Continuum Mechanics of Beam and Plate Flexure

Jönsson, Jeppe

Publication date:
1995

Document Version
Publisher's PDF, also known as Version of record

Continuum Mechanics of Beam and Plate Flexure

Jeppe Jönsson

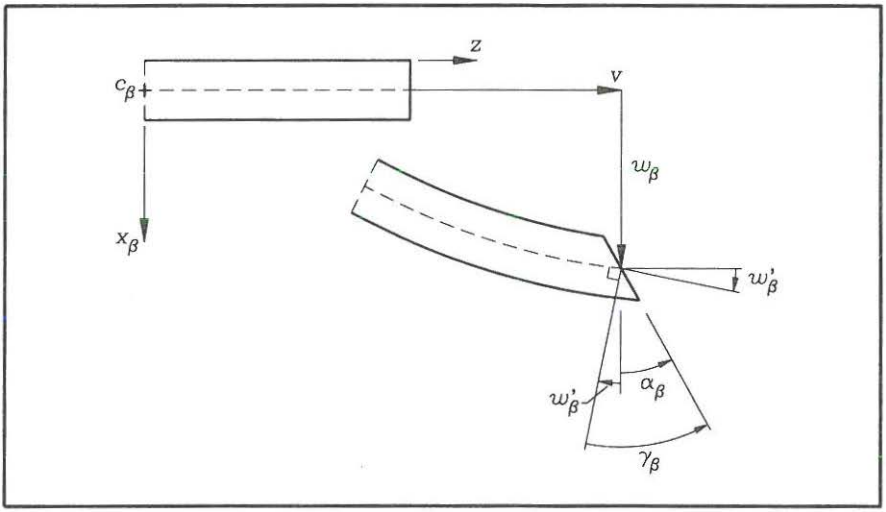

Aalborg University

July 1995

Preface

This text has been written and used during the spring of 1995 for a course on flexural mechanics of beams and plates at Aalborg University. The idea has been to concentrate on basic principles of the theories, which are of importance to the modern structural engineer. Today's structural engineer must be acquainted with the classic beam and plate theories, when reading manuals and using modern software tools such as the finite element method. Each chapter includes supplementary theory and derivations enabling consultation of the notes also at a later stage of study.

A preliminary chapter introduces the modern notation used in textbooks and in research today. It further gives an introduction to three-dimensional continuum mechanics of elastic bodies and the related principles of virtual work. The idea is to give the students a basic understanding of the stresses and strains, the equilibrium equations and the principle of virtual work.

The chapters of this text present the classic flexural beam theories and the stability theory for columns. For analysis of continuous beam and frame structures the flexibility method for statically indeterminate beam structures is presented. Plastic hinge analysis of beam structures is presented and includes both upper and lower-bound solution techniques. The remaining chapters are devoted to plates. The classic elastic plate theories are presented. The plastic yield line theory for plates is presented including both upper and lower-bound techniques.

The text serves as a proposal for a renewal in the line of presentation and it is used in structural mechanics at the Department of Building Technology and Structural Engineering at Aalborg University. Furthermore, it also serves as a proposal for a unified line of presentation within the Danish educational network for structural engineers, KONMAT. The text is to be used within the KONMAT framework for a post-graduate course in the autumn of 1995. The idea has been to use an advanced and modern notation from the beginning, and to use the principle of virtual work to derive the theories in a kinematic manner.

The presentation is greatly enhanced by the illustrations drawn by Mrs. Norma Hornung and by the language corrections performed by Mrs. Kirsten Aakjær.

Aalborg, July 31, 1995
Jeppe Jönsson

Contents

Chapter 1

Preliminaries

This chapter introduces the notation used in modern textbooks and in research today. Index notation used in combination with Einstein's summation convention enables a short and clear presentation of multi-dimensional problems, especially when we deal with scalar fields, vector fields and tensors in Cartesian coordinate systems. The index notation is used for flexural beam theory in order to avoid having to repeat equations of the two planes (later it is used to decouple the flexural equations). In plate theory it is used for the two in-plane directions. The chapter also gives an introduction to three-dimensional continuum mechanics of elastic bodies and the related principle of virtual work. This enables a clear and straightforward explanation of the assumptions in flexural beam and plate theories.

1.1 Index Notation and Cartesian Tensors

The notation intoduced by Einstein in his development of the Theory of Relativity simplifies the presentation of many equations and expressions. A more detailed introduction to index notation of Cartesian tensors and tensor analysis can be found in Simmonds [1], Kay [2] or Synge & Shield [3]. Index notation is often used for the components of vectors, matrices or tensors. Taking the dot product between two vectors $\mathbf{a}$ and $\mathbf{b}$ having three components each, a_i and b_i, where the index i assumes the values from 1 to 3, the expression can be written as

$$\mathbf{a} \cdot \mathbf{b} = a_1 b_1 + a_2 b_2 + a_3 b_3 = \sum_{i=1}^{3} a_i b_i. \tag{1.1}$$

Instead of using the summation symbol $\sum$ the strategy is to use the repeated index (here i) as a summation index. The dot product can thus simply be written as

Einstein summation used for the dot product

$$\mathbf{a} \cdot \mathbf{b} = a_i b_i \tag{1.2}$$

Einstein summation convention

A repeated index within a term is a summation index

which is indeed much shorter and just as clear as the dot product. All indices should have the same range unless otherwise stated.

Dummy and Free Indices

It is necessary to emphasize that it is a repeated index, which acts as a summation index. An index can thus only appear twice in the same term and the two indices are called dummy indices or just the dummy index. Other indices are called free indices. The expression $a_{ij}b_k$ does not indicate summation, it has three free indices, but both $a_{ii}b_j$ and $a_{ij}b_j$ indicate different sums with one free index.

- **Example 1.1** Expansion of dummy indices.

  Assuming the range of i to be $1\ldots3$ the two terms discussed above expand as follows:

$$\begin{aligned} a_{ii}b_j &= a_{11}b_j + a_{22}b_j + a_{33}b_j = (a_{11} + a_{22} + a_{33})b_j \\ a_{ij}b_j &= a_{i1}b_1 + a_{i2}b_2 + a_{i3}b_3 \end{aligned}$$

  It should be clear that the use of i as the notation for the repeated index is insignificant. The expression a_{ii} is equivalent to a_{kk}.

Multiple Sums

An expression may involve multiple summation indices. For example $a_{ij}b_{ij}$ or $a_{ij}b_ic_j$. If an expression involves two summation (dummy) indices with the range $1\ldots n$, there will be n^2 terms in the sum.

- **Example 1.2** Expansion of a double sum.

  The result of the latter expression $a_{ij}b_ic_j$ can be evaluated by expanding first the dummy index i, then the dummy index j. Assuming the range to be $1\ldots3$, the result is

$$\begin{aligned} a_{ij}b_ic_j &= a_{1j}b_1c_j + a_{2j}b_2c_j + a_{3j}b_3c_j \\ &= a_{11}b_1c_1 + a_{21}b_2c_1 + a_{31}b_3c_1 \\ &\quad + a_{12}b_1c_2 + a_{2j}b_2c_2 + a_{32}b_3c_2 \\ &\quad + a_{13}b_1c_3 + a_{23}b_2c_3 + a_{33}b_3c_3 \end{aligned}$$

  The result is the same if we sum over j, and then over i.

The Kronecker Delta

A symbol used to extract the "diagonal" terms in a double summation and to change indices is the Kronecker delta defined as

The Kronecker delta

$$\delta_{ij} = \delta_{ji} = \begin{cases} 1 & \text{if } i = j \\ 0 & \text{if } i \neq j \end{cases} \tag{1.3}$$

The trace of the components a_{ij} of a matrix (a tensor) can be found by multiplying it by Kronecker's delta. If the range is $1 \ldots 3$ we find

$$\delta_{ij} a_{ij} = a_{ii} = a_{jj} = a_{11} + a_{22} + a_{33} \tag{1.4}$$

It is seen that the trace has been found as the sum of the diagonal components. It can be seen that the symbol can also change the index. For example, the term a_{ij} changes index j to k, when multiplied by δ_{kj} or δ_{jk}

$$\delta_{kj} a_{ij} = \delta_{k1} a_{i1} + \delta_{k2} a_{i2} + \delta_{k3} a_{i3} = a_{ik} \tag{1.5}$$

which can be seen by using the fact that the delta has the value 1 only when $k = j$. Notice that the free indices are i and k, meaning that the result is a_{ik} and NOT a_{ij}.

The Permutation Symbol

The permutation symbol is a symbol which can be used in connection with cross products between two vectors, but it has many other applications. The symbol can be used in different dimensions with a corresponding number of indices. With a range of $1 \ldots 2$ for indices α and β the symbol $e_{\alpha\beta}$ is defined as

$$e_{\alpha\beta} = \begin{cases} +1 & \text{for } \alpha, \beta \text{ in an even permutation} \\ -1 & \text{for } \alpha, \beta \text{ in an odd permutation} \\ 0 & \text{otherwise} \end{cases} \tag{1.6}$$

Thus the even permutation results in $e_{12} = 1$ and the odd in $e_{21} = -1$. The symbol can be used to describe differences in sign between behaviour in the two coordinate directions. This can be used in the kinematic description of the torsional behaviour of beams.

With a range of $1 \ldots 3$ for indices i, j and k the permutation symbol is defined by

$$e_{ijk} = \begin{cases} +1 & \text{for } i, j, k \text{ in an even permutation} \\ -1 & \text{for } i, j, k \text{ in an odd permutation} \\ 0 & \text{otherwise} \end{cases} \tag{1.7}$$

The even permutations are e_{123}, e_{312}, e_{231} and the odd ones are e_{321}, e_{132}, e_{213}. The components of the vector cross product $\mathbf{c} = \mathbf{a} \times \mathbf{b}$ can be written as

$$c_i = e_{ijk} a_j b_k \tag{1.8}$$

Interchange of the order of the vectors $\mathbf{a}$ and $\mathbf{b}$ changes the sign and thereby the direction of the vector cross product.

Comma Notation for Partial Derivatives

When using the Einstein summation convention it is convenient also to introduce the comma as a symbol for partial derivatives. The approach is that all indices following the comma are partial derivatives in the corresponding coordinate direction

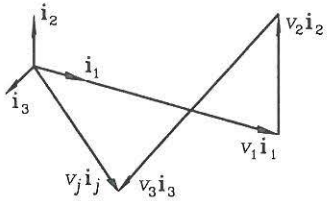

Fig. 1.1: Cartesian components of a vector.

x_i (where the three coordinate directions are x_1, x_2 and x_3)

Partial derivatives by use of comma index

$$\frac{\partial(\,)}{\partial x_i} = (\,)_{,i} \tag{1.9}$$

Examples

$$\frac{\partial^2(\,)}{\partial x_i \partial x_j} = (\,)_{,ij} \tag{1.10}$$

$$\frac{\partial^2(\,)}{\partial x_i x_3} = (\,)_{,i3} \tag{1.11}$$

- **Example 1.3** The gradient of a scalar

  The gradient of a scalar a is a vector ∇a with the partial derivatives as the components. It could be written in component form as $\frac{\partial a}{\partial x_i} = a_{,i}$.

Expanded Concept

For convenience in the present text lower case Greek indices $\alpha, \beta, \gamma, \nu$ have the two-dimensional range $1 \ldots 2$ and lower case Latin indices i, j, k, l have the three-dimensional range $1 \ldots 3$. Upper case indices are not summation indices. If other ranges are used it will be explicitly noted.

Mathematical Operators

The index notation with Einstein's summation convention also simplifies mathematical manipulations and can be of great help to the trained user of the matematical operators. Let us work with a Cartesian (orthonormal) coordinate system with the base vectors $\mathbf{i}_j$ and the related coordinates x_i. A vector $\mathbf{v} = v_j\mathbf{i}_j$ is thus described by its components v_j, as shown in fig. 1.1. The gradient operator is defined by

The gradient operator

$$\begin{aligned}\nabla &= \frac{\partial}{\partial x_1}\mathbf{i}_1 + \frac{\partial}{\partial x_2}\mathbf{i}_2 + \frac{\partial}{\partial x_3}\mathbf{i}_3 \\ &= \frac{\partial}{\partial x_j}\mathbf{i}_j \\ &= (\,)_{,j}\mathbf{i}_j \end{aligned} \tag{1.12}$$

Since the operator is a vector we use a boldface type to illustrate this. Denoting a scalar function by $s = s(x_i)$ and a vector quantity by $\mathbf{v} = \mathbf{v}(x_i)$ some well-known operations are decomposed in the following for the three-dimensional space. The operators and the index notation easily degenerate to two-dimensional space. The gradient of a scalar field is

$$\begin{aligned}\text{grad } s &= \nabla s \\ &= \frac{\partial s}{\partial x_1}\mathbf{i}_1 + \frac{\partial s}{\partial x_2}\mathbf{i}_2 + \frac{\partial s}{\partial x_3}\mathbf{i}_3 \\ &= \frac{\partial s}{\partial x_j}\mathbf{i}_j \\ &= s_{,j}\mathbf{i}_j \end{aligned} \tag{1.13}$$

It is seen that the gradient operator applied to a scalar results in a vector, since the gradient operator is a vector. The divergence of a vector is just applying the gradient operator to a vector through a scalar (dot) product, which results in a scalar.

$$\begin{aligned}\text{div } \mathbf{v} &= \nabla \cdot \mathbf{v} \\ &= (\frac{\partial}{\partial x_1}\mathbf{i}_1 + \frac{\partial}{\partial x_2}\mathbf{i}_2 + \frac{\partial}{\partial x_3}\mathbf{i}_3) \cdot (v_1\mathbf{i}_1 + v_2\mathbf{i}_2 + v_3\mathbf{i}_3) \\ &= \frac{\partial v_1}{\partial x_1} + \frac{\partial v_2}{\partial x_2} + \frac{\partial v_3}{\partial x_3} \\ &= \frac{\partial v_j}{\partial x_j} \\ &= v_{j,j} \end{aligned} \tag{1.14}$$

Instead of applying the gradient operator to a vector through the scalar (dot) product lets us use the cross product. This is the rotation or curl of the vector field defined by

$$\begin{aligned}\text{rot } \mathbf{v} &= \text{curl } \mathbf{v} = \nabla \times \mathbf{v} \\ &= (\frac{\partial}{\partial x_1}\mathbf{i}_1 + \frac{\partial}{\partial x_2}\mathbf{i}_2 + \frac{\partial}{\partial x_3}\mathbf{i}_3) \times (v_1\mathbf{i}_1 + v_2\mathbf{i}_2 + v_3\mathbf{i}_3) \\ &= \left(\frac{\partial v_3}{\partial x_2} - \frac{\partial v_2}{\partial x_3}\right)\mathbf{i}_1 + \left(\frac{\partial v_1}{\partial x_3} - \frac{\partial v_3}{\partial x_1}\right)\mathbf{i}_2 + \left(\frac{\partial v_2}{\partial x_1} - \frac{\partial v_1}{\partial x_2}\right)\mathbf{i}_3 \\ &= -e_{ijk}\frac{\partial v_i}{\partial x_j}\mathbf{i}_k \\ &= -e_{ijk}\, v_{i,j}\, \mathbf{i}_k \end{aligned} \tag{1.15}$$

It is seen that the permutation symbol has many applications, since it is used in the description of rotations. The Laplacian operator also enters many mechanical equations. The Laplacian of a scalar is given by

$$\begin{aligned} \text{div}(\text{grad } s) &= \nabla^2 s = \boldsymbol{\nabla} \cdot (\boldsymbol{\nabla} s) \\ &= \frac{\partial^2 s}{\partial^2 x_1} + \frac{\partial^2 s}{\partial^2 x_2} + \frac{\partial^2 s}{\partial^2 x_3} \\ &= s_{,jj} \end{aligned} \tag{1.16}$$

Notice that the Laplacian symbol ∇^2 is not a boldface symbol, since it works like a scalar. The Laplacian of a vector field is given by

$$\begin{aligned} \text{grad}(\text{div } \mathbf{v}) &= \nabla^2 \mathbf{v} = \boldsymbol{\nabla}(\boldsymbol{\nabla} \cdot \mathbf{v}) \\ &= \frac{\partial^2 \mathbf{v}}{\partial^2 x_1} + \frac{\partial^2 \mathbf{v}}{\partial^2 x_2} + \frac{\partial^2 \mathbf{v}}{\partial^2 x_3} \\ &= \mathbf{v}_{,jj} \\ &= v_{i,jj} \mathbf{i}_i \end{aligned} \tag{1.17}$$

Since the Laplacian operator works as a scalar the Laplacian of a vector is a vector and the Laplacian of a scalar is a scalar.

Another important mathematical tool is the divergence theorem which has a few alternate names in literature, it is also referenced as the Gauss theorem or the Green theorem. In vector notation the theorem is written

$$\int_V \text{div } \mathbf{v} \, dV = \int_{\partial V} \mathbf{n} \cdot \mathbf{v} \, dA \tag{1.18}$$

where $\mathbf{n}$ is the surface normal and ∂V is the boundary of the continuum volume as shown in fig. 1.2. In component form the divergence theorem takes the form:

The divergence theorem

$$\int_V v_{i,i} \, dV = \int_{\partial V} n_i \, v_i \, dA \tag{1.19}$$

In mechanics the divergence theorem can be used to transform differential field equations, (strong form), into a virtual work equation (weak form) involving lower order of the partial derivatives.

Cartesian Coordinate Transformation

Analysis often simplifies if performed in a Cartesian coordinate system, which has been rotated compared to the original system. This corresponds to a change of base vectors from an original base $\mathbf{i}_j$ to a new base $\bar{\mathbf{i}}_j$. The components of a vector $\mathbf{v}$ can be given in the original base

$$\begin{aligned} \mathbf{v} &= v_1 \mathbf{i}_1 + v_2 \mathbf{i}_2 + v_3 \mathbf{i}_3 \\ &= v_j \mathbf{i}_j \end{aligned} \tag{1.20}$$

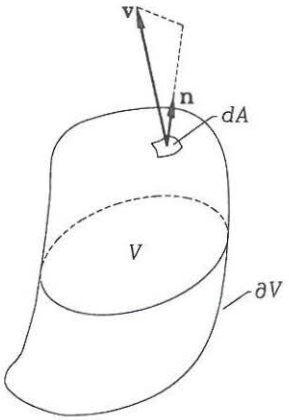

Fig. 1.2: Volume V, surface ∂V, vector field $\mathbf{v}$ and infinitesimal surface area dA with the normal $\mathbf{n}$.

or in the new base

$$\begin{aligned} \mathbf{v} &= \bar{v}_1\bar{\mathbf{i}}_1 + \bar{v}_2\bar{\mathbf{i}}_2 + \bar{v}_3\bar{\mathbf{i}}_3 \\ &= \bar{v}_j\bar{\mathbf{i}}_j \end{aligned} \tag{1.21}$$

Transformations between the two Cartesian coordinate systems are defined in the following. The new base vectors $\bar{\mathbf{i}}_j$ can be expressed by components in the original base, where the components are the projections of the new base onto the original base:

$$\begin{aligned} \bar{\mathbf{i}}_j &= (\bar{\mathbf{i}}_j \cdot \mathbf{i}_1)\,\mathbf{i}_1 + (\bar{\mathbf{i}}_j \cdot \mathbf{i}_2)\,\mathbf{i}_2 + (\bar{\mathbf{i}}_j \cdot \mathbf{i}_3)\,\mathbf{i}_3 \\ &= \ell_{j1}\mathbf{i}_1 + \ell_{j2}\mathbf{i}_2 + \ell_{j3}\mathbf{i}_3 \\ &= \ell_{jk}\mathbf{i}_k \end{aligned} \tag{1.22}$$

in which the direction cosines have been introduced as $\ell_{jk} = \bar{\mathbf{i}}_j \cdot \mathbf{i}_k = \cos(\angle\ \bar{\mathbf{i}}_j, \mathbf{i}_k)$. Note that the direction cosines are not symmetric, i.e. $\ell_{jk} \neq \ell_{kj}$. For example the first new base vector $\bar{\mathbf{i}}_1$ is given by:

$$\begin{aligned} \bar{\mathbf{i}}_1 &= (\bar{\mathbf{i}}_1 \cdot \mathbf{i}_1)\,\mathbf{i}_1 + (\bar{\mathbf{i}}_1 \cdot \mathbf{i}_2)\,\mathbf{i}_2 + (\bar{\mathbf{i}}_1 \cdot \mathbf{i}_3)\,\mathbf{i}_3 \\ &= \ell_{11}\mathbf{i}_1 + \ell_{12}\mathbf{i}_2 + \ell_{13}\mathbf{i}_3 \\ &= \ell_{1k}\mathbf{i}_k \end{aligned} \tag{1.23}$$

The opposite transformation from the "new" $\bar{\mathbf{i}}_k$ to the "original" base $\mathbf{i}_j$ is given by

$$\begin{aligned} \mathbf{i}_j &= (\mathbf{i}_j \cdot \bar{\mathbf{i}}_k)\,\bar{\mathbf{i}}_k = (\bar{\mathbf{i}}_k \cdot \mathbf{i}_j)\,\bar{\mathbf{i}}_k \\ &= \ell_{kj}\bar{\mathbf{i}}_k \end{aligned} \tag{1.24}$$

in which the indices of the direction cosines have changed places, corresponding to transposing a matrix.

The direction cosines ℓ_{jk} can be thought of as the components of a direction cosine matrix $\mathbf{L}$, which can be transposed $\mathbf{L}^T$ or inverted $\mathbf{L}^{-1}$. Since Cartesian coordinate systems are orthonormal the inverse of the direction cosine matrix is equal to its transpose, i.e. $\mathbf{L}^{-1} = \mathbf{L}^T$, and the components of the inverse direction cosine matrix are thus given by:

$$\ell_{jk}^{-1} = \ell_{jk}^T = \ell_{kj} \tag{1.25}$$

in which the order of the indices must be noted. This is in agreement with the transformations derived above.

Let us turn to the transformation of vector components. Transformation from components in the original base to components in the new base is given by:

$$\begin{aligned} v_k \mathbf{i}_k &= v_k \ell_{jk} \bar{\mathbf{i}}_j = \bar{v}_j \bar{\mathbf{i}}_j \quad \Downarrow \\ \bar{v}_j &= \ell_{jk} v_k \end{aligned} \tag{1.26}$$

and transformation from the new base to the original base is given by

$$\begin{aligned} \bar{v}_k \bar{\mathbf{i}}_k &= \bar{v}_k \ell_{kj} \mathbf{i}_j = v_j \mathbf{i}_j \quad \Downarrow \\ v_j &= \ell_{kj} \bar{v}_k \end{aligned} \tag{1.27}$$

It is seen that the vector components transform in the same manner as the base vectors. To summarize we have:

Cartesian transformations

$$\begin{aligned} \bar{\mathbf{i}}_j &= \ell_{jk}\, \mathbf{i}_k & \bar{v}_j &= \ell_{jk} v_k \\ \mathbf{i}_j &= \ell_{kj}\, \bar{\mathbf{i}}_k & v_k &= \ell_{kj} \bar{v}_k \end{aligned} \tag{1.28}$$

where the direction cosine matrix components are $\ell_{jk} = \bar{\mathbf{i}}_j \cdot \mathbf{i}_k = \cos(\angle\, \bar{\mathbf{i}}_j, \mathbf{i}_k)$. *The components of the inverse direction cosine matrix are found by* $\ell_{jk}^{-1} = \ell_{jk}^T = \ell_{kj}$.

These transformations are extensively used in analytical mechanics.

- **Example 1.4** Rotated two-dimensional base.

  Let us find the direction cosines of the transformation matrix from an original base $\mathbf{i}_\alpha$ to a new base $\bar{\mathbf{i}}_\beta$, which is rotated by an angle θ, as shown in fig. 1.3. In this two-dimensional case the direction cosine matrix and its components are:

$$\begin{aligned} \mathbf{L} = (\ell_{\alpha\beta}) &= \begin{bmatrix} \cos(\angle\, \bar{\mathbf{i}}_1, \mathbf{i}_1) & \cos(\angle\, \bar{\mathbf{i}}_1, \mathbf{i}_2) \\ \cos(\angle\, \bar{\mathbf{i}}_2, \mathbf{i}_1) & \cos(\angle\, \bar{\mathbf{i}}_2, \mathbf{i}_2) \end{bmatrix} \\ &= \begin{bmatrix} \cos\theta & \cos(\frac{\pi}{2} - \theta) \\ \cos(\frac{\pi}{2} + \theta) & \cos\theta \end{bmatrix} = \begin{bmatrix} \cos\theta & \sin\theta \\ -\sin\theta & \cos\theta \end{bmatrix} \end{aligned}$$

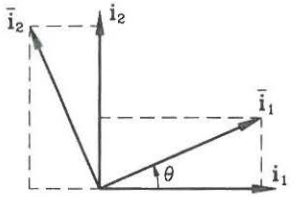

Fig. 1.3: Rotated two-dimensional base.

Cartesian Tensors

The mathematical modelling of mechanical systems often involves components, which depend on directions in space, and a specific choice of coordinate system. However, other choices may be convenient in part of the mathematical analysis. Tensor analysis deals with the change of coordinate systems and the related transformations of the direction dependent components of the mathematical model. Our main interest is related to the transformations between different Cartesian coordinate systems.

An N'th order tensor is a mathematical quantity which has components that refer to N choices of coordinate systems (which most often are chosen to be the same). Cartesian tensors are defined by the manner in which they transform from one Cartesian coordinate system to another. More extensive definitions that introduce covariant, contravariant and mixed tensors can be found in [1], [2] or [3], but the following definition will be sufficient in the present text.

Cartesian tensors *(Cartesian transformation: $\bar{\mathbf{i}}_j = \ell_{jk}\,\mathbf{i}_k$)*

A first order tensor $\mathbf{t} = t_j\,\mathbf{i}_j$ with components t_j in the Cartesian base $\mathbf{i}_j$ is a quantity, whose components transform to a new Cartesian base $\bar{\mathbf{i}}_j$ by:

$$\bar{t}_j = \ell_{jk}\,t_k \tag{1.29}$$

A second order tensor $\mathbf{t} = t_{jk}\,\mathbf{i}_j\mathbf{i}_k$ with components t_{jk} in the Cartesian base $\mathbf{i}_j$ is a quantity, whose components transform to a new Cartesian base $\bar{\mathbf{i}}_j$ by:

$$\bar{t}_{mn} = \ell_{mj}\ell_{nk}\,t_{jk} \tag{1.30}$$

An N'th order tensor $\mathbf{t} = t_{j\ldots n}\,\mathbf{i}_j \ldots \mathbf{i}_n$ with components $t_{j\ldots n}$ in the Cartesian base $\mathbf{i}_j$ is a quantity, whose components transform to a new Cartesian base $\bar{\mathbf{i}}_j$ by:

$$\bar{t}_{o\ldots s} = \ell_{oj} \ldots \ell_{sn}\,t_{j\ldots n} \tag{1.31}$$

A zero order tensor has one component t which does not change when the base is changed, i.e. it is a scalar.

Vectors are thus first order Cartesian tensors, since they transform in the same

manner. An example of a zero order tensor is the temperature, which is scalar. The temperature is typically a field variable, which is a function of the position, but has no direction components. The temperature component is the same in all coordinate systems, whereas a velocity field is a first order tensor, which has a direction and has components which are dependent on the coordinate system used. The highest order Cartesian tensor used in the present work is a fourth order and the most used are second order tensors. The second order tensors have much in common with the matrix concept. Originally it was the mechanical concept of stress, which has led to the introduction of tensor analysis (tension in French is "tenseur"). It is important to note that the three-dimensional Latin indices can be replaced by the two-dimensonal Greek indices.

- **Example 1.5** The tensor of inertia

  In mechanics the tensor of inertia is a second order Cartesian tensor defined as

$$I_{\alpha\beta} = \int_A (x_\alpha - c_\alpha)(x_\beta - c_\beta)\, dA$$

  where x_α are the Cartesian coordinates, c_α is the point about which the inertia is sought and the small area $dA = dx_1 dx_2$. It can be written in a matrix format as:

$$\mathbf{I} = (I_{\alpha\beta}) = \begin{bmatrix} I_{11} & I_{12} \\ I_{21} & I_{22} \end{bmatrix}$$

  To verify that this is a tensor let us seek the components in a rotated Cartesian base. We can just transform the coordinates independently:

$$\begin{aligned} \bar{I}_{\nu\gamma} &= \int_A (\bar{x}_\nu - \bar{c}_\nu)(\bar{x}_\gamma - \bar{c}_\gamma)\, dA \\ &= \int_A \ell_{\nu\alpha}\ell_{\gamma\beta}(x_\alpha - c_\alpha)(x_\beta - c_\beta)\, dA \\ &= \ell_{\nu\alpha}\ell_{\gamma\beta}\int_A (x_\alpha - c_\alpha)(x_\beta - c_\beta)\, dA \\ &= \ell_{\nu\alpha}\ell_{\gamma\beta}\, I_{\alpha\beta} \end{aligned}$$

  Thus it is seen that the inertia quantities are components of a second order tensor.

  In a rotated coordinate system the tensor components can be found by $\bar{I}_{\nu\gamma} = \ell_{\nu\alpha}\ell_{\gamma\beta}I_{\alpha\beta}$. For an angle of rotation θ the direction cosine components written in matrix format can be found as:

$$\mathbf{L} = (\ell_{\alpha\beta}) = \begin{bmatrix} \cos\theta & \sin\theta \\ -\sin\theta & \cos\theta \end{bmatrix} = \begin{bmatrix} c & s \\ -s & c \end{bmatrix}$$

  where $c = \cos\theta$ and $s = \sin\theta$ have been introduced, see example 1.4. In the rotated Cartesian coordinate system the moments of inertia can thus be found. In matrix notation the calculation procedure becomes:

$$\bar{\mathbf{I}} = \mathbf{L}\,\mathbf{I}\,\mathbf{L}^T \quad \Downarrow$$

$$\begin{bmatrix} \bar{I}_{11} & \bar{I}_{12} \\ \bar{I}_{21} & \bar{I}_{22} \end{bmatrix} = \begin{bmatrix} c & s \\ -s & c \end{bmatrix} \begin{bmatrix} I_{11} & I_{12} \\ I_{21} & I_{22} \end{bmatrix} \begin{bmatrix} c & -s \\ s & c \end{bmatrix}$$

By use of the index notation and $I_{12} = I_{21}$ it is easy to show that the resulting components are:

$$\begin{aligned}
\bar{I}_{11} &= \ell_{1\alpha}\ell_{1\beta}I_{\alpha\beta} &&= c^2 I_{11} + 2csI_{12} + s^2 I_{22} \\
\bar{I}_{22} &= \ell_{2\alpha}\ell_{2\beta}I_{\alpha\beta} &&= s^2 I_{11} - 2csI_{12} + c^2 I_{22} \\
\bar{I}_{12} &= \ell_{1\alpha}\ell_{2\beta}I_{\alpha\beta} &&= -csI_{11} + (c^2 - s^2)I_{12} + csI_{22} \\
\bar{I}_{21} &= \bar{I}_{21}
\end{aligned}$$

It is now possible to find an angle of rotation θ which diagonalizes the tensor of inertia by solving the equation $\bar{I}_{12} = 0$ which takes the form:

$$\begin{aligned}
cs(I_{22} - I_{11}) + (c^2 - s^2)I_{12} &= 0 \quad \Downarrow \\
(I_{22} - I_{11})\frac{\sin 2\theta}{2} + I_{12}\cos 2\theta &= 0 \quad \Downarrow \\
\tan 2\theta &= \frac{2I_{12}}{I_{11} - I_{22}}
\end{aligned}$$

The mechanical system simplifies when rotated by θ since $\bar{I}_{12} = 0$. The related axes are called the principal axes. In a following subsection it is shown that the principal axes can be found by solving an eigenvalue problem.

Isotropic and Deviatoric Tensors

An isotropic tensor is a tensor, whose components are the same in any coordinate system. A scalar is for example a zero order tensor, which is isotropic. It can be shown that second order isotropic tensors are of the form $p\delta_{ij}$, where p is a scalar. A tensor may include an isotropic part and a remaining non-isotropic part. The isotropic part of a second order tensor t_{ij} is determined by its trace as

$$p = \frac{1}{3}t_{ii} \tag{1.32}$$

A deviatoric tensor is a tensor without an isotropic part. A deviatoric second order tensor s_{ij} is a tensor, whose trace is zero in all coordinate systems, i.e. $s_{ii} = 0$. The non-isotropic part of a second order tensor, which deviates from isotropy, is the deviatoric part. Thus a second order tensor t_{ij} can always be decomposed into an isotropic part $p\delta_{ij}$ with $p = \frac{1}{3}t_{ii}$ and a deviatoric part s_{ij} as follows:

$$t_{ij} = p\delta_{ij} + s_{ij} \tag{1.33}$$

and the deviatoric part s_{ij} may thus be found by:

$$s_{ij} = t_{ij} - \frac{1}{3}t_{kk}\delta_{ij} \tag{1.34}$$

This decomposition is sometimes used in the mechanical description of (pressure), stress and strain.

Quadratic Forms

This subsection is just to remind the reader about the mathematical concepts related to analysis of quadratic forms. From analytic geometry and mathematics it is known that quadratic forms can be brought into a canonical form by coordinate transformation. Symmetric second order Cartesian tensors $t_{ij} = t_{ji}$ appear in quadratic forms, where they are multiplied twice by a first order tensor:

$$\begin{aligned} x_i t_{ij} x_j &= (x_1, x_2, x_3) \begin{bmatrix} t_{11} & t_{12} & t_{13} \\ t_{21} & t_{22} & t_{23} \\ t_{31} & t_{32} & t_{33} \end{bmatrix} \begin{pmatrix} x_1 \\ x_2 \\ x_3 \end{pmatrix} \\ &= t_{11}x_1^2 + t_{22}x_2^2 + t_{33}x_3^2 + 2t_{23}x_2x_3 + 2t_{13}x_1x_3 + 2t_{12}x_1x_2 \end{aligned} \tag{1.35}$$

By rotation of coordinate axis this quadratic form can be cast into a canonical form, where the second order tensor is diagonalized. In this rotated system the quadratic form thus takes the following canonical form

$$\begin{aligned} \bar{x}_i \bar{t}_{ij} \bar{x}_j &= (\bar{x}_1, \bar{x}_2, \bar{x}_3) \begin{bmatrix} \bar{t}_{11} & 0 & 0 \\ 0 & \bar{t}_{22} & 0 \\ 0 & 0 & \bar{t}_{33} \end{bmatrix} \begin{pmatrix} \bar{x}_1 \\ \bar{x}_2 \\ \bar{x}_3 \end{pmatrix} \\ &= \bar{t}_{11}\bar{x}_1^2 + \bar{t}_{22}\bar{x}_2^2 + \bar{t}_{33}\bar{x}_3^2 \end{aligned} \tag{1.36}$$

where the transformed second order tensor $\bar{t}_{ij} = \ell_{ik}\ell_{jl}t_{kl}$ is diagonal and $\bar{x}_j = \ell_{jk}x_k$ are the transformed components of the first order tensor. The diagonal components $\bar{t}_{11}$, $\bar{t}_{22}$, and $\bar{t}_{33}$ are the principal components and the associated axes $\bar{\mathbf{i}}_j$ are the principal axes. Sometimes the principal components are written with just one index $\bar{t}_{11} = t_{(1)}$, $\bar{t}_{22} = t_{(2)}$, and $\bar{t}_{33} = t_{(3)}$. To find the principal directions the related eigenvalue problem is solved. The eigenvalue problem results in eigenvalues, which are the principal components, and in eigenvectors, which are the principal directions.

Principal Axes and Invariants

Principal axes are the coordinate axes, which diagonalize symmetric second order tensors. The principal axes and the principal components are of interest when dealing with symmetric second order tensors, wether or not they appear in a quadratic form. The mechanical analysis is eased and the theoretical derivations can be enhanced by the use of principal axes.

Let us assume that the unit direction vector (tensor) $\mathbf{n} = n_j\mathbf{i}_j$ is in one of the three principal directions $\bar{\mathbf{i}}_{(n)}$, i.e. the direction $\bar{\mathbf{i}}_1$, $\bar{\mathbf{i}}_2$ or $\bar{\mathbf{i}}_3$. The index n in parenthesis refers to the principal direction 1, 2 or 3, and the parenthesis states that it is *not* a summation index. Let us further assume that the unit direction vector $\mathbf{m} = m_i\mathbf{i}_i$ is also directed in any one of the three principal directions $\bar{\mathbf{i}}_{(m)}$. According to equation (1.22) the components of the direction tensors are given by the direction cosines of the rotated principal axes as $n_j = \ell_{(n)j}$, since $\bar{\mathbf{i}}_{(n)} = \ell_{(n)j}\mathbf{i}_j$, and $m_i = \ell_{(m)i}$, since $\bar{\mathbf{i}}_{(m)} = \ell_{(m)i}\mathbf{i}_i$.

A first order tensor v_i is given by the product of the second order tensor t_{ij} and the unit direction tensor n_j as follows:

$$v_i = t_{ij} n_j \tag{1.37}$$

The components of v_i in one of the three principal directions m_i can then be found by the projection product $m_i v_i$, which takes the form

$$m_i v_i = m_i t_{ij} n_j = \ell_{(m)i} t_{ij} \ell_{(n)j} = \bar{t}_{(mn)} = \begin{cases} t_{(n)} & \text{if } m = n \\ 0 & \text{if } m \neq n \end{cases} \tag{1.38}$$

This shows us that the first order tensor v_i only has a component $t_{(n)}$ in the chosen direction n_i:

$$v_i = t_{(n)} n_i = \lambda n_i \tag{1.39}$$

where $\lambda = t_{(n)}$ has been introduced, since we do not yet know the principal value $t_{(n)}$. To find the principal directions we use the equality given by equation (1.37) and (1.39) as follows:

$$\begin{aligned} t_{ij} n_j &= \lambda n_i \quad \Downarrow \\ t_{ij} n_j - \lambda n_i &= 0 \quad \Downarrow \\ (t_{ij} - \lambda \delta_{ij})\, n_j &= 0 \end{aligned} \tag{1.40}$$

This is a linear eigenvalue problem, which has three solutions corresponding to three eigenvalues λ_n and three normalized eigenvectors $n_{(n)j}$. The three eigenvalues correspond to the three principal components of the diagonalized tensor $t_{(n)} = \lambda_{(n)}$ and the three eigenvectors give us the three orthonormal principal directions $n_{(n)j} = \ell_{(n)j}$. The eigenvalues and thereby the principal components $t_{(n)}$ are invariants, since they are the same no matter, which Cartesian coordinate system is used. Other invariants can be found by algebraic combinations of these eigenvalues.

The eigenvalue problem only has non-trivial solutions when the determinant of the coefficients vanishes, i.e. when

$$\begin{aligned} |t_{ij} - \lambda \delta_{ij}| &= 0 \quad \Downarrow \\ \begin{vmatrix} t_{11} - \lambda & t_{12} & t_{13} \\ t_{21} & t_{22} - \lambda & t_{23} \\ t_{31} & t_{32} & t_{33} - \lambda \end{vmatrix} &= 0 \end{aligned} \tag{1.41}$$

The determinant can be written in the form of a so-called characteristic equation:

$$\lambda^3 - I_1 \lambda^2 + I_2 \lambda - I_3 = 0 \tag{1.42}$$

which must be invariant since the solutions are invariants. Thus, the coefficients I_1, I_2 and I_3 are also invariants. The invariant coefficients are

$$I_1 = t_{11} + t_{22} + t_{33} = t_{ii} \tag{1.43}$$

$$I_2 = \begin{vmatrix} t_{22} & t_{23} \\ t_{32} & t_{33} \end{vmatrix} + \begin{vmatrix} t_{11} & t_{13} \\ t_{31} & t_{33} \end{vmatrix} + \begin{vmatrix} t_{11} & t_{12} \\ t_{21} & t_{22} \end{vmatrix} = \frac{1}{2}(t_{ii}t_{jj} - t_{ij}t_{ji}) \tag{1.44}$$

$$I_3 = \begin{vmatrix} t_{11} & t_{12} & t_{13} \\ t_{21} & t_{22} & t_{23} \\ t_{31} & t_{32} & t_{33} \end{vmatrix} = |t_{ij}| = \det(t_{ij}) \tag{1.45}$$

Using the diagonalized tensor components $t_n = t_{(n)}$ the invariants take the form

$$I_1 = t_1 + t_2 + t_3 \tag{1.46}$$
$$I_2 = t_2t_3 + t_1t_3 + t_1t_2 \tag{1.47}$$
$$I_3 = t_1t_2t_3 \tag{1.48}$$

In some problems of mechanics it is the deviatoric part of a tensor which is of interest. In this connection it should be noted that the principal directions of a tensor t_{ij} and its deviatoric part s_{ij} are the same. To show this we just introduce the decomposition of the tensor t_{ij} into its isotropic part $p\delta_{ij} = \frac{1}{3}t_{ii}$ and its deviatoric part s_{ij} as follows:

$$\begin{aligned} (t_{ij} - \lambda\delta_{ij})\, n_j &= 0 \quad \Downarrow \\ (s_{ij} - (\lambda - p)\delta_{ij})\, n_j &= 0 \quad \Downarrow \\ (s_{ij} - \tilde{\lambda}\delta_{ij})\, n_j &= 0 \end{aligned} \tag{1.49}$$

which is just a shifted eigenvalue problem with the eigenvalues shifted by the isotropic component $\tilde{\lambda} = \lambda - p$ and with the same eigenvectors n_j.

Principal Axes in Two-Dimensional Problems

In two-dimensional problems, where the principal directions are needed, the eigenvalue problem simplifies a little, since we just need to solve a quadratic equation. Let us find the principal components and directions of the tensor $t_{\alpha\beta}$ with $t_{12} = t_{21} \neq 0$ by solving the eigenvalue problem:

$$\begin{aligned} (t_{\alpha\beta} - \lambda\delta_{\alpha\beta})\, n_\beta &= 0 \quad \Downarrow \\ \begin{bmatrix} t_{11} - \lambda & t_{12} \\ t_{12} & t_{22} - \lambda \end{bmatrix} \begin{pmatrix} n_1 \\ n_2 \end{pmatrix} &= \begin{pmatrix} 0 \\ 0 \end{pmatrix} \end{aligned} \tag{1.50}$$

The non-trivial solutions exist when the determinant of the coefficients vanishes:

$$\lambda^2 - I_1\lambda + I_2 = 0 \tag{1.51}$$

where the invariants are $I_1 = t_{\alpha\alpha} = t_{11} + t_{22}$ and $I_2 = |t_{\alpha\beta}| = t_{11}t_{22} - t_{12}^2$. The two eigenvalues are thus given by

$$\begin{aligned} \lambda &= \frac{1}{2}\left(I_1 \pm \sqrt{I_1^2 - 4I_2}\right) \\ &= \frac{1}{2}\left(t_{11} + t_{22} \pm \sqrt{(t_{11} - t_{22})^2 - 4t_{12}^2}\right) \end{aligned} \tag{1.52}$$

By assuming that the eigenvalues are real, the eigenvectors may be found as follows. The components of the eigenvector must differ from zero since $t_{12} \neq 0$, let us then take the value of the first component as $n_1 = \cos\theta$. The direction vector should be a unit vector and we can thus take the second component as $n_2 = \sin\theta$. The angle θ is found by inserting the direction vector into the eigenvalue problem:

$$\begin{aligned} (t_{11} - \lambda)\cos\theta + t_{12}\sin\theta &= 0 \\ t_{12}\cos\theta + (t_{22} - \lambda)\sin\theta &= 0 \end{aligned} \tag{1.53}$$

These equations result in the following two formulas:

$$\begin{aligned} \tan\theta &= \frac{\lambda - t_{11}}{t_{12}} \\ \cot\theta &= \frac{\lambda - t_{22}}{t_{12}} \end{aligned} \tag{1.54}$$

Both of these equations may be used with the two eigenvalues $\lambda_{(1)}$ and $\lambda_{(2)}$. However, subtracting the second equation from the first equation we get one equation for θ, which is independent of λ

$$\tan 2\theta = \frac{2t_{12}}{t_{11} - t_{22}} \tag{1.55}$$

Where θ is the angle with the principal coordinate system in which the tensor $t_{\alpha\beta}$ becomes diagonal. The same equation was derived in example 1.5.

- **Problem 1.1**
  Use the summation convention to write the following systems in a more compact form. State which indices are free and which are dummy indices:

$$(a) \qquad \begin{aligned} c_{11}x_1 + c_{12}x_2 + c_{13}x_3 &= d_1 \\ c_{21}x_1 + c_{22}x_2 + c_{23}x_3 &= d_2 \\ c_{31}x_1 + c_{32}x_2 + c_{33}x_3 &= d_3 \end{aligned}$$

$$(b) \qquad \begin{aligned} c_{11}x_1 + c_{21}x_2 + c_{31}x_3 &= d_1 \\ c_{12}x_1 + c_{22}x_2 + c_{32}x_3 &= d_2 \\ c_{13}x_1 + c_{23}x_2 + c_{33}x_3 &= d_3 \end{aligned}$$

  Write the equations in matrix/vector format.

- **Problem 1.2**
  If a_{ij} are constants, calculate the partial derivative

$$(a_{ij}x_ix_j)_{,k}$$

  Use that $\frac{\partial(\,)}{\partial x_k} = (\,)_{,k}$ and that the Kronecker delta can change the indices. Note that the number of free indices should remain the same.

- **Problem 1.3**
  Expand the following terms into a sum of the individual components

$$(a) \quad a_{ijk}e_{ijk}$$
$$(b) \quad \delta_{\alpha\beta}e_{\alpha\beta}$$

  Remember that e_{ijk} and $e_{\alpha\beta}$ are permutation symbols.

- **Problem 1.4**
  The equation $\sigma_{\alpha\beta,\alpha} + q_\beta = 0$ is not only one equation but two equations. It has one free index β and a dummy index α. Greek indices have the range $1 \ldots 2$. Expand the two equations (they are equilibrium equations for a plane continuum).

- **Problem 1.5**
  The Laplace equation in Cartesian coordinates has the (strong) form $s_{,ii} = 0$ where the scalar $s(x_i)$ is a function of the coordinates. The equation is multiplied by an arbitrary scalar function $a(x_i)$ and integrated over the volume. This integral is also zero:

$$\int_V a s_{,ii}\, dV = 0 \qquad \text{in the volume } V \tag{1.56}$$

  Use the divergence equation to transform this equation into a weak form, which includes only single derivatives $a_{,i}$, $s_{,i}$ and an area integral $\int_{\partial V} \ldots dA$ over the surface of the volume. To do this use the rules for taking derivatives in a product $(as_{,i})_{,i} = a_{,i}s_{,i} + as_{,ii}$. Write the derivation first using index notation and then the gradient operator (vector) notation.

1.2 Continuum Mechanics

This section gives an introduction to continuum mechanics of elastic solids. Continuum mechanics is concerned with problems such as motion, deformation and equilibrium of continuous bodies. The main emphasis is put on a pictorial and intuitional understanding of strain and stress in deforming three-dimensional bodies. A geometrical derivation and description of the deformation of a cube leads to the non-linear Lagrange definition of strains. The non-linear strain definition is needed for a complete description of stability. The strains are linearized for the theory of small strains and small rotations. The stresses are introduced as traction vectors on a cube with surfaces parallel to the Cartesian coordinate axes. To clarify that all components are included in this description a tetrahedral element is also considered. The elastic theory can then be completed by introducing the constitutive relation between stresses and strains (sometimes referenced as Hooke's law). The section is completed by the principle of virtual work and potential energy. The book by Washizu [4] gives a thorough treatment of energy principles and variational methods used in mechanics. The manuscript by Krenk [5] for a book on three-dimensional elastic beam theory includes chapters on continuum mechanics and energy principles related to beam theories. Malvern [6] gives a unified and thorough presentation of concepts and principles of modern continuum mechanics including both solid and fluid mechanics. For further studies one may consult

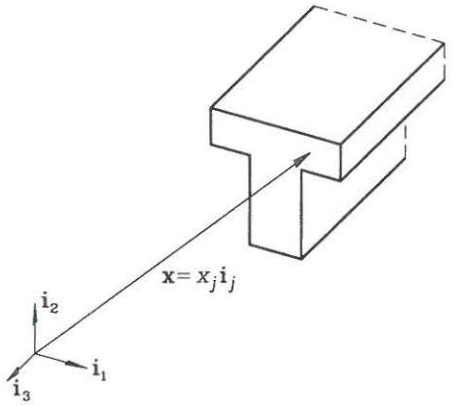

Fig. 1.4: Initial configuration with orthonormal base vectors $\mathbf{i}_j$.

Flügge [7], who gives an advanced treatment of tensor analysis and continuum mechanics involving skew coordinates, (covariant and contravariant properties).

Kinematics - Displacements, Rotations and Strains

Following Washizu [4] a Cartesian coordinate system with orthogonal unit base vectors $\mathbf{i}_1, \mathbf{i}_2, \mathbf{i}_3$ is introduced. As shown in fig. 1.4 the material points are described in the undeformed configuration by their position vector

$$\mathbf{x} = x_1\mathbf{i}_1 + x_2\mathbf{i}_2 + x_3\mathbf{i}_3 \tag{1.57}$$

The components (x_1, x_2, x_3) of the position vector can be written in a convenient form using index notation as x_j, whereby the coordinate decomposition of the material vector in equation (1.57) takes the form

$$\mathbf{x} = x_j\mathbf{i}_j \tag{1.58}$$

Each material coordinate x_j defines a particle position in the initial undeformed configuration. Let us use a Lagrangian deformation description. Each material particle is displaced from its initial configuration to its deformed position z_j by a displacement vector $\mathbf{u}(x_j)$. The displacement vector is a function of the particle position. The deformed particle position is thus given by

$$\mathbf{z} = \mathbf{x} + \mathbf{u} = (x_j + u_j)\mathbf{i}_j \tag{1.59}$$

If we consider a material point we can describe a particle using a local orthonormal set of base vectors $\mathbf{i}$, which we attatch to the material points. As the body deforms the particle also deforms and the initial orthonormal material base is no longer orthogonal nor of unit length. The deformed material base vectors $\tilde{\mathbf{i}}_j$ are determined by the gradients of the components of the new position vector

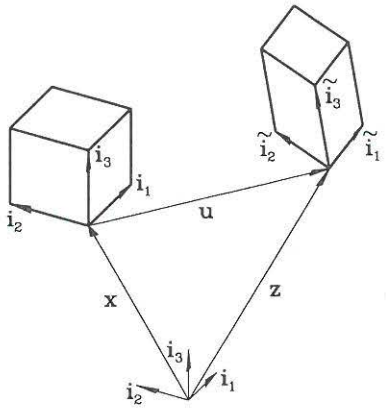

Fig. 1.5: Lagrangian deformation description.

Deformed base vector

$$\begin{aligned}\tilde{\mathbf{i}}_k &= \frac{\partial \mathbf{z}}{\partial x_k} = \frac{\partial}{\partial x_k}(z_j \mathbf{i}_j) = \frac{\partial z_j}{\partial x_k}\mathbf{i}_j \\ &= z_{j,k}\mathbf{i}_j \\ &= (x_j + u_j)_{,k}\mathbf{i}_j \\ &= (\delta_{jk} + u_{j,k})\mathbf{i}_j \end{aligned} \tag{1.60}$$

since $x_{j,k} = \frac{\partial x_j}{\partial x_k} = \delta_{jk}$. Figure 1.5 shows that the original cube spanned by the undeformed material base vectors has now been translated, rotated and deformed into a parallelepiped, where the side lengths and the angles between base vectors are altered. The result in equation (1.60) is clarified by expanding the deformed first base vector:

$$\tilde{\mathbf{i}}_1 = \mathbf{i}_1 + \frac{\partial u_1}{\partial x_1}\mathbf{i}_1 + \frac{\partial u_2}{\partial x_1}\mathbf{i}_2 + \frac{\partial u_3}{\partial x_1}\mathbf{i}_3 \tag{1.61}$$

The components are shown in fig. 1.6. The extensions of the material base vectors are measures of the axial strains, and the changes in angles between the material base vectors are measures of the shear strains. Let us see how this knowledge can be used.

The geometry of any parallelepiped can be described by scalar products of its three edge vectors. The scalar product of two different vectors is directly related to the angle between them and the scalar product of a vector by itself is related to its length. So let us take the scalar products of the initial undeformed material base and order them in a geometric second order tensor g_{ij} as follows

$$\begin{aligned} g_{ij} &= \mathbf{i}_i \cdot \mathbf{i}_j \\ &= \delta_{ij} \end{aligned} \tag{1.62}$$

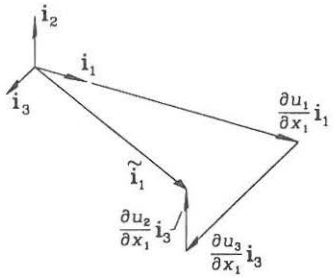

Fig. 1.6: The components of the deformed base vector $\tilde{\mathbf{i}}_1$.

which shows that the initial material base vectors are orthonormal. The geometry of the parallelepiped spanned by the deformed material base vectors is fully described by the geometric second order tensor $\tilde{g}_{ij}$ as follows

$$\begin{aligned}
\tilde{g}_{ij} &= \tilde{\mathbf{i}}_i \cdot \tilde{\mathbf{i}}_j \\
&= (z_{k,i}\mathbf{i}_k) \cdot (z_{l,j}\mathbf{i}_l) \\
&= z_{k,i} z_{l,j} \delta_{kl} \\
&= z_{k,i} z_{k,j} \\
&= (\delta_{ki} + u_{k,i})(\delta_{kj} + u_{k,j}) \\
&= \delta_{ki}\delta_{kj} + \delta_{ki}u_{k,j} + \delta_{kj}u_{k,i} + u_{k,i}u_{k,j} \\
&= \delta_{ij} + u_{i,j} + u_{j,i} + u_{k,i}u_{k,j} \qquad (1.63)
\end{aligned}$$

This was rather tedious index work but let us pick the fruits. It is seen that by taking the difference between the two geometric second order tensors $\tilde{g}_{ij} - g_{ij}$ we can get a strain measure. However, engineeres define the axial strains of linearized theory as the axial derivatives of axial displacements and it is thus necessary to divide the difference by 2. The Lagrangian strain tensor is thereby defined as

Lagrange strain tensor *(Finite strains)*

$$\begin{aligned}
\varepsilon_{ij} &= \frac{1}{2}(\tilde{g}_{ij} - g_{ij}) \\
&= \frac{1}{2}(u_{i,j} + u_{j,i} + u_{k,i}u_{k,j}) \qquad (1.64)
\end{aligned}$$

This is a non-linear strain measure with the non-linearity in the last term. Due to the symmetry of indices there are only six independent strain measures. The Lagrangian strain tensor is used in theories involving finite displacements. For infinitesimal strains we can linearize this definition and obtain the conventional linear strain measure. If all displacement derivatives $u_{i,j} \ll 1$ it justifies the use of the following linearized strain definition

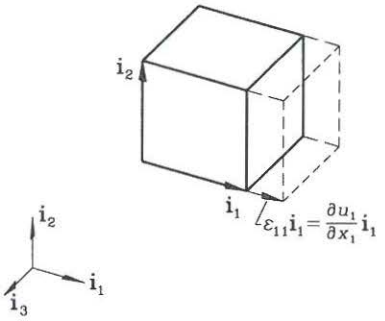

Fig. 1.7: Axial strain component ε_{11}.

Linear strain tensor *(Infinitesimal strains)*

$$\varepsilon_{ij} = \frac{1}{2}(u_{i,j} + u_{j,i}) \tag{1.65}$$

Thus the diagonal strain component ε_{11} illustrated in fig. 1.7 is found as

$$\begin{aligned} \varepsilon_{11} &= \frac{1}{2}(u_{1,1} + u_{1,1}) \\ &= u_{1,1} \\ &= \frac{\partial u_1}{\partial x_1} \end{aligned} \tag{1.66}$$

which is just the axial derivative of the axial displacement. The "off-diagonal" shear strain components are exemplified by

$$\varepsilon_{12} = \frac{1}{2}(u_{1,2} + u_{2,1}) = \frac{1}{2}\left(\frac{\partial u_1}{\partial x_2} + \frac{\partial u_2}{\partial x_1}\right) \tag{1.67}$$

The physical interpretation follows from consideration of the angle θ_{12} between the deformed material base vectors $\tilde{\mathbf{i}}_1$ and $\tilde{\mathbf{i}}_2$ as fig. 1.8 shows

$$\cos(\theta_{12}) = \frac{\tilde{\mathbf{i}}_1 \cdot \tilde{\mathbf{i}}_2}{\left|\tilde{\mathbf{i}}_1\right| \left|\tilde{\mathbf{i}}_2\right|} \tag{1.68}$$

For infinitesimal displacement derivatives, $u_{i,j} \ll 1$, we can neglect the axial elongation of the base vectors and use the Taylor expansion of $\cos(\theta_{12})$ about $\pi/2$, this yields $\cos(\theta_{12}) = \pi/2 - \theta_{12} + \ldots \simeq \gamma_{12}$, where γ_{12} is the conventional engineering shear strain angle, shown in fig. 1.8.

$$\begin{aligned} \gamma_{12} &= \tilde{\mathbf{i}}_1 \cdot \tilde{\mathbf{i}}_2 \\ &= \tilde{g}_{12} \\ &= 2\varepsilon_{12} \end{aligned} \tag{1.69}$$

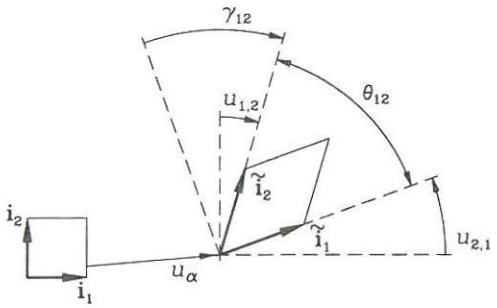

Fig. 1.8: Shear deformation, angles and strains ε_{12}.

It is important to notice the factor 2 between the shear strain ε_{12} and the engineering shear strain angle $\gamma_{12} = u_{1,2} + u_{2,1} = 2\varepsilon_{12}$. Some textbooks use a different notation!

We postulated that the components had contributions from strain and rotation. This can now be shown for the theory of infinitesimal strains and rotations, i.e. $u_{i,j} \ll 1$. In the components of the deformed base equation (1.60), we can rewrite the gradients of the displacement components $u_{j,k}$ as follows

$$\begin{aligned} u_{j,k} &= \frac{1}{2}(u_{j,k} + u_{k,j}) + \frac{1}{2}(u_{j,k} - u_{k,j}) \\ &= \varepsilon_{jk} + \omega_{jk} \end{aligned} \tag{1.70}$$

where the rotion tensor ω_{kj} has been defined as follows:

Linear rotation tensor *(Infinitesimal rotations)*

$$\omega_{jk} = \frac{1}{2}(u_{j,k} - u_{k,j}) \tag{1.71}$$

In mechanics it is sometimes convenient to work with a rotation vector. The relation between the second order rotation tensor and the rotation vector becomes clear, when we introduce the tensor components as follows:

$$(\omega_{jk}) = \begin{bmatrix} 0 & -\omega_3 & \omega_2 \\ \omega_3 & 0 & -\omega_1 \\ -\omega_2 & \omega_1 & 0 \end{bmatrix} \tag{1.72}$$

in which we have introduced the components of the vector of rotation $\omega_k \mathbf{i_k}$ as half the rotation of the displacement vector field $\omega = \frac{1}{2}$ rot $\mathbf{u} = \frac{1}{2}\,\boldsymbol{\nabla} \times \mathbf{u}$, see equation (1.15),

$$\omega_k = -\frac{1}{2} e_{ijk} u_{i,j} \quad \Downarrow \tag{1.73}$$

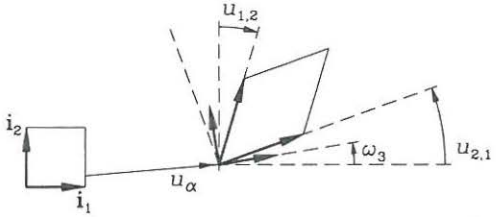

Fig. 1.9: The rotation $\omega_3 = \omega_{21} = \frac{1}{2}(u_{2,1} - u_{1,2})$ is the mean of the base vector rotations $u_{2,1}$ and $-u_{1,2}$.

$$\begin{aligned} \omega_1 &= \tfrac{1}{2}(u_{3,2} - u_{2,3}) \\ \omega_2 &= \tfrac{1}{2}(u_{1,3} - u_{3,1}) \\ \omega_3 &= \tfrac{1}{2}(u_{2,1} - u_{1,2}) \end{aligned} \tag{1.74}$$

The deformed base vector can then be rewritten as

Deformed base vector for infinitesimal strain and rotation

$$\tilde{\mathbf{i}}_k = (\delta_{jk} + \varepsilon_{jk} + \omega_{jk})\mathbf{i}_j \tag{1.75}$$

The rotation component $\omega_3 = \omega_{21}$ is illustrated in fig. 1.9. The figure shows that the rotation components are the mean rotations of the base vectors. This explains why the rotation components are defined as half of the rotation of the displacement vector field, i.e. $\boldsymbol{\omega} = \frac{1}{2}$ rot $\mathbf{u}$

It is important to note that the strain components are not completely independent nor are the rotation components. The strains and rotations must fulfil the so-called compatibility equations, if they are to be integrated to give the displacements. This corresponds to requiring that the related differentials are exact. A differential form $dF = \frac{\partial F}{\partial x_i} dx_i = F_{,i} dx_i$ is exact in a continuous continuum without holes if the cross differentials are equal, i.e. $\frac{\partial^2 F}{\partial x_i \partial x_j} = \frac{\partial^2 F}{\partial x_j \partial x_i}$ or with comma notation $F_{,ij} = F_{,ji}$. Supplementary conditions are needed, if there are holes.

To find the displacement field u_i and the rotation field ω_{ij} from a given strain field ε_{ij} and given boundary conditions for displacements $u_i^o = u_i(x_p^o)$ and rotations $\omega_{ij}^o = \omega_{ij}(x_p^o)$, we first find the rotation field. Let us show that the derivatives of the rotations (1.71) can be found by the derivatives of the strains as follows:

$$\begin{aligned} \omega_{ij,k} &= \frac{1}{2}(u_{i,jk} + u_{j,ik}) \\ &= \frac{1}{2}(u_{i,jk} + u_{k,ij}) - \frac{1}{2}(u_{j,ik} + u_{k,ij}) \\ &= \frac{1}{2}(u_{i,k} + u_{k,i})_{,j} - \frac{1}{2}(u_{j,k} + u_{k,j})_{,i} \\ &= \varepsilon_{ik,j} - \varepsilon_{jk,i} \end{aligned} \tag{1.76}$$

The rotations can thus be found by integration along any internal curve C from x_p^o

to the internal point x_p as follows:

$$\begin{aligned} \omega_{ij} &= \omega_{ij}^o + \int_C d\omega_{ij} \\ &= \omega_{ij}^o + \int_C \omega_{ij,k}\, dx_k \\ &= \omega_{ij}^o + \int_C (\varepsilon_{ik,j} - \varepsilon_{jk,i})\, dx_k \end{aligned} \tag{1.77}$$

if the differential $d\omega_{ij}$ is exact. Let us return to this later. Having found the rotations we can find the displacements by integrating the displacement differential $du_i = u_{i,j}dx_k$ along an internal curve C as follows:

$$\begin{aligned} u_i &= u_i^o + \int_C du_i \\ &= u_i^o + \int_C u_{i,j}\, dx_j \\ &= u_i^o + \int_C (\varepsilon_{ij} + \omega_{ij})\, dx_j \end{aligned} \tag{1.78}$$

Once again the differential du_i must be exact. It is thus clear that the strains must fulfil certain conditions that make the differential forms exact. Let us first check the cross derivatives of the displacements, i.e. $u_{i,jk} = u_{i,kj}$, which expressed by strains gives us:

$$\begin{aligned} (\varepsilon_{ij} + \omega_{ij})_{,k} &= (\varepsilon_{ik} + \omega_{ik})_{,j} \qquad \Downarrow \\ \varepsilon_{ij,k} + \varepsilon_{ik,j} - \varepsilon_{jk,i} &= \varepsilon_{ik,j} + \varepsilon_{ij,k} - \varepsilon_{kj,i} \qquad \Downarrow \\ -\varepsilon_{jk,i} &= -\varepsilon_{kj,i} \end{aligned} \tag{1.79}$$

which is fulfilled by the symmetry of the strains $\varepsilon_{jk} = \varepsilon_{kj}$. Let us next check the cross derivatives of the tensor of rotation, i.e. $\omega_{ij,kl} = \omega_{ij,lk}$, which gives us:

Compatibility equations

$$\varepsilon_{ik,jl} - \varepsilon_{jk,il} = \varepsilon_{il,jk} - \varepsilon_{jl,ik} \tag{1.80}$$

In two-dimensional problems the equations are similar:

$$\varepsilon_{\alpha\gamma,\beta\nu} - \varepsilon_{\beta\gamma,\alpha\nu} = \varepsilon_{\alpha\nu,\beta\gamma} - \varepsilon_{\beta\nu,\alpha\gamma} \tag{1.81}$$

This compatibility equation and the symmetry of the strain tensor ensures that the displacements found are compatible in the whole continuum. Note that the compatibility equations are fulfilled automaticly, if the strains are derived from a geometricly possible displacement field.

This concludes our journey into the kinematics of a continuum and we turn to the description of the stresses in a continuum and the equilibrium equations.

Stress and Equilibrium

Between neighbouring pariticle points of a continuum there will be action and reaction forces. These internal forces can be measured per area as force intensities

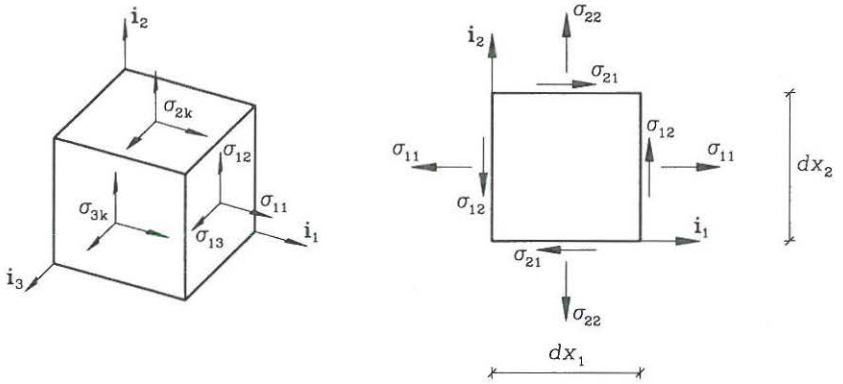

Fig. 1.10: Cartesian stress components σ_{ij}.

or stresses. However, the internal surface dA has an orientation with a surface normal. In a material point it is possible to make three orthogonal cuts each corresponding to an internal surface dA with a coordinate direction $\mathbf{i}_i$ as normal. Taking $\mathbf{t}_i$ as the stress vectors on each of the three surfaces of equal area dA and $d\mathbf{F}_i$ as the corresponding three internal forces we can define the stress vectors on the surfaces with normal $\mathbf{i}_i$ by

$$\mathbf{t}_i = \frac{d\mathbf{F}_i}{dA} \tag{1.82}$$

The stress vector acting on a surface, which has the first base vector $\mathbf{i}_1$ as normal, can be decomposed along the undeformed material base vectors as

$$\mathbf{t}_1 = \sigma_{11}\mathbf{i}_1 + \sigma_{12}\mathbf{i}_2 + \sigma_{13}\mathbf{i}_3 = \sigma_{1j}\mathbf{i}_j \tag{1.83}$$

where σ_{1j} are the three components of the vector $\mathbf{t}_1$. The decomposition of all three stress vectors $\mathbf{t}_i = [\mathbf{t}_1, \mathbf{t}_2, \mathbf{t}_3]$ using the force vectors $\mathbf{F}_i = [\mathbf{F}_1, \mathbf{F}_2, \mathbf{F}_3]$ in the undeformed material base directions $\mathbf{i}_j$ can be written as

$$\mathbf{t}_i = \sigma_{ij}\mathbf{i}_j = \frac{dF_{ij}}{dA}\mathbf{i}_j \quad \Downarrow$$

$$\sigma_{ij} = \frac{dF_{ij}}{dA} \tag{1.84}$$

It is seen that σ_{ij} is the component j of the force per surface area which has the base vector $\mathbf{i}_i$ as its normal. The Cartesian stress components are shown in fig. 1.10. This definition of the stress is acceptable for infinitesimal strains and rotations $u_{i,j} \ll 1$, but not for infinitesimal strains, $\varepsilon_{ij} \ll 1$, with moderate (infinitesimal) rotations, $\varepsilon_{ij} \ll \omega_{ij} \ll 1$, or with finite rotations. We shall consider this later, but it should be mentioned here that we could decompose the stress vectors along the deformed material base $\tilde{\mathbf{i}}_j$.

The stress tensor σ_{ij} has nine components. Let us consider an infinitesimal material cube as our particle and then see if we can obtain torsional equilibrium.

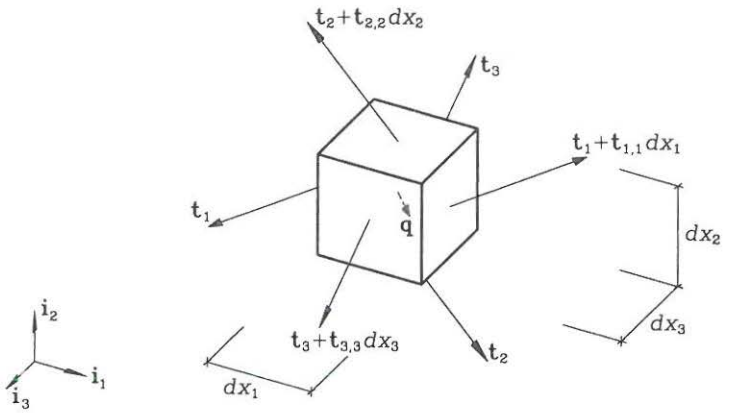

Fig. 1.11: Traction stress vectors on an infinitesimal parallelepiped.

For the sake of simplicity we just consider the plane spanned by the base vectors $\mathbf{i}_\alpha$ as included on the right-hand side of fig. 1.10. The torsional equilibrium gives

$$\begin{aligned}(\sigma_{12}dx_2)dx_1 - (\sigma_{21}dx_1)dx_2 &= 0 \quad \Downarrow \\ \sigma_{12} &= \sigma_{21}\end{aligned} \tag{1.85}$$

Thus, the stress tensor only has six independent components due to the symmetry

$$\sigma_{ij} = \sigma_{ji} \tag{1.86}$$

It is worth emphasizing that the first index i in the stress tensor σ_{ij} corresponds to the normal direction of the surface and the second index j to the directions of the local components of the stress vector acting on the surface.

Equilibrium equations can be found by use of the infinitesimal cube (or parallelepiped) shown in fig. 1.11. The cube is loaded by a volume load vector $\mathbf{q}$. Equilibrium can be expressed in vector format as

$$\begin{aligned}&(-\mathbf{t}_1 + \mathbf{t}_1 + \mathbf{t}_{1,1}dx_1)\, dx_2dx_3 \\ &\quad +(-\mathbf{t}_2 + \mathbf{t}_2 + \mathbf{t}_{2,2}dx_2)\, dx_1dx_3 \\ &\quad\quad +(-\mathbf{t}_3 + \mathbf{t}_3 + \mathbf{t}_{3,3}dx_3)\, dx_1dx_2 + \mathbf{q}\, dx_1dx_2dx_3 = \mathbf{0}\end{aligned} \tag{1.87}$$

By cancellation of terms and division by the infinitesimal volume, $dx_1dx_2dx_3$, the equilibrium equation becomes

$$\begin{aligned}\mathbf{t}_{1,1} + \mathbf{t}_{2,2} + \mathbf{t}_{3,3} + \mathbf{q} &= \mathbf{0} \quad \Downarrow \\ \mathbf{t}_{i,i} + \mathbf{q} &= \mathbf{0}\end{aligned} \tag{1.88}$$

This vector equation can be decomposed in the undeformed material base $\mathbf{i}_j$ for infinitesimal strain and rotation theory yielding the equilibrium equations in component form as

$$(\sigma_{ij,i} + q_j)\,\mathbf{i}_j = \mathbf{0} \tag{1.89}$$

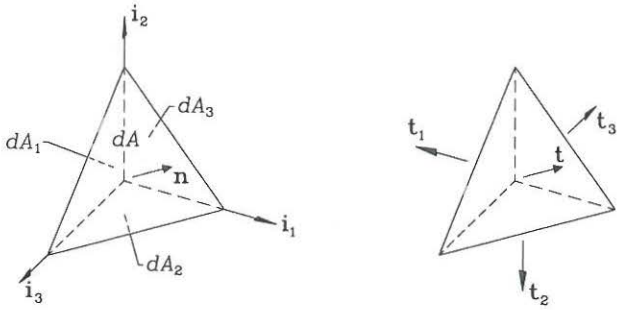

Fig. 1.12: Tetrahedral element with surface areas dA_i and dA.

Thus, the equilibrium equations in component form are

Linear equilibrium equations	*(Infinitesimal strains and rotations)*
$\sigma_{ij,i} + q_j = 0$	(1.90)

The equilibrium equations are linear in the displacements if the stresses are linear functions of the displacements. Let us expand the equilibrium equation to clairify the number of terms and equations

$$\begin{aligned} \sigma_{11,1} + \sigma_{21,2} + \sigma_{31,3} + q_1 &= 0 \\ \sigma_{12,1} + \sigma_{22,2} + \sigma_{32,3} + q_2 &= 0 \\ \sigma_{13,1} + \sigma_{23,2} + \sigma_{33,3} + q_3 &= 0 \end{aligned} \tag{1.91}$$

Sometimes the symbol τ is used for the shear stress components, for example $\sigma_{12} = \tau_{12}$ introducing these and using the conventional partial derivative symbol the equilibrium equations become

$$\begin{aligned} \frac{\partial \sigma_{11}}{\partial x_1} + \frac{\partial \tau_{21}}{\partial x_2} + \frac{\partial \tau_{31}}{\partial x_3} + q_1 &= 0 \\ \frac{\partial \tau_{12}}{\partial x_1} + \frac{\partial \sigma_{22}}{\partial x_2} + \frac{\partial \tau_{32}}{\partial x_3} + q_2 &= 0 \\ \frac{\partial \tau_{13}}{\partial x_1} + \frac{\partial \tau_{23}}{\partial x_2} + \frac{\partial \sigma_{33}}{\partial x_3} + q_3 &= 0 \end{aligned} \tag{1.92}$$

To clairify that we are able to find the stress components for any surface using the six independent stress components, we consider the equilibrium of an infinitesimal tetrahedral shown in fig. 1.12. The surface areas of the coordinate planes are denoted dA_i and the inclined surface area dA with its normal vector $\mathbf{n} = n_i \mathbf{i}_i$ (of cosine direction components). The areas are thus related by

$$n_i \, dA = dA_i \tag{1.93}$$

The stress traction vectors acting on the coordinate planes are $\mathbf{t}_i$ and on the inclined surface just $\mathbf{t}$. Equilibrium of the tetrahedral requires that

$$\begin{aligned} \mathbf{t}\, dA &= \mathbf{t}_i\, dA_i \quad \Downarrow \\ \mathbf{t}\, dA &= \mathbf{t}_i\, n_i\, dA \quad \Downarrow \\ \mathbf{t} &= n_i \mathbf{t}_i \end{aligned} \tag{1.94}$$

Introducing the strain components in the undeformed base of $\mathbf{t}$ as t_j and the components of $\mathbf{t}_i$ as σ_{ij} the tractions of any inclined surface with normal vector components n_i can be found by

Tractions *(Infinitesimal strains and rotations)*

$$t_j = n_i \sigma_{ij} \tag{1.95}$$

When the rotations are finite or moderate the equilibrium equation (1.88) and the stress tractions (1.94) must be resolved in the deformed base $\tilde{\mathbf{i}}_j$ since they follow (translate and rotate with) the material surface. This corresponds to equilibrium in the deformed state, which is necessary if stability is to be included in the theory. The related stresses σ_{ij} are called Piola Kirchhoff stresses and they are illustrated in fig. 1.13. The first index is a reference to the undeformed material surface with normal $\mathbf{i}_i$ and the second index is referred to the deformed material base $\tilde{\mathbf{i}}_j$. It is thus assumed that the strains are so small, that the initial infinitesimal area is an adequate approximation to the deformed infinitesimal area, for example $\varepsilon_{ij} \ll 1$. We assume that the volume forces maintain their original directions (as gravity forces). Decomposing the equilibrium equation (1.88) in the deformed material base and using equation (1.60) result in

$$\begin{aligned} \mathbf{t}_{i,i} + \mathbf{q} &= \mathbf{0} \quad \Downarrow \\ (\sigma_{ik} \tilde{\mathbf{i}}_k)_{,i} + q_j \mathbf{i}_j &= \mathbf{0} \quad \Downarrow \\ (\sigma_{ik}(\delta_{jk} + u_{j,k}))_{,i}\, \mathbf{i}_j + q_j \mathbf{i}_j &= \mathbf{0} \end{aligned} \tag{1.96}$$

These are equilibrium equations for a continuum in the deformed case using Piola Kirchhoff stress components. If the stresses are functions of the displacements then the equilibrium equations are non-linear in the displacements. In component form we get:

Non-linear equilibrium equations *(Small strain and finite rotations)*

$$(\sigma_{ik}(\delta_{jk} + u_{j,k}))_{,i} + q_j = 0 \tag{1.97}$$

The strains should be so small that an original infinitesimal area is an acceptable approximation for the deformed infinitesimal area. The traction stress vector (1.94) takes the following form when the tractions $\mathbf{t}_i$ are resolved in the deformed material base

$$\mathbf{t} = n_i\, \sigma_{ik} \tilde{\mathbf{i}}_k = n_i\, \sigma_{ik} (\delta_{jk} + u_{j,k})\, \mathbf{i}_j \tag{1.98}$$

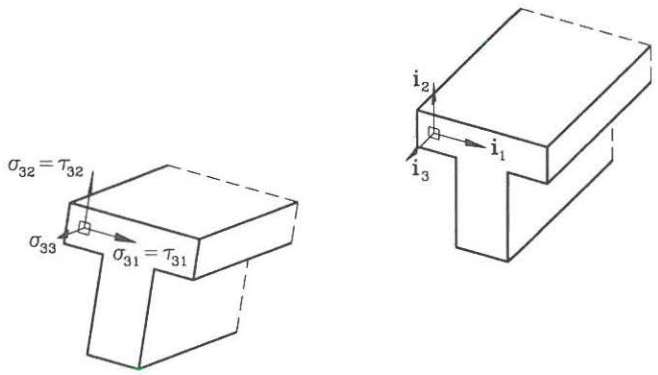

Fig. 1.13: Piola Kirchhoff stress components.

The components of the original surface normal n_i in equation (1.94) remains unchanged since they are the area ratios, which are assumed unchanged for small strains. In component form we just write:

Piola Kirchhoff tractions	*(Small strain and finite rotations)*
$t_j = n_i \sigma_{ik}(\delta_{jk} + u_{j,k})$	(1.99)

The Piola Kirchhoff stress components are illustrated in fig. 1.13 for a beam section. If the strains in the beam are small the cross-section does not deform in its own plane and the deformed material base will be approximately orthonormal. It is thus clear that the Piola Kirchhoff stress components are essentially the usual stress components except for being expressed in the deformed base.

Elasticity

The previous sections have defined strains and stresses in a deforming continuum body. A simple matematical model which enables us to approximate the real material behaviour is a linear model, as Hooke's law for springs ($F = ku$). Our intuition tells us that there must be a functional relationsship between stress σ_{ij} and strain ε_{ij}, which will enable us to find the displacement response of a continuum body when forces are applied to it. The linear relationship is called Hooke's law for linear elastic materials. The linear theory of elasticity is a classic subject described by many. Some classic references are Love [8] and Timoshenko & Goodier [9].

For simplicity we assume that the undeformed continuum is unstressed and without any imperfections, whereby the most general linear constitutive relation becomes

General linear elastic constitutive relation

$$\sigma_{ij} = a_{ijkl}\varepsilon_{kl} \tag{1.100}$$

where a_{ijkl} are the $3^4 = 9^2 = 81$ elasticity constants in the form of a fourth order tensor. However, since both the stress and strain tensors are symmetric with six independent components each then the number is reduced to $6^2 = 36$ elasticity constants for a general material. This implies that also the elasticity tensor a_{ijkl} has symmetry properties. For materials that are orthotropic materials, which have different propperties in the three orthogonal coordinate directions, the number of constants reduces to 9. If the material is isotropic it can be shown that only two constants remain. The isotropic fourth order elasticity tensor can be written as

$$a_{ijkl} = \frac{E}{2(1+\nu)}\left(\delta_{ik}\delta_{jl} + \delta_{il}\delta_{jk} + \frac{2\nu}{1-2\nu}\delta_{ij}\delta_{kl}\right) \tag{1.101}$$

where E is Young's modulus of elasticity and ν is Poisson's ratio. The linear relationship can also be expressed directly as

$$\sigma_{ij} = \lambda\delta_{ij}\varepsilon_{kk} + 2\mu\varepsilon_{ij} \tag{1.102}$$

$$\varepsilon_{ij} = \frac{1+\nu}{E}\sigma_{ij} - \delta_{ij}\frac{\nu}{E}\sigma_{kk} \tag{1.103}$$

where λ and μ are the Lamé constants, defined as

$$\lambda = \frac{E\nu}{(1-2\nu)(1+\nu)} \tag{1.104}$$

$$\mu = G = \frac{E}{2(1+\nu)} \tag{1.105}$$

The Lamé konstant μ is in fact the shear modulus G. The linear relationship is further clarified by introducing the component relationship through a vector format, which is also used in the computational finite element method:

$$\begin{pmatrix} \sigma_{11} \\ \sigma_{22} \\ \sigma_{33} \\ \sigma_{23} \\ \sigma_{13} \\ \sigma_{12} \end{pmatrix} = \frac{E}{(1+\nu)(1-2\nu)} \begin{bmatrix} 1-\nu & \nu & \nu & 0 & 0 & 0 \\ \nu & 1-\nu & \nu & 0 & 0 & 0 \\ \nu & \nu & 1-\nu & 0 & 0 & 0 \\ 0 & 0 & 0 & \frac{1-2\nu}{2} & 0 & 0 \\ 0 & 0 & 0 & 0 & \frac{1-2\nu}{2} & 0 \\ 0 & 0 & 0 & 0 & 0 & \frac{1-2\nu}{2} \end{bmatrix} \begin{pmatrix} \varepsilon_{11} \\ \varepsilon_{22} \\ \varepsilon_{33} \\ 2\varepsilon_{23} \\ 2\varepsilon_{13} \\ 2\varepsilon_{12} \end{pmatrix} \tag{1.106}$$

The shear stress and strain components are thus related directly through the elastic shear modulus G by

$$\begin{aligned} \sigma_{23} &= 2G\varepsilon_{23} = G\gamma_{23} \\ \sigma_{13} &= 2G\varepsilon_{13} = G\gamma_{13} \\ \sigma_{12} &= 2G\varepsilon_{12} = G\gamma_{12} \end{aligned} \tag{1.107}$$

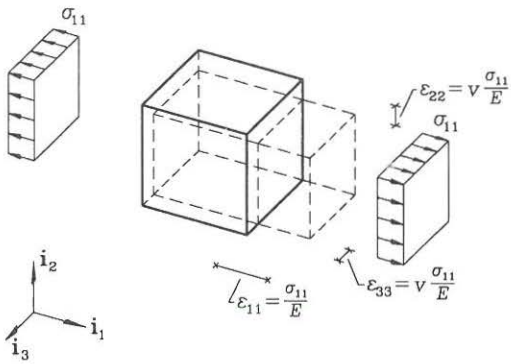

Fig. 1.14: Strains in a uniaxial stress situation.

The constitutive relations can be illustrated by a uniaxial stress situation and a pure shear stress situation. The axial strains ε_{11} and transverse axial strains ε_{22} and ε_{33} for a uniaxial stress situation $\sigma_{11} \neq 0$ are shown in fig. 1.14 and the uniform shear stress-strain situation is shown in fig. 1.15.

The classic beam and plate theories often neglect the transverse contraction associated with Poisson's ratio ν and it is then convenient to consider just the elastic modulus E and the shear modulus G. The simplest theories only use the elastic modulus E.

Virtual Work

The energy principles and the principle of virtual work are the basis of many mechanical derivations. They can be used for theoretical derivations and for analysis of engineering structures. The principles are related to scalar functionals which hold information about mechanical systems of for example force and displacement vectors. The scalar form makes the principles independent of particular coordinate systems. This independence makes the principles suitable for formulation of approximate theories for structural elements, such as beams and plates. The modern approaches to the principle of virtual work and related energy principles can be found in Washizu [4] and Lanczos [13].

The equilibrium equation (1.88) is expressed in terms of vectors. The left-hand side expresses the force "resultant" $\mathbf{F}$ on the infinitesimal cube or rather material points. Let us make an imaginary experiment and assume a virtual (not real) displacement vector field $\delta\mathbf{u}$, where the δ symbolizes the virtual concept, and let the force "resultant" $\mathbf{F}$ work through these displacements. Then by integrating the work over the volume we get the total virtual work $\delta W = \int_V \mathbf{F} \cdot \delta\mathbf{u}\, dV$, which should be zero, $\delta W = 0$, if the cube is in equilibrium. This is in fact the basic principle of virtual work.

Let us assume infinitesimal strains, infinitesimal rotations and work with a linear

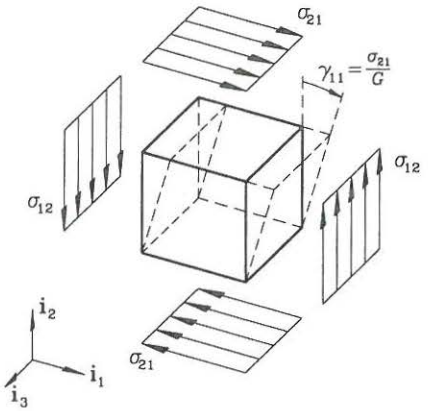

Fig. 1.15: Strains in a pure shear stress situation.

theory. The equilibrium equations (1.90) are multiplied by kinematicly admissible virtual displacements δu_j and integrated over the volume V of the continuum, thus giving

$$\int_V (\sigma_{ij,i} + q_j)\, \delta u_j \, dV = 0 \tag{1.108}$$

Kinematicly admissible virtual displacements δu_j are virtual displacements that satisfy the (kinematic) displacement boundary conditions. If this is not done it is necessary to include the work of the reactions, which are probably unknown at the time of making virtual variations in the displacements. Using the rules for taking partial derivatives of factors

$$(\sigma_{ij}\, \delta u_j)_{,i} = \sigma_{ij,i}\, \delta u_j + \sigma_{ij}\, \delta u_{j,i} \tag{1.109}$$

it is possible to rewrite the equation (1.108) and get

$$\int_V (\sigma_{ij}\, \delta u_j)_{,i}\, dV - \int_V \sigma_{ij}\, \delta u_{j,i}\, dV + \int_V q_j\, \delta u_j\, dV = 0 \tag{1.110}$$

Using the divergence theorem, see equation (1.19), on the first term introduces the components n_i of the vector normal to the surface of the continuum (use $v_i = \sigma_{ij}\delta u_j$ in equation (1.19)). Since the stress tensor σ_{ij} is symmetric we might as well write $\delta u_{j,i}$ as the virtual strain tensor $\delta\varepsilon_{ji} = \frac{1}{2}(\delta u_{j,i} + \delta u_{i,j})$. Introducing this the virtual work equation becomes:

$$\int_{\partial V} n_i\, \sigma_{ij}\, \delta u_j\, dA - \int_V \sigma_{ij}\, \delta\varepsilon_{ji}\, dV + \int_V q_j\, \delta u_j\, dV = 0 \tag{1.111}$$

Rearranging the terms and introducing equation (1.95) $t_j = n_i\sigma_{ij}$ the virtual work equation is revealed as

$$\int_V \sigma_{ij}\, \delta\varepsilon_{ji}\, dV = \int_V q_j\, \delta u_j\, dV + \int_{\partial V} t_j\, \delta u_j\, dA \tag{1.112}$$

On the left-hand side stresses are performing internal work through the virtual strains and on the right-hand side volume loads and boundary tractions are performing external work through the virtual displacements. A virtual work functional δW can thus be defined as the internal work minus the external work $\delta W = \delta W_{int} - \delta W_{ext}$ as follows:

The virtual work functional

$$\delta W = \int_V (\sigma_{ij}\, \delta\varepsilon_{ji} - q_j\, \delta u_j)\, dV - \int_{\partial V} t_j\, \delta u_j\, dA \tag{1.113}$$

The principle of virtual work

$$\delta W = 0 \quad \Leftrightarrow \quad \text{Equilibrium state} \tag{1.114}$$

Kinematicly admissible virtual displacements

Virtual displacements must satisfy kinematic boundary conditions

In an equilibrium state the virtual work must be zero $\delta W = 0$ or we would not have equilibrium. The stability of the equilibrium state is discussed in the section on potential energy.

It can be shown, by use of base vector manipulation, that the virtual work equation for the Piola Kirchhoff stresses and the non-linear Lagrangian strains are written as δW in (1.113). The virtual strains $\delta\varepsilon_{ji}$ are, however, quite complicated in this non-linear case with (small) Lagrangian strains and finite rotations:

$$\delta\varepsilon_{ji} = \frac{1}{2}(\, \delta u_{j,i} + \, \delta u_{i,j} + u_{k,j}\, \delta u_{k,i} + u_{k,i}\, \delta u_{k,j}) \tag{1.115}$$

It is seen that the real and virtual kinematic quantities do not separate.

- **Example 1.6** A sprung mass.

  A mass m is suspended by a spring with the spring stiffness k. An external load P is applied to the mass. The internal spring force is $F = kU$, where U is the end displacement of the spring. A virtual work functional can then be defined for a static situation as the internal virtual work minus the external virtual work:

$$\begin{aligned} \delta W &= \delta W_{int} - \delta W_{ext} \\ &= F\delta U - P\delta U \end{aligned}$$

  The principle of virtual work $\delta W = 0$ leads to

$$\begin{aligned} F\delta U - P\delta U &= 0 \quad \Downarrow \\ F &= P \end{aligned}$$

  which is in fact the force equilibrium equation. If we introduce our knowledge about the internal force $F = kU$ the displacement can be found as

$$U = \frac{P}{k}$$

If the external load is the gravity force $P = mg$, where g is the gravity constant, then we find the elongation of the spring due to the mass as $U = \frac{mg}{k}$. Since the example is very simple, let us emphasize that the main point is that the equilibrium equation, $F = P$, was derived directly from the principle of virtual work.

- **Example 1.7** An elastic rod.

A rod has the cross-sectional area A, its material is linear elastic with the elasticity modulus E and the length L. The coordinate z is used in the axial direction. The rod is fixed at $z = 0$, i.e. $u(z = 0) = 0$ and at the other end it is free with the displacement $u(L) = U$. The free end is loaded by an external load P. The rod could be the spring in the previous example 1.6 and we could just introduce the spring stiffness as $k = \frac{EA}{L}$, but let us instead use internal stresses and strains. The axial stress is σ and the internal axial force is given as $N = A\sigma$. The virtual displacements δu lead to virtual strains $\delta\varepsilon = \delta u'$, where the prime corresponds to differentiation with respect to the axial coordinate, i.e. $(\,)' = \frac{d(\,)}{dz}$. The virtual work functional takes the following form:

$$\begin{aligned}
\delta W &= \delta W_{int} - \delta W_{ext} \\
&= \int_V \sigma\, \delta\varepsilon\, dV - P\delta U \\
&= \int_0^L A\sigma\, \delta\varepsilon\, dz - P\delta U \\
&= \int_0^L N\delta\varepsilon\, dz - P\delta U
\end{aligned}$$

Using the principle of virtual work $\delta W = 0$ and introducing the virtual strains as $\delta\varepsilon = \delta u'$ lead to:

$$\begin{aligned}
\int_0^L N\delta u'\, dz - P\delta U &= 0 \quad \Downarrow \\
[N\delta u]_0^L - \int_0^L N'\delta u\, dz - P\delta U &= 0 \quad \Downarrow \\
-\int_0^L N'\delta u\, dz + (N(L) - P)\delta U &= 0
\end{aligned}$$

in which we have used partial integration. This equation is very informative, since we can use any kinematicly admissible virtual displacements δu. Since the equation must be satisfied for any local internal virtual displacement δu the integral term must also vanish:

$$N' = 0$$

This is the differential equilibrium equation for the axial force in the truss without distributed axial load. The conclusion is that the axial force is constant. Next let us use a local virtual end displacement $\delta U \neq 0$ and internally for $z \in]0, L[$ we have that $\delta u = 0$. The equation is only satisfied if:

$$N(L) = P$$

which is a boundary condition for the differential equilibrium equation. Thus the solution of the differential equilibrium equation is

$$N = P$$

Let us introduce the constitutive relation $N = A\sigma = EA\varepsilon$ and the strain definition $\varepsilon = u'$ into the solution for the axial force. Then let us integrate the equation as follows:

$$\begin{aligned} EAu' &= P \qquad \Downarrow \\ u &= \frac{P}{EA}z \end{aligned}$$

Inserting $z = L$ we find $U = \frac{PL}{EA}$, which corresponds to the spring solution with $k = \frac{EA}{L}$. Note again that the differential equilibrium equation and its boundary condition were derived directly by use of the principle of virtual work.

Complementary Virtual Work

A complementary principle of virtual work can be derived by the same principles as the virtual work. The idea is to use a virtual stress field $\delta\sigma_{ij}$, which satisfies the equilibrium equations (1.90) or (1.97). Typically the homogeneous equations (without virtual volume loads, $\delta q = 0$) are used to find a statically admissible stress field that can be used as the field of variation. The kinematic conditions used are the strain definitions and the kinematic boundary conditions. The linear strain equation is written in the form

$$\varepsilon_{ij} - \frac{1}{2}(u_{i,j} + u_{j,i}) = 0 \tag{1.116}$$

and the boundary conditions as

$$u_j - \bar{u}_j = 0 \tag{1.117}$$

where $\bar{u}_j$ are the prescribed boundary conditions. These equations are multiplied by the virtual stress field $\delta\sigma_{ji}$ and the virtual boundary tractions $\delta t_j = n_i\delta\sigma_{ij}$, respectively. This virtual work density is integrated over the volume and by use of the divergence theorem we can derive the complementary virtual work functional for the linear stress and strain as

The complementary virtual work functional

$$\delta W_c = \int_V (\varepsilon_{ij}\,\delta\sigma_{ji} - u_j\,\delta q_j)\,dV - \int_{\partial V} \bar{u}_j\,\delta t_j\,dA \tag{1.118}$$

The principle of complementary virtual work

$$\delta W_c = 0 \quad \Leftrightarrow \quad \text{Equilibrium state} \tag{1.119}$$

Statically admissible virtual stress field

Virtual stresses and virtual loads must satisfy the equilibrium equations $\delta\sigma_{ij,i} + \delta q_j = 0$

Use of the Lagrangian strain definition and the Piola Kirchhoff stress definition also leads to the same complementary virtual work functional. (For other non-linear strain measures the strain and stress must be complementary measures so that in combination they give exactly this virtual work and complementary virtual work)

Potential Energy

Irrespective of the constitutive relations of the material the virtual work equation (1.113) holds, and the forces need not be conservative. However, assuming that the material is elastic and that the forces are conservative, a potential energy exists. This energy can be integrated from the virtual work δW in (1.113).

With an elastic constitutive relation we assume that a strain energy density $A(\varepsilon_{ij})$ exists and that an infinitesimal change in strain $d\varepsilon_{ij}$ leading to a change in the internal energy density is given by

$$\sigma_{ij}\, d\varepsilon_{ji} = \frac{\partial A}{\partial \varepsilon_{ij}}\, d\varepsilon_{ji} \tag{1.120}$$

The left-hand side is the change in internal energy density found using the work of the stresses σ_{ij} through the strain increment $d\varepsilon_{ij}$, and the right-hand side is the change in internal energy density found using the assumed strain energy density. The relation defines the stress in terms of the partial derivative of the internal energy density

$$\sigma_{ij} = \frac{\partial A}{\partial \varepsilon_{ij}} \tag{1.121}$$

For a linear elastic material the constitutive equation $\sigma_{ij} = a_{ijkl}\varepsilon_{kl}$ can be introduced into (1.121) and the equation integrated. This gives the the strain energy density for a linear elastic material as

$$A = \frac{1}{2}\varepsilon_{ij} a_{ijkl} \varepsilon_{kl} \tag{1.122}$$

The resemblance with the linear elastic spring with a potential energy $\frac{1}{2}ku^2 = \frac{1}{2}uku$ is pleasant. The extensional potential energy per length of a truss $\frac{1}{2}EA\varepsilon^2$ is quite similar.

With conservative volume loads and traction forces and with a strain energy density for linear elastic materials the potential energy is given by

Potential energy

$$V = \int_V (\frac{1}{2}\varepsilon_{ij}\, a_{ijkl}\, \varepsilon_{kl} - q_j u_j)\, dV - \int_{\partial V} t_j u_j\, dA \tag{1.123}$$

In an equilibrium position the potential energy will be at a minimum. Let us analyse the variation of the potential energy if we make a virtual variation in the displacements δu_i when the current displacements are u_i. Taylor expansion about

the current displacement position gives

$$\begin{aligned} \Delta V &= \frac{\partial V}{\partial u_i}\,\delta u_i + \frac{1}{2}\frac{\partial^2 V}{\partial u_i\,\partial u_j}\,\delta u_i\,\delta u_j + \dots \\ &= \delta V + \delta^2 V + \dots \end{aligned} \tag{1.124}$$

where $\delta V = \frac{\partial V}{\partial u_i}\,\delta u_i$ is the first variation and $\delta^2 V = \frac{1}{2}\frac{\partial^2 V}{\partial u_i\,\partial u_j}\,\delta u_i\,\delta u_j$ is the second variation of the potential energy. Note that the virtual strains are determined by the virtual displacements as $\delta\varepsilon_{ij} = \frac{1}{2}\left(\delta u_{i,j} + \delta u_{j,i}\right) = \frac{1}{2}\left((\delta u_i)_{,j} + (\delta u_j)_{,i}\right)$ and that $\frac{\partial V}{\partial u_i}\delta u_i$ therefore also implies $\frac{\partial V}{\partial \varepsilon_{ij}}\delta\varepsilon_{ij}$. It should also be noted that the first variation of the potential energy is equal to the virtual work functional:

$$\delta V = \delta W \tag{1.125}$$

For minimum of the potential energy the first variation must vanish $\delta V = \delta W = 0$. This is only a necessary condition for a minimum, but if the second variation is positive, i.e. $\delta^2 V > 0$, it is sufficient. For linear elastic materials and linear strains $\varepsilon_{ij} \ll 1$ the second variation is always positive since

$$\begin{aligned} \delta^2 V &= \frac{1}{2}\int_V \frac{\partial^2 A}{\partial\varepsilon_{ij}\,\partial\varepsilon_{kl}}\,\delta\varepsilon_{ij}\,\delta\varepsilon_{kl}\,dV \\ &= \frac{1}{2}\int_V a_{ijkl}\,\delta\varepsilon_{ij}\,\delta\varepsilon_{kl}\,dV \\ &> 0 \end{aligned} \tag{1.126}$$

in which a_{ijkl} is positive definite. The second variation does not necessarily remain positive for non-linear variations in the displacements leading to instability situations. The section on initial stress is concerned with approximate stability analysis.

If the first variation of the potential energy is zero $\delta V = 0$, then the potential energy is stationary and the structure is in equilibrium. However, this equilibrium position must be stable. Stability is ensured if the second variation is positive $\delta^2 V > 0$.

- **Example 1.8** A loaded spring.

  In the previous sprung mass example 1.6 we used the virtual work functional and the principle of virtual work to derive the equilibrium equations, but in this example we show that it is possible to start by using the potential energy. The internal elastic spring energy is $V_{int} = \frac{1}{2}kU^2$, where the spring stiffness is determined by $F = kU$. The potential of the external load is $V_{ext} = PU$, which is well-known for the gravity field where $P = mg$ and thus $V_{ext} = mgU$. The total potential energy is thus given as

$$\begin{aligned} V &= V_{int} - V_{ext} \\ &= \frac{1}{2}kU^2 - PU \end{aligned}$$

Let us make a small virtual displacement variation and find the first variation of the potential energy δV as follows:

$$\begin{aligned} \delta V &= \frac{\partial V}{\partial U}\delta U \\ &= kU\,\delta U - P\,\delta U \end{aligned}$$

A necessary condition for a minimum of the potential energy is that the first variation vanishes $\delta V = 0$, which gives us the equilibrium equation:

$$\begin{aligned} kU &= P \quad \Downarrow \\ F &= P \end{aligned}$$

The first variation of the potential energy is equal to the virtual work functional from example 1.6, if we insert $kU = F$ into δV. Thus, for this linear elastic spring we can make exactly the same derivations using the virtual work functional or the potential energy. The second variation of the potential energy is

$$\delta^2 V = \frac{\partial^2 V}{\partial U^2}(\delta U)^2 = k(\delta U)^2 > 0$$

since the spring stiffness is positive $k > 0$.

- **Example 1.9** An elastic rod.

Let us continue example 1.7. The potential energy of the rod is given by:

$$\begin{aligned} V &= \int_V \frac{1}{2}\varepsilon E\varepsilon \, dV - PU \\ &= \int_0^L \frac{1}{2} EA\varepsilon^2 \, dz - PU \end{aligned}$$

The first variation of the potential energy is:

$$\delta V = \int_0^L EA\varepsilon\,\delta\varepsilon \, dz - P\delta U$$

by inserting the constitutive relation $EA\varepsilon = A\sigma = N$ it is clear that the first variation of the potential energy is equal to the virtual work functional $\delta V = \delta W$ and the same derivations can be made as in the previous example 1.7. The second variation of the potential energy is

$$\delta^2 V = \frac{\partial^2 V}{\partial u^2} = \int_0^L EA(\delta\varepsilon)^2 \, dz > 0$$

since the product of the modulus of elasticity and the area is positive $EA > 0$.

Complementary Potential Energy

As we could define a complementary virtual work equation we can also define a complementary potential energy. The arguments follow the same route as for the potential energy derivation. If we assume linear elasticity the constitutive relation (1.100) can be inverted to yield an alternative linear elastic constitutive equation

$$\varepsilon_{ij} = b_{ijlk}\sigma_{kl} \tag{1.127}$$

A stress energy density can then be derived

$$B = \frac{1}{2}\sigma_{ij}b_{ijlk}\sigma_{kl} \tag{1.128}$$

The complementary energy can then be defined as

Complementary potential energy

$$V_c = \int_V (\frac{1}{2}\sigma_{ij}\, b_{ijkl}\, \sigma_{kl} - q_j u_j)\; dV - \int_{\partial V} t_j u_j\, dA \tag{1.129}$$

Stationarity of the complementary energy $\delta V_c = 0$ implies that the structure is in an equilibrium state. The first variation δV_c in the complementary potential energy is equivalent to the complementary virtual work functional, $\delta V_c = \delta W_c$. These complementary work and energy functionals can be used to analyse statically indeterminate beam structures. It can further be seen that the potential energy and the complementary potential energy are closely related since $A = \varepsilon_{ij}a_{ijkl}\varepsilon_{kl} = \sigma_{ij}\varepsilon_{ji} = \sigma_{ij}b_{ijkl}\sigma_{kl} = B$. This relation will not be discussed further.

Initial Stress and Stability

As we have just seen, the second variation of the potential energy is always positive for infinitesimal strains and rotations. This implies that the equilibrium found by use of the virtual work equation $\delta W = 0$ is always a stable equilibrium position. However, through the use of initial stress (without initial strains and displacements) it is possible to consider the stability of structures within a linear framework. The initial stress method is often called the Euler method of linearized stability analysis, see Washizu [4]. The stability problems which can be treated by this method are socalled buckling problems, where the structure suddenly loses its stability and its mode of deformation is altered completely. Typical problems are flexural stability of columns, lateral stability of beams and stability of plates in compression.

The basic idea of linearized stability analysis is first to solve an initial problem, for example the compression of a column, and find the stress distribution. Then use this stress as an initial (strain and displacement free) stress distribution σ^0_{ij} to solve an eigenvalue problem, where the eigenvalue is a scaling factor determining the critical buckling load (or stability load). The linearized stability analysis thus has two basic steps. First the initial stress field has to be found and then an eigenvalue problem has to be solved. This will be considered further in later chapters.

In this section a linear equilibrium equation including initial stress σ^0_{ij} will be derived and the additional contributions to the virtual work functional and potential energy will be given. This will enable the solution of the secondary problem.

The initial stress field σ^0_{ij} has to satisfy the equilibrium equations (1.90). For our study we assume that the linear equilibrium equations will be adequate

$$\sigma^0_{ij,i} + q^0_j = 0 \tag{1.130}$$

The continuum with the initial stress field σ^0_{ij} and load q^0_j now deforms under the action of conservative loads q_j. At a material point the total stress σ^t_{ij} and total load q^t_j are

$$\begin{aligned} \sigma^t_{ij} &= \sigma^0_{ij} + \sigma_{ij} \\ q^t_j &= q^0_j + q_j \end{aligned} \tag{1.131}$$

To include the influence of initial stress we need to define equilibrium in the deformed position. The equilibrium equation for the deformed position (1.97) gives

$$\begin{aligned} \left(\sigma^t_{ik}(\delta_{jk} + u_{j,k})\right)_{,i} + q^t_j &= 0 \quad \Downarrow \\ \sigma^t_{ik,i}(\delta_{jk} + u_{j,k}) + \sigma^t_{ik} u_{j,ki} + q^t_j &= 0 \quad \Downarrow \\ \sigma^t_{ij,i} + \sigma^t_{ik,i} u_{j,k} + \sigma^t_{ik} u_{j,ki} + q^t_j &= 0 \end{aligned} \tag{1.132}$$

Introducing the total stress and load from equation (1.131) and linearizing (the initial stresses are constants), the equilibrium equation takes the form

$$\sigma^0_{ij,i} + \sigma_{ij,i} + \sigma^0_{ik,i} u_{j,k} + \sigma^0_{ik} u_{j,ki} + q^0_j + q_j = 0 \tag{1.133}$$

Combining the two initial stress terms into one and using the initial stress equilibrium (1.130) yield the final equilibrium equation for a linearized initial stress problem:

Linear equilibrium with initial stress

$$\sigma_{ij,i} + (\sigma^0_{ik} u_{j,k})_{,i} + q_j = 0 \tag{1.134}$$

This is the basic equilibrium equation, which can be used for linearized stability analysis. It is worth writing it in an alternative manner which makes comparison with the beam theory more direct

$$\frac{\partial \sigma_{ij}}{\partial x_i} + \frac{\partial}{\partial x_i}\left(\sigma^0_{ik} \frac{\partial u_j}{\partial x_k}\right) + q_j = 0 \tag{1.135}$$

The tractions in an initial stress problem are found in the same manner: We introduce the total stress components σ^t_{ij} from equation (1.131) and use that the initial tractions $t^0_j = n_i \sigma^0_{ij}$ satisfy the boundary conditions and finally we linearize the equation. The boundary tractions including initial stress are

Tractions with initial stress in linear theory

$$t_j = n_i \left(\sigma_{ij} + \sigma^0_{ik} u_{j,k}\right) \tag{1.136}$$

Let us turn to the virtual work formulation of this problem. We will just outline how to find the virtual work. The linearized equations (1.134) are multiplied by virtual displacemnts δu_j, integrated over the volume and then the equation is transformed by use of the divergence theorem. This gives the virtual work including the effect of initial stress. The modified virtual work functional is:

Virtual work functional including initial stress

$$\delta W = \int_V \left(\sigma_{ij}\, \delta\varepsilon_{ji} + \sigma^0_{ij} u_{k,j}\, \delta u_{k,i} - q_j\, \delta u_j\right) dV - \int_{\partial V} t_j\, \delta u_j\, dA \tag{1.137}$$

A related potential energy is found by "integration"

Potential energy including initial stress

$$V = \int_V \left(\frac{1}{2}\varepsilon_{ij}\, a_{ijkl}\, \varepsilon_{kl} + \frac{1}{2} u_{k,i} \sigma^0_{ij} u_{k,j} - q_j u_j\right) dV - \int_{\partial V} t_j u_j\, dA \tag{1.138}$$

It is worth noting the similarity of the linear elastic contribution and the initial stress contribution. The first term in the potential energy $\frac{1}{2}\varepsilon_{ij}\, a_{ijkl}\, \varepsilon_{kl}$ holds the elastic energy of the structure and the second term $\frac{1}{2} u_{k,i} \sigma^0_{ij} u_{k,j}$ holds the geometric energy of the initial stresses. It is clear that the potential energy is reduced for compression $\sigma^0_{ij} < 0$ thus reducing the stiffness of the structure. For large compression stresses the geometric energy can thus lead to instability. This concludes the treatment of initial stress in this section.

Initial Strain

Strains are not only produced by stresses, but also by material shrinkage or expansion, which can be caused for example by temperature variations, moisture variations, plastic strain and other mechanical or chemical processes. The present section only considers the influence of isotropic expansion and we will present the equations for isotropic thermal expansion.

In the case of a temperature change ΔT, where the material is completely free to expand the thermal strains are:

Isotropic thermal expansion strain

$$\varepsilon^T_{kl} = \beta \Delta T \delta_{kl} \tag{1.139}$$

where the coefficient of thermal expansion β has been introduced. The Kronecker delta gives the isotropic expansion. Since the geometric strain measure $\varepsilon_{kl} = \frac{1}{2}(u_{k,l} + u_{l,k})$ is the total strain, the thermal expansion with initially positive strains will reduce the total strain. This gives the following modified linear elastic

constitutive relation

Modified linear elastic constitutive relation

$$\sigma_{ij} = c_{ijkl}(\varepsilon_{kl} - \varepsilon^T_{kl}) \tag{1.140}$$

Thermal problems can be converted into initial stress problems.

Imperfections

Most structures are imperfect and sometimes it is necessary to analyse if the imperfections are such that they should be taken into account. The disagreement between theoretical and experimental buckling loads, is mainly caused by small deviations from the assumed initial shape of the structure. The imperfection in the present analysis is introduced as a stress free imperfection (or initial) displacement field $\hat{u}_j$. The total displacements u^t_j can thus be defined as

$$u^t_j = u_j + \hat{u}_j \tag{1.141}$$

We substitute the displacements u_j in the non-linear equilibrium equations (1.97) for the total displacements u^t_j and then linearize the equations. This linearized equilibrium equation including an imperfection displacement field is given as

$$(\sigma_{ik}(\delta_{jk} + \hat{u}_{j,k}))_{,i} + q_j = 0 \tag{1.142}$$

which looks the same as the non-linear equation, but it is quite different since we know the imperfections. The tractions are found in the same manner

$$t_j = n_i\, \sigma_{ik}(\delta_{jk} + \hat{u}_{j,k}) \tag{1.143}$$

It is seen that the imperfections enter the equations as a correction factor, which is a function of the position of the material point.

The major interest in imperfections is within stability analysis. Imperfections reduce the buckling capacity of columns, beam columns and plates. As mentioned, linearized stability analysis is often performed by an initial stress method. In the following both initial stress and imperfections will be included. It is assumed that the initial stress satisfies the linear equilibrium equations with imperfections (1.142). The total stress, the total loads (1.131) and total displacements (1.141) are substituted for the equivalent parameters in the non-linear equilibrium equation (1.97). This equation is modified by the fact that the initial stress field is in equilibrium with the initial loads in the imperfect state. Furthermore, we linearize the equation to

Linear equilibrium with initial stress and imperfections

$$(\sigma_{ij} + \sigma_{ik}\hat{u}_{j,k} + \sigma^0_{ik}u_{j,k})_{,i} + q_j = 0 \tag{1.144}$$

The tractions can also be found by the same procedure

Tractions with initial stress and imperfections for linear theory

$$t_j = n_i \left(\sigma_{ij} + \sigma_{ik}\hat{u}_{j,k} + \sigma^0_{ik}u_{j,k}\right) \tag{1.145}$$

The virtual work equation can also be derived in this case.

Virtual work functional including initial stress and imperfections

$$\delta W = \int_V (\sigma_{ij}\,\delta\varepsilon_{ji} + \sigma_{ij}\hat{u}_{k,j}\,\delta u_{k,i} + \sigma^0_{ij}u_{k,j}\,\delta u_{k,i} - q_j\,\delta u_j)\,dV - \int_{\partial V} t_j\,\delta u_j\,dA \tag{1.146}$$

A related potential energy is found by integration

Potential energy including initial stress and imperfections

$$V = \int_V (\frac{1}{2}\varepsilon_{ij}a_{ijkl}\varepsilon_{kl} + \frac{1}{2}\hat{u}_{k,i}\sigma_{ij}u_{k,j} + \frac{1}{2}u_{k,i}\sigma^0_{ij}u_{k,j} - q_j u_j)\,dV - \int_{\partial V} t_j u_j\,dA \tag{1.147}$$

Notice again that initial imperfections destabilize the structure in compression, if the imperfection displacement mode is of the same form as the buckling mode.

- **Problem 1.6**
  Expand the Lagrangian strain tensor for plane strain, which is given by

$$\varepsilon_{\alpha\beta} = \frac{1}{2}(u_{\alpha,\beta} + u_{\beta,\alpha} + u_{\gamma,\alpha}u_{\gamma,\beta})$$

- **Problem 1.7**
  What are the equilibrium equations for plane stress situations with infinitesimal strains and rotations. Plane stress $\sigma_{\alpha\beta}$ is a situation where the three stresses σ_{3j} corresponding to the third coordinate direction are zero $\sigma_{3j} = 0$. Try drawing an infinitesimal rectangle, add the in-plane stress components and a load term q_β and find the three equilibrium equations.

- **Problem 1.8**
  State six independent stress components.

- **Problem 1.9**
  How many independent stress components are found in plane stress?

- **Problem 1.10**
  Why do infinitesimal strains $\varepsilon_{ij} \ll 1$ not automaticly imply infinitesimal rotations?

- **Problem 1.11**
  In beam theory with the beam axis along the third axis $\mathbf{i}_3$ we simplify the continuum description by assuming that the transverse stress components $\sigma_{\alpha\beta} = 0$ are zero and introduce a simplified stress notation by setting $\sigma = \sigma_{33}$ and $\tau_\alpha = \sigma_{3\alpha}$. A similar notation is introduced for the strains $\varepsilon = \varepsilon_{33}$ and $\gamma_\alpha = \gamma_{3\alpha} = 2\varepsilon_{3\alpha}$. Propose a linear elastic constitutive relation for the beam stresses and strains, using the inverse stress strain relationship for general isotropic linear elastic materials.

Chapter 2

Flexural Beam Theories

A beam is a continuum with one primary dimension, the length, which is considerably larger than the other two cross-sectional dimensions. Beams are used as structural elements mainly to carry transverse loads and, when doing this, they deform in a socalled flexural mode. In this chapter the two classical flexural beam theories are derived in a consistent way using the principle of virtual work. Simple kinematic modes of deformation, socalled shape functions, are introduced as approximations to the kinematics of the three-dimensional continuum. The theories are developed by inserting the assumed shape functions into the linear strain definitions, then the linear elastic constitutive law is evaluated and finally the principle of virtual work is used to close the formulation by delivering the equilibrium equations. This approach has been chosen since it clarifies the definition of the elastic centre and the decoupling of differential equilibrium equations. The approach is also the basic approach used in the development of modern computational approximation methods such as the finite element method.

The theories of beams have roots back to the investigations of strength of materials by Galileo in 1638 and the investigations of springs and one-dimensional elastic bodies by Hooke in 1678. The assumption of plane sections remaining plane and perpendicular to the deflection curve was made by Bernoulli in 1694. In spite of an erroneous assumption regarding the neutral axis (elastic centre) made by Bernoulli it was possible for Euler in 1744 to formulate a one-dimensional beam theory and to find the well-known Euler formula for column buckling, which will be treated in the next chapter. Later in 1826 Navier formulated the beam theory including moments of inertia as we know today. Later in our century (1921) Timoshenko included shear deformation in a modified Euler-Bernoulli theory. The history of strength of materials and the people behind has been described by Timoshenko [10].

Cartesian Reference

To use the power of index notation we assume that the beam axis is parallel to the third base direction $\mathbf{i}_3$, see fig. 2.1, and for convenience the material coordinate along the beam axis is introduced as $z = x_3$. The material points within a cross-

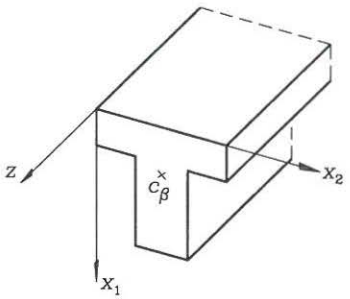

Fig. 2.1: Cartesian reference and the point of intersection c_α.

section of the beam are thus described by the two first coordinates x_α. The exact position of a material point is referenced by the components (x_α, z). The Cartesian reference frame is introduced in the cross-section of the beam with a given starting position along the beam axis $z = 0$. The derivatives in the axial directions will some places be written explicitly as $\frac{\partial()}{\partial z}$, $\frac{d()}{dz}$ or just denoted by an upper prime index as $()'$ for the sake of clarity.

2.1 Formulation of Flexural Beam Theories

Even though Euler-Bernoulli theory was developed first it is thought that the natural way to present the theories with the approach used is in the opposite order. However, all assumptions made also pertain to the Euler-Bernoulli beam theory, which just includes one extra assumption implying that the shear effects can be neglected. Therefore, the common assumptions, definitions and formulations are presented in this section in a common format including shears. Then the details are treated in specific sections on Timoshenko theory and Euler-Bernoulli theory.

The Timoshenko beam theory includes the effects of shear deformations, which are important for "short" beams, for example as a rule of thumb for beams of isotropic material with cross-sectional depth d to length L ratios of $\frac{d}{L} > \frac{1}{15}$. The shear effects were included by Timoshenko in 1921 by relaxing the assumptions made by Euler and Bernoulli. Euler-Bernoulli theory is well suited for "long" beams, for example as a rule of thumb for beams of isotropic material with cross-sectional depth d to length L ratios of $\frac{d}{L} < \frac{1}{15}$. However, shear effects can also be important in long beams with large transverse loads near the supports. Beam theories also only pertain to structural elements with a depth to length ratio of about $\frac{d}{L} < \frac{1}{4}$. The shorter the beam the poorer the beam assumptions made in the following. In one of the problems following the first section an explicit expression is found, which makes it possible to derive the above limit of about $\frac{1}{15}$. The typical beam depth to length ratios $\frac{d}{L}$ vary from $\frac{1}{10}$ to $\frac{1}{40}$ depending on cross-sectional type and material.

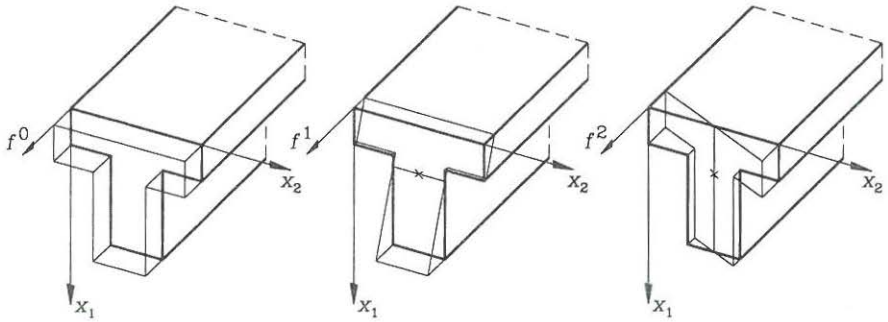

Fig. 2.2: The shape functions of simple beam theories $(1,\ x_1 - c_1,\ x_2 - c_2)$.

Beam Kinematics

The theories of beams are derived on the basis of assumed displacement fields $u_i(x_\beta, z)$. The main idea is to separate the axial displacements from the in-plane cross-sectional displacements $u_i = f(x_\beta)g_i(z)$. This is like separation of variables used in solution of differential equations. The displacements are not only separated in functions of x_β and functions of z, they are also expanded in a sum of separated products.

$$u_i(x_\beta, z) = \sum_k f^k(x_\beta) g_i^k(z) \tag{2.1}$$

For beam theories the fewest possible number of terms is included. Some simple shape functions are shown in fig. 2.2 and include the linear functions $f^0(x_\beta) = 1$, $f^1(x_\beta) = x_1 - c_1$ and $f^2(x_\beta) = x_2 - c_2$, where c_β has been introduced as the point of intersection for the two inclined shape functions f^1 and f^2, so we do not make the same mistake as Bernoulli and Euler. (It will later be shown that an intelligent choice of the intersection point c_β is the elastic centre). Since the geometric assumptions made are important let us introduce one assumption at a time. Concerning the geometric form of the cross-section the following assumption is made.

Assumption 1:

Cross-sections do not distort within their own plane

This means that the form of the cross-section is not altered by the deformation and we thereby conclude that only the shape function $f^0 = 1$ is needed to describe the transverse displacements of the cross-sections, as shown in fig. 2.3. Concerning the axial displacements the following assumption is made

Assumption 2:

Cross-sections remain plane during deformation

This limits the shape functions in the axial direction to the linear ones already

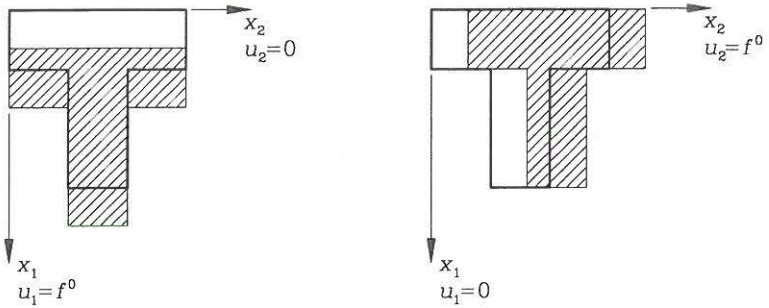

Fig. 2.3: Transverse displacements using the shape function $f^o = 1$.

introduced and with the displacement modes directly shown in fig. 2.2. The kinematic approximations made so far determine the displacement field of the beam as:

$$u_1(x_\beta, z) = f^0(x_\beta)w_1(z) = w_1(z) \tag{2.2}$$
$$u_2(x_\beta, z) = f^0(x_\beta)w_2(z) = w_2(z) \tag{2.3}$$

$$\begin{aligned} u_3(x_\beta, z) &= f^0(x_\beta)v(z) + f^1(x_\beta)\alpha_1(z) + f^2(x_\beta)\alpha_2(z) \\ &= v(z) + (x_1 - c_1)\alpha_1(z) + (x_2 - c_2)\alpha_2(z) \end{aligned} \tag{2.4}$$

Where $w_\beta(z)$ are the transverse displacements (of all points in the cross-section), $v(z)$ is the axial displacement of the intersection point c_β, and $\alpha_\beta(z)$ are the inclinations along the cross-sectional axes with c_β as the intersection point. The displacements can be written in the compact form as

Assumed displacements

$$u_\beta = w_\beta \tag{2.5}$$
$$u_3 = v + (x_\beta - c_\beta)\alpha_\beta \tag{2.6}$$

where the five unknown kinematic functions are

$$v(z)\,, \quad w_\beta(z)\,, \quad \alpha_\beta(z)$$

These displacements are illustrated in fig. 2.4 in a common coordinate view for x_β, where we can just substitute $\beta = 1$ or $\beta = 2$.

Using the linear strain definition (1.65) we find the following non-vanishing strain components

$$\begin{aligned} \varepsilon = \varepsilon_{33} &= \frac{\partial u_3}{\partial z} \\ &= \frac{dv}{dz} + (x_\beta - c_\beta)\frac{d\alpha_\beta}{dz} \end{aligned}$$

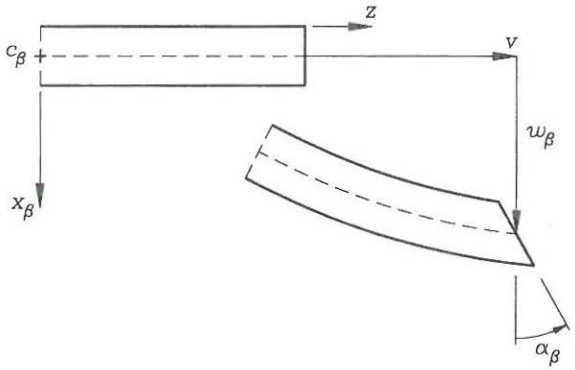

Fig. 2.4: The kinematic displacement functions.

$$\begin{aligned} &= v' + (x_\beta - c_\beta)\alpha'_\beta \\ &= \bar{\varepsilon} + (x_\beta - c_\beta)\kappa_\beta \end{aligned} \tag{2.7}$$

$$\begin{aligned} \gamma_\beta \;=\; \gamma_{3\beta} \;&=\; \frac{\partial u_3}{\partial x_\beta} + \frac{\partial u_\beta}{\partial z} \\ &= \alpha_\beta + \frac{dw_\beta}{dz} \\ &= \alpha_\beta + w'_\beta \end{aligned} \tag{2.8}$$

where the axial strain $\bar{\varepsilon} = v'$ at c_β, the curvatures $\kappa_\beta = \alpha'_\beta$ and the engineering shear strain γ_β have been introduced including the adopted notation for the axial strain $\varepsilon = \varepsilon_{33}$ and the shear strain $\gamma_\beta = \gamma_{3\beta} = \alpha_\beta + w'_\beta$ at any point. (In Euler-Bernoulli theory it is assumed that the shear strains can be neglected $\gamma_\beta = \alpha_\beta + w'_\beta = 0$, which implies that the intensity of the cross-section inclination is determined by $\alpha_\beta = -w'_\beta$. The assumption is described in detail in the Euler-Bernoulli section).

The axial strain is

$$\varepsilon = \bar{\varepsilon} + (x_\beta - c_\beta)\kappa_\beta \tag{2.9}$$

in which the axial strain $\bar{\varepsilon}$ at c_β and the curvatures κ_β are defined as

$$\bar{\varepsilon} = v' = \frac{dv}{dz} \qquad\qquad \kappa_\beta = \alpha'_\beta = \frac{d\alpha_\beta}{dz} \tag{2.10}$$

The engineering shear strains in Timoshenko theory are

$$\gamma_\beta = \alpha_\beta + w'_\beta = \alpha_\beta + \frac{dw_\beta}{dz} \tag{2.11}$$

(*In Euler-Bernoulli theory $\gamma_\beta = 0$, whereby $\kappa_\beta = \alpha'_\beta = -w''_\beta = -\frac{d^2 u_\beta}{dz^2}$* .)

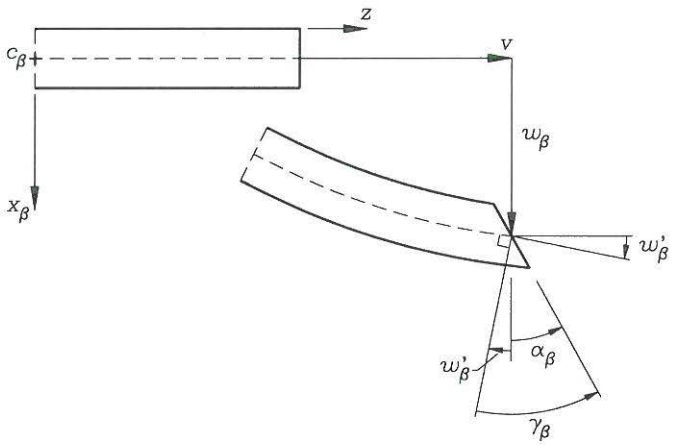

Fig. 2.5: The shear strain γ_ν in Timosheko beams.

The shear strain deformation is visualized in fig. 2.5. This concludes the subsection on the beam kinematics, which will be sufficient for Timoshenko theory. For Euler-Bernoulli theory the assumption leading to the neglection of shear strains is to be formulated in a later section on Euler-Bernoulli theory.

The Constitutive Relations

The kinematic assumptions lead to transverse strain components $\varepsilon_{\alpha\beta}$, which are all zero. This is actually not the case in a real beam, since the material will expand or contract due to the Poisson effect. To derive an intelligent constitutive relation for the beam strains we need a third assumption. In beams the transverse loads will produce small stresses σ_{11} or σ_{22}. However, experience shows that these stresses are very small compared to the axial stress due to beam moments as shown in fig. 2.6. This can be used to derive the constitutive relation from the three-dimensional linear elastic constitutive relation.

Assumption 3:

The transverse stress components are negligible

$$\sigma_{11} = \sigma_{22} = 0 \tag{2.12}$$

Using the inverse constitutive equation (1.103) it is possible, see problem 1.11, to derive the following constitutive relations

$$\sigma_{33} = E\varepsilon_{33} \tag{2.13}$$

$$\tau_{3\alpha} = G\gamma_{3\alpha} \tag{2.14}$$

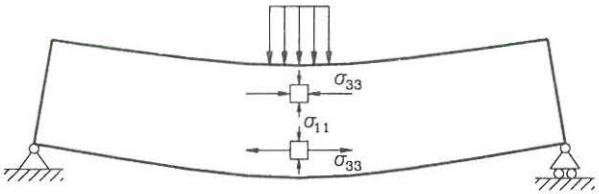

Fig. 2.6: Negligible transverse stress σ_{11}.

In terms of beam strains defined in (2.9) and (2.11) the constitutive relations are introduced. We further introduce the notation $\sigma(x_\beta, z)$ for the axial stress and $\tau_\beta(x_\alpha, z)$ for the shear stress

Axial beam stress

$$\begin{aligned} \sigma &= E\varepsilon \\ &= E\ (\bar{\varepsilon} + (x_\beta - c_\beta)\kappa_\beta) \end{aligned} \tag{2.15}$$

Transverse beam shear stress in Timoshenko theory

$$\tau_\beta = G\,\gamma_\beta \tag{2.16}$$

Sometimes it is also convenient to use the axial beam stress (2.15) in a vector format as follows:

$$\sigma \;=\; E[\,f^0,\, f^1,\, f^2] \begin{bmatrix} \varepsilon \\ \kappa_1 \\ \kappa_2 \end{bmatrix} \;=\; E[\,1,\, x_1 - c_1,\, x_2 - c_2] \begin{bmatrix} \varepsilon \\ \kappa_1 \\ \kappa_2 \end{bmatrix} \tag{2.17}$$

In the given constitutive relations we did not use that the kinematic assumptions result in zero transverse strains $\varepsilon_{11} = \varepsilon_{22} = 0$, instead we have used the third assumption of zero transverse stress $\sigma_{11} = \sigma_{22} = 0$. Due to this the section is not constitutively constrained. If we had constrained the section not only in the kinematics but also in the constitutive equations extra stresses would be induced, since we constrain the Poisson effect, and the theory would be very inaccurate. It is worth noting that the three-dimensional linear elastic constitutive relation has been developed later in time than the beam theory and therefore incoorporates the elasticity modulus E and the shear modulus G in such a convenient way for beam theories. It must be mentioned that the shear determined by the beam theory is constant over the section. This is not correct and is only an approximation. When performing displacement analysis on specific sections a correction factor is often introduced into the shear term. (The factor can be found by use of Grashof's static method for determining shear stress as described later).

Let us integrate the stresses σ and τ_β, shown in fig. 2.7, over the cross-sectional area and define the generalized internal forces (as the resultants of the cross-sectional stress components, sometimes referred to as the stress resultants). We

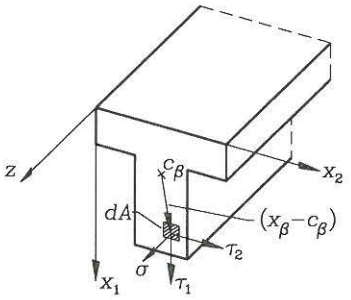

Fig. 2.7: Cross-sectional stress components.

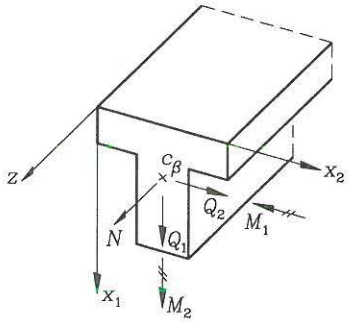

Fig. 2.8: The internal forces in a beam.

define the internal bending moments M_β as the moments of the stress distribution about the intersection point c_α, the internal axial force (or just the axial force) N as the resultant of the stress distribution acting at the point c_α (in the direction of the normal) and the internal shear force Q_β as the resultant of the shear stresses as shown in fig. 2.8. Let us make the unnessesary, but a little simplifying, assumption that the material parameters E and G are constant throughout the beam, then we get

Axial force *Constant E and G*

$$\begin{aligned} N &= \int_A \sigma \, dA = \int_A E\,(\bar{\varepsilon} + (x_\beta - c_\beta)\kappa_\beta)\, dA \\ &= E\,A\,\bar{\varepsilon} + E\,S_\beta\,\kappa_\beta \end{aligned} \tag{2.18}$$

Bending moments

$$\begin{aligned} M_\beta &= \int_A (x_\beta - c_\beta)\sigma \, dA = \int_A (x_\beta - c_\beta) E\,(\bar{\varepsilon} + (x_\beta - c_\beta)\kappa_\beta)\, dA \\ &= E\,S_\beta\,\bar{\varepsilon} + E\,I_{\alpha\beta}\kappa_\alpha \end{aligned} \tag{2.19}$$

Shear forces in Timoshenko theory

$$\begin{aligned} Q_\beta &= \int_A \tau_\beta \, dA = \int_A G\gamma_\beta \, dA \\ &= G\,A\,\gamma_\beta \qquad\qquad (\,=\psi_{\alpha\beta}GA\gamma_\beta) \end{aligned} \tag{2.20}$$

where the cross-sectional area, first moments and second moments of area are

$$A = \int_A 1 \, dA \tag{2.21}$$

$$S_\beta = \int_A (x_\beta - c_\beta)\, dA \tag{2.22}$$

$$I_{\alpha\beta} = \int_A (x_\alpha - c_\alpha)(x_\beta - c_\beta)\, dA \tag{2.23}$$

Be aware of the definition of the second moments of area also called moments of inertia. The definition varies with the naming convention for the reference coordinates. The notation used here is in agreement with the index notation. The transition equations for the first and second order geometric moments are easily derived as:

$$S_\beta = \int_A (x_\beta - c_\beta)\, dA = \int_A x_\beta \, dA - c_\beta A$$

$$I_{\alpha\beta} = \int_A (x_\alpha - c_\alpha)(x_\beta - c_\beta)\, dA = \int_A x_\alpha x_\beta \, dA - c_\alpha S_\beta - c_\beta S_\alpha + c_\alpha c_\beta A \tag{2.24}$$

These transition equations are often used to perform a transition of geometric moments about one set of axes to another set of axes.

The shear force definition is sometimes modified by the factors $\psi_{\alpha\beta}$, see the last section of this chapter on stresses in beams. The constitutive relations (2.18) and (2.19) can also be written in the following informative matrix format

$$\begin{pmatrix} N \\ M_1 \\ M_2 \end{pmatrix} = E \begin{bmatrix} A & S_1 & S_2 \\ S_1 & I_{11} & I_{12} \\ S_2 & I_{21} & I_{22} \end{bmatrix} \begin{pmatrix} \bar{\varepsilon} \\ \kappa_1 \\ \kappa_2 \end{pmatrix} \tag{2.25}$$

With known static values (N, M_β) it is possible to invert the above equation and use the axial beam stress equation (2.17) to find the stresses.

It can be seen that the constitutive equations for the internal forces will simplify considerably if $S_\beta = 0$ and if $I_{12} = I_{21} = 0$. If we use the elastic centre as the intersection point c_β then $S_\beta = 0$, and if the coordinate system can be rotated until the principal axes are obtained then $I_{12} = 0$. For single symmetric sections we can use the symmetry axis for one of the cross-sectional axes and obtain $I_{12} = 0$. The elastic centre can be defined as follows

The elastic centre is defined as the point c_β which satisfies

$$\int_A (x_\beta - c_\beta)\, dA = S_\beta = 0 \tag{2.26}$$

For cross-sections with constant E modulus we find

$$c_\beta = \frac{1}{A}\int_A x_\beta\, dA \tag{2.27}$$

It should be noticed that if we use the elastic centre as the origin of our Cartesian reference system we will have that $c_\beta = 0$. As mentioned the transition equations (2.24) can be used in this process.

If the elastic modulus varies within the cross-section it is a function of the cross-sectional coordinates x_ν. Let us therefore denote it by $\tilde{E}(x_\nu)$ and use E as a referencial elastic modulus. The definition of the cross-sectional parameters must then be altered as follows:

Definition of cross-sectional parameters, when the elastic modulus varies within the cross-section.

$$A = \int_A \eta\, dA \tag{2.28}$$

$$S_\beta = \int_A \eta\, (x_\beta - c_\beta)\, dA \tag{2.29}$$

$$I_{\alpha\beta} = \int_A \eta\, (x_\alpha - c_\alpha)(x_\beta - c_\beta)\, dA \tag{2.30}$$

in which the variation of the elastic modulus $\tilde{E}(x_\nu)$ is introduced through the use of a reference modulus E by the variation function

$$\eta = \frac{\tilde{E}(x_\nu)}{E} \tag{2.31}$$

These cross-sectional parameters are sometimes referred to as the transformed cross-sectional parameters.

Potential Energy and Virtual Work

Inserting the beam strain equations (2.9) and (2.11) into the potential energy function for a three-dimensional continuum given in equation (1.123) and using the constitutive equations (2.15) and (2.16) result in the following reduced potential

energy, see Washizu [4],

$$\begin{aligned} V &= \int_V (\frac{1}{2}\varepsilon E\varepsilon + \frac{1}{2}\gamma_\beta G\gamma_\beta - q_j u_j)\, dV - \int_A t_j u_j dA \\ &= \int_V (\frac{1}{2}\sigma\varepsilon + \frac{1}{2}\tau_\beta\gamma_\beta - q_j u_j)\, dV - \int_A t_j u_j dA \\ &= \int_V \left(\frac{1}{2}\sigma(\bar{\varepsilon} + (x_\beta - c_\beta)\kappa_\beta) + \frac{1}{2}\tau_\beta\gamma_\beta - q_j u_j\right) dV - \int_A t_j u_j\, dA \end{aligned} \quad (2.32)$$

Note that the potential energy is only a function of the displacement functions (v, w_ν, α_ν), since the stresses are functions of the strains, which in turn are functions of the displacement functions. Integrating over the cross-sectional area and using the constitutive relations in equations (2.18),(2.19) and (2.20) we find the potential energy for a beam:

Potential energy

$$\begin{aligned} V(v,\, w_\nu, \alpha_\nu) &= \int_0^L (\frac{1}{2}N\bar{\varepsilon} + \frac{1}{2}M_\beta\kappa_\beta + \frac{1}{2}Q_\beta\gamma_\beta \\ &\qquad -pv - p_\beta w_\beta - m_\beta\alpha_\beta)\, dz \\ &\quad - \left[\bar{N}v + \bar{M}_\beta\alpha_\beta + \bar{Q}_\beta w_\beta\right]_0^L \end{aligned} \quad (2.33)$$

where the internal beam forces N, M_β and Q_β are given by (2.18),(2.19) and (2.20) as functions of the displacements. Furthermore, axial, transverse and moment loads are

$$p = \int_A q_3\, dA, \quad p_\beta = \int_A q_\beta\, dA, \quad m_\beta = \int_A (x_\nu - c_\beta) q_3\, dA \quad (2.34)$$

and the boundary forces are

$$\bar{N} = \int_A t_3\, dA, \quad \bar{Q}_\beta = \int_A t_\beta\, dA, \quad \bar{M}_\beta = \int_A (x_\nu - c_\beta) t_3\, dA \quad (2.35)$$

The first variation of the potential energy functional with respect to all the unknown displacement variables yields the virtual work functional. As mentioned previously the first variation can be thought of as the change in potential energy when making small variations in the unknown displacements $(\delta v,\, \delta w_\beta,\, \delta\alpha_\nu)$. The first variation of the potential energy can thus be found as:

$$\delta V(v, w_\nu, \alpha_\nu) = \frac{\partial V}{\partial v}\delta v + \frac{\partial V}{\partial w_\beta}\delta w_\beta + \frac{\partial V}{\partial \alpha_\beta}\delta\alpha_\beta \quad (2.36)$$

(For Euler-Bernoulli theory α_β does not vary independently, since $\alpha_\beta = -w'_\beta$, but the total variation (2.36) remains correct if we insert $\alpha_\beta = -w'_\beta$).

Using that the variation of the potential energy with respect to the kinematic quantities is equal to the virtural work $\delta W = \delta V$ and that the internal forces are functions of the displacements $(N(\bar{\varepsilon}, \kappa_\beta))$, $M(\bar{\varepsilon}, \kappa_\beta)$, $Q(\gamma_\beta))$ we find:

Virtual work functional for beams

$$\begin{aligned}\delta W &= \int_0^L (N\,\delta\bar{\varepsilon} + M_\beta\,\delta\kappa_\beta + Q_\beta\,\delta\gamma_\beta \\ &\qquad -p\,\delta v - p_\beta\,\delta w_\beta - m_\beta\,\delta\alpha_\beta)\,dz \\ &\quad - \left[\bar{N}\,\delta v + \bar{M}_\beta\,\delta\alpha_\beta + \bar{Q}_\beta\,\delta w_\beta\right]_0^L \end{aligned} \tag{2.37}$$

The potential energy functional is equal to the complementary potential energy functional, if we include distributed loads and rewrite the functional in generalized stresses. This means that we can find the variation of the complementary potential energy functional with respect to the static quantities and find the complementary virtual work functional as:

Complementary virtual work functional for beams

$$\begin{aligned}\delta W^c &= \int_0^L (\bar{\varepsilon}\,\delta N + \kappa_\beta\,\delta M_\beta + \gamma_\beta\,\delta Q_\beta \\ &\qquad -v\,\delta p - w_\beta\,\delta p_\beta - \alpha_\beta\,\delta m_\beta)\,dz \\ &\quad - \left[v\,\delta\bar{N} + \alpha_\beta\,\delta\bar{M}_\beta + w_\beta\,\delta\bar{Q}_\beta\right]_0^L \end{aligned} \tag{2.38}$$

When using the complementary virtual work functional, it is common to take virtual variations of the internal forces which are in equilibrium without virtual loads (δp, δp_β, δm_β). The virtual internal forces must satisfy the equilibrium equation, which will be derived in the next section.

It should be noted that both the virtual work and complementary virtual work functionals can be derived even if the elastic potential does not exist (non-conservative forces, plastic energy dissipation).

- **Problem 2.1**
  A plane cantilever beam with the length $L = 6$ m and depth $d = 1$ m has the following kinematic displacement functions (let us use the coordinates (x_1, z)):

  $$\alpha_1(z) = 0 \qquad\qquad w_1(z) = \frac{1}{3}z$$

  a) Draw the displaced beam showing a few cross-sections along the beam.

  b) Calculate the shear strain γ_1 and the curvature $\kappa_1 = \alpha_1'$.

  c) It should be clear that this is a pure shear deformation mode. If the beam is rectangular with a width of $b = 1$ m, the elasticity modulus is $E = 1\ \mathrm{N/m^2}$ and the shear modulus $G = \frac{3}{8}E$, what is the shear energy density $\frac{1}{2}Q_1\gamma_1$ along the beam and what is the total shear energy $\int_0^L \frac{1}{2}Q_1\gamma_1\,dz$?

- **Problem 2.2**
  The plane cantilever beam with the length $L = 6$ m, rectangular cross-section with depth $d = 1$ m, width $b = 1$ m, elastic modulus $E = 1\ \mathrm{N/m^2}$ and shear modulus $G = \frac{3}{8}E$ has the following kinematic displacement functions

  $$\alpha_1(z) = -\frac{2}{3}\frac{z}{L} \qquad\qquad w_1(z) = \frac{1}{3}\frac{z^2}{L}$$

a) Draw the displaced beam showing a few cross-sections along the beam.

b) Calculate the shear strain γ_1 and the curvature $\kappa_1 = \alpha_1'$.

c) It should be clear that this is a pure bending deformation mode, i.e. pure bending. What is the bending energy density $\frac{1}{2}M_1\kappa_1$ along the beam and what is the total bending energy $\int_0^L \frac{1}{2}M_1\kappa_1\, dz$?

d) The cantilever beam in this and the previous problem has a tip displacement of 2 m (it must be a sponge to be so flexible). Compare the two total energy terms. What is the conclusion? Which energy is the largest? Will the displacements of a cantilever beam with a point load at the tip mainly displace in a bending mode or in a shear mode? (a combination, but which is governing)?

- **Problem 2.3**

A plane simply supported beam has a length of $L = 6\,\mathrm{m}$, a rectangular cross-section with depth $d = 1\,\mathrm{m}$, width $b = 1\,\mathrm{m}$, elastic modulus $E = 1\,\mathrm{N/m^2}$ and shear modulus $G = \frac{3}{8}E$.

a) Draw the displaced beam showing a few cross-sections along the beam, if the displacement functions are:

$$\alpha_1(z) = 0 \qquad\qquad w_1(z) = 4(1 - \frac{z}{L})\frac{z}{6}$$

Also, find the curvature $\kappa_1 = \alpha_1'$ and the shear strain γ_1 along the beam.

b) Draw the displaced beam showing a few cross-sections along the beam, if the displacement functions are

$$\alpha_1(z) = -\frac{2}{3}(1 - 2\frac{z}{L}) \qquad\qquad w_1(z) = 0$$

Also, find the curvature $\kappa_1 = \alpha_1'$ and the shear strain γ_1 along the beam.

c) Draw the displaced beam showing a few cross-sections along the beam, if the displacement functions are

$$\alpha_1(z) = -\frac{2}{3}(1 - 2\frac{z}{L}) \qquad\qquad w_1(z) = 4(1 - \frac{z}{L})\frac{z}{6}$$

Also, find the curvature $\kappa_1 = \alpha_1'$ and the shear strain γ_1 along the beam.

d) Which load can accomplish the displacements given in c) and what is its magnitude?

- **Problem 2.4**

A plane simply supported beam has the length L, rectangular cross-section with the depth d, the width b, the elastic modulus E and the shear modulus $G = \frac{3}{8}E$. The beam is loaded by a uniform transverse load p_1.

a) Find an explicit value for the total bending energy $V^\kappa = \int_0^L \frac{1}{2}M_1\kappa_1\, dz$

b) Find an explicit value for the total shear energy $V^\gamma = \int_0^L \frac{1}{2}Q_1\gamma_1\, dz$, including a correction term of $\psi_{11} = \frac{5}{6}$ for the constitutive relation $Q_1 = \psi_{11}GA\gamma_1$.

c) Find the numerical value of the ratio $r = \frac{V^\gamma}{V^\kappa}$ (in per cent) between shear energy and bending energy if the cross-sectional depth to beam length ratios are $\frac{d}{L} = \frac{1}{10}$ and $\frac{1}{30}$.

Since the energy terms are based on the square of the displacement quantities, we can also use the square root of this ratio, $\sqrt{r}$, to estimate the displacement ratios $\frac{w_1^\gamma}{w_1^\kappa}$ between the shear displacement component and the bending displacement component

d) Find an estimate of the displacement ratios $\frac{w_1^\gamma}{w_1^\kappa}$ of the shear component and the bending component for the depth to length ratios of $\frac{d}{L} = \frac{1}{10}$ and $\frac{1}{30}$. For engineering problems we are usually content with an error margin of $5-10\%$. In which case is it necessary to take shear deformation into account

- **Problem 2.5**
Derive the virtual work functional for beams (2.37) by taking the first variation of the potential energy functional (2.33). Use the general constitutive equations (2.18), (2.19) and (2.20) to express everything in strain measures. Take independent variations with respect to $\delta\bar{\varepsilon}$, $\delta\kappa_\beta$, $\delta\gamma_\nu$, $\delta\alpha_\beta$ and δw_β and add them to get the total variation. This is possible since $\delta\bar{\varepsilon} = \delta v'$, $\delta\kappa_\beta = \delta\alpha'_\beta$, and $\delta\gamma_\nu = \delta\alpha_\beta + w'_\beta$. End up by using the constitutive relations to reenter the internal forces N, M_β, and Q_β.

2.2 Timoshenko Beam Theory

The beam theory is based on the assumptions 1 to 3 and the formulations of displacements and strains made in the previous section. In this section the virtual work equation for Timoshenko beams and the equilibrium equations will be formulated.

In the first chapter we derived the equilibrium equations for a continuum by considering equilibrium of an infinitesimal cube. We will also in the last part of this section use this method to derive the equilibrium equations for a beam. However, to illustrate the value of the energy and work functionals in complicated problems we start by using these to derive the equilibrium equations. For very complex structural systems it is much easier to define the equilibrium equations through the use of stationarity of virtual work, as in modern computational finite element methods for analysing complex structures. This approach also validates the consistence of the assumptions made in the formulation of the theory.

Let us continue directly from the virtual work functional for beams (2.37) and introduce the virtual kinematic quantities $\delta\bar{\varepsilon} = \delta v'$, $\delta\kappa_\beta = \delta\alpha'_\beta$ and $\delta\gamma_\beta = \delta\alpha_\beta + \delta w'_\beta$. The virtural work equation for a Timoshenko beam thus takes the form

Virtual work functional for Timoshenko beams

$$\begin{aligned}\delta W \;=\; & \int_0^L \left(N\,\delta v' + M_\beta\,\delta\alpha'_\beta + Q_\beta\,(\delta\alpha_\beta + \delta w'_\beta)\right. \\ & \qquad \left. -p\,\delta v - p_\beta\,\delta w_\beta - m_\beta\,\delta\alpha_\beta\right)\,dz \\ & - \left[\bar{N}\,\delta v + \bar{M}_\beta\,\delta\alpha_\beta + \bar{Q}_\beta\,\delta w_\beta\right]_0^L \end{aligned} \tag{2.39}$$

Using partial integration we can rewrite the virtual work. It is in fact easy to remember the rule for partial integration by using the rule for derivatives of products for example $(M_\beta\,\delta\alpha_\beta)' = M'_\beta\,\delta\alpha_\beta + M_\beta\,\delta\alpha'_\beta$ is rearranged to the form $M_\beta\,\delta\alpha'_\beta = -M'_\beta\,\delta\alpha_\beta + (M_\beta\,\delta\alpha_\beta)'$ and by integration on both sides and using that the last term is already integrated we find the partial integration rule. We can thus introduce the following modifications:

$$\begin{aligned}\int_0^L M_\beta\,\delta\alpha'_\beta\,dz &= -\int_0^L M'_\beta\,\delta\alpha_\beta\,dz + [M_\beta\,\delta\alpha_\beta]_0^L \\ \int_0^L Q_\beta\,\delta w'_\beta\,dz &= -\int_0^L Q'_\beta\,\delta w_\beta\,dz + [Q_\beta\,\delta w_\beta]_0^L \\ \int_0^L N\,\delta v'\,dz &= -\int_0^L N'\,\delta v\,dz + [N\,\delta v]_0^L \end{aligned} \tag{2.40}$$

Introducing the modifications and rearranging the virtual work terms we find a very informative version of the virtual work functional, which delivers the differential equations and the boundary conditions for the Timoshenko beam.

$$\begin{aligned}\delta W &= -\int_0^L \Big((N'+p)\delta v + (Q'_\beta + p_\beta)\delta w_\beta + (M'_\beta - Q_\beta + m_\beta)\delta\alpha_\beta\Big)\,dz \\ &\quad - \Big[(\bar{N}-N)\,\delta v + (\bar{M}_\beta - M_\beta)\,\delta\alpha_\beta + (\bar{Q}_\beta - Q_\beta)\,\delta w_\beta\Big]_0^L \end{aligned} \tag{2.41}$$

If the virtual work vanishes $\delta W = 0$ for any variation in the kinematic parameters the beam is in equilibrium. We can make a variation internally in the beam over a very short distance for any of the three kinematic quantities (δv, δw_β, $\delta\alpha_\beta$) and the virtual work must vanish. If this is to occur the terms in the parenthesis in front of each individual variational displacement must be equal to zero. We thus see that we have derived the differential equilibrium equations using internal forces which satisfy the principle of virtual work:

Beam equilibrium equations derived by Timoshenko theory

$$\begin{aligned} N' + p &= 0 \\ Q'_\beta + p_\beta &= 0 \\ M'_\beta - Q_\beta + m_\beta &= 0 \end{aligned} \tag{2.42}$$

The boundary conditions are found by taking the variations infinitely close to the boundary and using that these variations must also vanish. The boundary conditions are trivial in this case as opposed to those found for the Bernoulli beam. The boundary conditions for the Timoshenko beam are:

$$\bar{N} = N \qquad \bar{M}_\beta = M_\beta \qquad \bar{Q}_\beta = Q_\beta \tag{2.43}$$

These just tell us that the reactions or loads acting on the ends of the beam are equal to the internal forces, (which is quite important even though it seems trivial). For statically determinate structures we could use these equations to find the correct variation of the internal forces N, M_β and Q_β along the beam or we could use static principles to find them.

For statically indeterminate structures we need information about the materials to solve the problem. Let us see why by finding the kinematic equilibrium equations and boundary conditions. If we insert the constitutive equations (2.18), (2.19) and (2.20) and introduce the strain definitions (2.10) (2.11) into the static equilibrium equations, we find the following kinematic equilibrium equations for a Timoshenko beam:

$$\begin{aligned}(EAv' + ES_\beta\alpha'_\beta)' + p &= 0\\ (ES_\beta v' + EI_{\alpha\beta}\alpha'_\alpha)' - (GA\alpha_\beta + GAw'_\beta) + m_\beta &= 0\\ (GA\alpha_\beta + GAw'_\beta)' + p_\beta &= 0\end{aligned} \tag{2.44}$$

We see that these five equations are coupled differential equations. The way to handle these is to decouple them by using c_β as the elastic centre, so that $S_\beta = 0$ and to rotate the coordinate system so that the off-diagonal moment of inertia is zero $I_{12} = 0$. The nearly decoupled kinematic equations for a Timoshenko beam become:

$$\begin{aligned}(EAv')' + p &= 0\\ (EI_{11}\alpha'_1)'' + m'_1 + p_1 &= 0\\ (GA\alpha_1 + GAw'_1)' + p_1 &= 0\end{aligned} \qquad \begin{aligned}&\\ (EI_{22}\alpha'_2)'' + m'_2 + p_2 &= 0\\ (GA\alpha_2 + GAw'_2)' + p_2 &= 0\end{aligned} \tag{2.45}$$

These equations are much simpler to solve, we just solve them from top to bottom. For the kinematic differential equations we can find the boundary conditions by using the constitutive relations and strain definitions. For the uncoupled case with c_β as the elastic centre and $I_{12} = 0$ we find the following expressions for the static boundary conditions for the Timoshenko beam

$$\begin{aligned}\bar{N} &= Ev'\\ \bar{M}_1 &= EI_{11}\alpha'_1\\ \bar{Q}_1 &= GA(\alpha_1 + w'_1)\end{aligned} \qquad \begin{aligned}&\\ \bar{M}_2 &= EI_{22}\alpha'_2\\ \bar{Q}_2 &= GA(\alpha_2 + w'_2)\end{aligned} \tag{2.46}$$

These boundary conditions must be handled with care, since the shear force leads to shear deformation, which concerns both α_β and w'_β.

Having introduced kinematic assumptions and a constitutive law, we have used the principle of virtual work and by "just turning a handle" (or say using variational principles) out came the equilibrium equations and boundary conditions.

The static equilibrium equations can also be found by considering equilibrium of an infinitesimal part of the beam as shown in fig. 2.9. The equilibrium equations found (independently of the beam theory) are exactly the ones found already in (2.42). Let us do it by using the figure and ensuring lateral and vertical force equilibrium and moment equilibrium about the right-hand end of the section as follows:

$$\begin{aligned}N + N'dz - N + pdz &= 0\\ Q_\beta + Q'_\beta dz - Q_\beta + p_\beta dz &= 0\\ M_\beta + M'_\beta dz - M_\beta - Q_\beta dz + m_\beta dz &= 0\end{aligned} \tag{2.47}$$

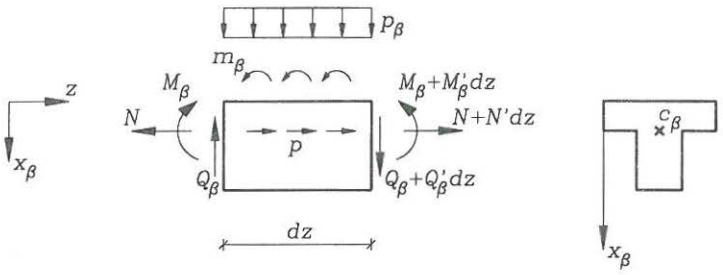

Fig. 2.9: Equilibrium of infinitesimal beam element.

where we deliberately have neglected small terms including $(dz)^2$. By cancellation of terms and division by dz these equations lead directly to the equilibrium equations in (2.42).

Problem

5. Use the kinematic equilibrium equations (2.45) and boundary conditions (2.46) for a Timoshenko beam to find the transverse displacements w_1 for a simply supported plane beam with a uniformly distributed transverse load p_1.

2.3 Euler-Bernoulli Beam Theory

Bernoulli made yet another assumption concerning the beam kinematics. Through experiments he saw that a transverse straight line remained straight during deformation and it also remained perpendicular to the transverse displacement curve. Let us make the same assumption and see what modifications it brings to the Timoshenko theory.

Assumption 4: *Euler-Bernoulli theory*

Cross-sections remain perpendicular to the displacement curve

this implies that shear strains are disregarded, since

$$\alpha_\beta = -w'_\beta \quad \Rightarrow \quad \gamma_\beta = \alpha_\beta + w'_\beta = 0 \tag{2.48}$$

That the assumption leads to $\alpha_\beta = -w'_\beta$ can be seen by comparing the displacements of Timoshenko theory in fig. 2.5 with the displacements of Euler-Bernoulli theory in fig. 2.10. The assumed displacements in Euler-Bernoulli theory are

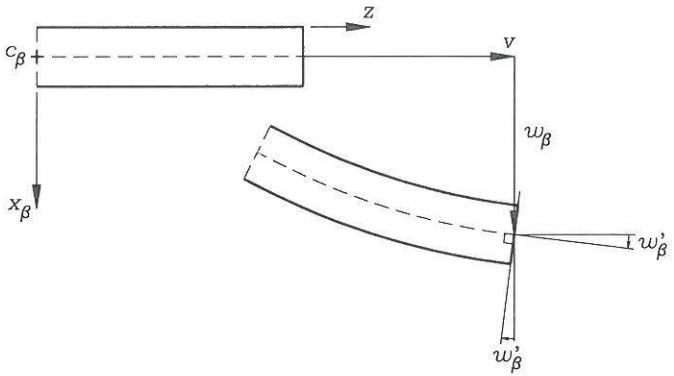

Fig. 2.10: Displacements of an Euler-Bernoulli beam.

Assumed displacements in Euler-Bernoulli theory

$$u_\beta = w_\beta \tag{2.49}$$
$$u_3 = v - (x_\beta - c_\beta)w'_\beta \tag{2.50}$$

where the three unknown functions are

$$v(z), \quad w_\beta(z)$$

The derivation of Euler-Bernoulli theory is equivalent to most of the derivations already performed and we will not repeat them here, since we can just insert $\gamma_\beta = 0$. However, the important formulas will be given. The axial strain is now defined by:

The axial strain is *Euler-Bernoulli theory*

$$\varepsilon = \bar{\varepsilon} + (x_\beta - c_\beta)\kappa_\beta \tag{2.51}$$

in which the axial strain $\bar{\varepsilon}$ at c_β and the curvatures κ_β are defined as

$$\bar{\varepsilon} = v' = \frac{dv}{dz} \qquad \kappa_\beta = \alpha'_\beta = -w''_\beta = -\frac{d^2 w_\beta}{dz^2} \tag{2.52}$$

Due to the altered definitions of the inclination $\alpha_\beta = -w'_\beta$ and the curvature $\kappa_\beta = -w''_\beta$ the virtual work functional for Euler-Bernoulli beams takes the form

Virtual work functional for Euler-Bernoulli beams

$$\begin{aligned}\delta W &= \int_0^L (N\,\delta v' - M_\beta\,\delta w_\beta'' - p\,\delta v - p_\beta\,\delta w_\beta + m_\beta\,\delta w_\beta')\,dz \\ &\quad - \left[\bar{N}\,\delta v - \bar{M}_\beta\,\delta w_\beta' + \bar{Q}_\beta\,\delta w_\beta\right]_0^L \end{aligned} \tag{2.53}$$

In our quest to find the equilibrium equations we need to perform partial integration twice on the displacement term $\delta w_\beta''$, which appears as the double derivative. Using partial integration once as done in the section on equilibrium equations for Timoshenko beams we find:

$$\begin{aligned}\delta W &= -\int_0^L \left((N' + p)\delta v - (M_\beta' + m_\beta)\delta w_\beta' + p_\beta \delta w_\beta\right)\,dz \\ &\quad - \left[(\bar{N} - N)\,\delta v - (\bar{M}_\beta - M_\beta)\,\delta w_\beta' + \bar{Q}_\beta\,\delta w_\beta\right]_0^L \end{aligned} \tag{2.54}$$

Using partial integration on the integral terms including $\delta w_\beta'$ we obtain the following very informative virtual work functional

$$\begin{aligned}\delta W &= -\int_0^L \left((N' + p)\delta v + (M_\beta'' + m_\beta' + p_\beta)\delta w_\beta\right)\,dz \\ &\quad - \left[(\bar{N} - N)\,\delta v - (\bar{M}_\beta - M_\beta)\,\delta w_\beta' + (\bar{Q}_\beta - M_\beta' - m_\beta)\,\delta w_\beta\right]_0^L \end{aligned} \tag{2.55}$$

If the virtual work vanishes $\delta W = 0$ for any variation in the kinematic parameters the beam is in equilibrium. For internal variations δv and δw_β the virtual work must vanish. Taking these variations we find the equilibrium equations:

Beam equilibrium equations derived by Euler-Bernoulli theory

$$\begin{aligned} N' + p &= 0 \\ M_\beta'' + m_\beta' + p_\beta &= 0 \end{aligned} \tag{2.56}$$

The boundary conditions are found by virtual variations infinitely close to the boundary and using that these variations must also vanish. The boundary conditions are not trivial in this case

$$\bar{N} = N \qquad \bar{M}_\beta = M_\beta \qquad \bar{Q}_\beta = M_\beta' + m_\beta \tag{2.57}$$

We see that the only way shear enters the Euler-Bernoulli theory is through the boundary condition $\bar{Q}_\beta = M_\beta' + m_\beta$. These equations can also be obtained by contracting the moment and equilibrium equations found by Timoshenko theory or by static equilibrium of an infinitesimal beam element.

For statically determinate beams it is possible to find the moments using the static equilibrium equations or using static priciples and then use the constitutive relation $M_1 = -EI_{11}w_1''$ to find the displacements by integration.

For statically indeterminate structures we need to introduce the kinematics and constitutive equations. Doing so results in a set of coupled differential equations in

v and w_β, however, we can decouple these. Assuming that c_β is the elastic centre, i.e. $S_\beta = 0$ and that the principal axes are used as coordinate axes, i.e. $I_{12} = 0$ we find the following kinematic equilibrium equations:

$$\begin{aligned} (EAv')' + p &= 0 \\ -(EI_{11}w_1'')'' + m_1' + p_1 &= 0 \end{aligned} \qquad -(EI_{22}w_2'')'' + m_2' + p_2 = 0 \tag{2.58}$$

with the associated boundary conditions

$$\begin{aligned} \bar{N} &= EAv' \\ \bar{M}_1 &= -EI_{11}w_1'' \\ \bar{Q}_1 &= -(EI_{11}w_1')' + m_1 \end{aligned} \qquad \begin{aligned} \bar{M}_2 &= -EI_{22}w_2'' \\ \bar{Q}_2 &= -(EI_{11}w_2')' + m_2 \end{aligned} \tag{2.59}$$

These equilibrium equations including boundary conditions can be used to solve statically indeterminate beams, however, when point loads act on the beam we have to split the beam in two and assemble the solutions using joint and boundary conditions or make use of delta functions. This becomes tedious and that is why we would like to use the complementary virtual work functional in the chapter on statically indeterminate beams.

Problem

6. Use the kinematic equilibrium equations (2.58) and boundary conditions (2.59) for an Euler-Bernoulli beam to find the transverse displacements w_1 for a simply supported plane beam with a uniformly distributed transverse load p_1.

2.4 Stresses in Beams

As mentioned earlier we can find the stresses using the constitutive equations and the definition of the internal forces. If we write these equations and definitions in a vector format as in (2.17) and (2.25) we find the following generalized Navier formula:

$$\sigma(x_\beta, z) = [\,1,\; x_1 - c_1,\; x_2 - c_2\,] \begin{bmatrix} A & S_1 & S_2 \\ S_1 & I_{11} & I_{12} \\ S_2 & I_{21} & I_{22} \end{bmatrix}^{-1} \begin{bmatrix} N \\ M_1 \\ M_2 \end{bmatrix} \tag{2.60}$$

However, if we use the elastic centre as the intersection point c_β, i.e. $S_\beta = 0$, and if we assume that the principal axes are used, i.e. $I_{12} = 0$, then the equations are simplified and we find the well-known Navier formula for beam stress:

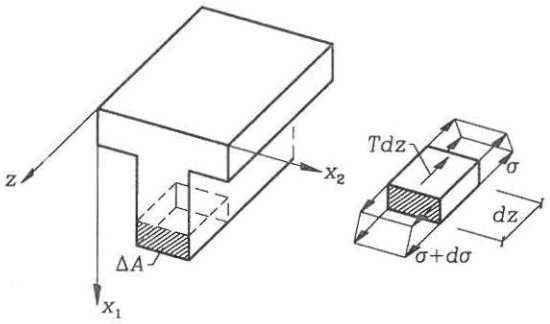

Fig. 2.11: Equilibrium of section cut-out.

Navier's formula: *Timoshenko and Euler-Bernoulli theories*

If $I_{12} = 0$ *then*

$$\sigma = \frac{N}{A} + \frac{M_1}{I_{11}}(x_1 - c_1) + \frac{M_2}{I_{22}}(x_2 - c_2) \tag{2.61}$$

and if also $c_\beta = 0$ *then*

$$\sigma = \frac{N}{A} + \frac{M_1}{I_{11}}x_1 + \frac{M_2}{I_{22}}x_2 \tag{2.62}$$

Even though Timoshenko theory includes shear deformation and an approximate determination of shear stress, it will be worthwile also to evaluate the Grashof formula, which is completely based on statics. Let us consider the equilibrium of a small cut-out element of the beam, shown in fig. 2.11. When the area of the cut-out is denoted ΔA the equilibrium equation can be written as

$$T = \int_{\Delta A} (\frac{d\sigma}{dz} + q)\, dA = \int_{\Delta A} (\sigma' + q)\, dA \tag{2.63}$$

where T is the total shear flow in the cut and $q = q_3$ is the longitudinal volume load. The equation is in fact an integral counterpart to the third continuum equilibrium equation (1.92). If again we assume that c_β is the elastic centre and that the beam is prismatic with identical cross-sections then we can use Navier's formula and find the shear flow by

$$\begin{aligned} T &= \int_{\Delta A} (\frac{N'}{A} + \frac{(x_1 - c_1)M_1'}{I_{11}} + \frac{(x_2 - c_2)M_2'}{I_{22}} + q)\, dA \\ &= \frac{N'\Delta A}{A} + \frac{M_1'\Delta S_1}{I_{11}} + \frac{M_2'\Delta S_2}{I_{22}} + \Delta p \end{aligned} \tag{2.64}$$

in which the following section cut-out parameters have been introduced

$$\Delta S_\beta = \int_{\Delta A} (x_\beta - c_\beta)\, dA \qquad \Delta p = \int_{\Delta A} q\, dA \tag{2.65}$$

The derivatives of the internal forces can be found by use of the equilibrium equations, i.e. $N' = -p$ and $M'_\beta = Q_\beta - m_\beta$ whereby we find the Grashof formula for the shear flow. The Grashof formula can be used to estimate the shear stresses by $\tau = \frac{T}{b}$, where b is the width over which the total shear stress "flows".

Grashof formula for the total shear stress "flow"

$$T = \frac{(Q_1 - m_1)\Delta S_1}{I_{11}} + \frac{(Q_2 - m_2)\Delta S_2}{I_{22}} + \Delta p - \frac{p\Delta A}{A} \tag{2.66}$$

Without distributed longitudinal and moment loads, (i.e. $p = m_1 = m_2 = 0$),

$$T = \frac{Q_1 \Delta S_1}{I_{11}} + \frac{Q_2 \Delta S_2}{I_{22}} \tag{2.67}$$

The shear stress approximation over the width b then is

$$\bar{\tau} \simeq \frac{T}{b} \tag{2.68}$$

It should be noted that the Timoshenko beam theory may overestimate the shear energy and the virtual work. This is due to the poor shear approximation with constant shear over the cross-section. An impoved approximation may be obtained by inserting correction factors into the constitutive equation

$$Q_\beta = \psi_{\alpha\beta} G A \gamma_\alpha \tag{2.69}$$

where $\psi_{\alpha\beta}$ are the correction factors. A better approximation of the potential energy or virtual work can be found by the use of Grashof's formula $\bar{\tau}_\beta = G\bar{\gamma}_\beta = T_\beta/b$ by anticipating that these shear stresses present a better approximation than the approximation by Timoshenko beam theory, see Krenk [5] and Gere & Timoshenko [12]. Equalizing the two energies by

$$\begin{aligned} \frac{1}{2}\int_A \bar{\tau}_\nu \bar{\gamma}_\alpha \, dA &= \frac{1}{2} Q_\nu \gamma_\alpha \quad \Downarrow \\ \frac{1}{2}\int_A \frac{\bar{\tau}_\nu \bar{\tau}_\alpha}{G} \, dA &= \frac{1}{2}\frac{Q_\nu Q_\beta}{\psi_{\alpha\beta} G A} \end{aligned} \tag{2.70}$$

whereby we find the correction factor

$$\psi_{\alpha\beta} = \frac{Q_\nu Q_\beta / A}{\int_A \bar{\tau}_\nu \bar{\tau}_\alpha \, dA} \tag{2.71}$$

in which it has been assumed that the shear modulus G is constant. It is customary to normalize the Grashof shear stress $\bar{\tau}_\beta$ by the shear force Q_β, (i.e. calculating with $Q_\beta = 1$). For a homogeneous, rectangular section it can be shown that $\psi_{11} = \frac{Q_1^2/A}{\int_A \bar{\tau}_1^2 \, dA} = \frac{5}{6}$ and $\psi_{12} = \psi_{21} = 0$, whereby we can write $\psi_{\alpha\beta} = \frac{5}{6}\delta_{\alpha\beta}$. For single and double symmetric cross-sections the off-diagonal factor is zero, $\psi_{12} = \psi_{21} = 0$, since

shear in one direction does not produce work through the shear strains in the other direction. For non-symmetric beams there may be off-diagonal terms $\psi_{12} \neq 0$.

This closes our development of beam theories, beam equilibrium equations and stress determination The statics of beams has not been treated, since it was assumed that the reader was acquainted with this. The determination of displacements by complementary virtual work will be treated in the section on statically indeterminate beams.

- **Problem 2.6**
  Show that the shear energy correction factor ψ_{11} for a rectangular beam is $\frac{5}{6}$. Use that the shear stress is parabolicly distributed, for example $\bar{\tau}_1 = \frac{3Q}{2A} 4\frac{x_1}{d}(1 - \frac{x_1}{d})$ where x_1 varies from 0 to d, where d is the cross-sectional depth.

Chapter 3

Stability of Columns

The flexural beam theories based on infinitesimal strains and rotation as developed in the previous chapter are great tools. However, for slender beams in compression, socalled columns, a stability phenomenon arises, which has to be included in the beam theories. If a column, for example a yardstick or just a ruler, is compressed as shown in fig. 3.1, it will initially remain straight and only have axial strains, but suddenly as the compression load is increased the column loses its stability by deflecting to the side in a flexural displacement mode. The column cannot carry more load without excessive displacements. Fig. 3.2 shows the load P as a function of both axial v and transverse displacements w in a three-dimensional view. As the load increases the compression path is followed and at the critical load the transverse displacement path is followed. This structural stability phenomenon is one of the simplest types and it was the first to be solved. The Swiss mathematician Leonhard Euler found the solution in 1744, even though he only knew the existence of a proportionality factor between the moment M and curvature κ. The proportionality factor EI was established in 1826 by Navier, i.e. $M = EI\kappa$. Many elastic stability problems of structural mechanics are treated by Timoshenko and Gere [11], which has become a classical reference when dealing with specific problems. An extensive treatment of stability of structures is given by Bazănt & Cedolin [14].

For small loads a straight column is well described by the linear beam theories, but in order to predict the critical load, the socalled buckling load, (Euler load or bifurcation load), a non-linear ingredient from large displacement theory is needed. According to linear theory the stationarity of the potential energy or the principle of virtual work always supplies a stable equilibrium position. However, this only applies if the linear assumptions made are correct. When the transverse displacements and the rotations become larger it is necessary to expand the theory by including non-linear terms in the strain definitions, whereby also the potential energy and virtual work functionals will include more terms. With the additional terms the stationarity of the potential energy and the principle of virtual work become necessary, but not sufficient, conditions for stable equilibrium. This is due to addition of possible negative terms in the potential energy or virtual work functionals. However, it is possible, following Washizu [4], to stay within a linear framework, with uncoupled linear differential equations, by using Euler's initial stress method and

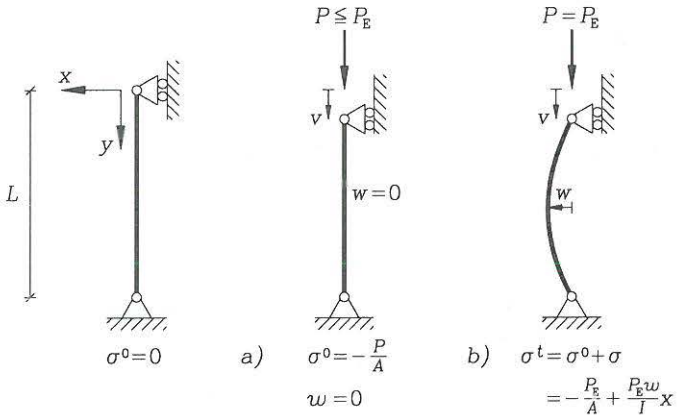

Fig. 3.1: Stability phenomenon for a simply supported column.

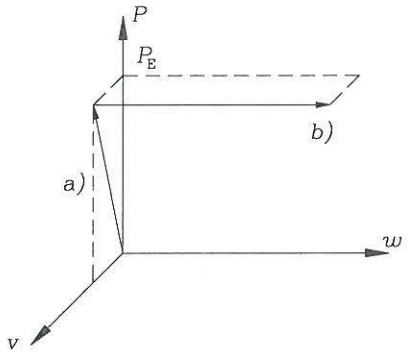

Fig. 3.2: The load path for an Euler column.

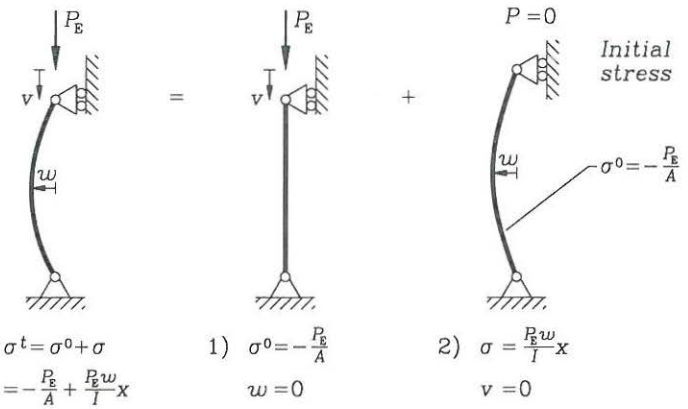

Fig. 3.3: Euler's initial stress method illustrated for a column.

still be able to predict the buckling load.

The idea of Euler's initial stress method is indicated in fig. 3.3. The solution can be viewed as two separate problems one for the trivial, compressed state and another for the buckled state. In the primary problem 1) the initial stress field σ^0 is found using linear infinitesimal strain and rotation theory. The secondary problem 2) then consists of finding the critical size of the initial stress field σ^0 at which a secondary deformed equilibrium (buckled) situation exists. The transition from the initial state to the buckled state is called bifurcation. For a column the bifurcation is the transition from the trivial compression load path with only axial displacements to the secondary flexural load path with transverse displacements.

The buckling load for uniformly compressed columns can be found using static methods and the constitutive equation for the moment. This is because the internal moments can be found explicitly, without considering rotation of internal forces. The first section of this chapter will treat uniformly compressed columns starting with a column with pinned ends, then other boundary conditions are treated and the idea of an effective length is introduced. The first section will also include a brief introduction to the influence of initial moments M^0, imperfections $\hat{w}$, non-linear material and shear deformation.

In the following section the general equilibrium equations for a deformed infinitesimal beam element will be derived and Euler's initial stress method will be used to linearize these equations. An alternative energy approach starting from the potential energy derived for a continuum will be used to derive the equilibrium equations. Approximate methods for estimating the buckling loads, including the well-known Rayleigh coefficient, will also be derived from the principle of virtual work.

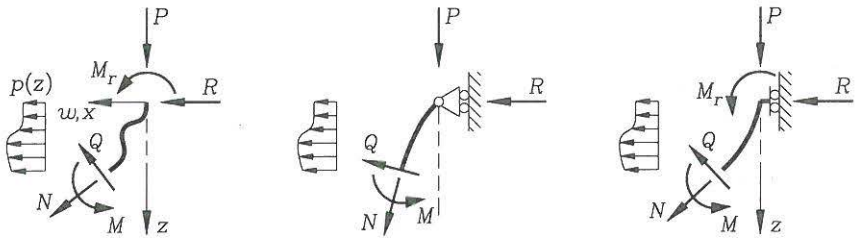

Fig. 3.4: Reactions and loads on uniformly compressed column end.

3.1 Uniformly Compressed Columns

In this section the index notation will be cancelled and we shall work in one of the principal planes (x_β, z) of the column cross-section, and just use the axes (x, z) neglecting the index β. It is assumed that the coordinate axes have their origin in the elastic centre, i.e. $c_\beta = 0$, $S_\beta = 0$ and $I_{12} = 0$.

Stability of columns can be evaluated for Euler-Bernoulli beams or Timoshenko beams, where the later solution will include the effects of shear. In this section we shall first treat the classical buckling problem for an Euler-Bernoulli column, since it is the one most often used. The uniformly compressed columns can be treated independently, since the internal moment due to the external compression load can be found explicitly as a function of the reaction forces. The geometric boundary conditions can be used if the reactions are statically indeterminate. Fig. 3.4 shows the lateral reaction force R and the moment reaction M_r on the end of a column which is in the displaced configuration and may have a varying transverse load $p(z)$. The moment in the deformed configuration in this column can be determined by use of statical equilibrium in the deformed configuration as

$$M(z) = Pw(z) - Rz - M_r - \int_0^z p(\bar{z})(z - \bar{z})\, d\bar{z} \tag{3.1}$$

If the column has initial transverse loads, the column deforms in the initial configuration and the problem is not a stability problem with a bifurcation point. However, if there are neither initial transverse loads nor initial reactions, but only the initial constant axial force $N^0 = -P$ then it is a stability problem. Notice that $N \neq N^0$ since the axial force in the column will change due to the rotation of the cross-section in the deformed position. It should be noted that we are using Euler's initial stress method, where the initial problem is the trivial compression problem of determining N^0. Notice also that we are not concerned about the axial and transverse equilibrium equations for the deformed situation.

The Euler Column with Pinned Ends

As mentioned, it is necessary to consider equilibrium in a deformed situation. It is possible to find the moment distribution $M(z, w, P)$ in the column for any trans-

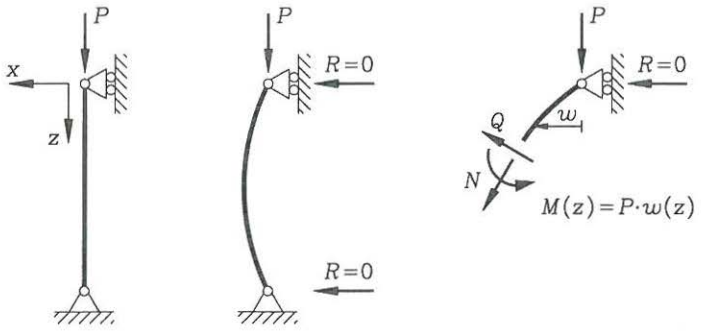

Fig. 3.5: Moment equilibrium for an Euler column in the deformed state.

verse displacement $w(z)$ with a uniform compressive axial force $N^0 = -P$. When the moment distribution is known the constitutive relation for the moment can be used to find the critical value of the axial load P. Using Euler-Bernoulli theory the relation is

$$w'' = -\frac{M(z,w,P)}{EI} \tag{3.2}$$

The use of this equation will be illustrated on a compressed column with pinned ends and without transverse loads, called the Euler column after Leonhard Euler. The column is illustrated in fig. 3.5. By formulating the moment equilibrium about the section at z the internal forces N and Q do not enter the equilibrium equation. It is thus seen that we can find the moment distribution $M(z) = Pw(z)$ as a function of an arbitrary displacement field $w(z)$, (which satisfies the boundary conditions). The differential relation (3.2) with the statically determinate moment thus becomes

$$\begin{aligned} w'' &= -\frac{P}{EI}w \quad \Downarrow \\ w'' + k^2 w &= 0 \end{aligned} \tag{3.3}$$

where the coefficient $k^2 = \frac{P}{EI}$ has been introduced (we have squared it to emphasize that it is always positive). This is an ordinary second order linear differential equation and if the bending stiffness EI is constant the differential equation has constant coefficients. The two boundary conditions needed are determined by the zero transverse displacements at the ends, $w(0) = w(L) = 0$. Note that $\frac{1}{k}$ has the dimension of length and we shall see later that it is in fact a measure of the problem length scale. (By multiplying the mathematical length scale by π an engineering length scale called the effective length is obtained as $L_s = \frac{\pi}{k}$).

The homogeneous equation (3.3) is a mathematical eigenvalue problem, where k^2 defines the eigenvalues which we want to find, and $w(z)$ define the corresponding eigenfunctions or socalled eigenmodes which we would also like to know.

The differential equation (3.3) is solved by assuming that $e^{\xi z}$ is a solution, whereby the characteristic equation $\xi^2 + k^2 = 0$ is found. The characteristic equation

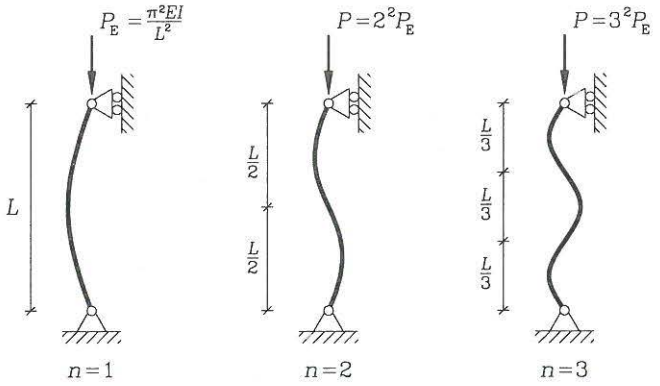

Fig. 3.6: Eigenmodes w and corresponding loads P for an Euler column.

has the solutions $\xi = \pm ik$, meaning that the solutions are of the form $e^{\pm ikz} = \cos(kz) \pm i\sin(kz)$ (using Leonard Euler's formula for complex exponentials. Euler published more than 886 papers on mathematics, mechanics, hydromechanics ...). Since the solution is real it can be written as:

$$w = A\sin(kz) + B\cos(kz) \tag{3.4}$$

in which A and B are arbitrary constants determined by the boundary conditions. (Notice that $L_s = \frac{\pi}{k}$ is a practical length scale for the displacement variation in the axial z direction). The boundary condition $w(0) = 0$ results in $B = 0$, whereby the last condition $w(L) = 0$ results in

$$A\sin(kL) = 0 \tag{3.5}$$

Two solutions are possible for this boundary equation. One solution is the trivial one $A = 0$, which corresponds to the primary undeformed state with $P > 0$ and $w(z) = 0$. The other solution is the non-trivial one corresponding to the secondary deformed state where A is arbitrary and eigenvalues are determined by

$$\begin{aligned} \sin(kL) &= 0 \quad \Downarrow \\ kL &= n\,\pi \qquad (n = 0, 1, 2, 3, \ldots) \end{aligned} \tag{3.6}$$

Using that $k^2 = \frac{P}{EI}$, i.e. $P = k^2 EI$, and discarding $kL = 0$ corresponding to no axial load $P = 0$ we find the following solution for the eigenvalue problem:

$$P = n^2 \frac{\pi^2 EI}{L^2} \qquad (n = 1, 2, 3, \ldots) \tag{3.7}$$

$$w = A\sin(n\,\pi \frac{z}{L}) \tag{3.8}$$

where A is an arbitrary constant. A few of the lower eigenvalues and corresponding displacement eigenmodes are shown in fig. 3.6. The lowest critical load at which

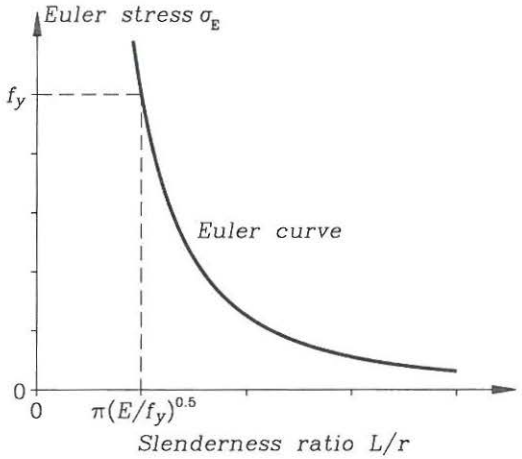

Fig. 3.7: The Euler buckling curve.

equilibrium in the deformed state exists is found for $n = 1$ and it is called the Euler load. The critical loads above the Euler load lie on the continued equilibrium path, which is unstable. The Euler load P_E and the corresponding displacement mode are thus given by the following equations.

The Euler load for a column with pinned ends is

$$P_E = \frac{\pi^2 EI}{L^2} \tag{3.9}$$

The column displacements are given by

$$w = A\sin(\pi\frac{z}{L}) \tag{3.10}$$

where A is an indeterminate arbitrary constant.

Dividing the Euler load (3.9) by the cross-sectional area we obtain the Euler stress

$$\sigma_E = \frac{\pi^2 EI}{AL^2} = \frac{\pi^2 E}{(L/r)^2} = \frac{\pi^2 E}{\lambda^2} \tag{3.11}$$

where the radius of inertia $r = \sqrt{I/A}$ of the cross-section has been introduced. Further, the ratio $\lambda = L/r$ is introduced as the slenderness ratio of the column. The slenderness ratio λ is the main geometric parameter, which governs the buckling behaviour. The plot in fig. 3.7 shows the Euler stress σ_E as a function of the slenderness ratio $\lambda = L/r$, the socalled elastic buckling curve. For columns with a maximum stress limit, typically the yield limit f_y, the buckling stress must be lower than the yield limit $\sigma_E < f_y$ as indicated in the figure, or the column will

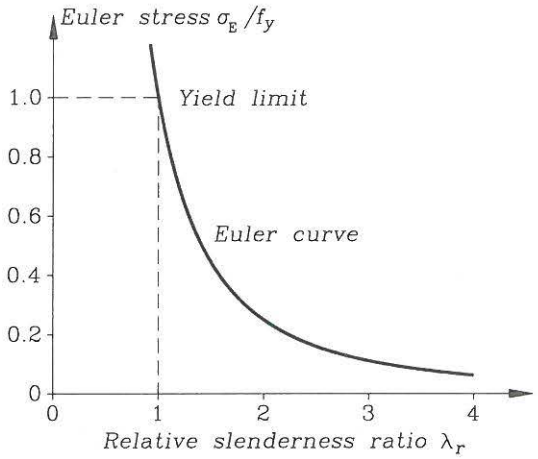

Fig. 3.8: The non-dimensional plot of the Euler buckling curve.

fail by yielding. Using this we find the corresponding limiting slenderness value as follows:

$$\frac{\pi^2 E}{(L/r)^2} \leq f_y \qquad \Rightarrow \qquad \pi\sqrt{E/f_y} \leq L/r \tag{3.12}$$

In codes of practice the slendernes ratio $\lambda = L/r$ is often normalized by this minimum slenderness value ($\pi\sqrt{E/f_y}$). The normalized slenderness ratio is called the relative slenderness ratio (since it is taken relative to the yield limit):

$$\lambda_r = \frac{L/r}{\pi\sqrt{E/f_y}} = \sqrt{\frac{f_y(L/r)^2}{\pi^2 E}} = \sqrt{\frac{f_y}{\sigma_E}} \tag{3.13}$$

The relative slenderness ratio enables buckling curves to be plotted in a non-dimensional form, as shown in fig. 3.8. This non-dimensional form is often used by codes of practice. The critical column stress can be found as the minimum of the Euler stress σ_E and the yield stress f_y, which can also be written as

$$\frac{\sigma_{cr}}{f_y} \leq \left\{ \begin{array}{c} 1 \\ \dfrac{\sigma_E}{f_y} \end{array} \right. = \frac{1}{\lambda_r^2} \tag{3.14}$$

However, in codes of practice the ideal Euler buckling curve is modified to taking imperfections, residual stresses and plasticity into account.

Other Columns and Effective Lengths

By the use of statics and the constitutive equation for the moment $M = -EIw''$ it is possible to find the buckling load for uniformly compressed single column

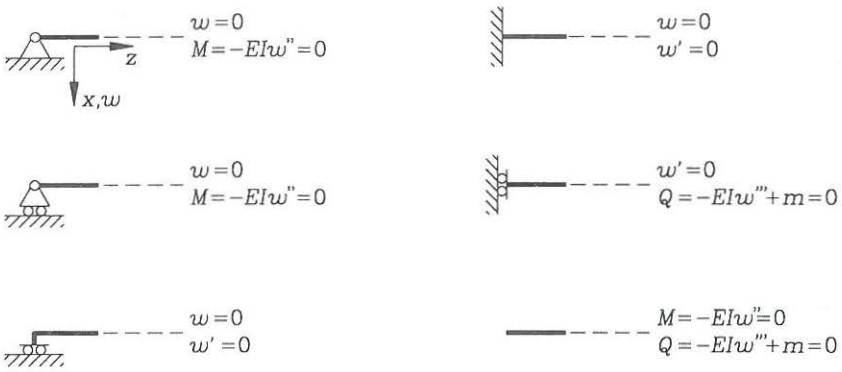

Fig. 3.9: Boundary conditions for the transverse displacements.

problems with known boundary conditions. It is also possible to include transverse loads and solve for the transverse displacements as a function of the axial load. However, we shall concentrate on the buckling problem. For columns with boundary conditions for the transverse displacements as illustrated on fig. 3.9 a general format for a buckling solution can be found. Some columns other than the Euler column with pinned ends are shown in fig. 3.10, which covers the most general boundary conditions. The moment in these columns is given by statical equilibrium and it can be written in the following general form

$$M(z) = Pw(z) - Rz - M_r \tag{3.15}$$

However, for simplification in the following we use that P is a constant and introduce $C = R/P$ and $D = M_r/P$, whereby the moment distribution becomes

$$M(z) = P\,(w(z) - Cz - D) \tag{3.16}$$

in which C and D determine an additional linear variation of the moment due to the reactions, as shown in fig. 3.10. The first column a) is statically determinate while the other three b), c) and d) are statically indeterminate. However, we can apply the unknown reactions to the columns, so that global equilibrium is satisfied. Using equation (3.16) and the constitutive equation (3.2) for the moment we find the governing differential equation

$$w'' + k^2 w - k^2 Cz - k^2 D = 0 \tag{3.17}$$

where $k^2 = \frac{P}{EI}$ is the problem constant as we have already seen. The non-homogeneous equation has the following general solution

$$w(z) = A\sin(kz) + B\cos(kz) + Cz + D \tag{3.18}$$

where A and B are constants determined by the remaining boundary conditions. The solution can be confirmed by substitution. It is seen that $L_e = \frac{\pi}{k}$ is a measure

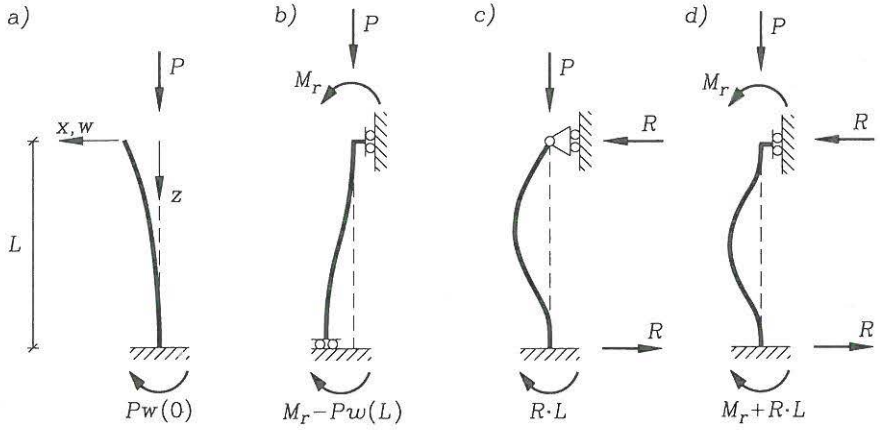

Fig. 3.10: Other simple columns.

of the problem length scale since it corresponds to the zero crossings of the sine and cosine functions. With this knowledge we might be able to guess the length scales for each of the columns in fig. 3.10 and use this to estimate the constant by $k = \pi/L_e$ and thus also the buckling load $P = k^2EI = \frac{\pi^2 EI}{L_e^2}$, which is similar to the Euler load for the column with pinned ends.

The column differential equation (3.17) can also be rewritten by taking the double derivative in the axial direction, whereby it takes the following form

$$w'''' + k^2 w'' = 0 \tag{3.19}$$

which has the same general solution as given in equation (3.18). This equation may be easier to use when boundary conditions become complicated (for example by springs). This equation can also be derived through the more general and robust approach used in the next section.

- **Example 3.1** Cantilever column.

  Let us treat the cantilever column a) and analyse the result. The cantilever column is statically determinate and we can find the constants $C = 0$ and $D = w(0)$ from fig. 3.10. Then we need to determine the constants A, B and $w(0)$. This is done by using three of the boundary conditions. First we can use that the moment is zero at the free end $w''(0) = 0$, which gives us that $B = 0$. As the second boundary condition we choose that the displacements at the fixed end are zero $w(L) = 0$, which results in $A = -w(0)$ Then we use that the column is restrained against rotation $w'(L) = 0$ at the fixed end:

$$\begin{aligned} w(0)k\cos(kL) &= 0 \quad \Downarrow \\ kL &= \frac{\pi}{2} + n\pi \quad (n = 1, 2, 3, \ldots) \end{aligned}$$

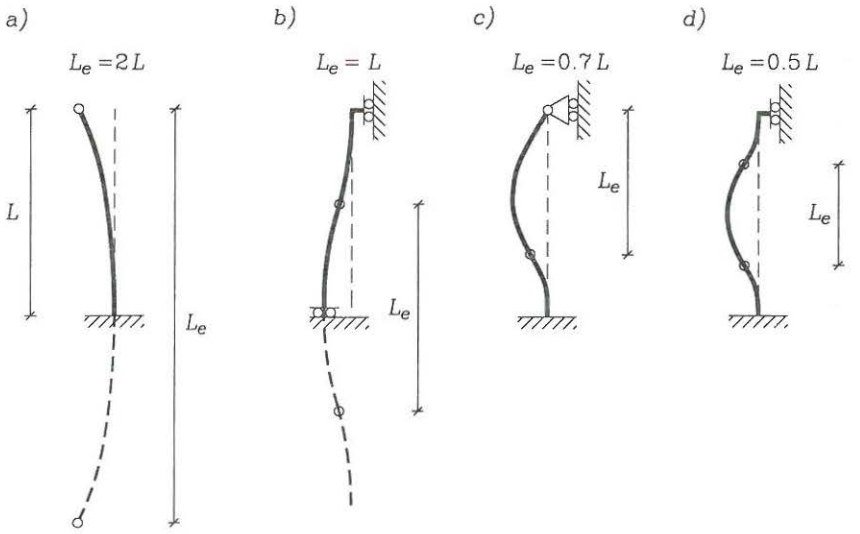

Fig. 3.11: Effective length of columns $L_e = \pi/k$.

The cantilever column thus has the lowest eigenvalue and lowest buckling load when $kL = \frac{\pi}{2}$. Using that $(kL)^2 = \frac{PL^2}{EI}$ we find the buckling load as

$$P = \frac{\pi^2 EI}{4L^2} = \frac{\pi^2 EI}{L_e^2}$$

where the effective length is defined using $kL = \frac{\pi}{2}$ as

$$L_e = \frac{\pi}{k} = 2L$$

The transverse column displacement (mode shape) is given by

$$w(z) = w(0)(1 - \sin(kz))$$

where $w(0)$ is an indeterminate arbitrary constant.

Effective lengths of the simple columns corresponding to the distance between curvature inflection points, i.e. points of zero moment, are shown in fig. 3.11 for the other columns.

Column	Boundary conditions	Problem solution	Eigen-value kL	Buckling load $P = \frac{\pi^2 EI}{L_e^2}$	Effective length L_e
a)	$w''(0) = 0$	$B = 0$			
$C = 0$	$w(L) = 0$	$A = \frac{-w(0)}{\sin(kL)}$			
$D = w(0)$	$w'(L) = 0$	$\cos(kL) = 0$	$\frac{\pi}{2}$	$\frac{\pi^2 EI}{(2L)^2}$	$2L$
b)	$w'(0) = 0$	$A = 0$			
$C = 0$	$w(0) = 0$	$B = \frac{-M_r}{P}$			
$D = M_r/P$	$w'(L) = 0$	$\sin(kL) = 0$	π	$\frac{\pi^2 EI}{L^2}$	L
c)	$w(0) = 0$	$B = 0$			
$C = R/P$	$w'(L) = 0$	$A = \frac{R}{Pk\cos(kL)}$			
$D = 0$	$w(L) = 0$	$\tan(kL) = kL$	$\sim \frac{\pi}{0.7}$	$\sim \frac{\pi^2 EI}{(0.7L)^2}$	$\sim 0.7L$
d)	$w(0) = 0$	Matrix			
$C = R/P$	$w'(0) = 0$	equation			
$D = M_r/P$	$w(L) = 0$	$\mathbf{Kc} = \mathbf{0}$			
	$w'(L) = 0$	$\det(\mathbf{K}) = 0$	2π	$\frac{\pi^2 EI}{(L/2)^2}$	$L/2$

Tab. 3.1: Solutions for the other columns.

The effective length is the distance between curvature inflection points

$$L_e = \frac{\pi}{k} = \sqrt{\frac{\pi^2 EI}{P}} \tag{3.20}$$

where P is the critical load.

When L_e is known the critical load is given by

$$P = \frac{\pi^2 EI}{L_e^2} \tag{3.21}$$

The solutions for the remaining columns can be found in a similar manner, with the major principles outlined in table 3.1. The boundary conditions give sets of

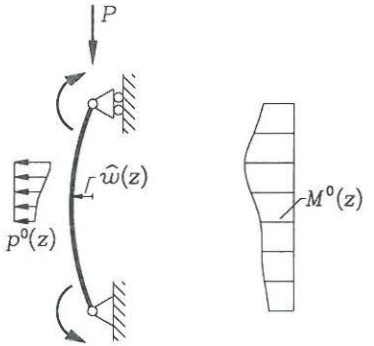

Fig. 3.12: Euler column with initial moments.

equations in the unknowns A, B, C, D (or equivalent A, B, M_r, R). These equations constitute a boundary eigenvalue problem. The column d) with both ends fixed gives us the greatest problems, since we have to solve some of the coupled boundary conditions as an eigenvalue problem. The table gives the solutions in the form of the lowest eigenvalue kL, the lowest buckling load P and the corresponding effective length L_e.

Initial Moments and Imperfections

Let us now turn to the influence of initial moments $M^0(z)$ from transverse loads $p^0(z)$, end moments and imperfections $\hat{w}$ on the Euler column with pinned ends as shown in fig. 3.12. The initial moment contribution could for example be given as

$$M^0(z) = P\hat{w}(z) - R^0 z - M_r^0 - \int_0^z p^0(\bar{z})(z - \bar{z})\, d\bar{z} \tag{3.22}$$

Imperfections are included in M^0 as an additional initial moment $P\hat{w}$. (We use $\hat{w}$ instead of w^0 since the imperfections have nothing to do with displacements due to M^0). The moment in the column becomes

$$M = M^0 + Pw \tag{3.23}$$

The governing differential equation is found by the use of the constitutive relation (3.2).

$$w'' + k^2 w + \frac{M^0}{EI} = 0 \tag{3.24}$$

With transverse loads or imperfections this differential equation is not an eigenvalue problem. The solution will determine an exact non-linear relationship between the column load P and the transverse displacements w for a given initial moment field M^0. The differential equation can be solved generally by expanding the initial

moment in a Fourier sine series:

$$M^0(z) = \sum_{n=1}^{\infty} M_n^0 \sin(\frac{n\pi z}{L}) \tag{3.25}$$

where the Fourier coefficients (corresponding to the weights of each sine function) are $M_n^0 = \frac{2}{L}\int_0^L M^0(z)\sin(\frac{n\pi z}{L})dz$, which can be determined when the initial moment distribution $M^0(z)$ is known. Fourier components M_n^0 for many different distributions can be found in mathematical handbooks. The displacements w which satisfy the boundary conditions $w(0) = w(L) = 0$ can be found as a Fourier series solution in the form:

$$w(z) = \sum_{n=1}^{\infty} w_n \sin(\frac{n\pi z}{L}) \tag{3.26}$$

in which all coefficients w_n are still unknown. Inserting the Fourier solution (3.26) and the Fourier expanded initial moment (3.25) in the differential equation (3.24) we find:

$$\sum_{n=1}^{\infty} \left(-\left(\frac{n\pi}{L}\right)^2 w_n + k^2 w_n + \frac{M_n^0}{EI} \right) \sin(\frac{n\pi z}{L}) = 0 \tag{3.27}$$

This equation must be satisfied for all z and n, therefore all the sine coefficents given in the parenthesis must be zero. This gives us the Fourier displacement coefficients:

$$-\left(\frac{n\pi}{L}\right)^2 w_n + k^2 w_n + \frac{M_n^0}{EI} = 0 \qquad \Downarrow$$

$$w_n = \frac{M_n^0}{EI((n\pi/L)^2 - k^2)} = \frac{M_n^0}{n^2 P_{\text{E}} - P} \tag{3.28}$$

The displacents are thus determined by the sum (3.26) and the coefficients (3.28). The moment in the column can then be found by use of the constitutive equation $M = -EIw''$ and by differentiation of the found displacements, which results in

$$M(z) = \sum_{n=1}^{\infty} \frac{n^2 P_{\text{E}}}{n^2 P_{\text{E}} - P} M_n^0 \sin(\frac{n\pi z}{L}) \tag{3.29}$$

This equation can give much information. It can be seen that the initial moment components in the Fourier expansion are magnified by a factor $\zeta(n)$ which depends on the component number n as follows

$$\zeta(n) = \frac{n^2 P_{\text{E}}}{n^2 P_{\text{E}} - P} \tag{3.30}$$

It is clear that the magnification is largest for the first term of the Fourier series expansion. If, for example, we assume that the initial moments are relatively small and that the column load is $P = 0.90 P_{\text{E}}$ we find the following magnification factors:

$$\zeta(1) = 10\,, \quad \zeta(2) = 1.29\,, \quad \zeta(3) = 1.11\,, \quad \zeta(4) = 1.06 \tag{3.31}$$

This shows that the first term of the Fourier series expansion dominates the magnification of the initial moment.

In engineering codes it is often assumed that the magnification of the initial moment $M^0(z)$ is well approximated by the magnification factor for the first term of the Fourier series expansion.

Magnification of initial moments

$$M(z) \simeq \frac{P_E}{P_E - P} M^0 \tag{3.32}$$

Note that for some cases with non-uniform transverse loads and also for some cases with clamped boundary conditions this may become a poor approximation.

Let us use the initial moment $M^0 = P\hat{w}$ to introduce some geometrical imperfections in the form of initial displacements $\hat{w}$. This also includes eccentric application of the compressive force. The moments are magnified as before and the total displacements $w^t = \hat{w} + w$ are also determined by use of the same magnification factor. This can be seen by use of equation (3.28) for the first term $n = 1$ as follows:

Magnification of initial displacements

$$w^t = \hat{w} + w \simeq \hat{w} + \frac{P\hat{w}}{P_E - P} = \frac{P_E}{P_E - P}\hat{w} \tag{3.33}$$

The imperfections $\hat{w}$ can also include the initial displacements w^0 from the transverse loads, which are determined from an initial linear analysis. It is worth noting that the magnification factor $\zeta(1)$ is exact if the initial moment and the initial imperfection have a sinusodial variation over the column length.

Let us use the relationship between the initial moment M^0, the imperfections $\hat{w}$, the column load P, the moments M and the displacements w. For sinusodial initial imperfections or initial moments with amplitudes $\hat{w}/L$ or $M^0/(P_E L)$ of 0.0001, 0.001 and 0.01 the column loads P are calculated using equations (3.32) and (3.33) and shown in fig. 3.13 as functions of the normalized total displacement or total moment. It is clear that as the Euler load is reached the displacements and moments grow very fast. It should further be noted that all the curves have the Euler load as a limit and that the buckling load is in fact an important value, also for columns with transverse loads.

In codes of practice the magnification factor is used to determine an approximate column stress, which has to be lower than the yield stress f_y. The column stress is approximated by

$$\sigma \simeq -\frac{P}{A} + \frac{P_E}{P_E - P}\frac{M_1^0}{I} x_{max} \leq f_y \tag{3.34}$$

in which M_1^0 is or is assumed to approximate the first Fourier component of the initial moment M^0 well. The codes usually specify methods for approximating M_1^0. The socalled Perry-Robertson column equation, used for buckling curves in codes of practice, is obtained by assuming an equivalent imperfection e and inserting $M_1^0 = Pe$ into the equation (3.34).

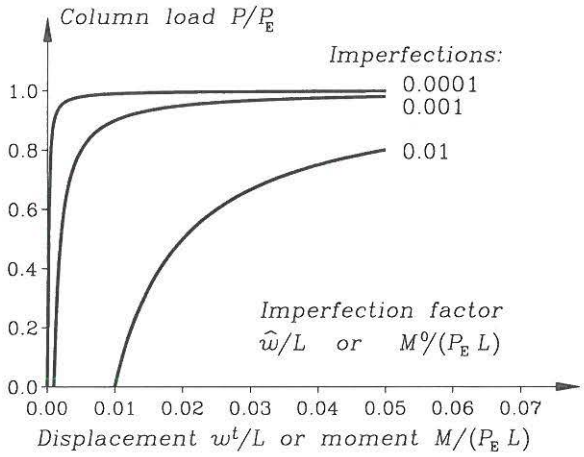

Fig. 3.13: Influence of initial imperfections or initial moments .

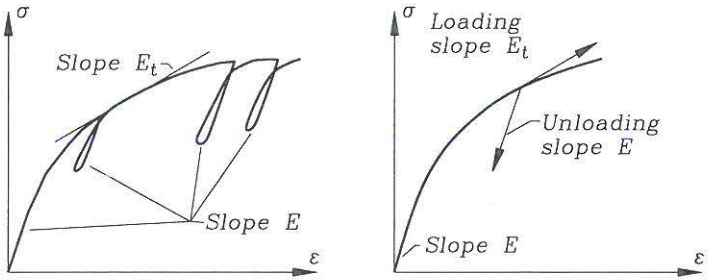

Fig. 3.14: Non-linear stress-strain relationship and the tangent-modulus.

Effect of Non-Linear Elasticity

The Euler formula found by Leonhard Euler in 1744 has formed the basis of column design since then. However, it has continuously been modified. First of all to account for plasticity and imperfections. Gere & Timoshenko [12] give a historical note on the development of the non-linear elastic buckling theory. In the present text the problem will just be introduced. For short columns, as already described, the Euler formula is limited by the yield stress. However, not all materials have a well defined yield stress as shown in fig. 3.14. For materials which have a non-linear stress-strain relationship it is necessary to modify Euler's buckling formula especially for the short columns. When the load on a perfect column increases the stiffness of the material is altered, as shown in fig. 3.14, and, as suggested by the German engineer F. Engesser in 1895, it is necessesary to use the tangent modulus $E_t = \frac{d\sigma}{d\varepsilon}$ instead of the initial modulus E in Euler's buckling formula.

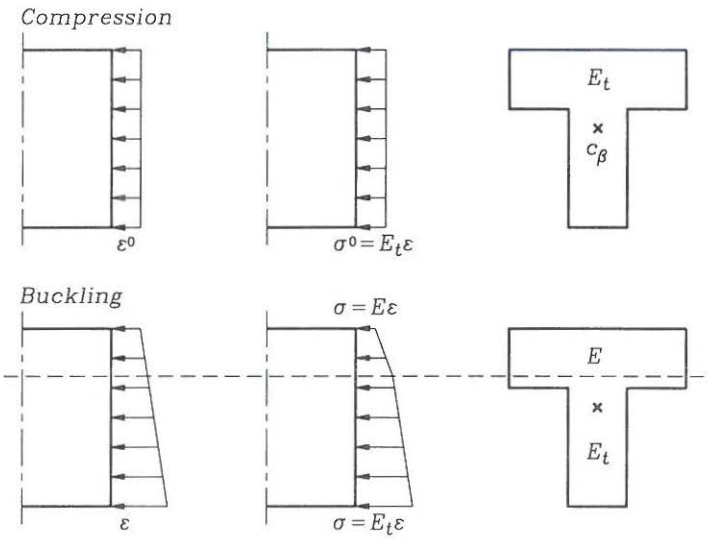

Fig. 3.15: Bending strains and stresses in column.

Engesscr's modified column formula

$$P_{E1} = \frac{\pi^2 E_t I}{L^2} \tag{3.35}$$

where $E_t = \partial\sigma/\partial\varepsilon$ is the tangent stiffness modulus

This is often referred to as Engesser's first column formula or just the Engesser theory. For the non-linear elastic column this is often used as the limiting column load. However, at this load the column starts buckling or let's say starts having small transverse displacements. When this occurs the column is further stressed on the compressed concave side, while on the convex side (not necessarily in tension) the stresses are reduced. This reduction of stress or local unloading of the material occurs with the larger initial stiffness modulus E as shown in fig. 3.14. The column bending stiffness is thus increased as the column begins to buckle. This leads to Engesser's second column formula, where the reduced stiffness modulus E_r is used instead. In fact the Euler formula holds the bending stiffness EI and it is this stiffness which is reduced to $(EI)_r$, seen from a global point of view. The reduced stiffness has to be calculated corresponding to the bending stiffness of a composite column which has a compressed material with stiffness modulus $E_t = \frac{d\sigma}{d\varepsilon}$ and a "tensioned" (stress reduced) material with the initial stiffness modulus $E = \left(\frac{d\sigma}{d\varepsilon}\right)_{\varepsilon=0}$ as illustrated in fig. 3.15. The reduced bending stiffness can thus be determined by cross-sectional analysis. However, as pointed out by Shanley in 1946, use of this stiffness in the Euler buckling formula is an upper bound, since

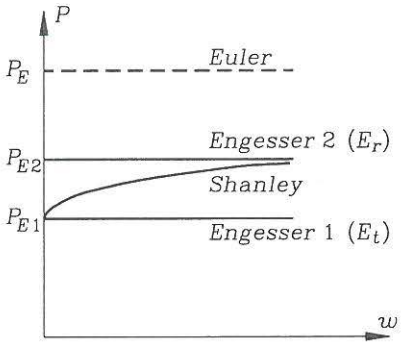

Fig. 3.16: Implications of Shanley's theory.

the column starts bending at Engesser's first column load using E_t, and due to the magnification (factor) of transverse displacements Engesser's second buckling load will not be reached, as illustrated in fig. 3.16. Shanley developed a theory on this basis. Today it is thus recognized that Engesser's first column load in manny cases gives an acceptable approximation of the column buckling load for non-linear elastic materials. Today, codes of practice often use different methods for the non-linear elastic materials, but most of them are based directly on on the above observations. Fig. 3.17 shows a buckling curve modified by the use of Engesser's theory for a material, which is linear elastic up to half of the compressive strength $\sigma_{pl} = 0.5 f_c$, and above this level plasticity gradually reduces the stiffness.

Effect of shear

The previous formulas have been derived using the assumptions of Euler-Bernoulli beam theory which covers most of the practical problems. However, for some problems, (short composite columns or columns of anisotropic material), shear effects might influence the buckling load and it will be necessary to use Timoshenko beam theory. For the uniformly compressed statically determinate column it is possible to derive the column buckling loads using exactly the same procedure, although complicated by the shear effects. It is assumed that the stiffness moduli and the cross-sectional parameters are constant. The constitutive relations for the moment M and shear force Q now are:

$$\alpha' = \frac{M}{EI} \tag{3.36}$$

$$\alpha + w' = \frac{Q}{\psi GA} \tag{3.37}$$

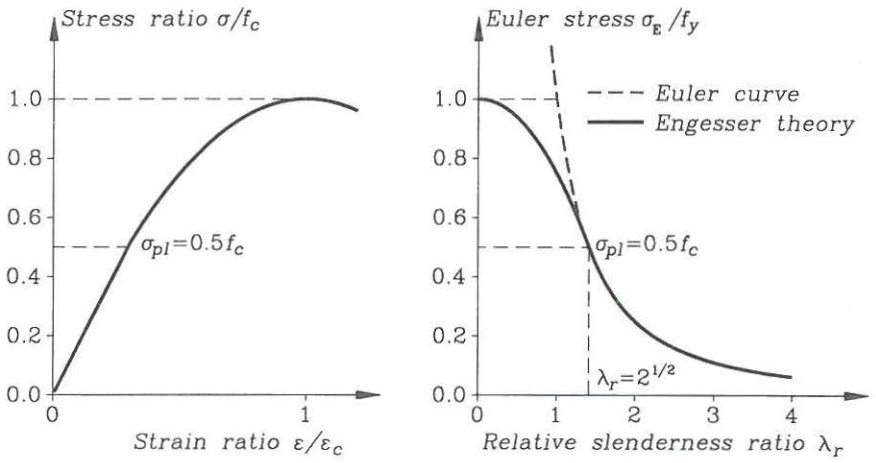

Fig. 3.17: Buckling curve using Engesser's theory.

Taking the axial derivative of the constitutive equation (3.37) and introducing the moment using the other constitive equation (3.36) we obtain

$$\frac{M}{EI} + w'' = \left(\frac{Q}{\psi GA}\right)' \tag{3.38}$$

The static relation between the moment and the shear force $Q = M'$ (no continuous moment load m) can now be used to eliminate the shear force. The kinematic/static differential equation for the column thus becomes

$$w'' = -\frac{M}{EI} + \left(\frac{M'}{\psi GA}\right)' \tag{3.39}$$

Moment equilibrium in the deformed position of the column results in $M = Pw$, which is inserted into this equation. After rearranging the terms this yields the column equation including shear effects

$$\begin{aligned} w'' &= -\frac{Pw}{EI} + \left(\frac{Pw'}{\psi GA}\right)' \qquad \Downarrow \\ \left(1 - \frac{P}{\psi GA}\right) w'' + k^2 w &= 0 \qquad \Downarrow \\ w'' + \tilde{k}^2 w &= 0 \end{aligned} \tag{3.40}$$

where the shear modified coefficient is

$$\tilde{k}^2 = \frac{k^2}{(1 - \frac{P}{\psi GA})} = \frac{P}{EI(1 - \frac{P}{\psi GA})} \tag{3.41}$$

The differential equation (3.40), which is an eigenvalue problem, has already been solved and the eigenvalues were found in equation (3.6). Using only the lowest non-zero eigenvalue and introducing the modified Euler column load $\tilde{P}_{\text{E}} = P$ we find

$$\begin{aligned} (\tilde{k}L)^2 &= \pi^2 \quad \Downarrow \\ \tilde{P}_{\text{E}} &= \frac{\pi^2 EI}{L^2(1+\pi^2\frac{EI}{\psi GA})} \end{aligned} \tag{3.42}$$

Thus, the Euler load is just modified by a simple factor. For isotropic materials the influence of this correction is negligible, but for anisotropic materials or composite columns like steel tubes filled with concrete the modification can be necessary.

The influence of initial moments can be determined from the non-homogeneous differential equation found by inserting $M = M^0 + Pw$ into equation (3.39)

$$w'' + \tilde{k}^2 w + \frac{M^0}{EI(1-\frac{P}{\psi GA})} - \frac{M^{0\prime\prime}}{\psi GA(1-\frac{P}{\psi GA})} = 0 \tag{3.43}$$

If we treat this equation as in the previous section it can be shown that the magnification factor is of the same type, the only difference being that the modified Euler column load should be used. The results concerning shear thus are:

The shear modified Euler buckling load is

$$\tilde{P}_{\text{E}} = \frac{P_{\text{E}}}{\eta} = \frac{\pi^2 EI}{\eta L^2} \tag{3.44}$$

where the shear modification factor is

$$\eta = 1 + \pi^2 \frac{EI}{\psi GA} \tag{3.45}$$

The magnification factor for initial moments and imperfections is

$$\zeta = \frac{\tilde{P}_{\text{E}}}{\tilde{P}_{\text{E}} - P} \tag{3.46}$$

This ends our discussion of the uniformly compressed columns and we shall turn to a general theoretical formulation of equilibrium in the deformed position and the equations for a general initial stress problem, including variation in the axial force.

- **Problem 3.1**
  Find the buckling load P of a linear elastic column with one end fixed and the other pinned. The column bending stiffness is EI and the column length is L.

  a) Find the moment variation in the deformed position and set up the differential equation.

  b) Solve the differential equation and use the boundary conditions to find the two lowest buckling loads by iteration (in kL).

c) Draw the transverse displacements (the eigenmodes) corresponding to the two lowest eigenvalues and illustrate the corresponding effective lengths.

- **Problem 3.2**

  A linear elastic column with pinned ends is loaded by a sinusodial transverse load $p(z) = \bar{p}\sin(\pi z/L)$. The column length is L and the bending stiffness is given as EI. The axial force in the column is $N^0 = -P$. The effect of shear is disregarded.

  a) Find the governing differential equation for this problem.

  b) Find the initial transverse displacements $w^0(z)$ of the column, when the axial load is zero $P = 0$ and state the maximum displacement W^0 and maximum initial moment M^0.

  c) Solve the differential equation from a) when the column is loaded by the transverse load $p(z)$ and is in compression $P > 0$.

  d) Find an expression for the maximum displacement W as a function of the axial load P and the maximum transverse load $\bar{p}$.

  e) Find an expression for the maximum total displacement W as a function of the axial load P, the column buckling load $P_E = \pi^2 EI/L^2$ and the initial displacement W^0. It should be compared with the magnification of initial displacements derived in the previous sections.

  f) Find an expression for the maximum moment M as a function of the axial load P, the column buckling load $P_E = \pi^2 EI/L^2$ and the initial moment M^0.

  g) Answer exactly the same questions from a) to f), when the transverse load is a constant load $p(z) = \hat{p}$. Furthermore, state the relative error when the approximate magnification factors are used in questions e) and f). (The error is measured relative to the exact result).

3.2 Linearized Stability Equations for Columns

The equilibrium equations for columns or beams can be derived in the deformed state. The internal forces must be related to the kinematic assumptions through strain definitions, which satisfy the principle of virtual work. These strain definitions become non-linear in the displacements and the equilibrium equations formulated in displacements are thus also non-linear in the displacements. In this section a linearized version of these equations will be formulated including initial stress to enable stability analysis. The non-linear equilibrium equations for a theory with non-linear infinitesimal strains and moderate (infinitesimal) rotations are derived in the last two subsections.

There are many related approaches to the derivation of linearized stability equations for columns. In the present section some of these approaches will be used to derive the same basic equations. The approaches are a little different, but each of them enlightens the basic structural theory and the modern methods in their own way. The stability equations will first be derived by equilibrium considerations for a column element with an initial stress field, then the virtual work functional for an initial stress problem will be used. The reader can then jump to the next section on

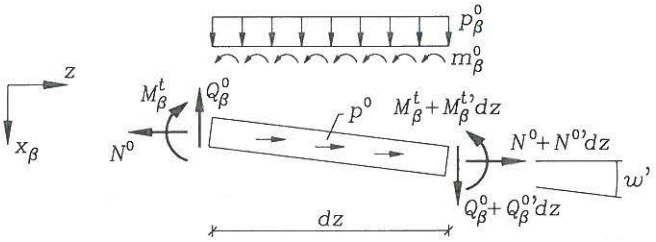

Fig. 3.18: Small displacement of column with initial stress.

approximate analysis or carry on to derive general non-linear equilibrium equations. The non-linear equations are linearized for stability analysis using Euler's initial stress method. The non-linear equilibrium equations are first derived directly in component form using a deformed geometric element and then using a vector based formulation on a more regular element.

The treatment is limited to Euler-Bernoulli beams, but the methods can be generalized, where necessary, to accommodate Timoshenko beam theory. The index notation is used again for the two transverse directions of a column. However, we assume that the column bends about the elastic centre c_β, i.e. $S_\beta = 0$, and that the principal axes are used $I_{12} = 0$.

Initial Stress Approach

A column is assumed to be in an initial state of stress N^0, Q^0_β and M^0_β, which fulfils the linear equilibrium equations with the initial loads p^0 and p^0_β

$$\begin{aligned} N^{o\prime} + p^0 &= 0 \\ M^{o\prime\prime}_\beta + m^{o\prime}_\beta + p^0_\beta &= 0 \end{aligned} \tag{3.47}$$

To see if an adjacent secondary equilibrium path exists it is assumed that the column undergoes small transverse displacements with moderate rotations and that the internal forces N^0, Q^0_β and M^0_β can be decomposed in the original base, $\mathbf{i}_\beta$ and $\mathbf{i}_3$, with acceptable approximation. Equilibrium of the column with initial stress is sought in the deformed position as shown in fig. 3.18 for the total moment $M^t_\beta = M^0_\beta + M_\beta$. It is seen that the longitudinal, transverse and moment equilibrium equations become

$$\begin{aligned} N^{o\prime} + p^0 &= 0 \\ Q^{o\prime} + p^0_\beta &= 0 \\ M^{t\prime}_\beta - Q^0_\beta + N^0 w'_\beta + m^0_\beta &= 0 \end{aligned} \tag{3.48}$$

The last two equations can be combined and we can use that $M^t_\beta = M^0_\beta + M_\beta$. Furthermore, we can use that the initial moments M^0_β are in equilibrium and thereby

find the stability equations:

$$M''_\beta + (N^0 w'_\beta)' = 0 \tag{3.49}$$

By inserting the constitutive relation and changing sign we find the governing linearized stability equations for columns in compression ($N^0 < 0$).

The general linearized stability equations for columns are $S_\beta = 0$

$$(EI_{\beta\alpha} w''_\alpha)'' + (-N^0 w'_\beta)' = 0 \tag{3.50}$$

When the bending stiffnesses $EI_{\alpha\beta}$ are constant and when the principal axes are used $I_{12} = 0$ these equations simplify to

$$\begin{aligned} w_1'''' + (k_1^2 w'_1)' &= 0 \\ w_2'''' + (k_2^2 w'_2)' &= 0 \end{aligned} \tag{3.51}$$

in which

$$k_1^2 = \frac{-N^0}{EI_{11}} \qquad k_2^2 = \frac{-N^0}{EI_{22}} \tag{3.52}$$

These equations are basicly the same as found in the previous section in equation (3.19), but with the possibility of a varying axial force. In the present formulation it becomes clear that the column can buckle with displacements in one of two transverse coordinate directions, depending on which bending stiffness is the smallest. Note that the sign in front of the factor k_α^2 changes in case of a tensile force ($N^0 > 0$), whereby the solutions become linear combinations of the hyperbolic sine and cosine functions.

The boundary conditions in this secondary stability problem are dictated by the fact that the column is already in equilibrium and that the additional moments should not alter this basic global equilibrium situation

$$\begin{aligned} \bar{M}_\beta &= 0 \\ \bar{Q}_\beta &= 0 \end{aligned} \tag{3.53}$$

The virtual work functional δW_2 related to this secondary problem can be found by multiplying the stability equations (3.49) by the virtual transverse displacements δw_β. After two partial integrations and a change of sign to obtain positive internal work it is found that

$$\delta W_2 = \int_0^L (M_\beta \delta\kappa_\beta + N^0 w'_\beta \delta w'_\beta)\, dz - [(M'_\beta + N^0 w'_\beta)\delta w_\beta - M_\beta \delta w'_\beta]_0^L \tag{3.54}$$

Identifying the boundary terms yields

$$\begin{aligned} \bar{M}_\beta &= M_\beta|_{z_b} = 0 \\ \bar{Q}_\beta &= (M'_\beta + N^0 w'_\beta)\big|_{z_b} = 0 \end{aligned} \tag{3.55}$$

in which z_b is the boundary coordinate. With the extra demand that the static boundary conditions above are fulfilled the virtual work functional thus becomes

$$\delta W_2 = \int_0^L (M_\beta \delta\kappa_\beta + N^0 w'_\beta \delta w'_\beta)\ dz \tag{3.56}$$

Assuming that the boundary forces vanish, the related potential energy functional is found as

$$V_2 = \int_0^L (\frac{1}{2} M_\beta \kappa_\beta + \frac{1}{2} w'_\beta N^0 w'_\beta)\ dz \tag{3.57}$$

In all the above functionals the curvature is defined as $\kappa_\beta = -w''_\beta$ and positive rotations as $-w'_\beta$.

This approach is in a way classic, however, the internal forces do not follow the rotation of the cross-sections, which is not consistent with the stress description given in the preliminary chapter on continuum mechanics, since it contradicts the idea of using Piola-Kirchhoff stresses in the deformed state. This is also emphasized by the boundary equation delivered by the principle of virtual work. However, the total internal force vector could be decomposed as done here, but the components are not necessarily the conventional internal forces and it would be necessary to review our geometric description and strain definitions. The stability equations found are the same as those derived by other methods.

Virtual Work Approach

Notice that the column stability equation (3.49) has the same format as the initial stress equation (1.135) derived in the continuum mechanics section of the chapter on preliminaries. An alternative approach as opposed to the preceding subsection is to use the virtual work functional (1.137) derived for initial stress problems in general continuae. This is the approach which is used in the chapter on beam theories and it has the advantage of being much more like a tool, than a way of reinventing everything each time a new theory or an extension of an existing theory has to be developed. Let us use this approach for the initial stress problem of a column.

Inserting the kinematic assumptions of Euler-Bernoulli theory into the virtual work functional with initial stress (1.137) leads to the virtual work functional for an Euler-Bernoulli beam δW given in equation (2.53) plus an additional contribution δW^0 from the initial stress terms

$$\begin{aligned} \delta W^0 &= \int_V \sigma^0_{ij} u_{k,j}\ \delta u_{k,i}\ dV \\ &\simeq \int_V \sigma^0_{ij} \omega_{kj}\ \delta\omega_{ki}\ dV \end{aligned} \tag{3.58}$$

where it is assumed that the strains ε_{ij} are infinitesimal and well approximated by the linear strain definitions, and the rotations ω_{ij} are moderate but infinitesimal, i.e. $\varepsilon_{ij} \ll \omega_{ij} \ll 1$. This enables us to make the approximation $u_{k,j} = \varepsilon_{kj} + \omega_{kj} \simeq \omega_{kj}$, see the derivations leading to equation (1.75). Be aware of the small difference in notation between transverse displacements w_β and rotations (omega) ω_{ij} used

in the present text. Using the beam kinematics the additional virtual work term becomes

$$\begin{aligned}\delta W^0 &= \int_V \sigma^0_{33}\omega_{\beta 3}\,\delta\omega_{\beta 3}\,dV \\ &= \int_V \sigma^0 w'_\beta\,\delta w'_\beta\,dV \\ &= \int_0^L N^0 w'_\beta\,\delta w'_\beta\,dz \end{aligned} \tag{3.59}$$

where it has been used that $\omega_{33} = \omega_{\alpha\beta} = 0$, $\omega_{\beta 3} = \frac{1}{2}(u_{\beta,3} - u_{3,\beta}) = w'_\beta$ and that $N^0 = \int_A \sigma^0\,dA$. The total virtual work functional for an Euler-Bernoulli beam with initial stress thus is

$$\begin{aligned}\delta W &= \int_0^L (N\,\delta\bar{\varepsilon} + M_\beta\,\delta\kappa_\beta + N^0 w'_\beta\,\delta w'_\beta \\ &\qquad -p\,\delta v - p_\beta\,\delta w_\beta + m_\beta\,\delta w'_\beta)\,dz \\ &\quad - \left[\bar{N}\,\delta v - \bar{M}_\beta\,\delta w'_\beta + \bar{Q}_\beta\,\delta w_\beta\right]_0^L \end{aligned} \tag{3.60}$$

This is the virtual work for a genereneral initial stress problem. Introducing the linear strain definitions and using partial integration up to two times yield the following modified virtual work equation

$$\begin{aligned}\delta W &= -\int_0^L \left((N' + p)\delta v + (M''_\beta + (N^0 w'_\beta)' + m'_\beta + p_\beta)\delta w_\beta\right)\,dz \\ &\quad - \left[(\bar{N} - N)\,\delta v - (\bar{M}_\beta - M_\beta)\,\delta w'_\beta \right. \\ &\qquad \left. +(\bar{Q}_\beta - M'_\beta - N^0 w'_\beta - m_\beta)\,\delta w_\beta\right]_0^L \end{aligned} \tag{3.61}$$

If the virtual work vanishes $\delta W = 0$ for any variation in the kinematic parameters, then the beam is in equilibrium. For internal variations δv and δw_β we thereby find the equilibrium equations

$$\begin{aligned} N' + p &= 0 \\ M''_\beta + (N^0 w'_\beta)' + m'_\beta + p_\beta &= 0 \end{aligned} \tag{3.62}$$

and by variation of the boundary displacements we find the boundary conditions and in fact also the correct definitions of the internal forces:

$$\begin{aligned} \bar{N} &= N \\ \bar{Q}_\beta &= M'_\beta + N^0 w'_\beta + m_\beta \\ \bar{M}_\beta &= M_\beta \end{aligned} \tag{3.63}$$

whereby it can be seen that it is only the internal shear force Q_β which needs redefinition for an initial stress problem.

However, it is the possibility of an adjacent secondary load path, which is sought in the present situation. As already mentioned all loads are carried by the initial state, and the secondary state does not carry any additional load (except through

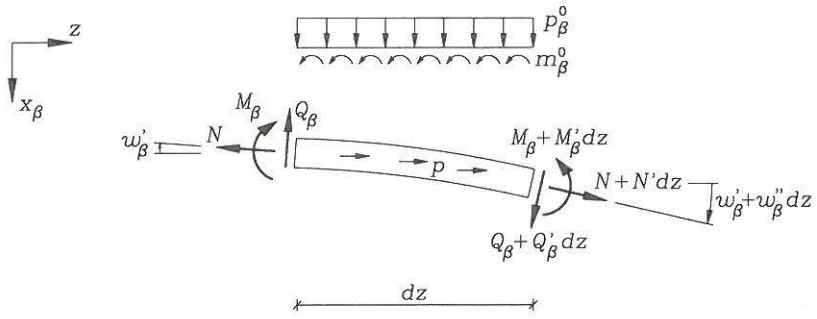

Fig. 3.19: Deformed infinitesimal beam element with curvature.

the initial stress), whereby we have $p = p_\beta = m_\beta = 0$, nor should there be any additional boundary loads $\bar{N} = \bar{Q}_\beta = \bar{M}_\beta = 0$. This leaves us with the following virtual work functional:

$$\delta W_2 \;=\; \int_0^L \left(N\,\delta\bar{\varepsilon} + M_\beta\,\delta\kappa_\beta + N^0 w'_\beta\,\delta w'_\beta\right) dz \tag{3.64}$$

and the following non-trivial stability equation

$$M''_\beta + (N^0 w'_\beta)' \;=\; 0 \tag{3.65}$$

which has already been found in the preceding section.

This ends the present subsection and the reader may go directly to the section on approximate stability analysis or read through the next two sections to see the derivation of the non-linear equilibrium equations for beams and the subsequent initial stress linearizations.

Component Approach

In this subsection it is the goal first to derive the equilibrium equations for a column or beam section in the deformed state and then to outline the introduction of initial stress and the linearization of the equilibrium equations. We shall dwell a little by the non-linear equilibrium equations in the deformed state and introduce the related strain definitions.

It is assumed that the stress components follow the deforming material base and that the geometry of the cross-section and the axial coordinate are described adequately by the undeformed state. It is also assumed that the non-linear strains are infinitesimal and rotations are moderate but infinitesimal, i.e. $\varepsilon_{ij} \ll \omega_{ij} \ll 1$. A deformed infinitesimal beam element with curvature is shown in fig. 3.19. Since the rotations are moderate the following approximations will be adequate:

$$\begin{aligned} \cos(w'_\beta) &\simeq 1 & \cos(w'_\beta + w''_\beta dz) &\simeq 1 \\ \sin(w'_\beta) &\simeq w'_\beta & \sin(w'_\beta + w''_\beta dz) &\simeq w'_\beta + w''_\beta dz \end{aligned} \tag{3.66}$$

Let us set up the three equilibrium equations neglecting the terms $(dz)^2$ which vanish in the infinitesimal limit. The loads are also assumed to keep their original direction. Using fig. 3.19 we find the following axial, transverse and moment equilibrium equations by first considering the left-hand end, then the right-hand end components and finally the loads. Moment equilibrium is sought about the right-hand end and the internal forces are projected on the original base directions before the moment contribution is found.

$$\begin{aligned} -N + Q_\beta w'_\beta + N + N'dz - Q(w'_\beta + w''_\beta dz) - Q'_\beta dz\, w'_\beta + p\, dz &= 0 \\ -Q_\beta - Nw'_\beta + Q_\beta + Q'_\beta dz + N(w'_\beta + w''_\beta dz) + N'w''_\beta dz + p_\beta\, dz &= 0 \\ -M_\beta + (N - Q_\alpha w'_\alpha)w'_\beta dz - (Nw'_\beta + Q_\beta)dz + M_\beta + M'_\beta dz + m_\beta dz &= 0 \end{aligned} \tag{3.67}$$

Cancellation of terms and division by dz yield the following result

$$\begin{aligned} N' - (Q_\beta w'_\beta)' + p &= 0 \\ Q'_\beta + (Nw'_\beta)' + p_\beta &= 0 \\ M'_\beta - Q_\beta(1 + w'_\alpha w'_\alpha) + m_\beta &= 0 \end{aligned} \tag{3.68}$$

In the following, some of our assumptions are put into use. Since the rotations are moderately infinitesimal their products will be even smaller and the approximation $1 + w'_\alpha w'_\alpha \simeq 1$ can be made. It is further assumed that the shear forces Q_β are small compared to the axial force N. This is in agreement with beam theories since the shear strains are an order of magitude lower than the axial strains. Using that AG has the same order of magnitude as EA it can be clarified as follows

$$\begin{aligned} Q_\beta &\ll N \quad \Downarrow \\ AG\gamma_\beta &\ll EA\varepsilon \quad \Downarrow \\ \gamma &\ll \varepsilon \end{aligned} \tag{3.69}$$

which is an assumption already made in beam theory, in Euler-Bernoulli beam theory it is used directly, since $\gamma_\beta = 0$. In Timoshenko beam theory it is also assumed that the shear strains are an order of magnitude lower than the axial stresses. The implication of this is that in the axial equilibrium equation the term $Q_\beta w'_\beta$ is much smaller than N and can be disregarded. In the transverse equilibrium equation we need to keep all terms since Q_β is of the same magnitude as Nw'_β. The equilibrium equations for a beam element in the deformed configuration thus are:

Equilibrium equations for a deformed beam element are:

$$\begin{aligned} N' + p &= 0 \\ Q'_\beta + (Nw'_\beta)' + p_\beta &= 0 \\ M'_\beta - Q_\beta + m_\beta &= 0 \end{aligned} \tag{3.70}$$

and by combining the last two equations they can be rewritten as

$$\begin{aligned} N' + p &= 0 \\ M''_\beta + (Nw'_\beta)' + m'_\beta + p_\beta &= 0 \end{aligned} \tag{3.71}$$

The strain definitions related to these internal forces and equilibrium equations must satisfy the principle of virtual work, if the theory is to be consistent. We multiply the equations (3.71) by virtual displacements $-\delta v$ and $-\delta w_\beta$ and use up to two partial integrations, whereby the following virtual work is found

$$\begin{aligned}\delta W &= \int_0^L \Big(N(\delta v' + w'_\beta\,\delta w'_\beta) - M_\beta\,\delta w''_\beta \\ &\qquad -p\,\delta v - p_\beta\,\delta w_\beta + m_\beta\,\delta w'_\beta\Big)\,dz \\ &\quad - \Big[N\,\delta v - M_\beta\,\delta w'_\beta + (M'_\beta + N w'_\beta + m_\beta)\,\delta w_\beta\Big]_0^L \end{aligned} \tag{3.72}$$

The stationarity of this virtual work functional defines the shear force through the boundary terms as $\bar{Q}_\beta = M'_\beta + N w'_\beta + m_\beta$ and the related strains as

$$\begin{aligned}\bar{\varepsilon} &= v' + \frac{1}{2} w'_\beta w'_\beta \\ \kappa_\beta &= -w''_\beta \end{aligned} \tag{3.73}$$

since $\delta\bar{\varepsilon} = \delta v' + w'_\beta \delta w'_\beta$ and $\delta\kappa_\beta = -\delta w''_\beta$. It is thus clear that the equilibrium equations are non-linear in the displacements. Using Hooke's constitutive law $\sigma = E\varepsilon$ the non-linear equilibrium equations with the assumptions of Euler-Bernoulli beam theory can be found by subsitituion of the strain definitions (3.73) into the equations in (3.71).

Non-linear differential equations for infinitesimal strains and moderate rotations

$$\begin{aligned}\Big(EA(v' + \frac{1}{2} w'_\alpha w'_\alpha)\Big)' + p &= 0 \\ (EI_{\beta\alpha} w''_\alpha)'' - \Big(EA(v' + \frac{1}{2} w'_\alpha w'_\alpha) w'_\beta\Big)' - m'_\beta - p_\beta &= 0 \end{aligned} \tag{3.74}$$

Since these equations are non-linear and coupled, it is necessary to use computerized approximation techniques to solve them.

The static equilibrium equations for a beam in the deformed state (3.71) can be used to derive the linearized stability equations by the use of Euler's initial stress method. Assuming that the problem is an initial stress problem the total internal forces $N^t = N^0 + N$ and $M^t_\beta = M^0_\beta + M_\beta$ and the total loads can be inserted $p^t = p^0 + p$, $p^t_\beta = p^0_\beta + p_\beta$, and $m^t_\beta = m^0_\beta + m_\beta$ into the above non-linear equations. Using that the initial stress field satisfies the linear equilibrium equations, linearizing the equations with respect to the displacement and using that the loads in the adjacent state are zero we find the linearized stability equations for columns (3.49) and (3.50).

Vector Approach

Let us try an alternative approach and derive the non-linear equilibrium equations using a vectorized approach. An infinitesimal beam element is shown in fig. 3.20 in

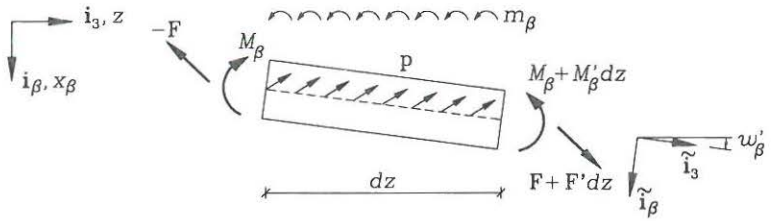

Fig. 3.20: Infinitesimal beam element in the deformed position.

the deformed position. The internal force vector $\mathbf{F}$ and its differential $d\mathbf{F}$ can be decomposed in the deformed material base $\tilde{\mathbf{i}}_\beta$ and $\tilde{\mathbf{i}}_3$ as follows

$$\begin{aligned} \mathbf{F} &= N\tilde{\mathbf{i}}_3 + Q_\beta \tilde{\mathbf{i}}_\beta \\ d\mathbf{F} &= \mathbf{F}'dz = (N\tilde{\mathbf{i}}_3 + Q_\beta \tilde{\mathbf{i}}_\beta)'dz \end{aligned} \tag{3.75}$$

Since the deformed material base is dependent on the axial coordinate through the displacements these must also be differentiated with respect to the axial coordinate z. The equilibrium equations in this vector format are

$$\begin{aligned} \mathbf{F}' + \mathbf{p} &= \mathbf{0} \\ M'_\beta - \mathbf{F} \cdot \tilde{\mathbf{i}}_\beta + m_\beta &= 0 \end{aligned} \tag{3.76}$$

The moment of the internal force vector $\mathbf{F}$ is found by projection on the transverse direction $\tilde{\mathbf{i}}_\beta$ and multiplication by the distance dz. The load vector is decomposed in the original base $\mathbf{p} = p\mathbf{i}_3 + p_\beta \mathbf{i}_\beta$ and the internal force vector is also decomposed, whereby the equilibrium equations take the form

$$\begin{aligned} (N\tilde{\mathbf{i}}_3 + Q_\beta \tilde{\mathbf{i}}_\beta)' + p\mathbf{i}_3 + p_\beta \mathbf{i}_\beta &= 0 \\ M'_\beta - (N\tilde{\mathbf{i}}_3 + Q_\alpha \tilde{\mathbf{i}}_\alpha) \cdot \tilde{\mathbf{i}}_\beta + m_\beta &= 0 \end{aligned} \tag{3.77}$$

Assuming infinitesimal strains and moderate rotations, $\varepsilon_{ij} \ll \omega_{ij} \ll 1$, i.e. strains are smaller than the rotations, the following approximation is appropriate:

$$\tilde{\mathbf{i}}_k \simeq (\delta_{jk} + \omega_{jk})\mathbf{i}_j \tag{3.78}$$

Splitting into axial and transverse base vectors and inserting the Euler-Bernoulli displacement assumptions we find

$$\begin{aligned} \tilde{\mathbf{i}}_3 &= \mathbf{i}_3 + w'_\beta \mathbf{i}_\beta \\ \tilde{\mathbf{i}}_\beta &= \mathbf{i}_\beta - w'_\beta \mathbf{i}_3 \end{aligned} \tag{3.79}$$

This is in agreement with our displacement assumptions shown in fig. 3.20. However, since we assume that the strains are infinitesimal the deformed base is still approximately an orthonormal system, whereby the scalar products between the deformed base vectors can be approximated by

$$\tilde{\mathbf{i}}_j \cdot \tilde{\mathbf{i}}_k \simeq \delta_{jk} \tag{3.80}$$

This can be used in the moment equilibrium equation. The approximation corresponds to the one made in the previous section regarding the term $1 + w'_\alpha w'_\alpha \simeq 1$. Decomposing the equilibrium equations in the original base and using our displacement assumptions give:

$$\begin{aligned} \left((N - Q_\beta w'_\beta)' + p\right)\mathbf{i}_3 + \left((Q_\beta + N w'_\beta)' + p_\beta\right)\mathbf{i}_\beta &= \mathbf{0} \\ M'_\beta - Q_\alpha \delta_{\alpha\beta} + m_\beta &= 0 \end{aligned} \tag{3.81}$$

Splitting the vector equation into the axial and transverse equations yields the following equilibrium equations

$$\begin{aligned} N' - (Q_\beta w'_\beta)' + p &= 0 \\ Q'_\beta + (N w'_\beta)' + p_\beta &= 0 \\ M'_\beta - Q_\beta + m_\beta &= 0 \end{aligned} \tag{3.82}$$

As in the preceding subsection we assume that the shear force is an order of magnitude lower than the axial force, i.e. $Q_\beta \ll N$ or $\gamma_\beta \ll \varepsilon$, which is in agreement with Euler-Bernoulli theory. The same non-linear equilibrium equations as in the previous subsection are found

$$\begin{aligned} N' + p &= 0 \\ Q'_\beta + (N w'_\beta)' + p_\beta &= 0 \\ M'_\beta - Q_\beta + m_\beta &= 0 \end{aligned} \tag{3.83}$$

in which we could combine the last two equations and proceed as in the previous subsection. This concludes our quick tour through formulation of equilibrium equations in the deformed state and subsequent linearizations.

3.3 Approximate Stability Analysis

The virtual work or potential energy functionals are used as the basis for approximate analysis in most problems of structural mechanics. Conventionally a set of (guessed) trial functions is used to estimate the displacement field or the force field. By use of a stationarity condition the combination of trial functions that minimize the work can be found. In this section two well-known methods of approximate analysis, namely the Galerkin method and the Rayleigh-Ritz method, will be outlined and used to give two versions of the Rayleigh coefficient. The Rayleigh coefficient gives an upper estimate of the buckling load. Furthermore as an extra precaution the magnification factor is treated again, since the buckling load represents a mathematical limit. Due to transverse loads and imperfections structures will behave differently, with a magnification of initial transverse deflections and initial moments. In this section the index notation is aborted and it is assumed that c_β is the elastic centre, i.e. $S_\beta = 0$, and let us work in a principal plane, i.e. $I_{12} = 0$.

The Galerkin Method

The Galerkin method is related to the principle of virtual work, even though it is not based on the (weak form) virtual work functional. The Galerkin method originates from the equilibrium equations (the strong form). In the present case of beam buckling the equilibrium equation is:

$$M'' + \lambda(N^0 w')' = 0 \tag{3.84}$$

in which we have introduced λ as a scale factor for a certain distribution of the axial force $N^0(z)$. The scale factor is thus independent of the axial coordinate z. In the Galerkin method the next step is to define a functional by multiplying the equilibrium equations by some weight functions $\eta(z)$ and integrating over the domain. Instead of taking the multiplicator function as a weight function we might as well take it as a virtual displacement function $\eta(z) = \delta w(z)$. We thus find the virtual work of the out of balance forces

$$\delta W = \int_L M'' \delta w \, dz + \lambda \int_L (N^0 w')' \delta w \, dz \tag{3.85}$$

For equilibrium the virtual work of forces should vanish, $\delta W = 0$. Using the constitutive relation for the moment, $M = -EIw''$, the principle of virtual work results in

$$\delta W = \int_L (EIw)'' \delta w \, dz + \lambda \int_L (N^0 w')' \delta w \, dz = 0 \tag{3.86}$$

Trial functions for the displacements $\tilde{w}$ and trial functions for the virtual displacements $\tilde{\eta}$ can now be inserted. It is important that the trial functions for the displacements are chosen so that the static boundary conditions (for example $\widetilde{M} = 0$ or $\widetilde{Q} = \widetilde{M}' = 0$) are satisfied and the trial functions for the virtual displacements must fulfil the kinematic boundary conditions (for example $\eta = \delta\tilde{w} = 0$ or $\eta' = \delta\tilde{w}' = 0$). The static boundary conditions have to be fulfilled, since the virtual work used does not include the work of the boundary forces. Instead of using two different sets of trial functions it is customary but not necessary to choose the same functions, so that $\tilde{\eta} = \tilde{w}$. The trial functions thus have to fulfil both static and kinematic boundary conditions.

Assuming that we only have one trial function $\tilde{w}(z)$ the principle of virtual work defines the critical value of the parameter λ as a coefficient known as the Rayleigh coefficient:

The Rayleigh buckling coefficient (based on the strong form)

$$\lambda = -\frac{\int_L (EI\tilde{w}'')''\tilde{w} \, dz}{\int_L (N^0\tilde{w}')'\tilde{w} \, dz} \tag{3.87}$$

in which the trial function $\tilde{w}(z)$ satisfies the static and the kinematic boundary conditions. The coefficient λ is an upper bound for the buckling load.

The Rayleigh coefficient gives an upper-bound value for the buckling load and this is explained as follows. When we assume a displacement trial function it does not

give the best possible minimum of internal work, which means that the numerator becomes too large. When the assumed displacement trial function absorbes too much work it becomes too stiff and the displacements smaller. The denominator therefore becomes too small and the Rayleigh coefficient is an upper bound.

Instead of using one trial function a linear combination of trial functions might be used for both displacements and virtual displacements

$$\begin{aligned} \tilde{w} &= \sum_{j=1}^{n} c_j \tilde{w}_j = \tilde{\mathbf{w}}^T \mathbf{c} \\ \delta\tilde{w} &= \sum_{i=1}^{n} (\delta c_i)\tilde{w}_i = (\delta \mathbf{c})^T \tilde{\mathbf{w}} \end{aligned} \tag{3.88}$$

where the coefficients c_j ordered in a vector $\mathbf{c}$ are the scale parameters of the individual displacement trial functions $\tilde{w}_j$, which are also ordered in a trial vector $\tilde{\mathbf{w}}$. The coefficients δc_i or $\delta \mathbf{c}$ are the virtual displacement coefficients for the same trial functions. With this notation we introduce the trial functions in the virtual work functional (3.86) as follows

$$\begin{aligned} \delta W &= \sum_{j=1}^{n}\sum_{i=1}^{n} \left(\int_L c_j (EI\tilde{w}_j'')''\tilde{w}_i \, \delta c_i dz + \lambda \int_L c_j (N^0 \tilde{w}_j')'\tilde{w}_i \, \delta c_i dz \right) \\ &= \delta \mathbf{c}^T \int_L \tilde{\mathbf{w}} \left((EI\tilde{\mathbf{w}}'')'' \right)^T dz \, \mathbf{c} + \lambda \, \delta \mathbf{c}^T \int_L \tilde{\mathbf{w}} \left((N^0 \tilde{\mathbf{w}}')' \right)^T dz \, \mathbf{c} \\ &= \delta \mathbf{c}^T \mathbf{A} \mathbf{c} + \lambda \, \delta \mathbf{c}^T \mathbf{B} \mathbf{c} \\ &= \delta \mathbf{c}^T (\mathbf{A} + \lambda \, \mathbf{B}) \mathbf{c} \end{aligned} \tag{3.89}$$

in which the matrices $\mathbf{A}$ and $\mathbf{B}$ have the following components

$$\begin{aligned} A_{ij} &= \int_L (EI\tilde{w}_j'')''\tilde{w}_i \, dz \\ B_{ij} &= \int_L (N^0 \tilde{w}_j')'\tilde{w}_i \, dz \end{aligned} \tag{3.90}$$

Note that the order of the indices is important. The virtual work should vanish, $\delta W = 0$, in order that an equilibrium state may exist. Since the weight functions or rather the virtual displacement coefficient vector $\delta \mathbf{c}$ can be chosen arbitrarily, the following eigenvalue equation must be satisfied:

$$\begin{aligned} \delta \mathbf{c}^T (\mathbf{A} + \lambda \mathbf{B}) \mathbf{c} &= 0 \quad \Downarrow \\ (\mathbf{A} + \lambda \mathbf{B}) \mathbf{c} &= \mathbf{0} \end{aligned} \tag{3.91}$$

This is a linear eigenvalue problem defining the critical values of λ and the corresponding linear coefficients $\mathbf{c}$ of the trial functions, which in turn define the displacement eigenmodes by $w = \tilde{\mathbf{w}}^T \mathbf{c}$. Note that the matrices $\mathbf{A}$ and $\mathbf{B}$ are not symmetric. The estimated critical values are upper-bound values and the lower eigenvalues are decreased by increasing the number of trial functions or using intuitivelly well chosen trial functions.

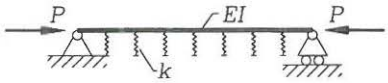

Fig. 3.21: Column with continuous transverse elastic springs.

The Rayleigh-Ritz Method

The Rayleigh-Ritz method is directly based on the stationarity of potential energy or the principle of virtual work formulated in stresses and strains, (the weak form). In the case of linearized stability analysis for an Euler-Bernoulli beam the virtual work functional takes the form

$$\delta W = \int_L EIw''\,\delta w''\,dz + \lambda \int_L N^0 w'\,\delta w'\,dz \tag{3.92}$$

in which λ is introduced as a scale factor for a specific distribution of the axial force $N^0(z)$. In this functional it is only necessary to fulfil the kinematic boundary conditions. In the Rayleigh-Ritz procedure we can choose to use the same trial functions for displacements and virtual displacements. This is natural, since it is clear that we are dealing with displacements in both situations. By using a single trial function for the displacements $\tilde{w}$, inserting it in the virtual work functional and using the principle of virtual work $\delta W = 0$ another form of the Rayleigh coefficient is found.

The Rayleigh buckling coefficient (based on the weak form)

$$\lambda = -\frac{\int_L EI\tilde{w}''\tilde{w}''\,dz}{\int_L N^0\tilde{w}'\tilde{w}'\,dz} \tag{3.93}$$

in which the trial function $\tilde{w}(z)$ satisfies the kinematic boundary conditions. The coefficient λ is an upper bound for the buckling load.

It is seen that this is much easier to work with since only first and second order derivatives of the displacements are involved. The accuracy of the approximation is also increased, since only the double derivative of a trial function is necessary. It is also much easier just to fulfil the kinematic boundary conditions.

- **Example 3.2** Column in an elastic medium.

  Let us use the principle of virtual work to analyse a column with pinned ends and with continuous elastic transverse springs, as shown in fig. 3.21. It is a compressed beam on elastic foundation, e.g. a rail in compression due to temperature expansion. To take the continuous elastic spring support into account we add the virtual work term corresponding to a continuous load $p(z) = -kw(z)$ where k is the spring stiffness per column length. The additional virtual work due to the elastic medium becomes

$$\delta W_k = -\int_L p\,\delta w\,dz = \int_L kw\,\delta w\,dz$$

corresponding to the first variation of a continuous spring potential of $\frac{1}{2}kw^2$. Assuming that the bending stiffness is constant and that the axial force is a contamt compression $N^0 = -P$ the Rayleigh coefficient, which is thus modified by the spring stiffness term, becomes

$$P = \frac{\int_L (EI\tilde{w}''\tilde{w}'' + k\tilde{w}\tilde{w})\, dz}{\int_L \tilde{w}'\tilde{w}'\, dz}$$

Let us use a sinusodial trial function with n buckles, which has the following properties:

$$\tilde{w} = \sin(n\pi\frac{z}{L}) \qquad \tilde{w}' = \frac{n\pi}{L}\cos(n\pi\frac{z}{L}) \qquad \tilde{w}'' = -(\frac{n\pi}{L})^2\sin(n\pi\frac{z}{L})$$

$$\int_0^L \tilde{w}^2 dz = \frac{L}{2} \qquad \int_0^L (\tilde{w}')^2 dz = \left(\frac{n\pi}{L}\right)^2\frac{L}{2} \qquad \int_0^L (\tilde{w}'')^2 dz = \left(\frac{n\pi}{L}\right)^4\frac{L}{2}$$

Inserting these functions the following buckling load is found

$$\begin{aligned} P &= \frac{EI\,(\frac{n\pi}{L})^4 + k}{(\frac{n\pi}{L})^2} \\ &= EI\left(\frac{n\pi}{L}\right)^2 + k\left(\frac{L}{n\pi}\right)^2 \end{aligned}$$

This is a classical result and it can be shown to be exact. The lowest buckling load depends on the stiffness parameters EI, k and the column length L. In each case the value of n minimizing the buckling load must be found.

In the column example a trial function was chosen that in fact held infinitely many functions. Let us instead introduce the Rayleigh-Ritz procedure where we introduce a linear combination of trial functions as in the previous subsection.

$$\begin{aligned} \tilde{w} &= \sum_{j=1}^{n} c_j\tilde{w}_j = \tilde{\mathbf{w}}^T\mathbf{c} \\ \delta\tilde{w} &= \sum_{i=1}^{n}(\delta c_i)\tilde{w}_i = (\delta\mathbf{c})^T\tilde{\mathbf{w}} \end{aligned} \tag{3.94}$$

where the vector $\mathbf{c}$ holds the displacement coefficients, the vector $\delta\mathbf{c}$ holds the virtual displacement coefficients and the vector $\tilde{\mathbf{w}}$ holds the trial functions. The trial functions are introduced into the virtual work functional equation (3.92) resulting in the following form of the discretized virtual work

$$\begin{aligned} \delta W &= \delta\mathbf{c}^T\int_L EI\tilde{\mathbf{w}}''(\tilde{\mathbf{w}}'')^T dz\,\mathbf{c} + \lambda\,\delta\mathbf{c}^T\int_L N^0\tilde{\mathbf{w}}'(\tilde{\mathbf{w}}')^T dz\,\mathbf{c} \\ &= \delta\mathbf{c}^T(\mathbf{K}_e + \lambda\,\mathbf{K}_g)\mathbf{c} \end{aligned} \tag{3.95}$$

in which the elastic stiffness matrix $\mathbf{K}_e$ and the geometric stiffness matrix $\mathbf{K}_g$ have the following components

$$\begin{aligned} \mathbf{K}_e(i,j) &= \int_L EI\tilde{w}_j''\tilde{w}_i''\, dz \\ \mathbf{K}_g(i,j) &= \int_L N^0\tilde{w}_j'\tilde{w}_i'\, dz \end{aligned} \tag{3.96}$$

These stiffness matrices are symmetric and we therefore only need to calculate the upper or lower triangular parts. Again, the principle of virtual work leads to an eigenvalue problem.

$$\begin{aligned} \delta \mathbf{c}^T (\mathbf{K}_e + \lambda \mathbf{K}_g)\mathbf{c} &= 0 \quad \Downarrow \\ (\mathbf{K}_e + \lambda \mathbf{K}_g)\mathbf{c} &= \mathbf{0} \end{aligned} \tag{3.97}$$

This is a linear symmetric eigenvalue problem, which is easier to solve compared to the eigenvalue problem found using the Galerkin procedure.

The Magnification Factor

The magnification factor can also be derived in an alternative way. Let us have a look at the linearized stability equation once again, but this time we introduce the moment as $M = M^t - M^0$, where M^t is the total moment and M^0 is the initial moment.

$$\begin{aligned} M'' + \bar{\lambda}(N^0 w')' &= 0 \quad \Downarrow \\ (M^t - M^0)'' + \bar{\lambda}(N^0 w')' &= 0 \end{aligned} \tag{3.98}$$

In this equation let us assume that the initial moments are proportional to the moments in the eigenmodes, when the perfect column buckles, $M^0 = \xi M^t$, whereby the equation becomes

$$\begin{aligned} (1-\xi)M^{t\prime\prime} + \bar{\lambda}(N^0 w')' &= 0 \quad \Downarrow \\ M^{t\prime\prime} + \frac{\bar{\lambda}}{1-\xi}(N^0 w')' &= 0 \end{aligned} \tag{3.99}$$

where $\bar{\lambda}$ is the scale factor for the axial forces in the column with initial moments. The equation has the same solution λ as the eigenvalue problem of the perfect column without initial moments. We thus find that the parameter ξ can be determined as follows:

$$\begin{aligned} \lambda &= \frac{\bar{\lambda}}{1-\xi} \quad \Downarrow \\ \xi &= \frac{\lambda - \bar{\lambda}}{\lambda} \end{aligned} \tag{3.100}$$

The total moment M^t can therefore be found as a function of the initial moments in the following manner

$$M^t = \frac{1}{\xi} M^0 = \frac{\lambda}{\lambda - \bar{\lambda}} M^0 \tag{3.101}$$

It is thus clear that the moment magnification factor is of the same type as given previously. The same is the case for imperfections in the transverse displacements. It should also be clear that the magnified part is the part of the initial moment which has the same distribution as the eigenmode moments.

- **Problem 3.3**

  A uniformly compressed column with pinned ends has the constant bending stiffness EI and the length L. Find upper bounds for the buckling load P using the two different Rayleigh buckling coefficients for the following trial function.

  Let us assume that the moment variation corresponds to a second order polynomial, then we can find the displacements by integrating it twice and fulfilling the boundary conditions. Our trial function then takes the following form.

$$\begin{aligned} \tilde{w} &= \int\int \frac{z}{L}(1-\frac{z}{L})\,dz + C_1 z + C_2 \\ &= \frac{L^2}{3\cdot 2}\left(\frac{z}{L}\right)^3 - \frac{L^2}{4\cdot 3}\left(\frac{z}{L}\right)^4 - \frac{L^2}{4\cdot 3}\frac{z}{L} \end{aligned}$$

  Compare the answers with the Euler load P_{E}.

Chapter 4

Statically Indeterminate Beams

In this chapter two calculation methods for statically indeterminate beams will be introduced. Since torsion has not been introduced and to shorten equations we shall restrict ourselves to plane structures, but the methods can equally well be applied to three-dimensional structural analysis. The Einstein index notation is therefore not used in this chapter.

Beam structures are called statically determinate, when internal forces and reactions can be determined by static principles alone, i.e. by the use of force and moment equilibrium equations. From a kinematic point of view the position of these structures in space is exactly determined by the hinges and boundary conditions without redundant kinematic constraints. Some statically determinate structures are shown in the left-hand part of fig. 4.1.

Determinateness

A statically determinate beam structure has internal forces and reactions, which can be determined by static principles alone.

These structures have exactly the number of kinematic conditions needed to determine their position in space.

Statically indeterminate beam structures are structures in which the internal forces and reactions cannot be determined by static principles alone, due to redundant internal forces or reactions. From a kinematic point of view the position of these structures in space is determined by internal hinges and boundary conditions with redundant kinematic conditions, which constrain the structure. In these structures it is necessary in addition to the static equilibrium equations, to take the deflections of the beams into account and obtain either equations of displacement compatibility or force equilibrium at beam joints. Some indeterminate beam structures are shown in the right-hand part of fig. 4.1.

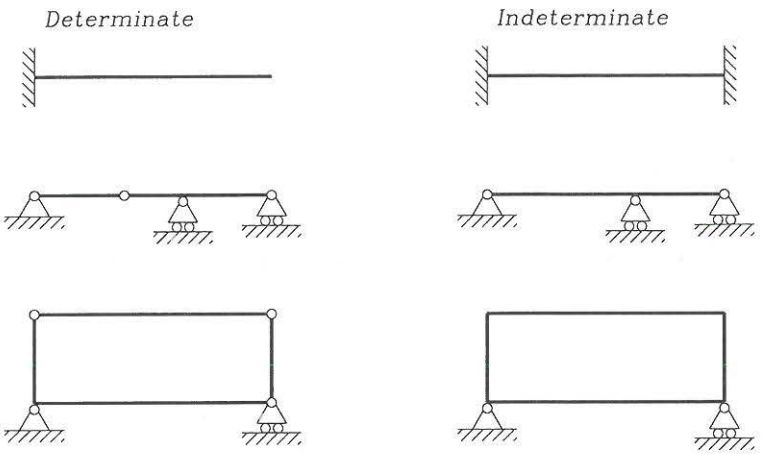

Fig. 4.1: Statically determinate and indeterminate structures.

Indeterminateness

A statically indeterminate beam structure has internal forces or reactions, which cannot be determined by static principles alone.

These structures have redundant internal forces or reactions corresponding to redundant kinematic conditions that constrain the structure.

Note the duality between the static and kinematic points of view, in fact the number of static redundancies is exactly equal to the number of kinematic redundancies, which is quite natural, since we need a force to enforce a kinematic constraint. The number of redundant forces or kinematic constraints is also referred to as the degree of statical indeterminateness. Structures which have too few or poorly chosen kinematic constraints are not static since they may accelerate, when external forces are applied.

The number of rendundancies in a statically indeterminate structure can be determined by geometrical investigation of the structure. The method consists of assembling the structure from scratch, so that its position in space is given, without redundant kinematic conditions. At places where redundant connections exist the unknown internal forces or external reactions are inserted as illustrated in figs. 4.2 and 4.3.

Identification of redundancies

Assemble the structure without introducing kinematic constraints. Insert the redundant forces and moments at the kinematic constraints.

The statically indeterminate structures are solved by the use of superposition

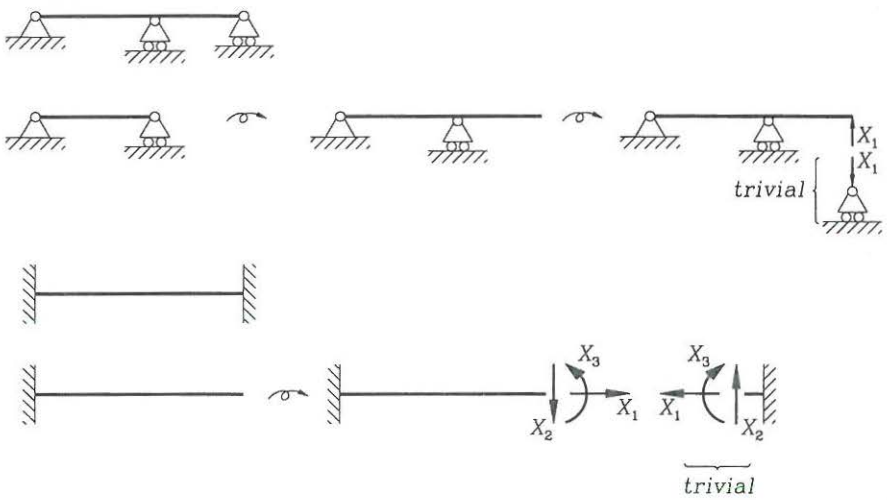

Fig. 4.2: Assemblage of structures to find redundancies.

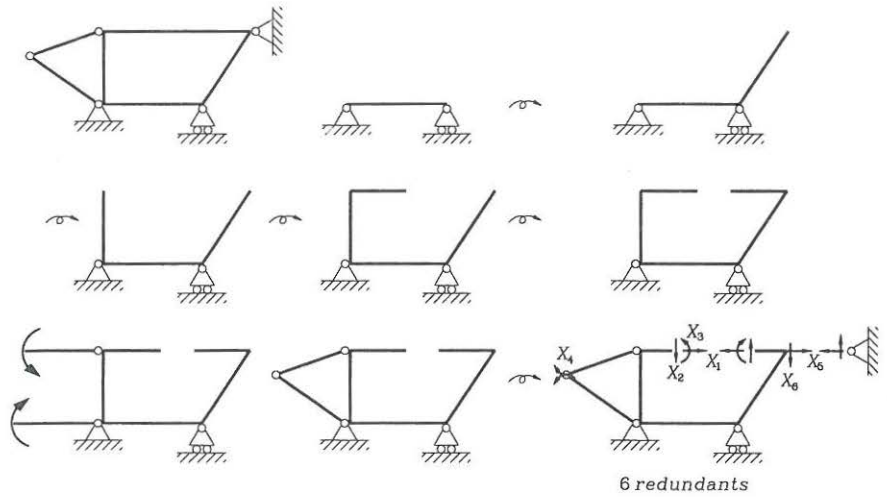

Fig. 4.3: Assemblage of a complex structure to find the redundancies.

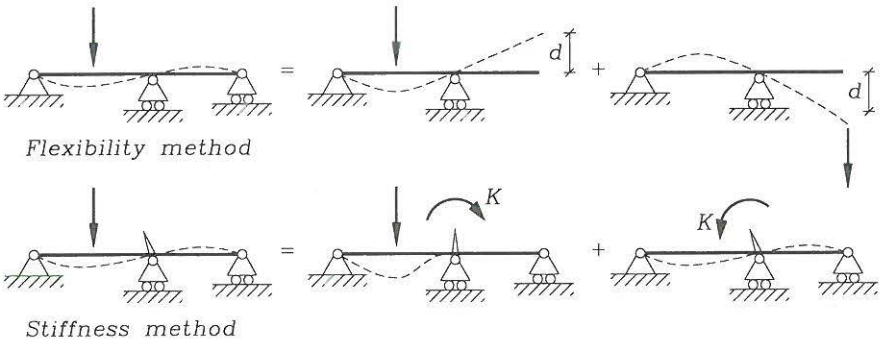

Fig. 4.4: Superposition used in the flexibility and stiffness methods.

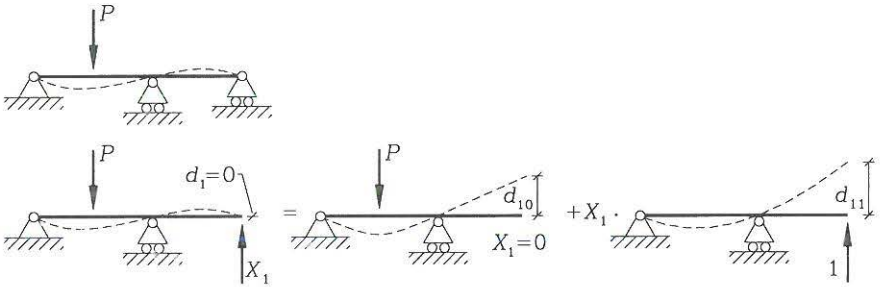

Fig. 4.5: The flexibility method, where d_{11} is a flexibility coefficient.

of different structural cases. Superposition is possible when materials are linear elastic and when the differential equations are linear in the displacements. Two complementary methods based on superposition are the flexibility method and the stiffness method, both illustrated in fig. 4.4. The flexibility method introduces redundant forces and uses compatibility of displacements to superimpose structural cases, whereas the stiffness method introduces redundant displacement constraints and uses equilibrium of constraint forces. Both methods have non-linear versions known as the force method and the displacement method, respectively.

Let us illustrate the two superposition principles starting with the flexibility method. The flexibility method uses superposition of statically determinate structural systems. The basic idea is to introduce the redundant forces and moments as unknowns and release the structure from the corresponding kinematic constraints. Fig. 4.5 illustrates the principle for a continuous beam with one redundant reaction. The reaction at the right-hand end of the beam is chosen as the unknown redundant force X_1. The corresponding kinematic constraint is that the mutual displacement between support and the end of the beam should be zero, i.e. $d_1 = 0$. Let us use superposition: First we release the kinematic constraint by assuming that $X_1 = 0$

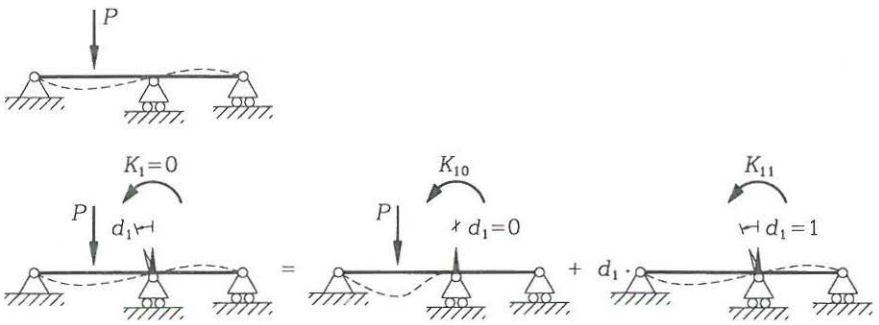

Fig. 4.6: The stiffness method, where K_{11} is a stiffness coefficient.

and find the mutual (end) displacement d_{10} for the statically determinate structure with loads. Then we find the mutual displacement d_{11} in the same statically determinate structure *without external load*, but with a unit load $X_1 = 1$ at the right-hand end. (The mutual displacement is just the displacement of the end of the beam, since the support is inflexible). Finally we scale the $X_1 = 1$ case so that the total mutual displacement at the end is zero $d_1 = 0$, (since the displacement, or let's say settlement of the support, is zero). Superimposing the two structural systems we find the redundant force:

$$\begin{aligned} d_1 &= d_{10} + d_{11} X_1 \quad \Downarrow \\ X_1 &= (d_1 - d_{10})/d_{11} \quad \Downarrow \\ X_1 &= -d_{10}/d_{11} \end{aligned} \tag{4.1}$$

in which we have used that $d_1 = 0$. The coefficient d_{11} is known as a flexibility coefficient. A flexibility coefficient is the displacement at a point for a unit load acting at the same or some other point. It is a coefficient, since we just need to multiply by the load magnitude to find the corresponding displacement.

Let us turn to the stiffness method in which kinematic redundancies are introduced. The stiffness method does not depend on the choice of a statically determinate structure, but uses basic beam displacement modes and load cases of which some are statically indeterminate. There are, however, a finite number of basic displacement modes and load cases of practical relevance. Instead of going into details let us just illustrate the superposition principle used in this case. Fig. 4.6 shows the principle of the stiffness method on the same continuous beam as just used. Let us first introduce a redundant kinematic condition in the original structure with external loads by constraining the rotation displacement at the central support to zero, i.e. $d_1 = 0$. To do this we need to apply a redundant moment K_{10}, (which in the present case would be negative), since the external load tries to rotate the beam. Then we need to superimpose a second structural case *without external loads*, but with a rotation at the central support. To do this we analyse a situation with a unit rotation $d_1 = 1$ and find the moment K_{11} needed to enforce

this rotation. Since the total external moment K_1 applied at the central support in the present case is zero, i.e. $K_1 = 0$, superimposing the two structural cases results in the determination of the unknown rotation, as follows:

$$\begin{aligned} K_1 &= K_{10} + K_{11} d_1 \quad \Downarrow \\ d_1 &= (K_1 - K_{10})/K_{11} \quad \Downarrow \\ d_1 &= -K_{10}/K_{11} \end{aligned} \tag{4.2}$$

The coefficient K_{11} is known as a stiffness coefficient. A stiffness coefficient is the force (or moment) needed at some point to obtain a required unit displacement mode.

The flexibility method is related to the complementary principle of virtual work, since virtual forces are used to find the unknown displacements. The unit load method is used and it is based on the complementary principle of virtual work. The stiffness method is based on the principle of virtual work, since we make use of virtual displacements in our search for equilibrium. The methods have many variants and they are related to many historical energy and work principles, which will not be treated in detail in the present text. Gere & Timoshenko describe many of the related methods and energy principles in their textbook on mechanics of materials [12]. In the following, only the flexural stiffness method will be described in detail. The stiffness method is treated in much more detail, when introducing the finite element method. The flexibility method is a great tool for hand calculations, whereas the stiffness method is the main tool in computational analysis of structures.

4.1 The Flexibility Method for Beams

The flexibility method has roots back to J. C. Maxwell, who in 1864 proposed the unit load method to determine displacements and the flexibility method to calculate statically indeterminate truss structures. Independently, O. Mohr proposed the same methods in 1874. The flexibility method for beam and truss structures has many names, some of these are: The Maxwell-Mohr method, the method of consistent deformation, the force method, the dummy load method and also the unit load method for statically indeterminate structures.

In the present section we shall first give a short presentation of the unit load method for determining displacements and then we shall give two examples. The first example is the one used in the previous introduction, it has one redundant force. The second example will have two redundant forces. To enable fast handling of integrals a simple integration formula is given. Having treated the examples a general flexibility procedure for hand calculation of statically indeterminate beam structures is described. The procedure is related to the complementary principle of virtual work and a simple method for determining displacements in the statically indeterminate beam structures is given. Furthermore, the effect of temperature variations and support settlements are considered. Statically indeterminate truss

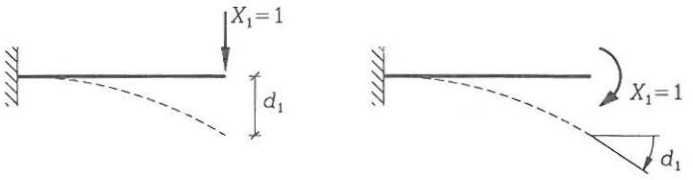

Fig. 4.7: Unit load method for finding a displacement or a rotation d_1.

structures can be treated by the same methods, since a truss is also a beam. For truss structures a few simplifications will be described.

Before proceeding a word about notation is helpful. For external point loads and internal forces we use capital letters. Redundant forces are denoted X_i and the corresponding mutual displacements d_i, where the lower index i referes to the number of this particular redundant force. Virtual internal force distributions N^i, Q^i and M^i corresponding to the redundant forces X_i are indicated by an upper index, so that we can differentiate the notation a little from the index notation in the previous chapters. (Upper indices are not power indices).

The Unit Load Method

The unit load method is used to find the displacement at a certain point. The method can be derived from the principle of complementary virtual work $\delta W^c = 0$. For beams the complementray virtual work is given in equation (2.38) and it takes the following form when a virtual point load $\delta\widetilde{P}$ and a virtual moment load $\delta\widetilde{M}$ are introduced at a point with the real displacement w and rotation α:

$$\delta W^c = \sum_{\text{beams}} \int_0^L \left(\bar{\varepsilon}\,\delta N + \gamma\,\delta Q + \kappa\,\delta M\right)\,dz - w\,\delta\widetilde{P} - \alpha\,\delta\widetilde{M} \tag{4.3}$$

in which the virtual internal forces δN, δQ and δM must correspond to (i.e. be in equilibrium with) the virtual loads $\delta\widetilde{P}$ and $\delta\widetilde{M}$.

A virtual unit load $\delta\widetilde{P}$ or $\delta\widetilde{M}$ denoted $X_1 = 1$ is applied at the point and in the direction in which the displacement (or rotation) d_1 is sought, as shown in fig. 4.7. To use the complementary principle of virtual work it is necessary to find a statically admissible virtual stress distribution. This virtual stress distribution corresponds to the internal forces N^1, Q^1, M^1 found when the unit load $X_1 = 1$ is applied to the structure *without external loads*. The complementary virtual work functional thus takes the following form

$$\delta W^c = \sum_{\text{beams}} \int_0^L \left(\bar{\varepsilon}N^1 + \gamma Q^1 + \kappa M^1\right)\,dz - d_1 X_1 \tag{4.4}$$

in which the axial strain $\bar{\varepsilon}$, the shear strains γ and the curvature κ are the real structural strains and the only external virtual work is performed by the virtual force X_1 through the real displacements d_1. Using the complementary principle of

virtual work $\delta W^e = 0$ and that the virtual load is a unit load $X_1 = 1$, we find the displacement (or rotation):

$$d_1 = \sum_{\text{beams}} \int_0^L \left(\bar{\varepsilon} N^1 + \gamma Q^1 + \kappa M^1 \right) \, dz \tag{4.5}$$

Introducing the uncoupled constitutive equations $\bar{\varepsilon} = \frac{N}{EA}$, $\gamma = \frac{Q}{\psi GA}$ and $\kappa = \frac{M}{EI}$ the internal work can be rewritten and the displacement is given as

$$d_1 = \sum_{\text{beams}} \int_0^L \left(\frac{NN^1}{EA} + \frac{QQ^1}{\psi GA} + \frac{MM^1}{EI} \right) dz \tag{4.6}$$

This equation corresponds to setting the external work of the virtual force equal to the internal work of the virtual internal forces, which is an alternative formulation of the complementary virtual work statement.

In case of a truss system the integration simplifies since both the axial forces and the cross-sectional areas are constant through each truss. For a structure including trusses we can thus find the displacement by the following formula:

Unit load displacement formula for beam and truss structures

$$d_1 = \sum_{\text{beams}} \int_0^L \left(\frac{NN^1}{EA} + \frac{QQ^1}{\psi GA} + \frac{MM^1}{EI} \right) dz + \sum_{\text{trusses}} \frac{NN^1}{EA} L \tag{4.7}$$

Neglecting axial extension and shear effects leads to

$$d_1 \simeq \sum_{\text{beams}} \int_0^L \frac{MM^1}{EI} \, dz + \sum_{\text{trusses}} \frac{NN^1}{EA} L \tag{4.8}$$

For "long" beams where the depth to length ratio is large, i.e. as a rule of thumb $\frac{d}{L} > \frac{1}{15}$, the shear effects can be neglected. Furthermore, the axial extension due to axial forces can also be neglected in most situations where bending is involved. The calculation of displacements can therefore be performed by neglecting the contributions from shear and axial force using the formula given above.

In connection with the flexibility method it is important to note that the displacements can also be mutual displacements. The mutual displacement is found by applying two opposite unit loads at the place where the mutual displacement is sought, as shown in fig. 4.8.

The integration of the moment products over the beam length is often performed for simple linear functions and in the case of a constant distributed load also for products of linear and quadratic functions. Fig. 4.9 illustrates a linear function $f(z)$ and a parabolic function $g(z)$. Integrating the products of these two functions yields:

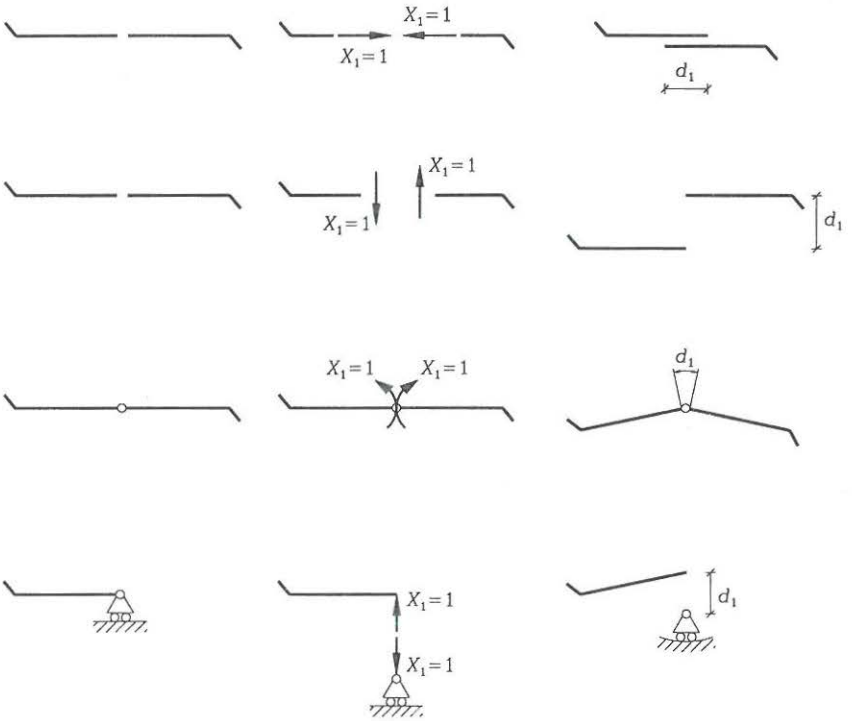

Fig. 4.8: Unit loads $X_1 = 1$ and corresponding mutual displacements d_1.

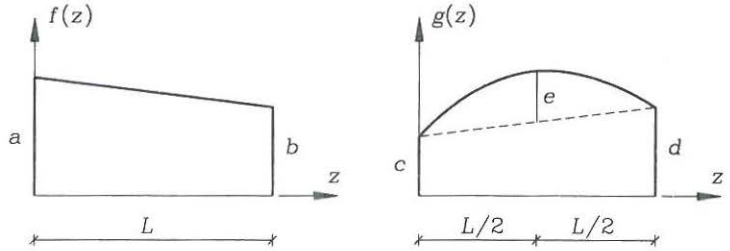

Fig. 4.9: A linear function $f(z)$ and a parabolic function $g(z)$.

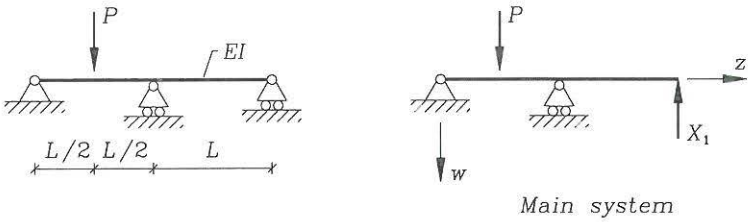

Fig. 4.10: Beam with one redundant force and the main system used.

Integration of the product of a linear and a quadratic function

$$\int_0^L f(z)g(z)\,dz = \frac{L}{6}(2ac + 2bd + ad + bc) + \frac{L}{3}e(a+b) \qquad (4.9)$$

The constants are defined in fig. 4.9

This formula is very easy to learn by heart once and for all. Notice the definition of the quadratic variation by e, which is easy to find for any part of a beam with constant transverse load ($e = \frac{1}{8}pL^2$), where L is the length of the part analysed. Note also that the formula includes integration of two linear functions by setting $e = 0$. The following example will illustrate the use of the integration formula and the unit load method.

- **Example 4.1** A continuous beam with one Redundant.

  Let us analyse a double span continuous beam with equal spans, constant bending stiffness EI, and a point load in the first span as shown in fig 4.10. The two ends of the beam are pinned and the right-hand end also has rollers that make horizontal movement possible. At the central support the beam is continuous and can transfer moments from the first span to the next span, the pin (or hinge) of the support is placed below the continuous beam and moments cannot be carried through to the support. The central support also has horizontal rollers. In the following the main points in the method are emphasized so that we can develop a general method of analysis.

  1: *Choose a statically determinate main structural system and introduce the redundant force.*

  If we assemble the structure from scratch, as shown in fig. 4.2, we find that the structure has one degree of indeterminateness and we add the corresponding redundant force X_1 as the unknown reaction. We could have made infinitely many other choices, as shown in fig. 4.11. For example by introducing a hinge anywhere in the beam and thereby choosing the internal moment at the hinge as the redundancy.

  Let us use the right-end reaction as the redundant force X_1 and neglect the influence of shear. The statically determinate system is called the main system, as shown in fig. 4.10. The first problem is to determine the displacement

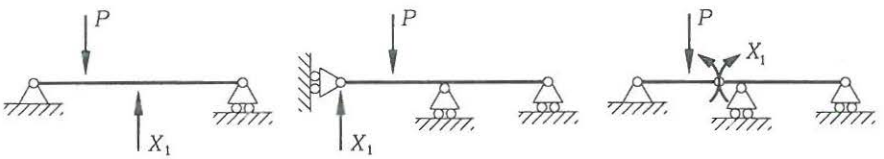

Fig. 4.11: Alternative choices of the redundancy.

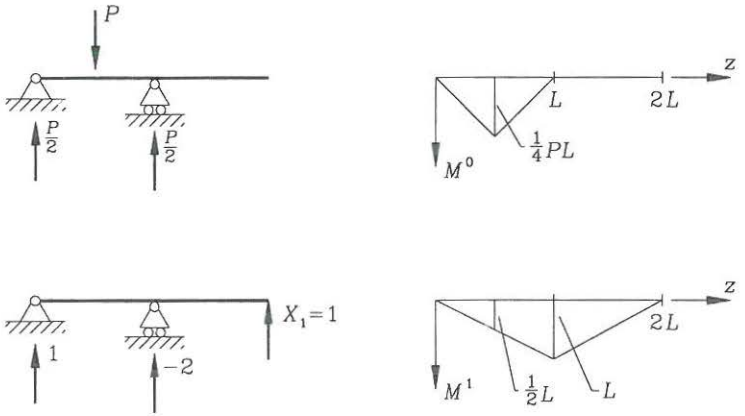

Fig. 4.12: Moment distributions in the main system.

d_{10} of the statically determinate structure. To do this we use the unit load method and apply a virtual unit load $X_1 = 1$ at the point where the displacement is to be found. To calculate the displacement using equation (4.8) we need the moment distribution M^0 from the external load on the main system with $X_1 = 0$ and the virtual moment distribution M^1 corresponding to the unit load $X_1 = 1$ and no external load. These moments are found and shown in fig. 4.12. Having found the moment distributions we can find the displacements. The things to do are:

2: *Find the moment distribution M^0 corresponding to an external load P on the main system without virtual load (i.e. $X_1 = 0$).*

3: *Find the moment distribution M^1 corresponding to a virtual unit load $X_1 = 1$ on the main system without external load (i.e. $P = 0$).*

4: *Find the (mutual) displacement d_{10} corresponding to the redundant force X_1 for an external load P on the main system.*

The displacement d_{10} from external load on the main system is calculated using equation (4.8), the integration formula in equation (4.9) and the moment distributions in fig. 4.12 as follows

$$d_{10} = \int_0^{2L} \frac{M^0 M^1}{EI}\, dz = \frac{1}{EI}\int_0^{L/2} \frac{M^0 M^1}{EI}\, dz + \frac{1}{EI}\int_{L/2}^{L} \frac{M^0 M^1}{EI}\, dz$$

$$= \frac{L/2}{6EI}\left(2\cdot\frac{1}{4}PL\cdot\frac{1}{2}L\right)+\frac{L/2}{6EI}\left(2\cdot\frac{1}{4}PL\cdot\frac{1}{2}L+\frac{1}{4}PL\cdot L\right)$$

$$= \frac{1}{16}\frac{PL^3}{EI}$$

This completes one case in our superposition of structural cases and the next step is to apply a redundant unit force $X_1 = 1$ and find the displacement d_{11}.

5: *Find the (mutual) displacement d_{11} corresponding to the redundant force X_1 for a unit load $X_1 = 1$ on the main system.*

The displacement d_{11} is found using the unit load method and since we have already found the moment distribution we can calculate it:

$$d_{11} = \int_0^{2L}\frac{M^1M^1}{EI}\,dz = 2\frac{L}{6EI}(2\cdot L\cdot L) = \frac{2}{3}\frac{L^3}{EI} \tag{4.10}$$

Now let us use that our differential equations are linear and superimpose displacements.

6: *Use displacement compatibility to find the redundant force.*

The total displacement at the redundant force X_1 is zero, $d_1 = 0$, since the support does not move. The total displacement is found by superposition as

$$d_1 = d_{10} + d_{11}X_1$$

This equation enforces compatibility between support displacement and structural displacement. The unknown redundant reaction can thus be found as

$$X_1 = (d_1 - d_{10})/d_{11} = -\frac{\frac{PL^3}{16EI}}{\frac{2L^3}{3EI}} = -\frac{3}{32}P \tag{4.11}$$

Having found the redundant reaction we can analyse the structure as usual, but why should we? The internal forces and the reactions in the real structure can be found by superposition of the structural cases already treated. An internal force or a reaction can be denoted S and found by the use of superposition, i.e. $S = S^0 + S^1X_1$. The next step thus is:

7: *Determine internal forces S and the remaining support reactions S by superposition, $S = S^0 + S^1X_1$.*

The moments M^0 and M^1 have already been determined in fig. 4.12 so let us start by superimposing these using the value found for the redundant force $X_1 = -\frac{3}{32}P$. The result is shown in fig. 4.13. The shear forces can be found by statics or simply by using the static relation $Q = M' + m = M'$, (since there is no distributed moment load $m = 0$). The reactions can be found using superposition or by inspection of the shear force distribution.

The next step is to find displacements at selected points. This can be done by superposition or by applying the unit load method to the real structure with known internal forces. To use superposition would mean that the displacement should be determined in both load cases, whereas use of the unit load method on the real structure would only need determination of one displacement, (i.e. half the work and even less with multiple redundant forces). Furthermore, since the unit load is a virtual load we can choose any structural sub-system which is statically determinate to define the virtual internal forces.

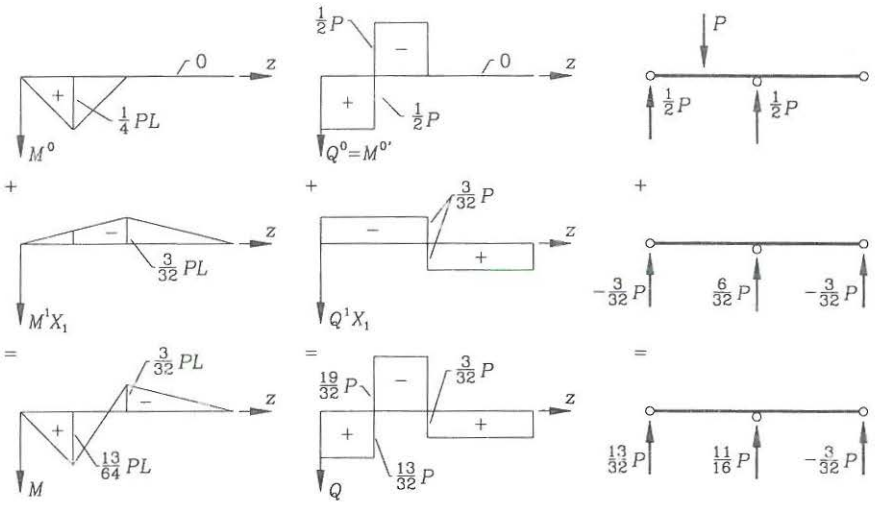

Fig. 4.13: Moment distributions in the main system.

8: *Find displacements by using a statically determinate sub-systems for definition of the virtual internal forces.*

Let us find the vertical displacement d_2 at the centre of the second span. To do this we apply a unit load X_2 to a statically determinate sub-system as shown in fig. 4.14 and we determine the corresponding virtual moment distribution M^2. The displacement can then be found as:

$$\begin{aligned} d_2 &= \int_L^{2L} \frac{M M^2}{EI}\, dz \\ &= \frac{L/2}{6EI}\left(2 \cdot \frac{3}{64} PL \cdot \frac{1}{4} L + \frac{3}{32} PL \cdot \frac{1}{4} L\right) + \frac{L/2}{6EI}\left(2 \cdot \frac{3}{64} PL \cdot \frac{1}{4} L\right) \\ &= \frac{3}{512} \frac{PL^3}{EI} \end{aligned}$$

This concludes the example with one redundant force.

Multiple Redundancies

In this subsection a general flexibility procedure for multiple redundancies will be described. The procedure has already been outlined in the introduction to the chapter and by the previous example. However, it is necessary to be aware of the fact that the redundancies affect each other as seen in fig. 4.15. The redundancies are enumerated from 1 to n and indices i and j will be used, with j referring to the load X_j and i to the mutual displacement d_i. A statically determinate structure is chosen as the main system, the redundant constraints are released and the main

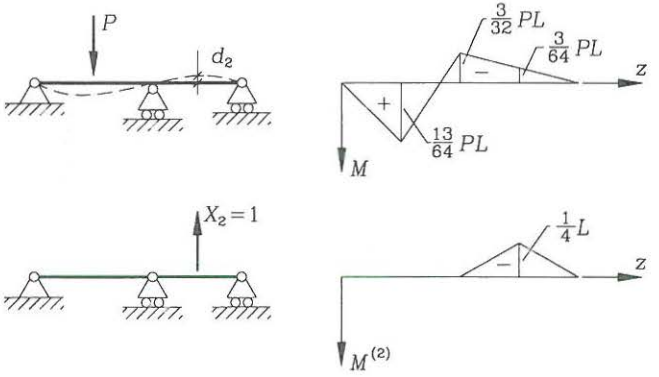

Fig. 4.14: Displacement determination.

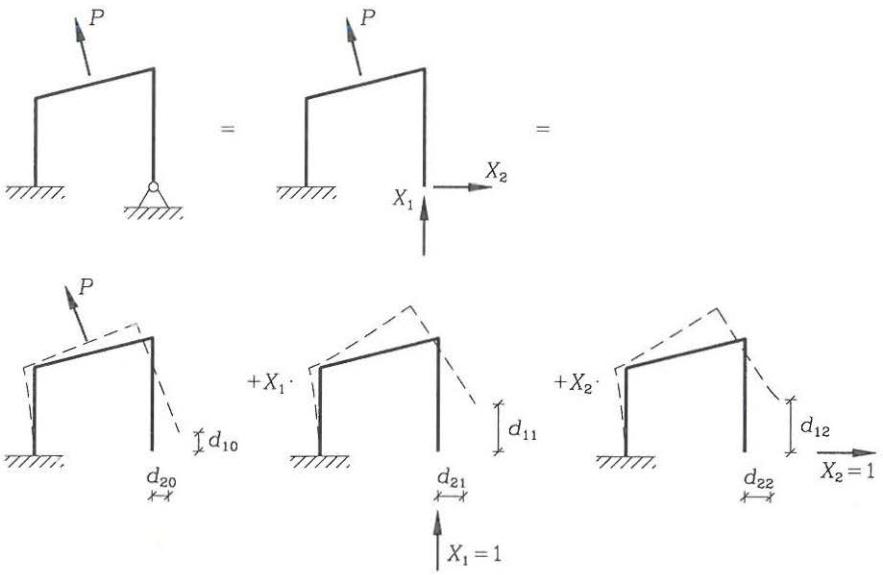

Fig. 4.15: A structure with two redundant forces.

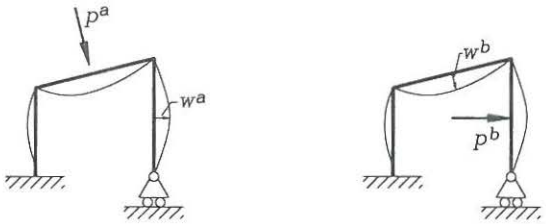

Fig. 4.16: Reciprocal displacements for Maxwell's theorem.

system is loaded by the external loads, thereby undergoing deformation. We see that displacements d_{i0} may occur at all the redundancies. This case is superimposed with the cases where the main system is loaded by unit loads $X_j = 1$. Also in this case displacements d_{ij} may occur at all redundancies. The compatibility equation in the case of multiple redundancies thus takes the following form:

$$\begin{aligned} d_{10} + d_{11}X_1 + d_{12}X_2 + \ldots &= d_1 \\ d_{20} + d_{21}X_1 + d_{22}X_2 + \ldots &= d_2 \\ &\vdots \\ d_{n0} + d_{21}X_1 + \ldots + d_{nn}X_n &= d_n \end{aligned} \tag{4.12}$$

in which d_i are the real mutual displacements, which in most cases will be zero. In matrix notation the compatibility equations take the following format:

$$\begin{pmatrix} d_{10} \\ d_{20} \\ \vdots \\ d_{n0} \end{pmatrix} + \begin{bmatrix} d_{11} & d_{12} & \ldots & d_{1n} \\ d_{21} & d_{22} & \ldots & d_{2n} \\ & & \vdots & \\ d_{n1} & d_{n2} & \ldots & d_{nn} \end{bmatrix} \begin{pmatrix} X_1 \\ X_2 \\ \vdots \\ X_n \end{pmatrix} = \begin{pmatrix} d_1 \\ d_2 \\ \vdots \\ d_n \end{pmatrix} \tag{4.13}$$

The compatibility equations can be written in compact form using the Einstein summation convention, where i and j have the range from 1 to the number of redundancies n:

$$d_{i0} + d_{ij}X_j = d_i \tag{4.14}$$

The redundant forces and moments are found by inverting the flexibility matrix d_{ij} as follows:

$$X_j = d_{ij}^{-1}(d_i - d_{i0}) \tag{4.15}$$

The flexibility matrix is symmetric $d_{ij} = d_{ji}$. The symmetry was shown by Maxwell 1864 and it applies to linear elastic materials. It is referred to as "Maxwell's reciprocal displacement theorem" and we can use the principle of virtual work to show it. Fig. 4.16 shows two situations a and b. In situation a a load P^a produces a displacement field w^a, strains ε^a and stresses σ^a and in situation b a load P^b

produces a displacement field w^b, strains ε^b and stresses σ^b. The principle of virtual work for situation a states that:

$$\begin{aligned} \int_V \sigma^a \delta\varepsilon \, dV - P^a \, \delta w &= 0 \quad \Downarrow \\ P^a \, \delta w &= \int_V \sigma^a \delta\varepsilon \, dV \end{aligned} \tag{4.16}$$

Using situation b for the virtual displacement field $\delta w = w^b$ and using the linear elastic constitutive equation $\sigma = E\varepsilon$ we find:

$$P^a w^b = \int_V \sigma^a \varepsilon^b \, dV = \int_V \varepsilon^a E \varepsilon^b \, dV = \int_V \varepsilon^a \sigma^b \, dV = P^b w^a \tag{4.17}$$

where the principle of virtual work for situation b has been used in the latter operation. This also shows that the flexibility matrix is symmetric, since the component d_{ij} corresponds to the displacement at i for a force at j and for d_{ji} vice versa. (The direct reciprocity of displacements can thus be seen as $P^a/w^a = P^b/w^b$).

The flexibility method for hand calculation of statically indeterminate beam and truss structures can thus be summarized in the enumerated steps given in tab. 4.1. It is assumed that axial extension and shear displacements can be neglected. If this is not the case all internal forces must be determined in steps 2 and 3, and the displacement formulas in steps 4 and 5 must be modified.

- **Example 4.2** A frame with two redundancies.

  A small frame shown in fig. 4.17 consists of three beams, each with the length L and the bending stiffness EI. The frame has one fixed support and one pinned support. The problem we set ourselves is to find the sidesway of the frame. To answer this it is neccesary to find the moment distribution in the frame. Let us use the procedure described in tab. 4.1.

  1: The chosen statically determinate structual system is shown in fig. 4.17. We choose the two mutual rotations as redundancies, since mutual rotations almost always ease the calculations, by localizing the influence of the virtual load.

  2: The hinges in the main system make it easy to find the linear variation from the point load and the quadratic variation from the distributed load. The moment distribution M^0 is also shown in fig. 4.17.

  3: The moment distributions M^1 and M^2 from the mutual moments, respectively $X_1 = 1$ and $X_2 = 1$ are shown in the figure.

  4: The mutual rotations for external loads only on the main system are:

$$d_{10} = \frac{L}{6EI}(-2PL - PL) + \frac{L}{3EI}(\frac{1}{2}PL) = -\frac{2}{6}\frac{PL^2}{EI}$$

$$d_{20} = \frac{L}{3EI}(\frac{1}{2}PL) + \frac{L}{6EI}(2(-1)(-PL)) = \frac{3}{6}\frac{PL^2}{EI}$$

Flexibility method for statically indeterminate beam and truss structures:

1: *Choose a statically determinate main system and introduce redundant forces and moments X_j. (Try to use moments where possible).*

2: *Find the moment distribution M^0 corresponding to external loads (P) on the main system without virtual load (i.e. $X_j = 0$).*

3: *For all j find the moment distribution M^j corresponding to the virtual unit load $X_j = 1$ on the main system* **without external load** *(i.e. $P = 0$ and $X_k = 0$ for $k \neq j$).*

4: *For all i find the (mutual) displacement d_{i0} corresponding to the redundancy i for external loads (P) on the main system*

$$d_{i0} \simeq \sum_{\text{beams}} \int_0^L \frac{M^0 M^i}{EI}\, dz + \sum_{\text{trusses}} \frac{N^0 N^i}{EA} L$$

5: *For all i and j find the (mutual) displacements d_{ij} corresponding to the redundancy i for a unit load $X_j = 1$ on the main system*

$$d_{ij} \simeq \sum_{\text{beams}} \int_0^L \frac{M^j M^i}{EI}\, dz + \sum_{\text{trusses}} \frac{N^j N^i}{EA} L$$

6: *Use displacement compatibility to find the redundant forces and moments X_j:*

$$\begin{aligned} d_{i0} + d_{ij} X_j &= d_i \quad \Downarrow \\ X_j &= d_{ij}^{-1}(d_i - d_{i0}) \end{aligned}$$

where d_i are the real mutual displacements, which may be equal to zero or to a given settlement.

7: *Determine internal forces S and the remaining support reactions S by superposition. Using Einstein summation:*

$$S = S^0 + S^j X_j$$

8: *Find displacements by* **using statically determinate sub-systems** *for definition of the virtual internal forces corresponding to a virtual unit load.*

Tab. 4.1: The flexibility method.

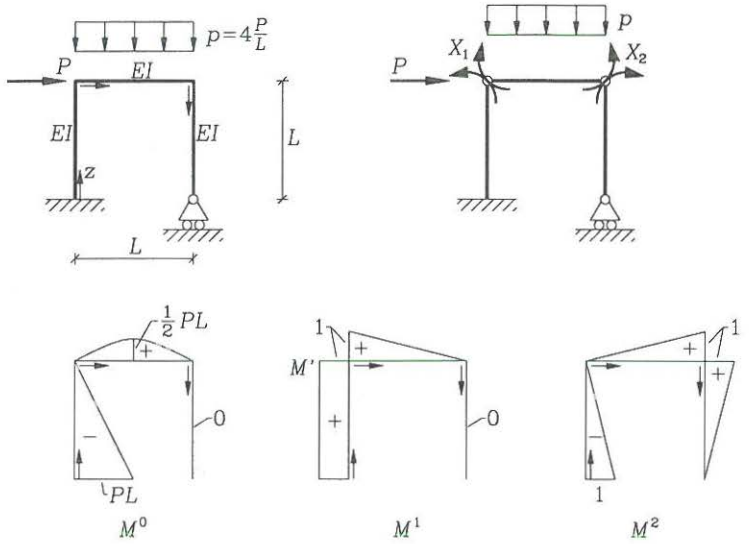

Fig. 4.17: A simple frame with two redundancies.

5: The mutual rotations for unit loads $X_j = 1$ on the structure are

$$d_{11} = \frac{L}{6EI}(2+2+1+1) + \frac{L}{6EI}(2) = \frac{8}{6}\frac{L}{EI}$$

$$d_{22} = 3\frac{L}{6EI}(2) = \frac{6}{6}\frac{L}{EI}$$

$$d_{12} = \frac{L}{6EI} + \frac{L}{6EI}(-2-1) = -\frac{2}{6}\frac{L}{EI}$$

$$d_{21} = d_{12}$$

6: Since the mutual rotations are zero $d_1 = d_2 = 0$ in the real structure we find the following matrix equation, which we solve:

$$\frac{L}{6EI}\begin{bmatrix} 8 & -2 \\ -2 & 6 \end{bmatrix}\begin{pmatrix} X_1 \\ X_2 \end{pmatrix} = -\frac{PL^2}{6EI}\begin{pmatrix} -2 \\ 3 \end{pmatrix} \quad \Downarrow$$

$$\begin{pmatrix} X_1 \\ X_2 \end{pmatrix} = -\frac{PL}{8\cdot 6 - 2^2}\begin{bmatrix} 6 & 2 \\ 2 & 8 \end{bmatrix}\begin{pmatrix} -2 \\ 3 \end{pmatrix} \quad \Downarrow$$

$$\begin{pmatrix} X_1 \\ X_2 \end{pmatrix} = \begin{pmatrix} 6 \\ -20 \end{pmatrix}\frac{PL}{44}$$

7: To determine displacements we only need the moment distribution. Using the above result we find the moments by superposition, and the result is shown in

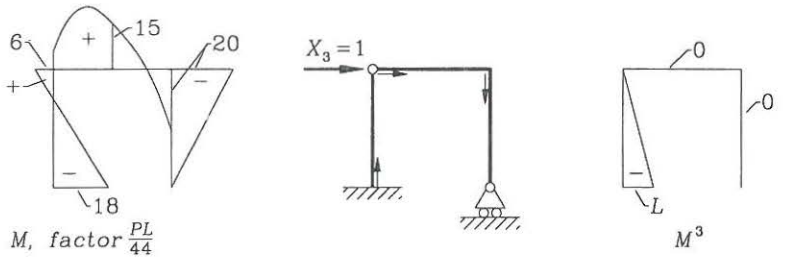

Fig. 4.18: Moment distribution and a unit load case for displacements.

fig. 4.18. Only one important comment will be given and that is concerning the quadratic moment variation. We have not found the maximum value, only the value at the centre of the beam. The central value is:

$$M_{centre} = \frac{1}{2}X_1 + \frac{1}{2}X_2 + \frac{1}{2}PL = \frac{3}{44}PL - \frac{10}{44}PL + \frac{22}{44}PL = \frac{15}{44}PL$$

8: The sidesway to the right can now be found using a unit load on the statically determinate system, as shown in fig. 4.18. The sidesway is:

$$d_3 = \frac{L}{6EI}(2 \cdot 18 \cdot L - 6 \cdot L)\frac{PL}{44} = \frac{5}{44}\frac{PL^3}{EI}$$

This concludes the example with 2 redundancies.

Support Settlement

There are two possible effects of settlements on the compatibility equations. One effect is the introduction of final (mutual) displacements d_i at the redundancies, due to settlements at the redundant supports. Another possible effect is the introduction of displacements d_{i0} in the directions of the redundancies due to settlements of the (non-redundant) supports of the main system. Both types are shown in fig. 4.19, where two of three supports settle. When the right-hand support settles upwards s_r and when we choose this support reaction as the redundant force X_1, then the final displacement of the support is $d_1 = s_r$. When the left-hand main system support settles downwards s_l a displacement $d_{10} = s_l$ is introduced at the redundant force.

As shown in fig. 4.20 the calculation method is the same for cases where internal moments are chosen as redundancies. We just have to find the mutual rotations d_{10} in the main system and remember that rotations are positive in the directions, where the work of redundancies would be positive.

- **Example 4.3** Using a redundant force.

  Let us analyse the situation shown in fig. 4.19 and find the moment at the central support introduced by the settlements. The displacement in the main system with

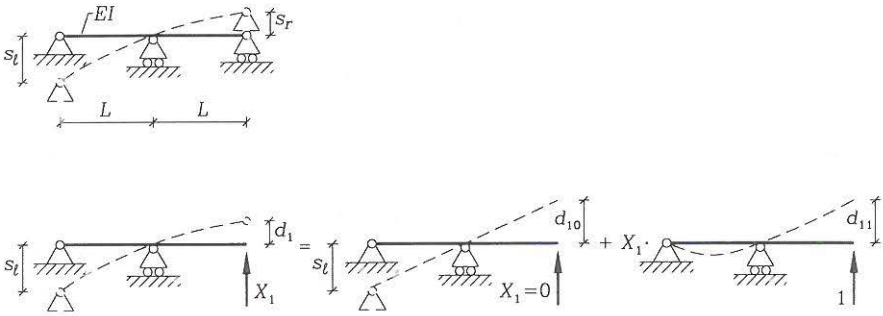

Fig. 4.19: Analysis of settlements using a redundant force.

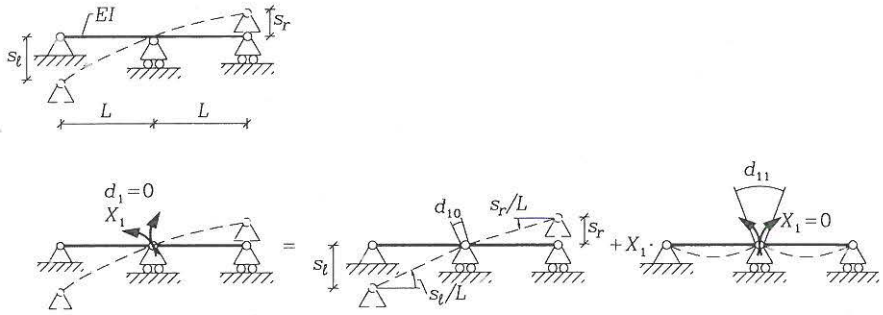

Fig. 4.20: Analysis of settlements using a redundant moment.

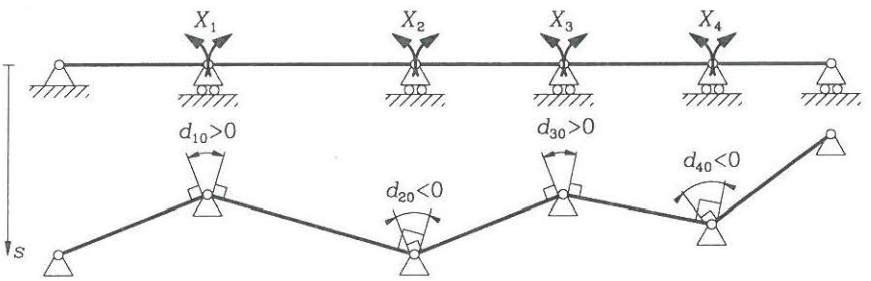

Fig. 4.21: Sign of mutual rotations for settlements in a main system.

external loads, i.e. settlements, is $d_{10} = s_l$. The displacement in the main system with the only load $X_1 = 1$ can be calculated as done previously in (4.10) for the same main system with the result $d_{11} = \frac{2}{3}\frac{L^3}{EI}$. The final displacement at the redundancy is, $d_1 = s_r$. The redundant reaction is thus determined as

$$X_1 = (d_1 - d_{10})/d_{11} = (s_r - s_l)\frac{3EI}{2L^3}$$

The moment at the central support is found by superposition as

$$\begin{aligned} M &= M^0 + M^1 X_1 = M^1 X_1 = L\,(s_r - s_l)\frac{3EI}{2L^3} \\ &= (s_r - s_l)\frac{3EI}{2L^2} \end{aligned}$$

- **Example 4.4** Using a redundant moment.

  Let us analyse the situation shown in fig. 4.20 and find the moment at the central support introduced by the settlements. The mutual rotation in the main system with external loads, i.e. settlements, is $d_{10} = (s_l - s_r)/L$. The displacement in the main system with the only load $X_1 = 1$ can be calculated as described in the previous subsections with the result $d_{11} = \frac{2}{3}\frac{L}{EI}$. The final mutual rotation at the redundancy is zero, $d_1 = 0$, since the beam is still continuous. The moment at the central support thus is

$$M = X_1 = -d_{10}/d_{11} = (s_r - s_l)\frac{3EI}{2L^2}$$

It is important to be aware of the positive and negative directions. Fig. 4.21 shows the influence of settlements in the main system for a continuous beam with multiple intermediate supports, where the moments at the supports have been chosen as redundancies. The signs of the mutual rotations are indicated in the figure.

Temperature Effects

There are two main effects of temperature changes $\Delta T(x_s, z)$. One effect is to change the initial length of beams and the other is to introduce curvatures in

beams. The difference between the current temperature field $T(x_\beta, z)$ and the initial temperature field $T^0(x_\beta, z)$ (at erection) is what we define as the temperature change $\Delta T = T^0 - T$. For the sake of generality the Einstein index notation is reintroduced in the first part of this subsection.

In the first chapter isotropic thermal strains ε^T_{ij} were introduced in equation (1.139). In beam theory we assume that the transverse expansion is free and therefore only axial strains will have an effect. The axial thermal strains are thus given by:

$$\varepsilon^T = \beta\, \Delta T \tag{4.18}$$

where β is the coefficient of thermal expansion.

The virtual work functionals and the potential energies must be expanded by an additional term due to the work of the stresses $\sigma = N/A + I^{-1}_{\beta\alpha} M_\alpha (x_\beta - c_\beta)$ through thermal strains ε^T. For example the additional term for the complementary virtual work functional δW^c which we use in the flexibility method can be found as follows:

$$\begin{aligned}
\delta W^c_T &= \int_V \varepsilon^T\, \delta\sigma\, dV \\
&= \int_0^L \int_A \varepsilon^T \delta \left(N/A + I^{-1}_{\beta\alpha} M_\alpha (x_\beta - c_\beta) \right) dA\, dz \\
&= \int_0^L \left(\frac{1}{A} \int_0^L \varepsilon^T dA\, \delta N + I^{-1}_{\beta\alpha} \int_A \varepsilon^T (x_\beta - c_\beta) dA\, \delta M_\alpha \right) dz \\
&= \int_0^L \left(\bar{\varepsilon}^T\, \delta N + \kappa^T_\alpha\, \delta M_\alpha \right) dz
\end{aligned} \tag{4.19}$$

where the temperature strain at the elastic centre and the temperature curvature have been introduced as:

$$\bar{\varepsilon}^T = \frac{1}{A} \int_A \varepsilon^T\, dA \tag{4.20}$$

$$\kappa^T_\alpha = I^{-1}_{\alpha\beta} \int_A \varepsilon^T (x_\beta - c_\beta)\, dA \tag{4.21}$$

For non-linear variations of the temperature changes the shear stiffness of beams will enforce a linear strain distribution, so that plane sections remain plane. This will introduce some stresses which cannot be accounted for by beam theories.

Let us return to the case of single symmetric cross-sections with the elastic centre at origo $c_\beta = 0$ and forget the Einstein index notation. We assume that the distribution of the temperature change is linear, as shown in fig. 4.22, with the following temperature changes: ΔT_c at the elastic centre, ΔT_u at the upper flange and ΔT_l at the lower flange. Using the cross-sectional depth h the linear variation of the temperature strain can be written as:

$$\varepsilon^T = \beta\, \Delta T_c + \beta (\Delta T_l - \Delta T_u) \frac{x}{h} \tag{4.22}$$

This leads to the following thermal strain at the elastic centre and thermal curvature:

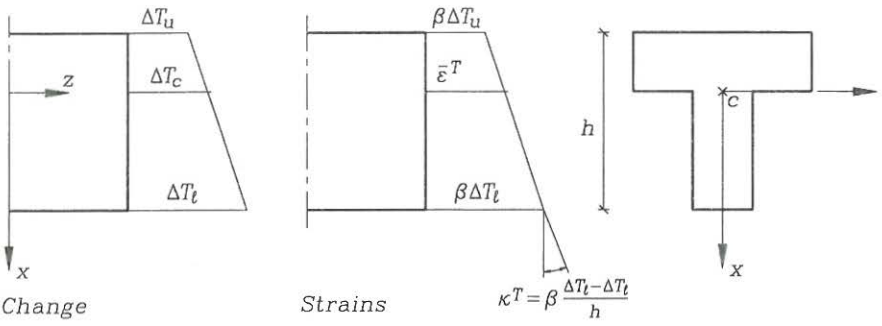

Fig. 4.22: The temperature strains for a linear temperature change.

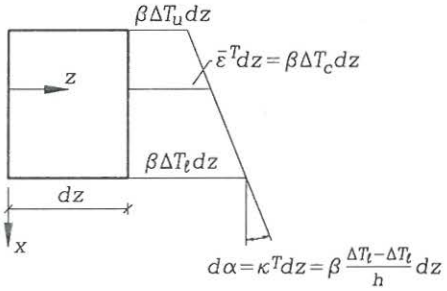

Fig. 4.23: The temperature induced displacements.

The thermal strain at the elastic centre and the thermal curvature for a linear variation of the temperature change through the cross-section are:

$$\bar{\varepsilon}^T = \beta\,\Delta T_c \tag{4.23}$$

$$\kappa^T = \beta\,\frac{\Delta T_l - \Delta T_u}{h} \tag{4.24}$$

where β is the coefficient of thermal expansion and the other quantities are shown in fig. 4.22.

For non-linear variations of the temperature change the mean values given by equations (4.20) and (4.21) can be used.

Sometimes an intuitive understanding can be achieved by the temperature induced displacements shown in fig. 4.23.

In statically determinate structures the axial displacements and curvatures induced by temperature changes will occur without introducing internal forces and reactions. However, in statically indeterminate structures the temperature changes can be regarded as a load that will induce internal forces and reactions. Thermal

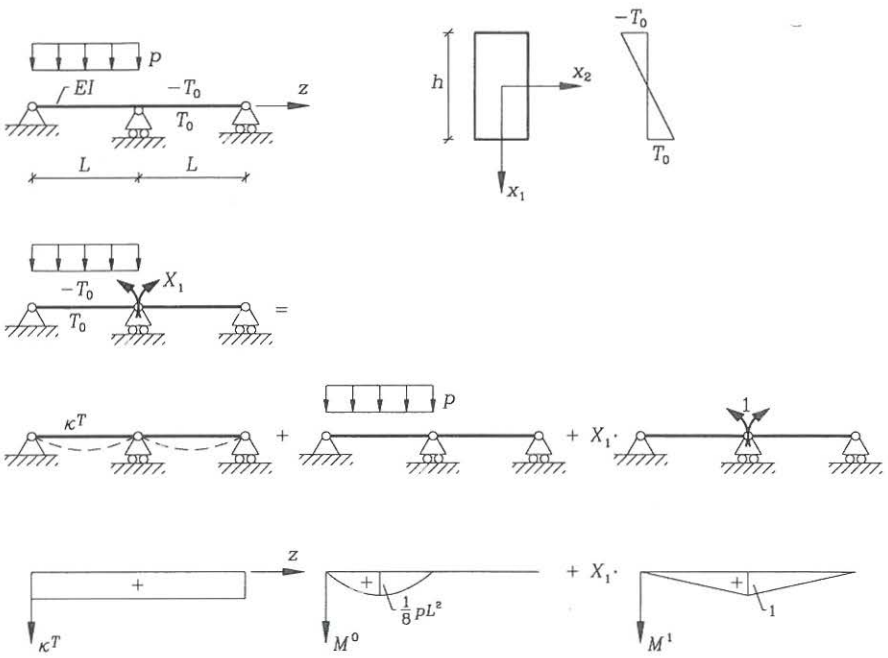

Fig. 4.24: Example with thermal curvature and transverse load.

changes can be included directly in the determination of the displacements due to external loads on the main system, using the original unit load formula in equation (4.5) as follows:

Thermal effects are introduced into the flexibility method by:

$$d_{i0} \simeq \sum_{\text{beams}} \int_0^L (\kappa^T + \frac{M^0}{EI}) M^i \, dz + \sum_{\text{trusses}} (\bar{\varepsilon}^T + \frac{N^0}{EA}) N^i \, L \qquad (4.25)$$

where $\bar{\varepsilon}^T$ and κ^T are the unrestrained thermal strains and curvatures on the main system. N^0 and M^0 are the internal forces from other loads.

- **Example 4.5** Thermal curvature and transverse load.

  Fig. 4.24 shows a continuous beam with one intermediate support. The upper temperature is decreased by T_0 and the lower temperature is increased by T_0. The first span is loaded by a uniform transverse load p. Let us calculate the moment at the central support. As shown in the figure we choose the central moment as the redundant moment X_1. The thermal curvature is found as:

$$\kappa^T = \beta \frac{2T_0}{h}$$

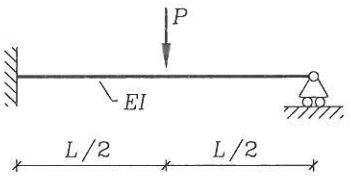

Fig. 4.25: A loaded beam.

The displacement d_{10} in the main statically determinate system can be found as follows:

$$\begin{aligned} d_{10} &= 2\frac{L}{6}(2+1)\kappa^T + \frac{L}{3EI}\frac{1}{8}pL^2 = (6EI\kappa^T + \frac{1}{4}pL^2)\frac{L}{6EI} \\ &= (12\frac{\beta T_0 EI}{h} + \frac{1}{4}pL^2)\frac{L}{6EI} \end{aligned}$$

The displacement d_{11} due to the unit load $X_1 = 1$ is

$$d_{11} = 2\frac{L}{6EI}(2) = 4\frac{L}{6EI}$$

The moment at the intermediate support thus becomes

$$M = X_1 = -\frac{d_{10}}{d_{11}} = -3\frac{\beta T_0 EI}{h} - \frac{1}{16}pL^2$$

It can thus be seen that both the temperature variation through the thickness and the transverse load contribute to the negative moment at the central support.

- **Problem 4.1**

A horizontal beam shown in fig. 4.25 has the length L, the material is linear elastic and the bending stiffness EI is constant. The beam is loaded downwards by a central point load P. The left-hand end is fixed (built in) and the right-hand end is pinned with horizontal rollers. Find the reactions, the moment distribution and the central displacement in the beam.

- **Problem 4.2**

The linear elastic frame shown in fig. 4.26 consists of two vertical beams, which are rigidly connected to a horizontal beam. The vertical beams are pinned at the lower end, they have a length of $L_1 = 5\,\mathrm{m}$ and a bending stiffness of EI_1. The horizontal beam has a length of $L_2 = 8\,\mathrm{m}$ and a bending stiffness of $EI_2 = \frac{1}{4}EI_1$. The beam is loaded downwards by a distributed load $p = 10\,\mathrm{kN/m}$ on the horizontal beam. Find the reactions and the moment distribution in the frame. Find also the vertical displacement at the centre of the horizontal beam.

- **Problem 4.3**

A plane frame $ABCD$, shown in fig. 4.27, is built in at the supports A and pinned at D. The vertical beams AB and DC have the length L and the bending stiffness EI. The horizontal beam BC has the length L and bending stiffness $\frac{1}{2}EI$. The frame is loaded by a uniform horizontal load p acting on beam AB. The effects of shear and axial forces are neglected and it is assumed that only moments contribute to the beam displacements.

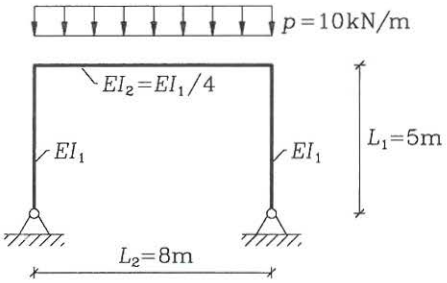

Fig. 4.26: A symmetric frame.

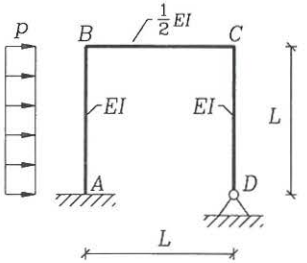

Fig. 4.27: A frame with lateral load.

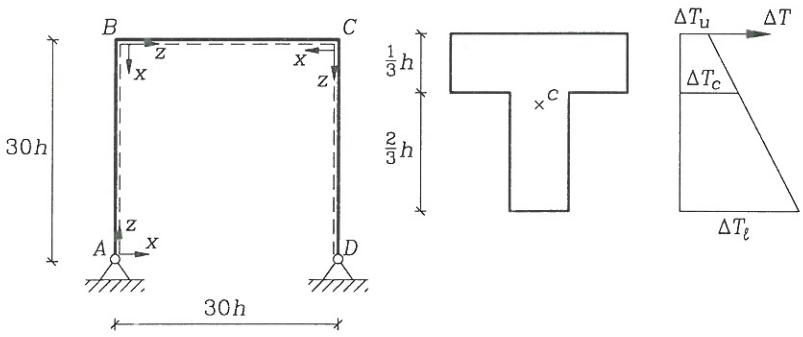

Fig. 4.28: Temperature change in plane frame.

a) Find the moment and shear force distributions in the frame. The sign conventions used must be stated and clearly drawn.

b) The support at D settles the distance s_D downwards due to the external load. Find the moment distribution in the frame due to this settlement alone (with $p = 0$).

- **Problem 4.4**

A plane frame $ABCD$, shown in fig. 4.28, is pinned at the supports A and D. All three beams have the length $L = 30h$, the modulus of elasticity E, the cross-sectional area $A = \frac{1}{2}h^2$ and the moment of inertia $I = \frac{1}{30}h^4$. The cross-sectional type is also shown in the figure. The effects of shear and axial forces are neglected and it is assumed that only moments contribute to the beam displacements.

A temperature change occurs. At the elastic centre it is $\Delta T_c = T_0$, at the outer surface it is half, $\Delta T_u = \frac{1}{2}T_0$, and at the inner surface it is double, $\Delta T_l = 2T_0$. The expansion coefficient is β and the temperature variation is linear through the cross-section.

a) Find the moment distribution and the reactions due to the temperature change. Remember the influence of axial temperature strain.

b) The cross-section is an uncracked reinforced concrete section with maximum compressive stress of $f_c = 40$ MPa. The depth is $h = 200$ mm, the elasticity modulus is $E = 36 \cdot 10^3$ MPa, the expansion coefficient is $\beta = 10 \cdot 10^{-6}$ and the elastic centre is located $\frac{1}{3}h$ from the outer surface. With the given temperature variation, what is the maximum permissible temperature change T_0 for this frame?

Chapter 5

Plastic Hinge Analysis

Since beam structures do not always remain linear elastic it is necessary to have tools which can take us beyond the elastic limit, especially for beams of materials that have a plastic capacity. In this section we shall first describe the plastification of beam cross-sections for some non-linear elastic constitutive relations. Then we shall introduce the concept of plastic hinges and relate the concept to the principle of virtual work and derive upper- and lower-bound theorems for plastic hinge analysis. Following this a method of combining plastic flow mechanisms is described and finally a method for estimating displacements is given. Detailed treatment of the subject is given by Massonnet & Save [15] or by Neal [16]. A modern approach to general plasticity theory is given by Chen & Han [18]. This book includes a small section on plastic hinge analysis and its relation to modern plasticity theory.

In this chapter we thus treat the load-carrying capacity of beam structures and we shall restrict ourselves to plane frames. The index notation will therefore not be used in this chapter.

Plastification of Beam Cross-Sections

In Bernoulli beam theory we assume that the beam is in a uniaxial state of stress and strain and the theory relies on a linear elastic constitutive material law. However, the linear elastic constitutive law $\sigma = E\varepsilon$ is only an assumption, which cannot always be applied to the complete stress-strain domain of the structure. The uniaxial behaviour of different materials is relavtivly simple to find by experiment. Some materials have stress-strain relationships, which can be idealized as shown in fig. 5.1. The first plot shows an example of a uniaxial stress-strain relation for a real material, the second plot shows an idealized linear elastic perfectly plastic constitutive material model and the third plot shows the highest level of idealization corresponding to a perfectly plastic material model. Note that in the plastic domain the strain cannot be determined uniquely from the stress, but must be determined by other kinematic conditions. When the material is unloaded the stress-strain curve follows a linear path, which is approximately parallel to the initial linear path, until it reaches the opposite yield stress. The plastic part of the strains thus becomes residual strains, which can be reduced by plastic straining in the oppo-

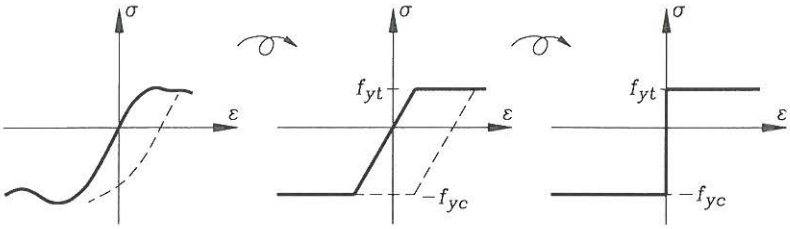

Fig. 5.1: Uniaxial stress-strain curves and two idealizations.

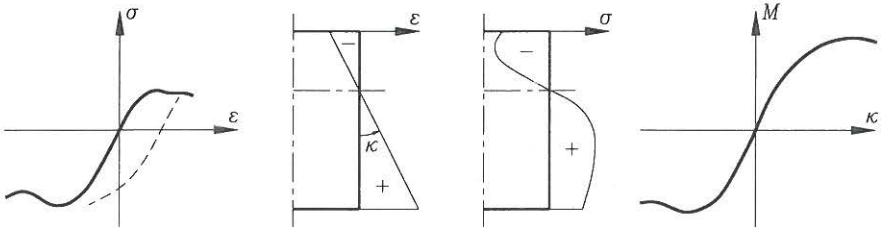

Fig. 5.2: Use of a real stress-strain relation.

site direction. The unloading paths are shown as dashed lines in the figure. In the idealized models the maximum tensile stress is the tensile yield stress f_{yt} and the maximum compressive stress is the compressive yield stress f_{yc} and if they are identical we just write f_y.

Let us see how the three types of stress-strain relations influence the constitutive moment-curvature relation $M = F(\kappa)$ for a beam in bending. We assume that cross-sections remain plane during deformation. The neutral axis is determined by the assumption of zero axial force, $N = \int_A \sigma \, dA = 0$. Fig. 5.2 illustrates the use of the real uniaxial stress-strain curve. With the assumption of cross-sections remaining plane the strain distribution becomes linear and the stress distribution is just a rotated part of the material stress-strain relation. The moment curvature relation is found by integrating the moment contribution of the stresses $M = \int_A (x - c)\sigma \, dA$ for the relevant curvature range, where c is the current position of the neutral axis. The moment curvature relation also becomes non-linear. In case of a linear elastic perfectly plastic material, as shown in fig. 5.3, the moment curvature relation is linear until a material point reaches the yield-stress f_y and the corresponding moment is called the initial yield moment M_y. After this the relation becomes non-linear and the moment asymptotically approaches the fully plastified situation corresponding to a fully plastic moment M_p. If we assume a perfectly plastic stress-strain relation, as illustrated in fig. 5.4, the moment curvature relation also becomes a perfectly plastic relation. The material moment-curvature relations depend on the geometry of the cross-section and the stress-strain relation assumed. For some cross-sections, especially steel I-beams, the non-linear part of the moment-curvature

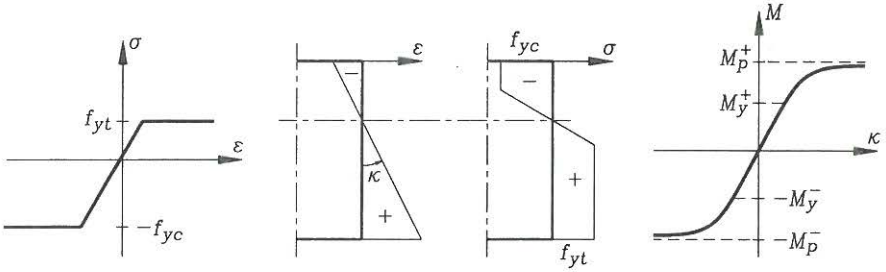

Fig. 5.3: Use of a linear elastic perfectly plastic stress-strain relation.

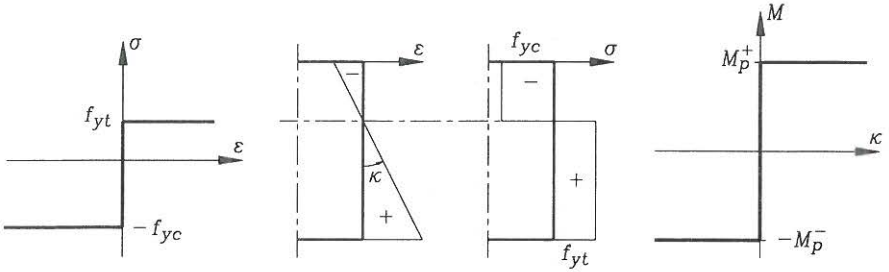

Fig. 5.4: Use of a perfectly plastic stress-strain relation.

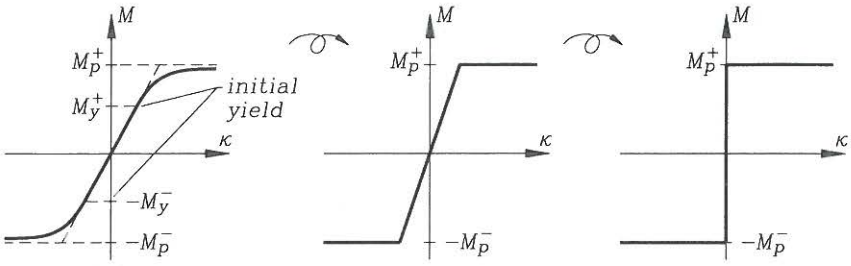

Fig. 5.5: Idealizations of the moment-curvature relationship.

relation in the linear elastic perfectly plastic case becomes negligible. Even though the moment-curvature relation has a non-linear part it is convenient and useful to assume a linear elastic perfectly plastic relation. In fig. 5.5 the first plot shows the resulting moment-curvature relation, when assuming a linear elastic perfectly plastic material model. The second plot shows an idealized linear elastic perfectly plastic moment-curvature relation, where the linear elastic part of the first curve has been extended. The third plot just shows the idealized perfecly plastic moment-curvature relation, which is the constitutive model used in plastic hinge analysis. The linear elastic perfectly plastic moment-curvature relation is used for simplified deflection analysis, whereas the perfectly plastic moment-curvature relation is used to derive the load-carrying capacity of a beam structure.

In the following we assume that the axial forces and the shear forces are small enough to be discarded in the analysis. If this is not the case an approach using plastic yield surfaces generalized from the von Mises and Tresca yield criteria, which are beyond the scope of the present chapter. Furthermore, it is assumed that the plastic domain is large enough to give the necessary rotation capacity in plastic hinges introduced in the following.

Virtual Work in a Plastic Hinge

In beam structures the maximum moments are often situated at discrete points and in a few situations a constant moment is transferred through a beam. Let us first assume that the maximum moments are situated at discrete points and that the moment-curvature relation is perfectly plastic. With this assumption the curvatures are localized to positions, where the moment has reached the plastification moment M_p. Let us use a beam with pinned ends and a central point load, as shown in fig. 5.6, to illustrate a plastic hinge. The beam remains straight with no deflections until the load reaches a value, where the midsection is plastified. With the given assumptions the curvature is zero except at the midpoint, where it is indeterminate. In this situation the structure flows (yields) and we assume that the structural behaviour is quasi static, so that the principle of virtual work can be used. When the beam flows at the midpoint the beam becomes kinematicly indeterminate and the possible kinematic motion is called a mechanism. The midpoint where all the

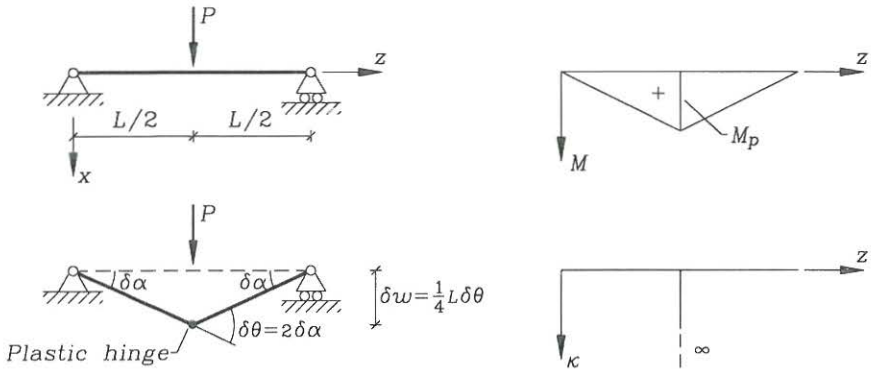

Fig. 5.6: A beam with pinned ends and a central point load.

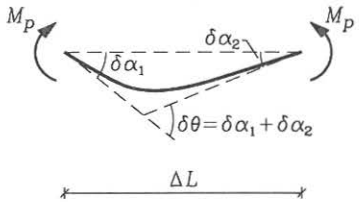

Fig. 5.7: Plastic beam section of the length ΔL.

material deformation is concentrated is a so-called plastic hinge.

The internal virtual work $\int_L M\,\delta\kappa\,dz$ corresponds to the virtual plastic energy dissipation. To use the principle of virtual work we need to find the internal virtual work. Let us show how we can find it in an indirect manner. A beam section of the length ΔL, shown in fig. 5.7, is loaded by end moments, $\bar{M} = M_p$, which are equal to the plastic yield moment. The beam section yields and the real as well as the virtual internal curvature is indeterminate. We assume that the end rotations are given by $\delta\alpha_1$ and $\delta\alpha_2$ and that the sum is $\delta\theta = \delta\alpha_1 + \delta\alpha_2$. Using the principle of virtual work $\delta W = \delta W_{int} - \delta W_{ext} = 0$ we can find the internal work expressed by the external work as follows:

$$\begin{aligned}
\int_{\Delta L} M\delta\kappa\,dz - \bar{M}(\delta\alpha_1 + \delta\alpha_2) &= 0 \quad \Downarrow \\
\int_{\Delta L} M_p\,|\delta\kappa|\,dz - M_p\,|(\delta\alpha_1 + \delta\alpha_2)| &= 0 \quad \Downarrow \\
\int_{\Delta L} M_p\,|\delta\kappa|\,dz &= M_p\,|\delta\theta| \qquad (5.1)
\end{aligned}$$

where the absolute value is introduced, since $M = -M_p$ and $\bar{M} = -M_p$ for negative curvatures, $\delta\kappa < 0$. Let the length of the section approach zero, thus defining the internal virtual work of a plastic hinge δW_{int} with an indeterminate infinite

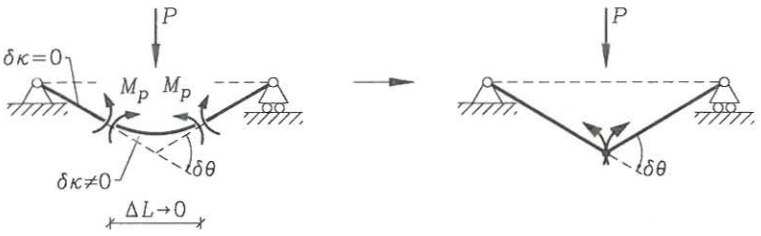

Fig. 5.8: Plastic hinge in the beam with pinned ends.

curvature as:

$$\delta W_{int} = \lim_{\Delta L \to 0} \int_{\Delta L} M_p \, |\delta\kappa| \, dz = M_p \, |\delta\theta| \tag{5.2}$$

Note that the internal work is positive. The idea is illustrated for a beam with pinned ends in fig. 5.8.

- **Example 5.1** A statically determinate beam with a plastic hinge

  The load-carrying capacity of the beam in fig. 5.8 with pinned ends and a central point load is sought. The external virtual work is determined as the work by the load P through its vertical displacement $\delta w = \frac{1}{4} L \, \delta\theta$. Now it is possible to find the load capacity of the beam by use of the principle of virtual work $\delta W = \delta W_{int} - \delta W_{ext} = 0$ as follows:

$$\begin{aligned} \int_L M \delta\kappa \, dz - P\delta w &= 0 \qquad \Downarrow \\ M_p \, \delta\theta - \frac{1}{4} P L \delta\theta &= 0 \qquad \Downarrow \\ P &= 4 \frac{M_p}{L} \end{aligned}$$

  In the present case this is the load-carrying capacity of the beam. However, in general, as we shall se later, the virtual work equation just gives an upper-bound value for the load-carrying capacity, since the virtual hinge has not necessarily been placed correctly, and therefore, the moment at the hinge may not have reached the plastic limit.

Virtual Work and Hinges

The virtual work functional for beams does not depend on the constitutive moment-curvature relation. The principle of virtual work can be extended to include discontinuities in the derivative of the virtual displacement, so-called virtual hinges. The internal work in a hinge is found by using the same procedure as in the previous sub-section, however, this time the end moments $\bar{M} = M$ in fig. 5.7 have not reached the plastic limit. Thus, the internal work in a virtual hinge is thus:

$$\delta W_{int} = \lim_{\Delta L \to 0} \int_{\Delta L} M \delta\kappa \, dz = M \, \delta\theta \tag{5.3}$$

Without making any constitutive assumption about the moment-curvature relation the general virtual work functional for virtual displacements with hinges and zero curvatures has the following form:

Virtual work functional with virtual hinges and zero virtual curvature

$$\begin{aligned} \delta W &= \delta W_{int} - \delta W_{ext} \\ &= \sum_{\text{hinges}} M\delta\theta - \sum_{\text{beams}} \int_L (p\,\delta w + m\delta\alpha)\,dz \end{aligned} \tag{5.4}$$

The principle of virtual work

$$\delta W = 0 \quad \text{for all virtual displacements} \quad \Leftrightarrow \quad \text{equilibrium} \tag{5.5}$$

where the displacements must be kinematicly admissible.

It is possible to find the moment at any point of a statically determinate beam by use of virtual hinge analysis. If a linear-elastic beam is statically indeterminate and the redundant forces are known, then it is also possible to find the internal moments by use of virtual hinge analysis. However, this method is beyond the scope of the present chapter.

If the beam structure includes only point loads P the virtual work functional takes the following form:

$$\delta W = \sum_{\text{hinges}} M\delta\theta - \sum_{\text{loads}} P\,\delta w \tag{5.6}$$

This is a trivial extension, which will be left to the reader in the following.

5.1 Theorems of Limit Analysis

The idea of limit analysis in perfect plasticity is to ease the "intuitional demand" for the real moment field M in the principle of virtual work. A kinematic and a static approach results in an upper-bound theorem and a lower-bound theorem, respectively. Before proceeding let us introduce a load factor λ to a set of given loads, i.e. λp and λm, and rewrite the principle of virtual work as follows:

$$\delta W = \sum_{\text{hinges}} M\delta\theta - \lambda \sum_{\text{beams}} \int_L (p\,\delta w + m\delta\alpha)\,dz = 0 \tag{5.7}$$

This equation is exact and gives the correct load factor, λ, corresponding to the real moment distribution M. Furthermore, let us also introduce a plastic virtual work functional δW_p in which we exchange the moments M at the virtual hinges by the plastic moments M_p and the load factor λ by the plastic load factor λ_p at which a flow mechanism is created. The plastic virtual work functional takes the form:

Plastic virtual work functional

$$\delta W_p = \sum_{\text{hinges}} M_p \, |\delta\theta| - \lambda_p \sum_{\text{beams}} \int_L (p \, \delta w + m \delta\alpha) \, dz \tag{5.8}$$

This plastic virtual work functional is used in the following.

The kinematic approach is to anticipate a kinematic mechanism with *virtual plastic* hinges, as illustrated in fig. 5.9 for a uniformly loaded beam with a fixed and a pinned end. Let us use the principle of virtual work $\delta W = 0$ to estimate an upper bound λ^+ for the plastic load factor λ_p at which a flow mechanism is created. Assuming that the moment at the *virtual* hinge is the *plastic* moment M_p, the demand for the real moment M at this point is violated, since $M_p \geq |M|$. The principle of virtual work is thus violated by increasing the internal work $\delta W_p \geq \delta W = 0$, since $M_p|\delta\theta| \geq M\delta\theta$. This leads to the following upper-bound theorem:

The upper-bound theorem

An upper bound, λ^+, for the plastic load-carrying capacity, λ_p, can be found by introducing kinematicly admissible virtual displacements with virtual plastic hinges into the virtual work functional and using that this virtual work is greater than or equal to zero, $\delta W_p \geq 0$.

The inequality leads to the following formulation:

$$\delta W_p = \sum_{\text{hinges}} M_p|\delta\theta| - \lambda_p \sum_{\text{beams}} \int_L (p \, \delta w + m\delta\alpha) \, dz \geq 0 \quad \Downarrow$$

$$\lambda_p \leq \lambda^+ \tag{5.9}$$

where the upper-bound load factor is given by

$$\lambda^+ = \frac{\sum_{\text{hinges}} M_p \, |\delta\theta|}{\sum_{\text{beams}} \int_L (p \, \delta w + m\delta\alpha) \, dz} \tag{5.10}$$

Note that the size of the plastic moment M_p may depend on the sign of the virtual rotation, i.e. the sign of the localized curvature, and on the position.

Many equivalent formulations of the upper-bound theorem exist, which in fact can be generalized to other structures.

- **Example 5.2** Use of the upper-bound theorem.

  The beam shown in fig. 5.9 has the length $L = 6$ m, the plastification moment $M_p = 20$ kNm and a uniformly distributed load $p = 2$ kN/m. Let us find an upper-bound load factor. The figure shows a kinematicly admissible virtual displacement field with virtual plastic hinges. The internal virtual work is $M_p\delta\theta + M_p\frac{5\theta}{2}$ and the external work kan either be integrated by the integration formula (4.9) or by finding the work of the load resultants for the load on each half of the beam by

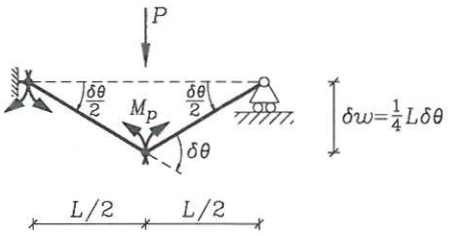

Fig. 5.9: Mechanism with virtual plastic hinge.

$2(\frac{1}{2}\lambda_p p\ \frac{1}{2}\delta w) = \frac{1}{2}\lambda_p pL\delta w$. The upper-bound principle for plastic virtual work $\delta W_p \geq 0$ gives:

$$\frac{3}{2}M_p\delta\theta - \frac{1}{2}\lambda_p pL\delta w \geq 0 \tag{5.11}$$

in which we can introduce either $\delta\theta = \frac{4}{L}\delta w$ or $\delta w = \frac{L}{4}\delta\theta$ and thereby find an upper bound for the load factor as:

$$\lambda_p \leq 12\frac{M_p}{pL^2} = 3.33 \tag{5.12}$$

Thus an upper bound for the load-carrying capacity is $p^+ = 3.33p = 6.67$ kN/m. This value can be decreased by letting the position of the virtual plastic hinge be variable and then minimizing the upper bound with respect to this position.

The static approach is based on statically admissible moment distributions M_s in the beam structure and limit the values of these moments by the plastic limit M_p. In a statically determinate beam structure there is only one way to carry the load and thus only one statically admissible moment distribution. In statically indeterminate beam structures with n redundants there are $n+1$ independent statically admissible moment distributions which may be combined. Fig. 5.10 shows a statically admissible moment field. When the structure is linear-elastic only one combination is possible and this combination can for example be found by the flexibility method as $M = M^0 + \sum_n M^i X_i$, where X_i are the values of the redundant forces. However, when the structure is no longer linear-elastic it must be some other combination, which results in the real moment distribution. Since the real moment distribution is unknown the idea of the static approach is to replace the real moment distribution M by a statically admissible moment distribution M_s. For the statically admissible moment distribution M_s to be a safe distribution the moments must be within the plasticfication limit $|M_s| \leq M_p$. This leads to a lower bound λ^- for the load factor.

First let us use the principle of virtual work (5.5) to find an expression for the exact plastic load factor λ_p. To do this we use the displacements of the real plastic flow mechanism as the virtual displacements, i.e. $\delta\theta = \dot{\theta}$, $\delta w = \dot{w}$ and $\delta\alpha = \dot{\alpha}$, and

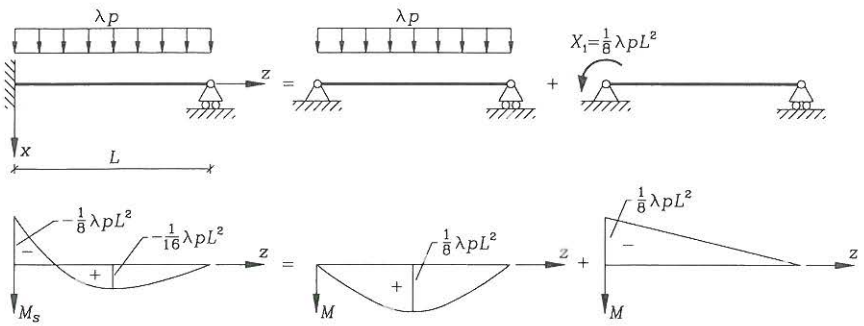

Fig. 5.10: A statically admissible moment field.

thus the real moment M_p at the hinges as follows:

$$\delta W = \sum_{\text{hinges}} M_p \, |\dot{\theta}| \; - \; \lambda_p \sum_{\text{beams}} \int_L (p\,\dot{w} + m\dot{\alpha})\, dz \; = \; 0 \quad \Downarrow$$

$$\lambda_p \; = \; \frac{\sum\limits_{\text{hinges}} M_p \, |\dot{\theta}|}{\sum\limits_{\text{beams}} \int_L (p\,\dot{w} + m\dot{\alpha})\, dz} \tag{5.13}$$

Next let us use a statically admissible moment distribution M_s in equilibrium with the loads $\lambda^- p$ and $\lambda^- m$. The principle of virtual work (5.5) is exact for this moment field, since it fulfils the equilibrium equations (it is statically admissible), we can thus use any virtual displacement field and find the same load factor λ^-. We will show that this load factor is a lower bound for the real plastic load factor if we just make sure that M_s is a safe statically admissible moment field, i.e. $|M_s| \leq M_p$. Since we can use any virtual displacement field let us try the real plastic flow mechanism as follows:

$$\delta W \; = \; \sum_{\text{hinges}} M_s \delta\theta - \lambda^- \sum_{\text{beams}} \int_L (p\,\delta w + m\delta\alpha)\, dz = 0 \quad \Downarrow$$

$$\lambda^- \; = \; \frac{\sum\limits_{\text{hinges}} M_s \delta\theta}{\sum\limits_{\text{beams}} \int_L (p\,\delta w + m\delta\alpha)\, dz} \; = \; \frac{\sum\limits_{\text{hinges}} M_s \dot{\theta}}{\sum\limits_{\text{beams}} \int_L (p\,\dot{w} + m\dot{\alpha})\, dz} \; \leq \; \lambda_p \tag{5.14}$$

where the last inequality is obtained using equation (5.13) and $M_s\dot{\theta} \leq M_p\,|\dot{\theta}|$, since the statically admissible moment distribution is safe, i.e. since $|M_s| \leq M_p$ and $M_p|\dot{\theta}|$ is always positive.

The lower-bound theorem

If a statically admissible moment distribution, M_s, in equilibrium with the factored external loads, $\lambda^- p$ and $\lambda^- m$, is safe, $|M_s| \leq M_p$, then the load factor, λ^-, is a lower bound for the real plastic load factor λ_p, i.e. $\lambda^- \leq \lambda_p$.

There are also many equivalent formulations of the lower-bound theorem, which can be generalized for other structures. The lower-bound theorem is used in combination with the upper-bound theorem to bound the plastic load factor. Furthermore, as we shall see in the second of the following examples, it may sometimes be profitable to use the statically admissible moment distribution corresponding to the upper-bound solution and scale it down to be a safe one.

If the upper-bound and lower-bound load factors are identical then the solution is exact. This is sometimes referred to as the uniqueness theorem and it is trivial with the already given theorems.

From the derivation of the lower-bound theorem, equation (5.14), it is clear that we can define a safe virtual work functional δW_s using the safe moment distribution M_s and the virtual work will be less than the real virtual work as follows:

$$\delta \quad _s \quad = \sum_{\text{hinges}} M_s \delta\theta - \lambda_p \sum_{\text{beams}} \int_L (p\,\delta w + m\delta\alpha)\,dz \;\leq\; 0 \tag{5.15}$$

However, we will not use this principle $\delta W_s \leq 0$ in the following, but it is worthwhile to compare it with the plastic principle of virtual work $\delta W_p \geq 0$.

- **Example 5.3** Use of the lower-bound theorem.

  The uniformly loaded beam with a fixed and a pinned end from the previous example 5.2 is analysed using the lower-bound theorem. As in the previous example the beam has the length $L = 6$ m, the plastification moment $M_p = 20$ kNm and a uniformly distributed load $p = 2$ kN/m. Let us find a lower-bound load factor.

  A statically admissible moment distribution is shown in fig. 5.10, where any value can be chosen for X_1. In the present example we choose to let the fixed end carry a moment equal to $-\frac{1}{8}\lambda pL^2$. The positive moments are thereby less than $\frac{1}{8}\lambda pL^2$ and the maximum is not at the centre. The statically admissible moment distribution is safe if $|M_s| \leq M_p$. Using the equal sign this results in the following lower-bound load factor:

$$\frac{1}{8}\lambda^- pL^2 = M_p \qquad \Downarrow$$

$$\lambda^- = 8\frac{M_p}{pL^2} = 2.22$$

  Comparing the result with the previous example it is seen that the plastic load factor is bounded by the two solutions:

$$8\frac{M_p}{pL^2} \leq \lambda_p \leq 12\frac{M_p}{pL^2} \qquad \Downarrow$$

$$2.22 \leq \lambda_p \leq 3.33$$

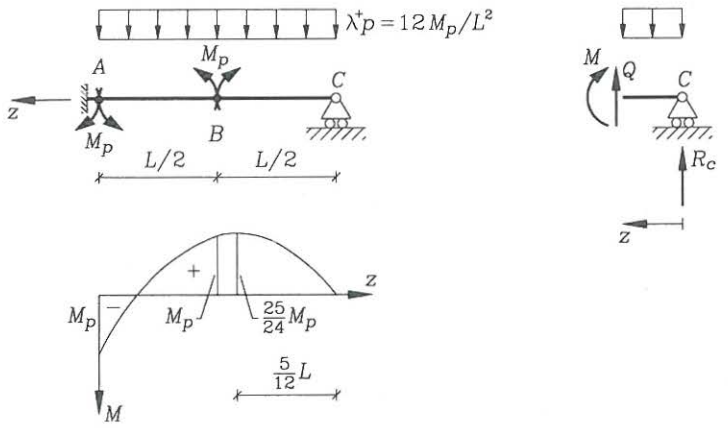

Fig. 5.11: Upper-bound moment distribution.

This can be used in two ways, if the beam is known, then we can find the plastification moment M_p, and the load-carrying capacity $p^t = \lambda_p p$ is then bounded as follows:

$$\begin{aligned} 8\frac{M_p}{L^2} &\leq p^t \leq 12\frac{M_p}{L^2} \quad \Downarrow \\ 4.44\,\mathrm{kN/m} &\leq p^t \leq 6.67\,\mathrm{kN/m} \end{aligned}$$

However, if we are at the design stage we know the total load $p = 2$ kN/m and want to find the necessary plastification momemt M_p, which is then bounded by:

$$\begin{aligned} \frac{1}{12}p^t L^2 &\leq M_p \leq \frac{1}{8}p^t L^2 \quad \Downarrow \\ 6\,\mathrm{kNm} &\leq M_p \leq 9\,\mathrm{kNm} \end{aligned}$$

The gap between the upper- and lower-bound value can be narrowed by finding a better lower bound, corresponding to a better statically admissible moment distribution, or by finding a better flow mechanism. In the current case we shall probably not gain much from moving the central plastic hinge, on the other hand, we can find a much better lower-bound solution.

- **Example 5.4** Finding an admissible moment distribution.

Let us use the upper-bound solution to find a statically admissible moment distribution and then scale it down to make it safe. To find the moment distribution corresponding to the upper-bound solution we assume that the moments at the hinges are given the yield moments M_p and the load is thus given by $\lambda^+ p = 12 M_p/L^2$, as shown in the upper left-hand part of fig. 5.11. To find the moment distribution we can first find the vertical reaction at C by moment equilibrium about B for the

part $B-C$ as follows:

$$-M_p - \lambda^+ p\frac{L}{2}\frac{L}{4} + R_c\frac{L}{2} = 0 \qquad \Downarrow$$
$$R_c = \frac{2}{L}(M_p + \frac{12}{8}M_p) = 5\frac{M_p}{L}$$

The moment distribution varies quadraticly, due to the transverse load. From A to B it varies from a negative plastic moment to a positive plastic moment. The maximum negative moment is thus at A and the maximum positive is assumed to be between B and C. The moment variation from C to B is found by moment equilibrium of the section shown in the right-hand part of the figure. With origin at the right-hand end we have that $z \leq L/2$ and find:

$$-M(z) - \frac{1}{2}\lambda^+ pz^2 + R_c z = 0 \qquad \Downarrow$$
$$M(z) = -\frac{12}{2}M_p\left(\frac{z}{L}\right)^2 + 5M_p\frac{z}{L}$$

The maximum value is found by demanding $M' = 0$ as follows:

$$M'(z) = -12M_p\frac{z}{L^2} + 5M_p\frac{1}{L} = 0 \qquad \Downarrow$$
$$z = \frac{5}{12}L \qquad \Downarrow$$
$$M_{max} = M(\frac{5}{12}L) = -\frac{12}{2}M_p\left(\frac{5}{12}\right)^2 + 5M_p\frac{5}{12} = \frac{25}{24}M_p$$

The statically admissible moment distribution corresponding to λ^+ is shown in the lower left-hand part of the figure. To make it safe we scale it by a factor β and require that the maximum moment is equal to the plastic moment. The lower bound is thus given by $\lambda^- = \beta\lambda^+$. Let us find the scaling factor:

$$\beta\, M_{max} = M_p \qquad \Downarrow$$
$$\beta\frac{25}{24}M_p = M_p \qquad \Downarrow$$
$$\beta = \frac{24}{25}$$

This gives the lower bound

$$\lambda^- = \frac{24}{25}\lambda^+ = \frac{24}{25}12\frac{M_p}{pL^2} \simeq 11.52\frac{M_p}{pL^2} \simeq 3.20$$

The difference between the upper-bound solution $\lambda^+ = 3.33$ and the lower-bound solution $\lambda^- = 3.20$ is about 4%, which is acceptable in design.

- **Problem 5.1**

Find upper-bound and lower-bound load factors for the beam shown in fig. 5.12. The number of plastic hinges is equal to the degree of indeterminateness plus one. For the upper bound assume a plastic hinge below the force and at the fixed end of the beam. Find the exact plastic load factor by finding equal upper and lower-bound load factors.

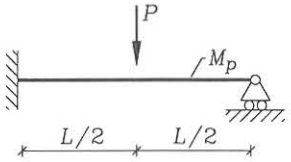

Fig. 5.12: Beam loaded by a point load.

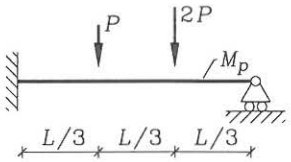

Fig. 5.13: Beam loaded by two point loads.

- **Problem 5.2**
  Find upper-bound and lower-bound load factors for the beam shown in fig. 5.13. Plastic hinges can be formed at the loads and at the fixed support, however, only two hinges are needed to define a plastic mechanism. Find the exact plastic load factor by finding equal upper and lower-bound load factors.

- **Problem 5.3**
  Find upper-bound and lower-bound load factors for the frame shown in fig. 5.14. Plastic hinges can be formed on either side of the corners and under the point load. Find three plastic mechanisms and the corresponding upper-bound load factors. Find a good lower-bound load factor.

5.2 Combination of Mechanisms

Today analysis of large three-dimensional beam structures can be performed by advanced computational methods based on modern plasticity theory, which takes axial forces, shear forces, biaxial moments and torsional moments into account, either by a yield surface directly based on internal forces or by a yield surface based on stresses. However, for small plane frames plastic hinge analysis is a simple tool, which can be used to determine the load-carrying capacity, and which can give a basic intuitional understanding of the structural behaviour. A method of combining mechanisms proposed by Neal & Symmonds [16], [17], is introduced in the present section.

The idea is to choose a sufficient number of possible basic mechanisms in the frame and then combine these. Through combination of mechanisms plastic hinges are introduced or eliminated in order to minimize the upper-bound load factor. The upper-bound load factor λ^+ is minimized by choosing combinations of mechanisms,

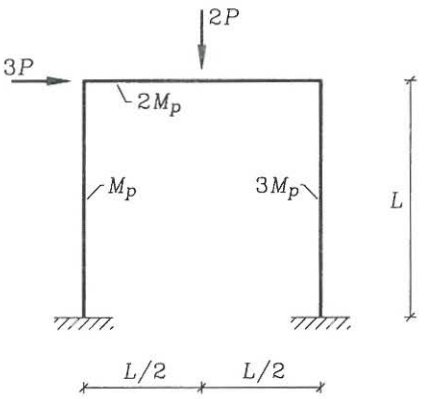

Fig. 5.14: Frame with varying plastification moment.

which minimize the virtual work of the plastic hinges and maximize the virtual work of the loads.

Frames often consist of beams with different plastification moments M_p and it is therefore very important to be precise about the position of plastic hinges at the joints. This can be done by placing the plastic hinges in the beams infinitely close to the joints as shown in the following figures. It is also necessary to be aware that plastification moments can be different for positive and negative moments.

Plastic collapse mechanisms in frame structures can be partial, thus involving a part of the structure, typically with a few local plastic hinges, or they can be complete, thus involving displacement of the complete structure (without separate statically indeterminate parts). In a structure with n redundancies a complete mechanism will involve $n+1$ plastic hinges, whereas partial mechanisms will involve fewer plastic hinges. Having chosen the basic mechanisms to be combined, the number of possible plastic hinges h is known. For a strucure with h possible plastic hinges there are $h - n$ independent mechanisms, which can be combined to form the total array of mechanisms (spanned by the chosen hinges).

Plastic hinges are typically situated at connections, at point loads or somewhere in the central part of the span for distributed loads. The choice of mechanisms to be combined can be simplified by introducing three basic types of mechanisms, namely beam, joint and sway mechanisms. These basic mechanisms are combined in the search for a collapse mechanism. Fig. 5.15 shows the basic mechanisms and two combinatory proposals representing partial collapse mechanisms. It is important to note that, it may be neccessary to include joint mechanisms even at unloaded joints, since it is difficult in advance to predict in which beams at the joint the plastic hinges will be formed.

To minimize the upper bound λ^+, it follows from the virtual work equation that the virtual work of the loads has to be maximized and that the virtual work of the plastic hinges must be minimized. Optimal combinations of mechanisms may

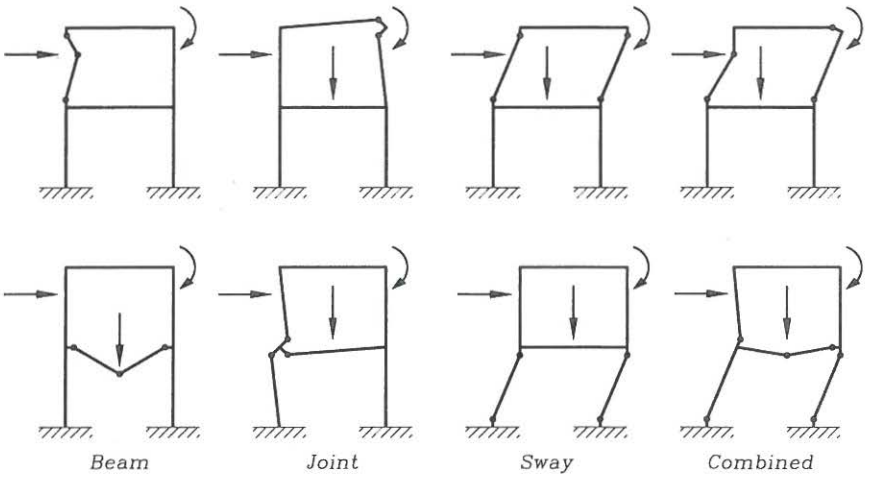

Fig. 5.15: Basic mechanisms and two combined mechanisms.

often be found by choosing mechanisms, which involve displacement of as many loads as possible, and by eliminating plastic hinges or exchanging plastic hinges for others, where the plastification moment is lower. The combined mechanisms should be described kinematicly by one free geometric parameter alone, for example $\delta\theta$ or δw. When a minimized upper-bound load factor λ^+ has been found, then the corresponding moment distribution M can be found. This moment distribution is then scaled down by a factor β, which makes it a safe moment distribution $\beta|M| \leq M_p$. A lower-bound load factor is then given by $\lambda^- = \beta\lambda_+$. In problems involving only point loads the mechanism combination method often leads to the exact solution for the plastic load factor. In problems involving distributed loads the lower-bound and upper-bound load factors are often very close. The mechanism combination method is summarized in tab. 5.1. It should be noted that assumptions concerning rotation capacity at plastic hinges and small displacements should be checked.

- **Example 5.5** Analysis of the frame in fig. 5.16.

  A frame consisting of a continuous beam $ABCD$ over the top of two columns EB, FC is shown in fig. 5.16. The geometry, loads and boundary conditions are shown in the figure. The factor λ has been introduced as a proportional load factor. The load is $P = 10$ kN and the length is $L = 5$ m. The plastification moment is $M_r = 100\,\mathrm{kNm}$ for the columns and $2M_r = 200\,\mathrm{kNm}$ for the beams. In the example M_r is used as a reference moment as indicated by the index r. In this example the problem is to find the exact plastic load factor for the given frame with the given combination of loads. The problem will be solved by the mechanism combination method following the procedure given in tab. 5.1.

  1. Inserting plastic hinges arround connections, fixed supports and at point

The mechanism combination method

1. *Find the number of possible plastic hinges, h.*
2. *Find the degree of static indeterminateness, n (i.e. the number of redundancies).*
3. *Find $h - n$ independent (beam, joint and sway) mechanisms and the corresponding upper-bound load factors λ^+.*
4. *Find the combination that minimizes the upper-bound load factor λ^+. (Combine the independent mechanisms by maximizing virtual work of the loads and minimizing the virtual work of the plastic hinges. It is a good idea to combine mechanisms with low upper-bound load factors. The maximum admissible number of plastic hinges in a mechanism is $n + 1$).*
5. *For the minimized upper-bound solution with the load factor λ^+, find the corresponding moment distribution M by statics.*
6. *Scale the upper-bound solution by the factor β, which makes the moment distribution safe, i.e. $\beta|M| \leq M_p$. A lower-bound load factor is thus given by $\lambda^- = \beta\,\lambda^+$.*
7. *If the lower-bound and the upper-bound load factors are identical, i.e. $\beta = 1$, then the exact plastic load factor has been found $\lambda_p = \lambda^+ = \lambda^-$.*

Tab. 5.1: The mechanism combination method.

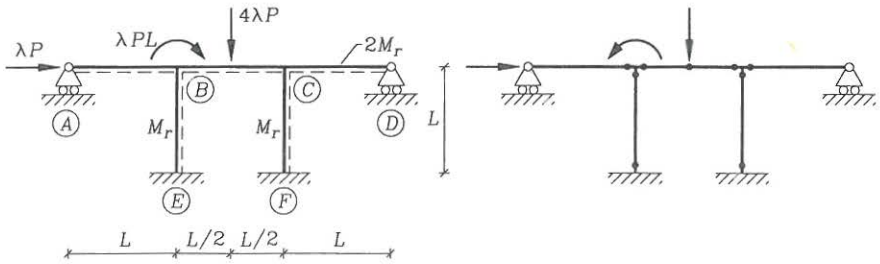

Fig. 5.16: Frame geometry and the possible location of plastic hinges.

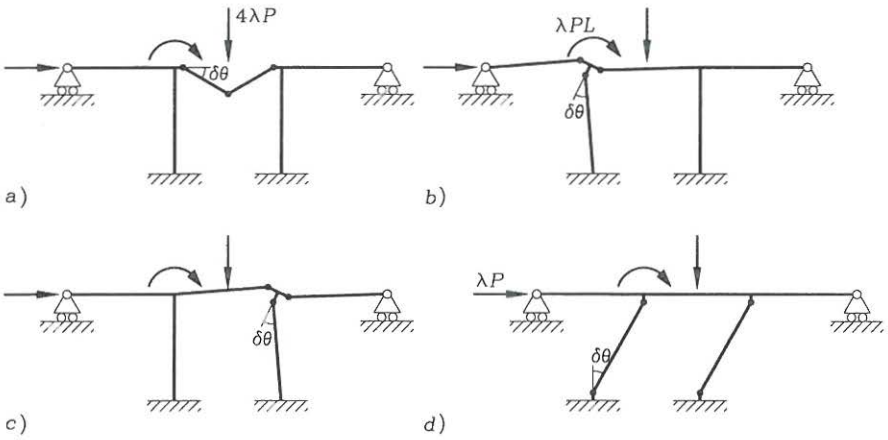

Fig. 5.17: Beam, joint and sway mechanisms.

Mechanism	a	b	c	d
δW_{int}	$8M_r\delta\theta$	$5M_r\delta\theta$	$5M_r\delta\theta$	$4M_r\delta\theta$
δW_{ext}	$2\lambda PL\delta\theta$	$\lambda PL\delta\theta$	0	$\lambda PL\delta\theta$
λ^+	$4\dfrac{M_r}{PL}$	$5\dfrac{M_r}{PL}$	∞	$4\dfrac{M_r}{PL}$

Tab. 5.2: Calculation results for basic mechanisms.

loads, we find that there are $h = 9$ possible plastic hinges as shown in the right-hand side of fig. 5.16.

2. The frame has $n = 5$ redundancies, since the structure will be stable with just one of the fixed column supports.

3. We thus have to find $h - n = 4$ independent mechanisms. Let us choose the basic beam, joint and sway mechanisms shown in fig. 5.17. The plastic virtual work functional is given by $\delta W_p = \delta W_{int} - \delta W_{ext}$, where the internal work is δW_{int} and the external work is δW_{ext}. To find an upper bound set $\delta W_p \geq 0$. Let us show the calculations for mechanism a.

$$\begin{aligned} \delta W_{int} &= 2M_r \cdot \delta\theta + 2M_r \cdot 2\delta\theta + 2M_r \cdot \delta\theta = 8M_r\delta\theta \\ \delta W_{ext} &= 4\lambda P \cdot \frac{L}{2}\delta\theta = 2\lambda PL\delta\theta \\ \delta W_p &\geq 0 \qquad \Rightarrow \qquad \lambda^+ = 4\frac{M_r}{PL} \end{aligned}$$

The calculations and results for the basic mechanisms are summarized in tab. 5.2. The mechanism c does not involve external work and thus corresponds to an infinite upper-bound load factor.

4. We can maximize the virtual work of the loads by combining the mechanisms so that all the loads perform virtual work. This can be done by combining

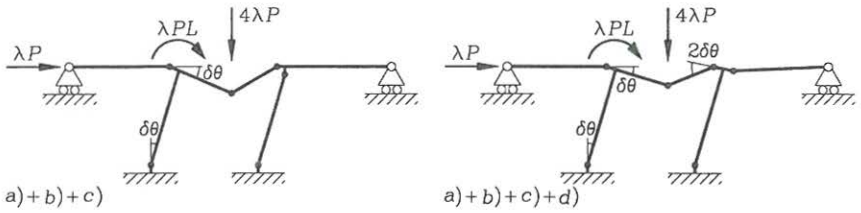

Fig. 5.18: Combined mechanisms.

Mechanism	$a+b+d$	$a+b+c+d$
δW_{int}	$11M_r\delta\theta$	$12M_r\delta\theta$
δW_{ext}	$4\lambda PL\delta\theta$	$4\lambda PL\delta\theta$
λ^+	$\frac{11}{4}\frac{M_r}{PL}$	$3\frac{M_r}{PL}$

Tab. 5.3: Calculation results for combined mechanisms.

mechanisms a and d. However, this leads to 7 plastic hinges, which is one too many. This defect can be healed by including the joint mechanism b, which closes two plasic hinges and opens a new one. The combined mechanism $a+b+d$ is shown in the left-hand side of fig. 5.18. Another related combined mechanism $a+b+c+d$ can be formed to analyse the effect of moving a plastic hinge at the joint C. This mechanism is shown in the right-hand part of fig. 5.18. The related upper-bound load factors can be calculated and the calculation results are shown in tab. 5.3. No other combinations seem to be attractive in the quest to find a lower value for the upper-bound load factor. Our best guess is the combination $a+b+d$ with the upper-bound load factor

$$\lambda^+ = \frac{11}{4}\frac{M_r}{PL} = = \frac{11}{4}\frac{100\text{kNm}}{10\text{kN}\cdot 5\text{m}} = 5.5$$

where the given values have been inserted.

5. Let us find the moment distribution in the frame for this upper-bound solution. The moments are known at the plastic hinges, so let us use statics to find the distribution along the beams. With no distributed loads we know from the moment equilibrium equation $M'' = 0$ that the variation must be linear between joints, boundaries and point loads. Fig. 5.19 shows an exploded view of the given information. The moments M_{BC}, M_{BE} and M_{CD} are unknown. To find them we need the horizontal reactions R_E, R_F, at points E and F.

   At C moment equilibrium of the joint gives us:

$$M_{CD} + 2M_r - M_r = 0 \quad \Rightarrow \quad M_{CD} = -M_r$$

   The horizontal reaction at F is found by considering moment equilibrium of the column CF at C:

$$M_r + M_r - LR_F = 0 \quad \Rightarrow \quad R_F = 2\frac{M_r}{L}$$

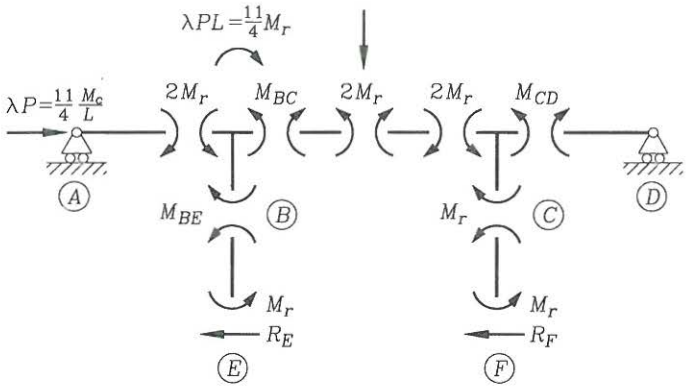

Fig. 5.19: Exploded view with internal moments for combination $a+b+d$.

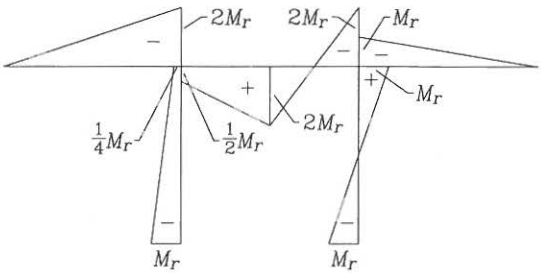

Fig. 5.20: Moment distribution for the upper-bound solution.

Horizontal equilibrium gives us the horizontal reaction at E:

$$\lambda P - R_E - R_F = 0 \quad \Rightarrow \quad R_E = (\frac{11}{4} - 2)\frac{M_r}{L} = \frac{3}{4}\frac{M_r}{L}$$

The moment M_{BE} is found by considering moment equilibrium of column BE at B:

$$M_{BE} + M_r - LR_E = 0 \quad \Rightarrow \quad M_{BE} = (-1 + \frac{3}{4})M_r = -\frac{1}{4}M_r$$

Finally moment equilibrium of joint B gives us

$$M_{BC} - M_{BE} + 2M_r - \lambda PL = 0 \quad \Rightarrow \quad M_{BC} = (-\frac{1}{4} - 2 + \frac{11}{4})M_r = \frac{1}{2}M_r$$

The moment distribution M is now given as the linearly varying moment distribution shown in fig. 5.20. With the factor $\beta = 1$ on the upper-bound moment distribution, it is seen that the moments in the continuous beam fulfil the lower-bound requirement $\beta M \leq 2M_r$ and the moments in the columns

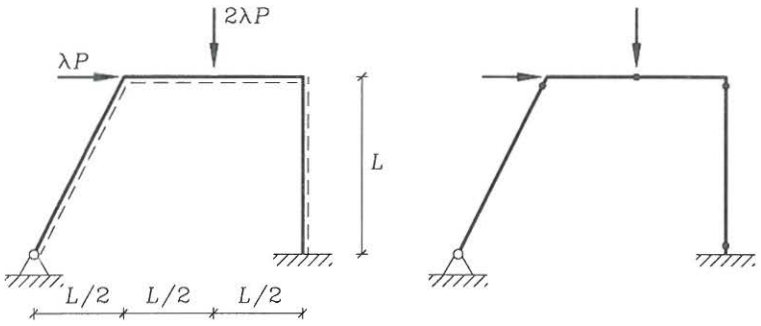

Fig. 5.21: Frame geometry and the possible location of plastic hinges.

fulfil the lower-bound requirement $\beta M \leq M_r$. It is thus seen that the exact plastification factor is

$$\lambda_p = \lambda^+ = \frac{11}{4}\frac{M_r}{PL} = 5.5$$

The given loads can thus be increased proportionally by 5.5, and the moment distribution at collapse is shown in fig. 5.20.

- **Example 5.6** Analysis of the frame in fig. 5.21.

A frame $ABCD$ shown in fig. 5.21 with a non-vertical column AB is analysed in order to illustrate how to tackle geometrically complicated mechanisms. The geometry, loads and boundary conditions are shown in the figure. The factor λ has been introduced as a proportional load factor. The plasticfication moments are different for the beams and columns. Furthermore, the positive plastification moments M_p^+ are different from the negative plastification moments M_p^-. Using M_r as a reference moment the plastification moments are given as:

Beam	M_p^+	M_p^-
AB, CD	M_r	$2M_r$
BC	$3M_r$	$4M_r$

In this example the problem is to find the exact plastic load factor for the given frame with the given combination of loads. The problem will be solved by the mechanism combination method following the procedure given in tab. 5.1.

1. In this example we know that the beam BC has higher plastification moments than the columns, so we need not include the joint mechanism, if we just place the plastic hinges in the columns. The $h = 4$ possible locations of plastic hinges are shown in the right-hand side of fig. 5.21.
2. The frame has $n = 2$ redundancies, since the structure will be stable with the support at D alone.

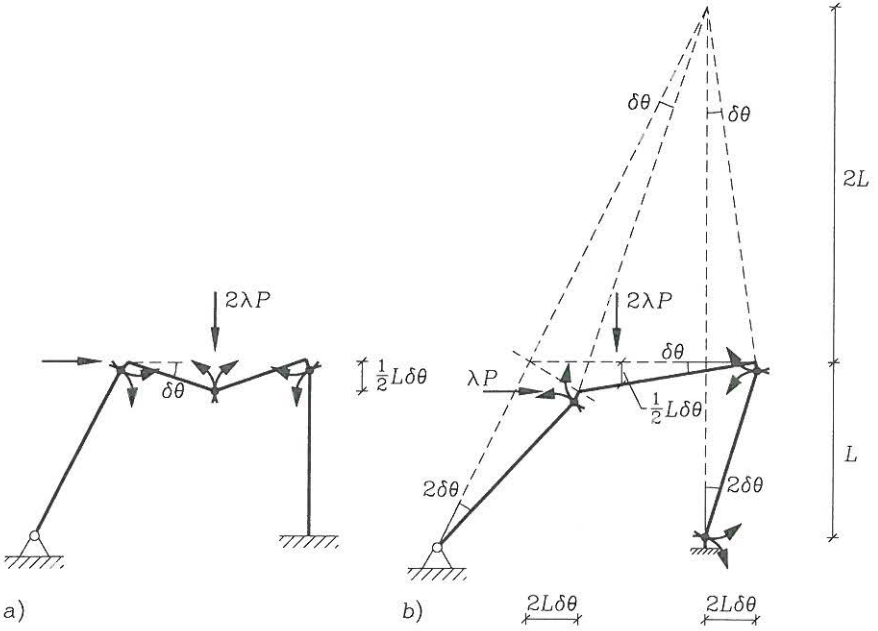

Fig. 5.22: Beam and sway mechanisms.

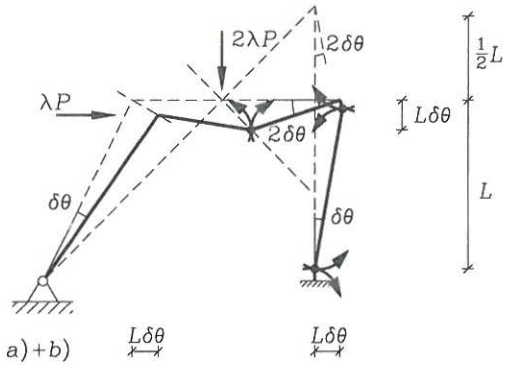

Fig. 5.23: The combined mechanism.

3. We thus have to find $h - n = 2$ independent mechanisms. Let us choose the beam related mechanism a and the sway mechanisms b shown in fig. 5.22. Let us first treat the mechanism a and find the corresponding upper-bound load factor; bearing in mind the different values of the plastification moments:

$$\begin{aligned} \delta W_{int} &= 2M_r \cdot \delta\theta + 3M_r \cdot 2\delta\theta + 1M_r \cdot \delta\theta = 9M_r\delta\theta \\ \delta W_{ext} &= 2\lambda P \cdot \frac{L}{2}\delta\theta = \lambda P\delta\theta \\ \delta W_p &\geq 0 \qquad \Rightarrow \qquad \lambda^+ = 9\frac{M_r}{PL} \end{aligned}$$

Next let us have a closer look at mechanism b. How are the kinematics defined? The *small* movement of the point B is perpendicular to the line AB, since the beam AB rotates about the point A. The movement of point C is perpendicular to the line CD, since the beam CD is fixed at D (no axial displacements). The movement of the beam BC is a rotation about the intersection point of the two lines AB and BC. The kinematics are thus defined by movements of points B and C along the straight lines perpendicular to the respective lines AB and BC. Let us find the upper-bound load factor corresponding to mechanism b:

$$\begin{aligned} \delta W_{int} &= M_r \cdot (2+1)\delta\theta + M_r \cdot (1+2)\delta\theta + 2M_r \cdot 2\delta\theta = 10M_r\delta\theta \\ \delta W_{ext} &= \lambda P \cdot 2L\delta\theta + 2\lambda P \cdot \frac{L}{2}\delta\theta = 3\lambda PL\delta\theta \\ \delta W_p &\geq 0 \qquad \Rightarrow \qquad \lambda^+ = \frac{10}{3}\frac{M_r}{PL} \end{aligned}$$

4. Thus, the only possible combined mechanism is $a+b$, shown in fig. 5.23. This mechanism may also be quite difficult for the beginner, but the principles are the same. The point C still moves perpendicular to the line CD. The midpoint of the beam BC moves on a line perpendicular to the line between the midpoint of BC and the point A. The movement of the right-hand part of the beam BC is a rotation about the point determined by the intersection

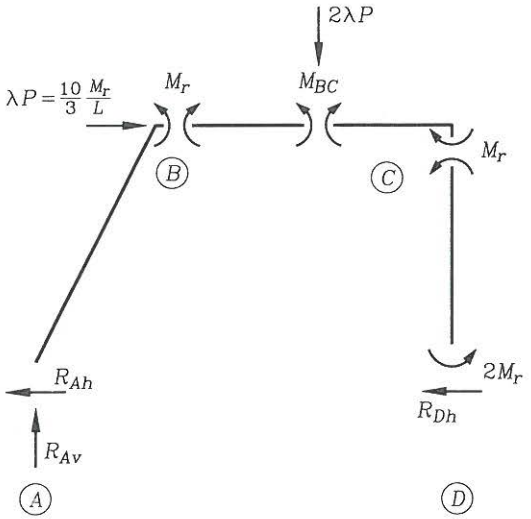

Fig. 5.24: Exploded view with internal moments for mechanism b.

of the extensions of these lines, (i.e. line CD and the line between point A and the midpoint of the beam BC).

Let us find the upper-bound load factor for the mechanism $a + b$:

$$\begin{aligned} \delta W_{int} &= 3M_r \cdot (1+2)\delta\theta + M_r \cdot (2+1)\delta\theta + 2M_r \cdot \delta\theta = 14M_r\delta\theta \\ \delta W_{ext} &= \lambda P \cdot L\delta\theta + 2\lambda P \cdot L\delta\theta = 3\lambda P\delta\theta \end{aligned}$$

$$\delta W_p \geq 0 \quad \Rightarrow \quad \lambda^+ = \frac{14}{3}\frac{M_r}{PL}$$

The best upper-bound guess corresponds to the mechanism b with the upper-bound load factor:

$$\lambda^+ = \frac{10}{3}\frac{M_r}{PL}$$

5. Let us find the moment distribution in the frame for this upper-bound solution. The moments are known at the plastic hinges, so let us use statics to find the distribution along the beams. Fig. 5.24 shows an exploded view of the given information. The moment M_{BC} is unknown and to find it we use the horizontal reactions R_{Dh}, R_{Ah} and the vertical reaction R_{Av} as described in the following.

   Moment equilibrium of the column CD at point C gives us the horizontal reaction at D as follows:

$$M_r + 2M_r - LR_{Dh} = 0 \quad \Rightarrow \quad R_{Dh} = -3\frac{M_r}{L}$$

   Horizontal equilibrium gives us the horizontal reaction at A:

$$\lambda P - R_{Ah} - R_{Dh} = 0 \quad \Rightarrow \quad R_{Ah} = (\frac{10}{3} - 3)\frac{M_r}{L} = \frac{1}{3}\frac{M_r}{L}$$

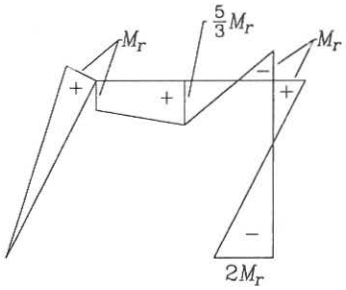

Fig. 5.25: Moment distribution for the upper-bound solution.

The vertical reaction at A is found by moment equilibrium of the column AB at the point B:

$$M_r - LR_{Ah} - \frac{L}{2}R_{Av} = 0 \quad \Rightarrow \quad R_{Av} = 2(1 - \frac{1}{3})\frac{M_r}{L} = \frac{4}{3}\frac{M_r}{L}$$

The moment M_{BC} is found by considering moment equilibrium of the left-hand part of the structure:

$$M_{BC} - LR_{Ah} - LR_{Av} = 0 \quad \Rightarrow \quad M_{BC} = (\frac{1}{3} + \frac{4}{3})M_r = \frac{5}{3}M_r$$

The moment distribution M is now given as the linearly varying moment distribution shown in fig. 5.25. With the factor $\beta = 1$ on the upper-bound moment distribution, it is seen that the moments in the frame fulfil the lower bound requirement $\beta M \leq M_p$. It is thus seen that the exact plastification factor is

$$\lambda_p \quad = \quad \lambda^+ \quad = \quad \frac{10}{3}\frac{M_r}{PL}$$

Having found the exact plastification factor the posed problem has been solved.

5.3 Displacement Estimation

In the previous subsections the displacements have been assumed small enough for the static equilibrium equations to be valid. To check this it is necessary to know or to have an estimate of the displacements just before the plastic collapse load is reached. There are a couple of ways to find the displacements. If the load history is known for a linear elastic perfectly plastic beam structure, it is possible to find the displacements by slowly loading the structure and introducing plastic hinges as they arise. This leads to subsequent analysis of several different related statically indeterminate structural systems with fewer and fewer redundancies, until the collapse load is finally reached for a statically determinate system. This procedure is well suited for computational implementation, but becomes quite time consuming

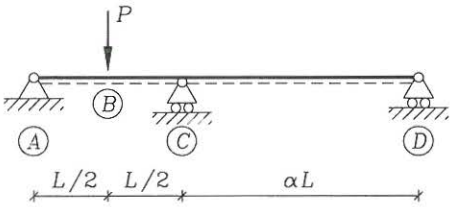

Fig. 5.26: Double span beam with a point load.

for hand calculations. A qualified guess on which plastic hinge is the last to be formed can directly lead to a good estimate of the displacements. Even if the load history is not known exactly, the estimate can tell us, if the displacemets are small enough for the plastic hinge analysis to be valid.

To find displacements we can use the unit load method based on the principle of virtual work and we can just assume a linear elastic perfectly plastic moment curvature relation. Let us guess which hinge is the last to be created. Then insert (moment free) hinges in the structure at all plastic hinges except at the last one created and load the structure with a unit load at the position, where the displacements are to be found. The moment distribution M^1 related to the unit load is then used to find the displacements by:

$$d_1 \simeq \sum_{\text{beams}} \int_0^L \frac{MM^1}{EI}\, dz \tag{5.16}$$

In which M is the moment distribution at the plastic collapse load. If the last formed plastic hinge is unknown, then try the hinges systematically and find the one giving the largest displacement; this one is the last formed plastic hinge. Even though we have only found an approximate upper-bound solution for the plastic collapse situation we can use this to estimate displacements.

Using the unit load method it is also possible to find the mutual rotations in the plastified hinges and use this to compare with the plastic rotation capacity of the beam.

- **Example 5.7** Displacement estimation.

  Let us analyse the double span beam with a point load in the centre of the first span, as shown in fig. 5.26. The elastic bending stiffness of the beam is EI and the plastification moment is M_p. The first span has the length L and the second span has the length αL, where the $\alpha > \frac{1}{8}$. The plastic collapse mechanism and the corresponding moment distribution are shown in fig. 5.27. The problem is to find the displacement at point B just before plastic collapse.

  If the second span is very short it will have a stiffening effect on the first span, and the moment at C will be large and be the first to become plastic. Let us assume that the plastic hinge at B is the last to be created. A unit load $X_1 = 1$ is thus placed on the structural system with a hinge at C as shown in fig. 5.27. The

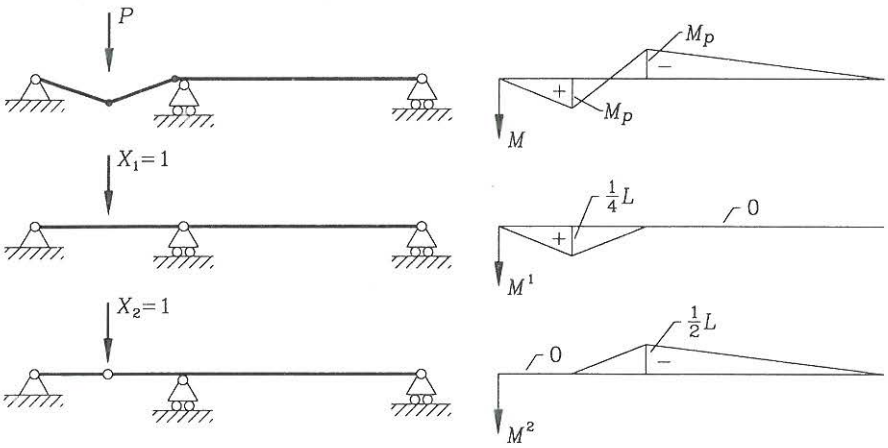

Fig. 5.27: Moment distributions of double span beam.

displacement at B, thus becomes:

$$d_1 = \frac{L/2}{6EI}(2M_p \cdot \frac{1}{4}L) + \frac{L/2}{6EI}(2M_p \cdot \frac{1}{4}L - M_p\frac{1}{4}L) = \frac{1}{16}\frac{M_pL^2}{EI}$$

However, if the second span is very long then a plastic hinge will first be created at B and then at C. We thus assume that the plastic hinge at C is the last to be created. A unit load $x_2 = 1$ is thus placed on the structural system with a hinge at B and the displacement becomes:

$$d_2 = \frac{L/2}{6EI}(2M_p \cdot \frac{1}{2}L - M_p\frac{1}{2}L) + \frac{\alpha L}{6EI}(2M_p \cdot \frac{1}{2}L) = \frac{1}{24}(1+4\alpha)\frac{M_pL^2}{EI}$$

If $\alpha > \frac{1}{8}$ we find that:

$$\begin{aligned} d_2 &> \frac{1}{24}(1+4\tfrac{1}{8})\frac{M_pL^2}{EI} \quad \Downarrow \\ &> \frac{1}{16}\frac{M_pL^2}{EI} = d_1 \end{aligned}$$

Since $d_2 > d_1$ the assumption is correct, i.e. the last plastic hinge to be created is at C, and the displacement at B is

$$d = d_2 = \frac{1}{24}(1+4\alpha)\frac{M_pL^2}{EI}$$

It is clear that d grows linearly with α. For large α the displacements at B may become so large that the plastic hinge cannot be created before the displacement limit is reached or before the rotational capacity of the plastic hinge at B is reached.

- **Problem 5.4**

Find the plastic load factor λ_p for the frame shown in fig. 5.28 and find the side sway of the frame just before plastic collaps. The plastification moment is M_p and the bending stiffness is EI for all the beams and columns.

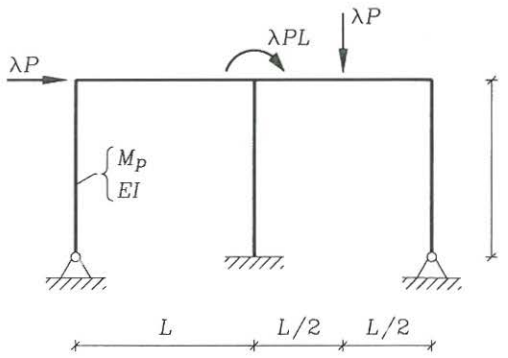

Fig. 5.28: Frame loaded two by point loads and a concentrated moment load.

Chapter 6

Flexural Plate Theories

A plate is a continuum with two primary dimensions, which are large compared to the third thickness dimension. The geometry of a plate is thus described by its contour in a plane and a thickness, which may vary across the plane. Plates are used as structural elements mainly to redistribute transverse loads to the plate boundaries. In fulfilling this purpose the plate deforms in the transverse direction in a two-dimensional flexural mode. Plates can also carry in-plane loads through a membrane action, just as beams can carry axial loads, with the important difference that the in-plane forces are two-dimensional. The theories are developed like the beam theories through a geometrical approach, where the kinematic assumptions and constitutive relations lead to the formulation of a potential energy. Variations in the potential energy lead to the equilibrium equations and the generalized internal force definitions. This approach is directly related to the modern formulations of the classic theories used in computational methods like the finite element method. Another approach which is often used is to introduce internal forces and then derive the equilibrium equations through equilibrium of an infinitesimal plate section. However, this approach may lead to difficulties concerning the shear force and its relation to the two classic plate theories.

The first attempts made on the theory of plates were those of Euler, who in 1766 studied the vibration of perfectly flexible membranes. The flexural theory of plates was studied by Bernoulli in 1789 and Navier in 1823. In 1811 Lagrange derived the biharmonic differential equation for deflection analysis of plates, even though his plate theory was not entirely satisfactory. The first convincing and today a classic plate theory was presented in 1850 by Kirchhoff [19], including the identification of proper boundary conditions, which can be quite difficult to understand. The theory of combined membrane and flexural effects was developed by Kirchhoff in 1877 and St. Venant in 1883. The large deflection differential equations for plates was derived by von Karman in 1910. Later in our century Reissner [20] in 1945 and Mindlin [21] in 1951 proposed a modification of the Kirchhoff plate theory to include the influence of shear. Kirchhoff plate theory, often referred to as thin-plate theory, gives a good approximation for thin plates, but when the plates become thick it is necessary to include the effects of shear through the use of Mindlin-Reissner plate theory, which is referred to as thick-plate

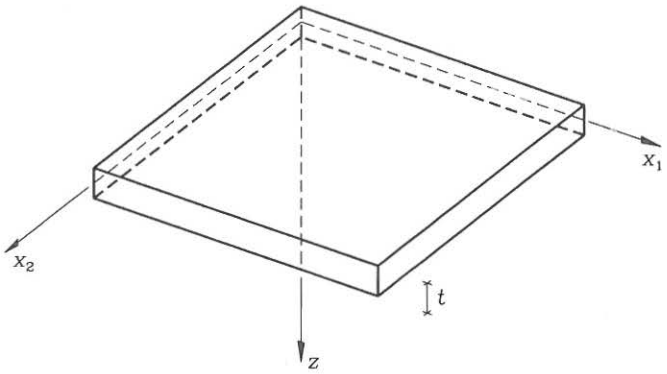

Fig. 6.1: Cartesian reference for a plate.

theory. However, in modern computational methods Mindlin-Reissner theory is often modified to enable thin-plate analysis. The development of plate theories is of course related to the development of beam theories and the derivation of the theories in the following should be compared to the chapter on beam theories. Timoshenko & Woinowsky-Krieger [22] give a thorough treatment of plates and shells. Furthermore, many textbooks on mechanics like Boresi et al. [23], Nielsen [24] and Nielsen & Rathkjen [25], [26], treat the classic theories of plates. The theories of plates are related to the many advanced theories of shells and we just refer the advanced tensor treatment of Flügge [7].

Cartesian Reference

To use the power of index notation we introduce the first two base vectors $\mathbf{i}_\nu$ in the elastic central surface of the plate and the third base vector $\mathbf{i}_3$ in the perpendicular direction. A point in the plate is thus defined by the vector $x_\nu \mathbf{i}_\nu + z\mathbf{i}_3$, where (x_ν, z) are the coordinates of the material point, as shown in fig. 6.1. In the present work we assume that the elastic central surface of the plate corresponds to the middle surface, so that $z \in [-\frac{1}{2}t, \frac{1}{2}t]$, where t is the thickness of the plate.

6.1 Mindlin-Reissner Plate Theory

Even though the Kirchhoff plate theory was developed first it is thought that the Mindlin-Reissner plate theory naturally leads to the Kirchhoff plate theory through one extra assumption. We therefore start with the Mindlin-Reissner plate theory, which corresponds to the Timoshenko beam theory. The plate theory is derived on the basis of assumed displacement fields $u_i(x_\nu, z)$, where we separate the displacement in the transverse direction u_3 from those in the in-plane directions u_β. It is assumed that the displacement in the transverse direction $u_3(x_\nu, z) = w(x_\nu)$ is constant through the thickness, so that all points on a normal have the same

transverse displacements $w(x_\nu)$. This means that the normal keeps its length during deformation.

Assumption 1:

Normals to the undeformed middle surface keep their length during deformation

Furthermore, it is assumed that the displacements in the in-plane directions have a linear variation through the thickness. This is equivalent with the following statement:

Assumption 2:

Normals to the undeformed middle surface remain straight during deformation

The two assumptions are sometimes combined and formulated as follows: Normals to the undeformed middle surface remain straight and inextensional during deformation. Note that the normals do not necessarily remain normals in the deformed states.

The linear variation through the thickness can be separated into the two middle surface displacements $v_\beta(x_\nu)$ and the two inclinations (rotations) $\alpha_\beta(x_\nu)$ and thus written as $u_\beta(x_\nu, z) = v_\beta + z\alpha_\beta$. The displacements of a material point (x_ν, z) are thus given by the following kinematics

Assumed displacements

$$u_\beta = v_\beta + z\,\alpha_\beta \tag{6.1}$$

$$u_3 = w \tag{6.2}$$

where the five unknown kinematic functions are

$$v_\beta(x_\nu)\,, \quad \alpha_\beta(x_\nu)\,, \quad w(x_\nu)$$

These kinematic assumptions are shown in fig. 6.2 in a common coordinate view for x_β, where we can just substitute $\beta = 1$ or $\beta = 2$ for the two orthogonal transverse sections through the plate.

Using the linear strain definition (1.65) we find the following non-vanishing strain components

$$\begin{aligned} \varepsilon_{\alpha\beta} &= \frac{1}{2}\left(\frac{\partial u_\alpha}{\partial x_\beta} + \frac{\partial u_\beta}{\partial x_\alpha}\right) = \frac{1}{2}(u_{\alpha,\beta} + u_{\beta,\alpha}) \\ &= \frac{1}{2}(v_{\alpha,\beta} + v_{\beta,\alpha}) + \frac{1}{2}(\alpha_{\alpha,\beta} + \alpha_{\beta,\alpha})\, z \\ &= \bar{\varepsilon}_{\alpha\beta} + \kappa_{\alpha\beta}\, z \end{aligned} \tag{6.3}$$

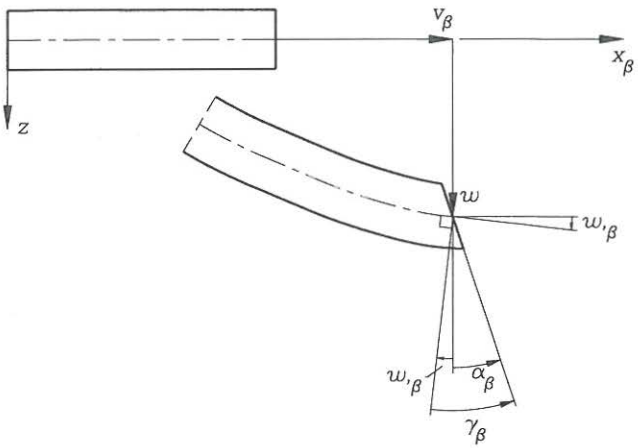

Fig. 6.2: The kinematics of a Mindlin-Reissner plate.

$$\begin{aligned}\gamma_\beta &= \gamma_{\beta 3} = 2\varepsilon_{\beta 3} = \frac{\partial u_\beta}{\partial z} + \frac{\partial u_3}{\partial x_\beta} = u_{\beta,3} + u_{3,\beta} \\ &= \alpha_\beta + w_{,\beta} \end{aligned} \tag{6.4}$$

where the in-plane strains at the middle surface (level of the elastic central surface) have been introduced as $\bar{\varepsilon}_{\alpha\beta}$, the curvatures as $\kappa_{\alpha\beta} = \frac{1}{2}(\alpha_{\alpha,\beta} + \alpha_{\beta,\alpha})$ and the engineering shear strains as $\gamma_\beta = \gamma_{\beta 3} = 2\varepsilon_{\beta 3}$. Thus the strains in the Mindlin-Reissner plate theory are defined as follows:

The in-plane strains in the Mindlin-Reissner plate theory are

$$\varepsilon_{\alpha\beta} = \bar{\varepsilon}_{\alpha\beta} + z\kappa_{\alpha\beta} \tag{6.5}$$

in which the strains at the middle surface are the membrane strains determined by:

$$\bar{\varepsilon}_{\alpha\beta} = \frac{1}{2}(v_{\alpha,\beta} + v_{\beta,\alpha}) = \frac{1}{2}\left(\frac{\partial v_\alpha}{\partial x_\beta} + \frac{\partial v_\beta}{\partial x_\alpha}\right) \tag{6.6}$$

and the curvatures are

$$\kappa_{\alpha\beta} = = \frac{1}{2}(\alpha_{\alpha,\beta} + \alpha_{\beta,\alpha}) = \frac{1}{2}\left(\frac{\partial \alpha_\alpha}{\partial x_\beta} + \frac{\partial \alpha_\beta}{\partial x_\alpha}\right) \tag{6.7}$$

The transverse engineering shear strains in the Mindlin-Reissner plate theory are

$$\gamma_\beta = \alpha_\beta + w_{,\beta} = \alpha_\beta + \frac{\partial w}{\partial x_\beta} \tag{6.8}$$

The transverse engineering shear strains are also shown in fig. 6.2 and the resem-

blance with beam theory should be noted, the difference being in the orientation of the axes.

The Constitutive Relations

As in beam theories we do not wish to introduce artificial constraints due to errors in our kinematic assumptions. The kinematic assumptions imply that all material points along a normal have the same transverse displacement and thus $\varepsilon_{33} = 0$. However, this is not the case in real plates, since they are free to expand in the transverse direction. To derive a useful constitutive relation, which is not constitutively constrained, we need an extra assumption. Since experience shows, that the transverse stress component σ_{33} in plates is negligible compared to the in-plane stress components $\sigma_{\alpha\beta}$, let us introduce this as a basic assumption.

Assumption 3:

The transverse stress component is negligible

$$\sigma_{33} = 0 \tag{6.9}$$

The assumption is inserted into the three-dimensional linear elastic constitutive relations (1.102) or (1.106) for isotropic materials. This results in an equation for the transverse strain component as follows:

$$\begin{aligned} \sigma_{33} &= 0 = \lambda(\varepsilon_{\nu\nu} + \varepsilon_{33}) + 2\mu\varepsilon_{33} \quad \Downarrow \\ \varepsilon_{33} &= -\frac{\lambda}{2\mu + \lambda}\varepsilon_{\nu\nu} \end{aligned} \tag{6.10}$$

Inserting this expression for ε_{33} into the three-dimensional constitutive relations and replacing the Lamé constants by conventional engineering constants result in the following expressions for the non-vanishing stresses:

$$\begin{aligned} \sigma_{\alpha\beta} &= \frac{2\mu\lambda}{2\mu + \lambda}\delta_{\alpha\beta}\varepsilon_{\nu\nu} + 2\mu\varepsilon_{\alpha\beta} \\ &= \frac{E}{1 - \nu^2}\left(\nu\delta_{\alpha\beta}\varepsilon_{\nu\nu} + (1 - \nu)\varepsilon_{\alpha\beta}\right) \end{aligned} \tag{6.11}$$

$$\tau_\beta = \sigma_{\beta 3} = 2G\varepsilon_{\beta 3} = G\gamma_{\beta 3} = G\gamma_\beta \tag{6.12}$$

By introducing additional Kronecker deltas and using the symmetry of both stresses and strains the constitutive relation for in-plane stresses $\sigma_{\alpha\beta}$ can also be written as follows:

$$\sigma_{\alpha\beta} = d_{\alpha\beta\gamma\nu}\,\varepsilon_{\gamma\nu} \tag{6.13}$$

in which the fourth-order isotropic tensor of material constants $d_{\alpha\beta\gamma\nu}$ becomes

$$d_{\alpha\beta\gamma\nu} = \frac{E}{1 - \nu^2}\left(\nu\delta_{\alpha\beta}\delta_{\gamma\nu} + \tfrac{1}{2}(1 - \nu)(\delta_{\alpha\gamma}\delta_{\beta\nu} + \delta_{\alpha\nu}\delta_{\beta\gamma})\right) \tag{6.14}$$

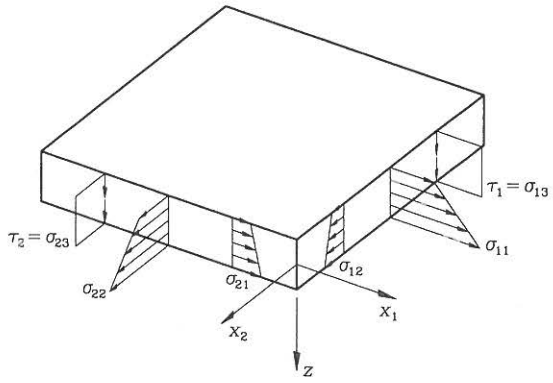

Fig. 6.3: Stress components in a Mindlin-Reissner plate.

The in-plane stress-strain relation can also be expressed in a matrix format as follows:

$$\begin{pmatrix} \sigma_{11} \\ \sigma_{22} \\ \sigma_{12} \end{pmatrix} = \frac{E}{1-\nu^2} \begin{bmatrix} 1 & \nu & 0 \\ \nu & 1 & 0 \\ 0 & 0 & \frac{1}{2}(1-\nu) \end{bmatrix} \begin{pmatrix} \varepsilon_{11} \\ \varepsilon_{22} \\ 2\varepsilon_{12} \end{pmatrix} \tag{6.15}$$

Where the symmetry of components has been used, i.e. $\varepsilon_{12} = \varepsilon_{21}$ and $\sigma_{12} = \sigma_{21}$. Thus, the basic stress-strain relations are given as follows:

In-plane stress-strain relation for a plate

$$\begin{aligned} \sigma_{\alpha\beta} &= d_{\alpha\beta\gamma\nu}\, \varepsilon_{\gamma\nu} \\ &= d_{\alpha\beta\gamma\nu}\, (\bar{\varepsilon}_{\gamma\nu} + z\, \kappa_{\gamma\nu}) \end{aligned} \tag{6.16}$$

where the fourth order isotropic linear elastic material tensor is given by

$$d_{\alpha\beta\gamma\nu} = \frac{E}{1-\nu^2} \left(\nu \delta_{\alpha\beta}\delta_{\gamma\nu} + \tfrac{1}{2}(1-\nu)(\delta_{\alpha\gamma}\delta_{\beta\nu} + \delta_{\alpha\nu}\delta_{\beta\gamma}) \right) \tag{6.17}$$

The relation between transverse engineering shear stresses and the engineering shear strains for Mindlin-Reissner plates is

$$\tau_\beta = G\gamma_\beta \tag{6.18}$$

where the $\tau_\beta = \sigma_{\beta 3}$ *and* $\gamma_\beta = \gamma_{\beta 3} = 2\varepsilon_{\beta 3}$.

Since the in-plane strain distribution $\varepsilon_{\alpha\beta}$ is assumed to vary linearly through the thickness and since the constitutive relation is linear, then the stress distribution will also vary linearly through the thickness. The kinematic assumption also leads to a constant transverse shear strain γ_β through the thickness and thus also to a constant transverse shear stress τ_β through the thickness. The stress components

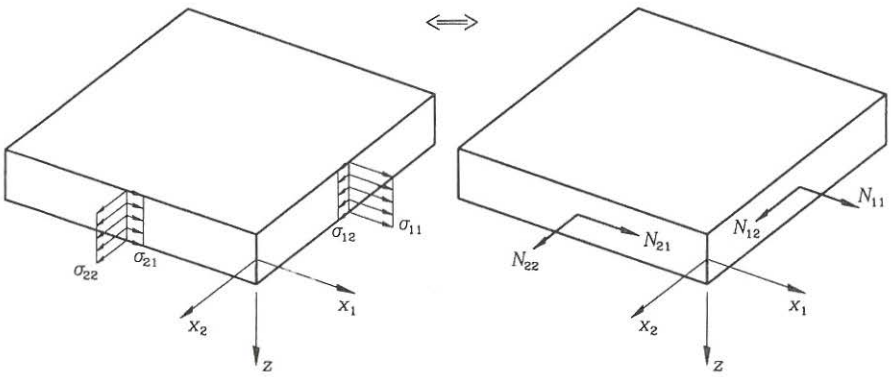

Fig. 6.4: Membrane forces in a plate.

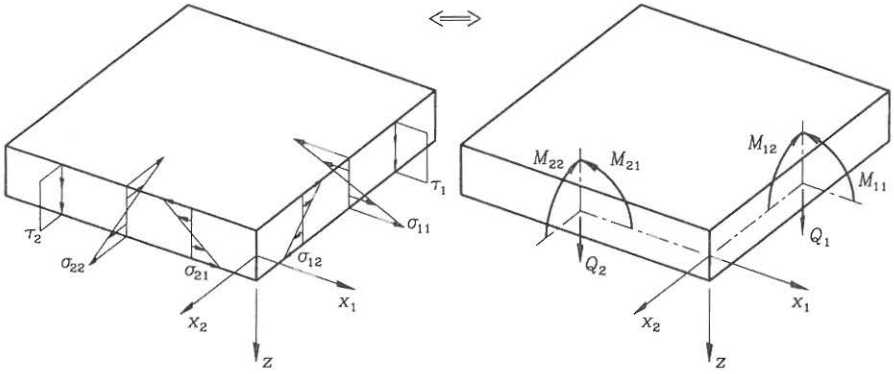

Fig. 6.5: Internal forces related to plate flexure.

of the Mindlin-Reissner plate theory are shown in fig. 6.3.

Let us integrate the stresses through the thickness and define a set of internal plate forces. Integrating the in-plane stresses $\sigma_{\alpha\beta}$ defines the membrane forces $N_{\alpha\beta}$, shown in fig. 6.4. The membrane forces are also referred to as in-plane forces or axial forces. We define the internal moments $M_{\alpha\beta}$ as the moments of the stress distribution $\sigma_{\alpha\beta}$ about the middle surface. The transverse shear forces Q_β are defined as the integral of the transverse shear stresses. The moments $M_{\alpha\beta}$ and the transverse shear forces Q_β are related to the out-of-plane bending behaviour of the plate and they are illustrated in fig. 6.5. For a plate of isotropic linear elastic material we thus have the following force definitions with the sign convention shown in fig. 6.6.

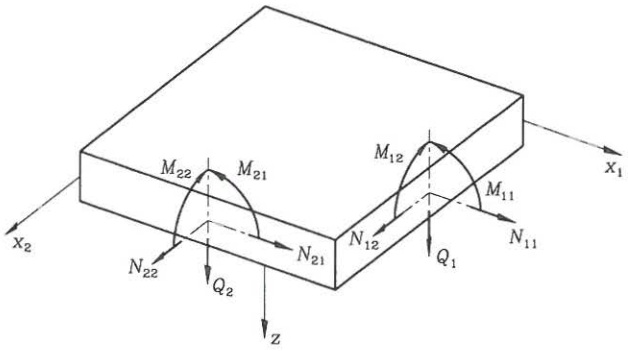

Fig. 6.6: Internal forces in a plate.

Membrane forces

$$\begin{aligned} N_{\alpha\beta} &= \int_{-\frac{t}{2}}^{\frac{t}{2}} \sigma_{\alpha\beta}\, dz = \int_{-\frac{t}{2}}^{\frac{t}{2}} c_{\alpha\beta\gamma\nu}\,(\bar{\varepsilon}_{\gamma\nu} + z\kappa_{\gamma\nu})\, dz \\ &= D^m_{\alpha\beta\gamma\nu}\,\bar{\varepsilon}_{\gamma\nu} \end{aligned} \tag{6.19}$$

Bending moments

$$\begin{aligned} M_{\alpha\beta} &= \int_{-\frac{t}{2}}^{\frac{t}{2}} z\sigma_{\alpha\beta}\, dz = \int_{-\frac{t}{2}}^{\frac{t}{2}} c_{\alpha\beta\gamma\nu}\,(z\bar{\varepsilon}_{\gamma\nu} + z^2\kappa_{\gamma\nu})\, dz \\ &= D^b_{\alpha\beta\gamma\nu}\,\kappa_{\gamma\nu} \end{aligned} \tag{6.20}$$

Transverse shear forces

$$\begin{aligned} Q_\beta &= \int_{-\frac{t}{2}}^{\frac{t}{2}} \tau_\beta\, dz = \int_{-\frac{t}{2}}^{\frac{t}{2}} G\gamma_\beta\, dz \\ &= D^s\,\gamma_\beta \end{aligned} \tag{6.21}$$

where the plate section properties for membrane, bending and shear action are

$$D^m_{\alpha\beta\gamma\nu} = t\, d_{\alpha\beta\gamma\nu} \tag{6.22}$$

$$D^b_{\alpha\beta\gamma\nu} = \tfrac{1}{12}\, t^3\, d_{\alpha\beta\gamma\nu} \tag{6.23}$$

$$D^s = \psi\, G\, t \tag{6.24}$$

in which $\psi = \frac{5}{6}$ has been introduced as a shear correction factor.

The stress in a plate can be found by use of the force and moment definitions above and the equations (6.16), (6.22), (6.23), (6.24) or just by using that the stress distribution is linear:

Stresses in a plate

$$\sigma_{\alpha\beta} = \frac{N_{\alpha\beta}}{t} + 12\,\frac{M_{\alpha\beta}}{t^3}z \tag{6.25}$$

$$\left(\tau_\beta \simeq \frac{6}{5}\frac{Q_\beta}{t}\right)$$

The shear stress is not the best possible approximation, since it is known by use of the Grashof formula that the shear is distributed parabolicly with a maximum shear stress of

$$\tau_\beta = \frac{3}{2}\frac{Q_\beta}{t} \tag{6.26}$$

The constitutive relations for Mindlin-Reissner plate theory can also be written in a more illustrative matrix form as follows:

$$\begin{pmatrix} N_{11} \\ N_{22} \\ N_{12} \end{pmatrix} = \frac{E\,t}{1-\nu^2}\begin{bmatrix} 1 & \nu & 0 \\ \nu & 1 & 0 \\ 0 & 0 & \frac{1}{2}(1-\nu) \end{bmatrix}\begin{pmatrix} \bar{\varepsilon}_{11} \\ \bar{\varepsilon}_{22} \\ 2\bar{\varepsilon}_{12} \end{pmatrix} \tag{6.27}$$

$$\begin{pmatrix} M_{11} \\ M_{22} \\ M_{12} \end{pmatrix} = \frac{E\,t^3}{12\,(1-\nu^2)}\begin{bmatrix} 1 & \nu & 0 \\ \nu & 1 & 0 \\ 0 & 0 & \frac{1}{2}(1-\nu) \end{bmatrix}\begin{pmatrix} \kappa_{11} \\ \kappa_{22} \\ 2\kappa_{12} \end{pmatrix} \tag{6.28}$$

$$\begin{pmatrix} Q_1 \\ Q_2 \end{pmatrix} = \frac{5}{6}\,G\,t\begin{bmatrix} 1 & 0 \\ 0 & 1 \end{bmatrix}\begin{pmatrix} \gamma_1 \\ \gamma_2 \end{pmatrix} \tag{6.29}$$

These matrix equations are based on the symmetry of both strains and stresses. Note that symmetry in stresses and strains implies that $N_{12} = N_{21}$ and $M_{12} = M_{21}$. In the flexural constitutive relations it is convenient to introduce the elastic plate bending modulus as:

The elastic plate bending modulus

$$D = \frac{E\,t^3}{12\,(1-\nu^2)} \tag{6.30}$$

Using this modulus we can write the flexural constitutive tensor as:

$$D^b_{\alpha\beta\gamma\nu} = D\,\left(\nu\delta_{\alpha\beta}\delta_{\gamma\nu} + \tfrac{1}{2}(1-\nu)(\delta_{\alpha\gamma}\delta_{\beta\nu} + \delta_{\alpha\nu}\delta_{\beta\gamma})\right) \tag{6.31}$$

For the sake of clarity the constitutive relations for membrane forces and bending moments can also be written in components as follows:

Constitutive relations (in expanded form)

$$\begin{aligned} N_{11} &= \tfrac{E\,t}{1-\nu^2}\,(\bar{\varepsilon}_{11} + \nu\bar{\varepsilon}_{22}) \\ N_{22} &= \tfrac{E\,t}{1-\nu^2}\,(\bar{\varepsilon}_{22} + \nu\bar{\varepsilon}_{11}) \\ N_{12} &= \tfrac{E\,t}{1-\nu^2}\,(1-\nu)\bar{\varepsilon}_{12} \end{aligned} \tag{6.32}$$

$$\begin{aligned} M_{11} &= D\,(\kappa_{11} + \nu\kappa_{22}) \\ M_{22} &= D\,(\kappa_{22} + \nu\kappa_{11}) \\ M_{12} &= D\,(1-\nu)\kappa_{12} \end{aligned} \tag{6.33}$$

It is seen that the constitutive relations simplify a little if Poisson's ratio ν is zero. This is seldom the case, however, sometimes it is possible to derive quite good approximate solutions by setting $\nu = 0$.

Potential Energy and Virtual Work

Inserting the plate strain equations (6.5) and (6.8) into the potential energy function for a three-dimensional continuum given in equation (1.123), but using the constitutive relations (6.16) and (6.18), results in the following reduced potential energy

$$\begin{aligned} V &= \int_V (\frac{1}{2}\varepsilon_{\alpha\beta}d_{\alpha\beta\gamma\nu}\varepsilon_{\gamma\nu} + \frac{1}{2}\gamma_\beta G\gamma_\beta - q_j u_j)\,dV - \int_{\partial V} t_j u_j dA \\ &= \int_V (\frac{1}{2}\sigma_{\alpha\beta}\varepsilon_{\alpha\beta} + \frac{1}{2}\tau_\beta\gamma_\beta - q_j u_j)\,dV - \int_A t_j u_j dA \\ &= \int_V \left(\frac{1}{2}\sigma_{\alpha\beta}(\bar{\varepsilon}_{\alpha\beta} + z\,\kappa_{\alpha\beta}) + \frac{1}{2}\tau_\beta\gamma_\beta - q_j u_j\right) dV - \int_A t_j u_j\,dA \end{aligned} \tag{6.34}$$

Note that t_i are the components of the stress tractions on the plate surface. Integrating through the thickness t and defining the membrane forces, plate moments and plate shear forces as in (6.19), (6.20) and (6.21) we find the potential energy for a Mindlin-Reissner plate:

Potential energy for a Mindlin-Reissner plate

$$V(v_\nu, w, \alpha_\nu) = \int_A (\frac{1}{2} N_{\alpha\beta}\bar{\varepsilon}_{\alpha\beta} + \frac{1}{2} M_{\alpha\beta}\kappa_{\alpha\beta} + \frac{1}{2} Q_\beta \gamma_\beta - p_\beta v_\beta - pw - m_\beta \alpha_\beta)\, dA - \int_{\partial A} \left(\bar{N}_\beta v_\beta + \bar{M}_\beta \alpha_\beta + \bar{Q} w\right) ds \tag{6.35}$$

Internal plate forces are given by (6.19), (6.20) and (6.21) and thus they are functions of the displacements. The membrane, transverse and moment loads are

$$p_\beta = \int_{-\frac{t}{2}}^{\frac{t}{2}} q_\beta \, dz, \quad p = \int_{-\frac{t}{2}}^{\frac{t}{2}} q_3 \, dz, \quad m_\beta = \int_{-\frac{t}{2}}^{\frac{t}{2}} z q_\beta \, dz \tag{6.36}$$

and the boundary forces are

$$\bar{N}_\beta = \int_{-\frac{t}{2}}^{\frac{t}{2}} t_\beta \, dz, \quad \bar{Q} = \int_{-\frac{t}{2}}^{\frac{t}{2}} t_3 \, dz, \quad \bar{M}_\beta = \int_{-\frac{t}{2}}^{\frac{t}{2}} z t_\beta \, dz \tag{6.37}$$

Taking the first variation of the potential energy function with respect to all the unknown functions yields the virtual work functional. The first variation can be thought of as the change in potential energy when making small variations in the unknown displacement functions (δv_β, δw, $\delta \alpha_\beta$). The first variation of the potential energy can thus be found as:

$$\delta V(v, w_\beta, \alpha_\beta) = \frac{\partial V}{\partial v_\beta}\delta v_\beta + \frac{\partial V}{\partial w}\delta w + \frac{\partial V}{\partial \alpha_\beta}\delta \alpha_\beta \tag{6.38}$$

The variation of the potential energy with respect to the kinematic quantities is equal to the virtural work $\delta W = \delta V$. Let us thus perform this variation using that the membrane forces, plate moments and plate shear forces are functions of the displacements, i.e. $N_{\alpha\beta}(v_\nu)$, $M(\alpha_\beta)$ and $Q(w, \alpha_\beta)$. We find:

Virtual work functional for a Mindlin-Reissner plate

$$\delta W = \int_A (N_{\alpha\beta}\, \delta\bar{\varepsilon}_{\alpha\beta} + M_{\alpha\beta}\, \delta\kappa_{\alpha\beta} + Q_\beta\, \delta\gamma_\beta - p_\beta \delta v_\beta - p\delta w - m_\beta \delta\alpha_\beta)\, dA - \int_{\partial A} \left(\bar{N}_\beta \delta v_\beta + \bar{M}_\beta \delta\alpha_\beta + \bar{Q}\delta w\right) ds \tag{6.39}$$

The virtual work functional can be derived even if a potential energy does not exist and thus it is in reality independent of the constitutive relations.

Plate Equilibrium Equations

The plate equilibrium equations will be derived using the principle of virtual work $\delta W = 0$, since this is the modern approach, used for developing mechanical models. However, the classic method of deriving the equilibrium equations by considering

equilibrium of an infinitesimal rectangular plate section will be left to the reader. Let us continue directly from the virtual work functional for Mindlin-Reissner plates (6.39) and introduce the virtual kinematic quantities $\delta\varepsilon_{\alpha\beta}$, $\delta\kappa_{\alpha\beta}$ and $\delta\gamma_\beta$. However, before doing so let us note that since $N_{\alpha\beta}$ and $M_{\alpha\beta}$ both have symmetric components we can just introduce the virtual kinematic quantities as

$$\begin{aligned} \delta\varepsilon_{\alpha\beta} &= \tfrac{1}{2}(\delta v_{\alpha,\beta} + \delta v_{\beta,\alpha}) \rightarrow \delta v_{\beta,\alpha} \\ \delta\kappa_{\alpha\beta} &= \tfrac{1}{2}(\delta\alpha_{\alpha,\beta} + \delta\alpha_{\beta,\alpha}) \rightarrow \delta\alpha_{\beta,\alpha} \\ \delta\gamma_\beta &= \delta\alpha_\beta + \delta w_{,\beta} \end{aligned} \tag{6.40}$$

The virtual work functional for the Mindlin-Reissner plate thus takes the form:

$$\begin{aligned} \delta W = \int_A & (N_{\alpha\beta}\,\delta v_{\beta,\alpha} + M_{\alpha\beta}\,\delta\alpha_{\beta,\alpha} + Q_\beta\,(\delta\alpha_\beta + \delta w_{,\beta}) \\ & -p_\beta\delta v_\beta - p\delta w - m_\beta\delta\alpha_\beta)\,dA \\ - \int_{\partial A} & \left(\bar{N}_\beta\delta v_\beta + \bar{M}_\beta\delta\alpha_\beta + \bar{Q}\delta w\right)\,ds \end{aligned} \tag{6.41}$$

The idea is to bring this virtual work functional into a form, which only holds the basic virtual quantities δv_β, δw and $\delta\alpha_\beta$ without derivatives of these. To find the integral transformations needed do this we first find the partial derivatives of the individual terms, then we integrate over the area of the plate (middle surface) and use the divergence theorem (1.19). For example let us consider the moment terms:

$$\begin{aligned} (M_{\alpha\beta}\,\delta\alpha_\beta)_{,\alpha} &= M_{\alpha\beta,\alpha}\,\delta\alpha_\beta + M_{\alpha\beta}\,\delta\alpha_{\beta,\alpha} \quad \Downarrow \\ M_{\alpha\beta}\,\delta\alpha_{\beta,\alpha} &= -M_{\alpha\beta,\alpha}\,\delta\alpha_\beta + (M_{\alpha\beta}\,\delta\alpha_\beta)_{,\alpha} \quad \Downarrow \\ \int_A M_{\alpha\beta}\,\delta\alpha_{\beta,\alpha}\,dA &= -\int_A M_{\alpha\beta,\alpha}\,\delta\alpha_\beta\,dA + \int_A (M_{\alpha\beta}\,\delta\alpha_\beta)_{,\alpha}\,dA \quad \Downarrow \\ \int_A M_{\alpha\beta}\,\delta\alpha_{\beta,\alpha}\,dA &= -\int_A M_{\alpha\beta,\alpha}\,\delta\alpha_\beta\,dA + \int_{\partial A} n_\alpha M_{\alpha\beta}\,\delta\alpha_\beta\,ds \end{aligned} \tag{6.42}$$

The other partial derivatives of the basic kinematic quantities can also be eliminated using this method. The remaining integral transformations are:

$$\int_A N_{\alpha\beta}\,\delta v_{\beta,\alpha}\,dA = -\int_A N_{\alpha\beta,\alpha}\,\delta v_\beta\,dA + \int_{\partial A} n_\alpha N_{\alpha\beta}\,\delta v_\beta\,ds \tag{6.43}$$

$$\int_A Q_\beta\,\delta w_{,\beta}\,dA = -\int_A Q_{\beta,\beta}\,\delta w\,dA + \int_{\partial A} n_\beta Q_\beta\,\delta w\,ds \tag{6.44}$$

Introducing the integral transformations and rearranging the virtual work terms we find the following informative version of the virtual work functional.

$$\begin{aligned} \delta W = & \\ & -\int_A \left((N_{\alpha\beta,\alpha} + p_\beta)\delta v_\beta + (Q_{\beta,\beta} + p)\delta w + (M_{\alpha\beta,\alpha} - Q_\beta + m_\beta)\delta\alpha_\beta\right)\,dA \\ & -\int_{\partial A} \left((\bar{N}_\beta - n_\alpha N_{\alpha\beta})\delta v_\beta + (\bar{Q} - n_\beta Q_\beta)\delta w + (\bar{M}_\beta - n_\alpha M_{\alpha\beta})\delta\alpha_\beta\right)\,ds \end{aligned} \tag{6.45}$$

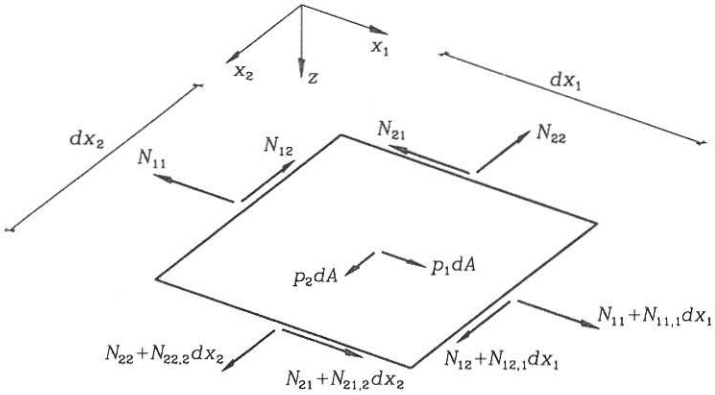

Fig. 6.7: In-plane forces on infinitesimal plate section.

Since the virtual work must vanish $\delta W = 0$ for any independent variation in the virtual kinematic parameters this virtual work functional delivers the differential equilibrium equations and the corresponding boundary conditions for a plate.

Plate equilibrium equations

$$N_{\alpha\beta,\alpha} + p_\beta = 0 \tag{6.46}$$

$$Q_{\beta,\beta} + p = 0 \tag{6.47}$$

$$M_{\alpha\beta,\alpha} - Q_\beta + m_\beta = 0 \tag{6.48}$$

Corresponding boundary conditions

$$\bar{N}_\beta = n_\alpha N_{\alpha\beta} \qquad \bar{Q} = n_\beta Q_\beta \qquad \bar{M}_\beta = n_\alpha M_{\alpha\beta} \tag{6.49}$$

where n_α is the normal on the boundary of the middle surface.

The five differential equations just derived must be satisfied for a loaded plate to be in static equilibrium. The equations correspond to force equilibrium in the two in-plane directions (6.46), force equilibrium in the transverse direction (6.47) and moment equilibrium about the in-plane axes (6.48). The in-plane equilibrium equations involve the membrane forces $N_{\alpha\beta}$ and the distributed in-plane loads p_β as shown in fig. 6.7 for an infinitesimal plate section. The three flexural equilibrium equations involve the shear forces Q_β, the moments $M_{\alpha\beta}$, the distributed transverse loads p and the distributed moment loads m_β as shown for an infinitesimal plate section in fig. 6.8. By combining the transverse equilibrium and the moment equilibrium equations we can eliminate the shear forces and find the following equation which just involves the moments and the transverse load:

$$M_{\alpha\beta,\alpha\beta} + m_{\beta,\beta} + p = 0 \tag{6.50}$$

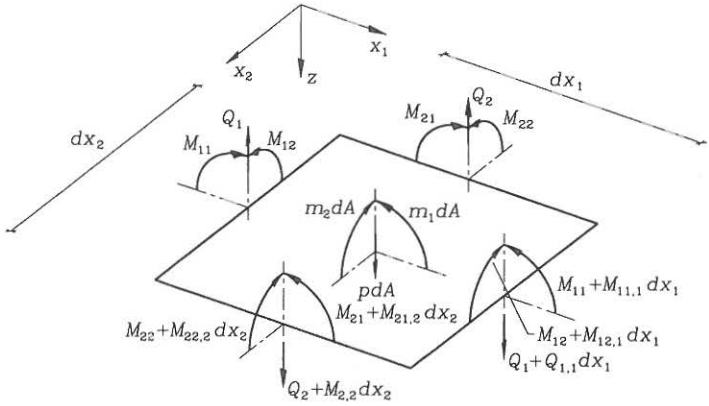

Fig. 6.8: Moments and transverse forces on infinitesimal plate section.

Force and moment distributions, which satisfy the static equilibrium equations, are said to be statically admissible, i.e. the static equilibrium equations can be used to check if a given set of force and moment distributions satisfies equilibrium. A plate is statically indeterminate, since the static equilibrium equations do not only have one solution, but many. However, if we introduce the linear elastic constitutive relations there is one unique solution. Let us introduce the constitutive relations and the kinematics of the Mindlin-Reissner plate theory, just to see how the equations and thereby the mechanical problems are coupled. We assume that the thickness and material properties are constant in the whole plate and find the following kinematic differential equations:

$$\tfrac{1}{2} D^m_{\alpha\beta\gamma\nu}(v_{\gamma,\nu\alpha} + v_{\nu,\gamma\alpha}) + p_\beta = 0 \tag{6.51}$$

$$D^s(\alpha_{\beta,\beta} + w_{,\beta\beta}) + p = 0 \tag{6.52}$$

$$\tfrac{1}{2} D^b_{\alpha\beta\gamma\nu}(\alpha_{\gamma,\nu\alpha} + \alpha_{\nu,\gamma\alpha}) - D^s(\alpha_\beta + w_{,\beta}) + m_\beta = 0 \tag{6.53}$$

It is thus clear that the in-plane problem (6.51) involving membrane forces $N_{\alpha\beta}$ and loads p_β is an independent problem, which is not coupled with the bending problem. The in-plane problem is a so-called plane stress problem. Some in-plane problems can be solved through the use of a stress potential, the so-called Airy's stress function. However, this will not be considered in the present text. The flexural plate problem is given by the coupled shear equation (6.52) and the two moment equations (6.53). We shall be content with a knowledge of the form of the static equilibrium equations and the two derived displacement differential equations. Today these equations are solved by approximate computational techniques, based on the principle of virtual work or minimum potential energy. Analytical solutions can be obtained for cases with simple geometric forms and boundary conditions. The similarity in the differential equations of the Mindlin-Reissner plate theory and the

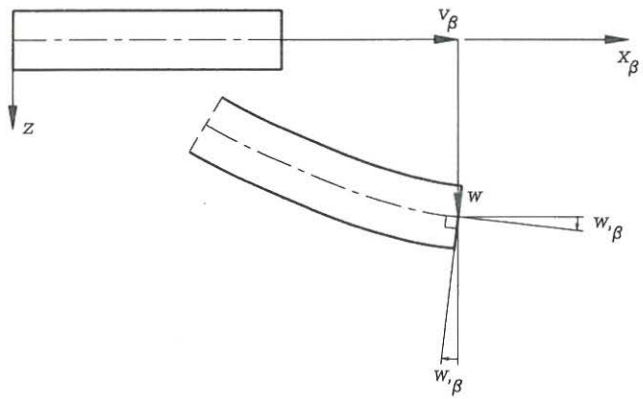

Fig. 6.9: Displacements of a Kirchhoff plate.

Timoshenko beam theory should be noted. The plate equations are complicated by the two-dimensional format of the coupled partial differential equations.

6.2 Kirchhoff Plate Theory

The behaviour of plates has much in common with the behaviour of beams and it is therefore not surprising that Kirchhoff introduced the same additional assumption that the normals remain normals to the plate surface even in the deformed state. The mechanical explanation is that the influence of shear vanishes for thin plates, i.e. the engineering shear strain components of the plate vanish.

Assumption 4:

Normals to the middle surface remain normals during deformation

this implies that the shear strains are disregarded, since:

$$\alpha_\beta = -w_{,\beta} \quad \Rightarrow \quad \gamma_\beta = \alpha_\beta + w_{,\beta} = 0 \tag{6.54}$$

The assumed displacements shown in fig. 6.9 are a two-dimensional version of the Euler-Bernoulli beam theory. The assumed displacements in Kirchhoff plates thus are:

Assumed displacements

$$u_\beta = v_\beta - z\, w_{,\beta} \tag{6.55}$$
$$u_3 = w \tag{6.56}$$

where the three unknown kinematic functions are

$$v_\beta(x_\nu)\,, \quad w(x_\nu)$$

The derivation of Kirchhoff theory is equivalent to the derivations already performed for the Mindlin-Reissner theory and we shall not go into details, since we can just insert $\gamma_\beta = 0$. However, as in the chapter on beam theory the important formulas will be given. The in-plane strains are now defined by:

The in-plane strains in Kirchhoff plate theory are

$$\varepsilon_{\alpha\beta} = \bar{\varepsilon}_{\alpha\beta} + z\kappa_{\alpha\beta} \tag{6.57}$$

in which the membrane strains are

$$\bar{\varepsilon}_{\alpha\beta} = \frac{1}{2}(v_{\alpha,\beta} + v_{\beta,\alpha}) = \frac{1}{2}\left(\frac{\partial v_\alpha}{\partial x_\beta} + \frac{\partial v_\beta}{\partial x_\alpha}\right) \tag{6.58}$$

and the curvatures are

$$\kappa_{\alpha\beta} = \tfrac{1}{2}(\alpha_{\alpha,\beta} + \alpha_{\beta,\alpha}) = -\tfrac{1}{2}(w_{,\alpha\beta} + w_{,\beta\alpha})$$
$$= -w_{,\alpha\beta} = -\frac{\partial^2 w}{\partial x_\alpha \partial x_\beta} \tag{6.59}$$

The constitutive relations are the same as for Mindlin-Reissner theory, with the only modification that the shear forces are irrelevant, since $\gamma_\beta = 0$. Due to the definitions of the inclinations as $\alpha_\beta = -w_{,\beta}$, and thereby the curvatures as $\kappa_{\alpha\beta} = -w_{,\alpha\beta}$, the virtual work functional for Kirchhoff plates takes the following form

Virtual work functional for Kirchhoff plates

$$\delta W = \int_A \left(N_{\alpha\beta}\,\delta v_{\beta,\alpha} - M_{\alpha\beta}\,\delta w_{,\alpha\beta} - p_\beta \delta v_\beta - p\delta w + m_\beta \delta w_{,\beta}\right) dA$$
$$- \int_{\partial A} \left(\bar{N}_\beta \delta v_\beta - \bar{M}_\beta \delta w_{,\beta} + \bar{Q}\delta w\right) ds \tag{6.60}$$

In the quest to find the equilibrium equations we need to perform partial integration and use the divergence theorem twice, since the virtual work equation involves double partial derivatives of a kinematic quantity, i.e. $\delta w_{,\alpha\beta}$. Using partial integration once as in the previous section we find:

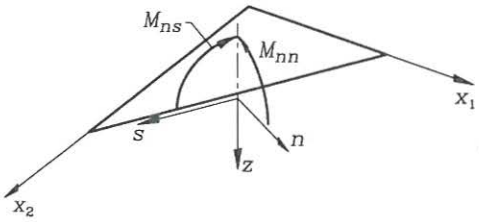

Fig. 6.10: Local (n, s)-coordinate system on boundary.

$$\begin{aligned}\delta W &= -\int_A \left((N_{\alpha\beta,\alpha} + p_\beta)\delta v_\beta - (M_{\alpha\beta,\alpha} + m_\beta)\delta w_{,\beta} + p\delta w\right)\, dA \\ &\quad -\int_{\partial A} \left((\bar{N}_\beta - n_\alpha N_{\alpha\beta})\delta v_\beta + \bar{Q}\delta w - (\bar{M}_\beta - n_\alpha M_{\alpha\beta})\delta w_{,\beta}\right)\, ds \qquad (6.61)\end{aligned}$$

Using partial integration on the terms including $\delta w_{,\beta}$ and the divergence theorem yields

$$\begin{aligned}\delta W &= -\int_A \left((N_{\alpha\beta,\alpha} + p_\beta)\delta v_\beta + (M_{\alpha\beta,\alpha\beta} + m_{\beta,\beta} + p)\delta w\right)\, dA \\ &\quad -\int_{\partial A} \left((\bar{N}_\beta - n_\alpha N_{\alpha\beta})\delta v_\beta \right. \\ &\qquad \left. +(\bar{Q} - n_\beta M_{\alpha\beta,\alpha})\delta w - (\bar{M}_\beta - n_\alpha M_{\alpha\beta})\delta w_{,\beta}\right)\, ds \qquad (6.62)\end{aligned}$$

In this virtual work functional we can use internal variations leading to the equilibrium equations (6.46) and (6.50) already derived. However, the boundary variations are not easy to introduce since the transverse displacement and its derivative along the boundary are coupled. In order to cope with this problem we introduce the tangential boundary vector with components s_β, which is orthogonal to the boundary normal with components n_β. These vectors define a local (n, s)-coordinate system as shown in fig. 6.10. We assume that the boundary is piecewise straight so that the partial derivatives become simple. The boundary rotations can be decomposed in the local coordinate system by projections and the components found as follows:

$$\delta w_{,n} = \delta\left(\frac{\partial w}{\partial n}\right) = n_\beta\, \delta w_{,\beta}\ , \qquad \delta w_{,s} = \delta\left(\frac{\partial w}{\partial s}\right) = s_\beta\, \delta w_{,\beta} \qquad (6.63)$$

in which the indices n and s refer to the components and they are not summation indices. We also use the notation $()_{,n} = \frac{\partial()}{\partial n}$ and $()_{,s} = \frac{\partial()}{\partial s}$, respectively, for partial derivatives in the normal and tangential directions. Corresponding to this notation we use the following notation for the internal moments in the local coordinate system as shown in fig. 6.10

$$M_{nn} = n_\alpha n_\beta M_{\alpha\beta}\ , \qquad M_{ns} = s_\beta n_\alpha M_{\alpha\beta} \qquad (6.64)$$

and for the (prescribed) boundary moments $\bar{M}_\beta$ we use the following component notation:

$$\bar{M}_n = n_\beta \bar{M}_\beta , \qquad \bar{M}_s = s_\beta \bar{M}_\beta \tag{6.65}$$

Furthermore, let us introduce the notation Q_β for the internal shear force , which is determined statically by:

$$Q_\beta = M_{\alpha\beta,\alpha} \tag{6.66}$$

Note that this shear force is determined statically and not kinematicly, since there are no shear strains in the Kirchhoff plate theory.

Having introduced the notations we rewrite the boundary integral term in (6.62) involving the derivatives of the boundary displacements $\delta w_{,\beta}$ as follows:

$$\begin{aligned}
&\int_{\partial A} (\bar{M}_\beta - n_\alpha M_{\alpha\beta}) \delta w_{,\alpha} \, ds \\
&\quad = \int_{\partial A} \left((\bar{M}_\beta n_\beta - n_\alpha M_{\alpha\beta} n_\beta) \delta w_{,n} + (\bar{M}_\beta s_\beta - n_\alpha M_{\alpha\beta} s_\beta) \delta w_{,s} \right) ds \\
&\quad = \int_{\partial A} \left((\bar{M}_n - M_{nn}) \delta w_{,n} + (\bar{M}_s - M_{ns}) \delta w_{,s} \right) ds
\end{aligned} \tag{6.67}$$

For the derivatives along the boundary in equation (6.67) we can use partial integration as follows:

$$\begin{aligned}
&\int_{\partial A} (\bar{M}_s - M_{ns}) \delta w_{,s} \, ds \\
&\qquad = -\int_{\partial A} (\bar{M}_{s,s} - M_{ns,s}) \delta w \, ds + \int_{\partial A} \left((\bar{M}_s - M_{ns}) \delta w \right)_{,s} ds \\
&\qquad = -\int_{\partial A} (\bar{M}_{s,s} - M_{ns,s}) \delta w \, ds
\end{aligned} \tag{6.68}$$

since the (circulation) integral $\int_{\partial A} (\ldots)_{,s} \, ds = 0$ around the boundary of the derivative along the boundary is zero, (the integral starts and ends at the same place). Introducing this (6.68) in equation (6.67) we get the following reformulation of the boundary term:

$$\begin{aligned}
&\int_{\partial A} (\bar{M}_\beta - n_\alpha M_{\alpha\beta}) \delta w_{,\alpha} \, ds \\
&\qquad = \int_{\partial A} \left((\bar{M}_n - M_{nn}) \delta w_{,n} - (\bar{M}_{s,s} - M_{ns,s}) \delta w \right) ds
\end{aligned} \tag{6.69}$$

Introducing this equality into the virtual work equation (6.62) yields the following informative form of the virtual work for Kirchhoff plates:

$$\begin{aligned}
\delta W = &- \int_A \left((N_{\alpha\beta,\alpha} + p_\beta) \delta v_\beta + (M_{\alpha\beta,\alpha\beta} + m_{\beta,\beta} + p) \delta w \right) dA \\
&- \int_{\partial A} \Big((\bar{N}_\beta - n_\alpha N_{\alpha\beta}) \delta v_\beta - (\bar{M}_n - M_{nn}) \delta w_{,n} \\
&\qquad + (\bar{Q} + \bar{M}_{s,s} - n_\beta M_{\alpha\beta,\alpha} - M_{ns,s}) \delta w \Big) \, ds
\end{aligned} \tag{6.70}$$

The principle of virtual work $\delta W = 0$ states that the virtual work functional must vanish for any independent virtual variation in the kinematic parameters. In this

informative virtual work functional (6.70) we can also vary in-plane displacements δv_β, transverse displacements δw and the normal derivative of the transverse displacements $\delta w_{,n}$ independently at the boundary, whereby the correct boundary conditions are revealed for any boundary.

Plate equilibrium equations

$$N_{\alpha\beta,\alpha} + p_\beta = 0 \tag{6.71}$$

$$M_{\alpha\beta,\alpha\beta} + m_{\beta,\beta} + p = 0 \tag{6.72}$$

Corresponding boundary conditions for Kirchhoff plate theory

$$\bar{N}_\beta = n_\alpha N_{\alpha\beta} \tag{6.73}$$

$$\bar{M}_n = n_\beta n_\alpha M_{\alpha\beta} \tag{6.74}$$

$$\begin{aligned} \bar{Q} + \bar{M}_{s,s} &= n_\beta Q_\beta + M_{ns,s} \\ &= n_\beta M_{\alpha\beta,\alpha} + M_{ns,s} \\ &= M_{nn,n} + 2\, M_{ns,s} \end{aligned} \tag{6.75}$$

Let us take a look at the differential equation (6.72), which describes the bending behaviour of the Kirchhoff plate. Let us assume that there are no distributed moment loads $m_\beta = 0$ and let us then expand the equation into components as follows:

$$\begin{aligned} M_{11,11} + M_{12,21} + M_{21,12} + M_{22,22} + p &= 0 \quad \Downarrow \\ M_{11,11} + 2M_{12,12} + M_{22,22} + p &= 0 \end{aligned} \tag{6.76}$$

where we have used that the moment components are symmetric and that the order of differentiation is irrelevant. The equation can also be written in the following notation:

$$\frac{\partial^2 M_{11}}{\partial x_1^2} + 2\,\frac{\partial^2 M_{12}}{\partial x_1 \partial x_2} + \frac{\partial^2 M_{22}}{\partial x_2^2} + p = 0 \tag{6.77}$$

This equation is a static equilibrium equation. If we want to consider transverse displacements, then we must introduce some constitutive relation between moments and displacements, i.e. curvatures. The linear elastic constitutive relation for Kirchhoff theory takes the following component form:

$$\begin{aligned} M_{11} &= -D\,(w_{,11} + \nu w_{,22}) \\ M_{22} &= -D\,(w_{,22} + \nu w_{,11}) \\ M_{12} &= -D\,(1-\nu) w_{,12} \end{aligned} \tag{6.78}$$

Introducing these constitutive relations in the static equilibrium equation (6.72) or (6.76) yields the differential equation for the transverse displacements in an isotropic linear elastic Kirchhoff plate:

Differential equation for displacements of Kirchhoff plate

$$w_{,1111} + 2\,w_{,1122} + w_{,2222} = \frac{p}{D} \tag{6.79}$$

where $D = \frac{Et^3}{12(1-\nu^2)}$ *is the elastic plate bending modulus.*

This equation is the biharmonic equation derived in 1811 by Lagrange, even though his plate theory was not entirely satisfactory. The equation may also be presented as follows:

$$\begin{aligned} w_{,\alpha\beta\alpha\beta} &= \frac{p}{D} \\ \nabla^2\nabla^2 w &= \frac{p}{D} \\ \frac{\partial^4 w}{\partial x_1^4} + 2\,\frac{\partial^4 w}{\partial x_1^2 \partial x_2^2} + \frac{\partial^4 w}{\partial x_2^4} &= \frac{p}{D} \end{aligned} \tag{6.80}$$

To solve the biharmonic equation we need boundary conditions, which can either be of a static or a kinematic type. The boundary conditions for the flexural problem are given in equations (6.74) and (6.75), where the second one is the most complicated. The first states that the moment corresponding to stress components in the normal direction is directly related to the boundary tractions or moments by $\bar{M}_n = n_\alpha n_\beta M_{\alpha\beta} = M_{nn}$. The second and more complicated boundary condition (6.75) is related to the boundary shear $\bar{Q}$ and change in the torsional boundary moment $\bar{M}_{s,s}$. These boundary forces/loads are transmitted to the plate in the form of a shear force $n_\beta Q_\beta = n_\beta M_{\alpha\beta,\alpha}$ and gradients in the torsional moment $M_{ns,s}$ (i.e. $s_\nu s_\alpha n_\beta M_{\alpha\beta,\nu}$), but since the shear force and torsional moment gradient are statically equivalent in the Kirchhoff theory we cannot separate them, only their sum is known.

Kirchhoff boundary condition

$$\bar{Q} + \bar{M}_{s,s} = n_\beta Q_\beta + M_{ns,s} \tag{6.81}$$

where the internal shear forces are $Q_\beta = n_\beta M_{\alpha\beta,\alpha}$.

At the boundary there is a transition zone where the boundary forces/loads $\bar{Q}$ and $\bar{M}_{s,s}$ transform into an internal indeterminate combination of shear force $n_\beta Q_\beta$ and torsional moment gradient $M_{ns,s}$.

The equivalence between the shear force and the moment gradient along the boundary is illustrated in fig. 6.11. The left-hand part of the figure shows the torsional moment M_{ns} and its variation $M_{ns,s}ds$. The right-hand part shows an equivalent set of forces M_{ns} and $M_{ns} + M_{ns,s}ds$. It is clear that a variation in the torsional moment leads to differences in adjacent forces $M_{ns,s}ds$, which thereby produces a continuous shear force $M_{ns,s}$ and some concentrated corner shear forces M_{ns}, as illustrated in fig. 6.12.

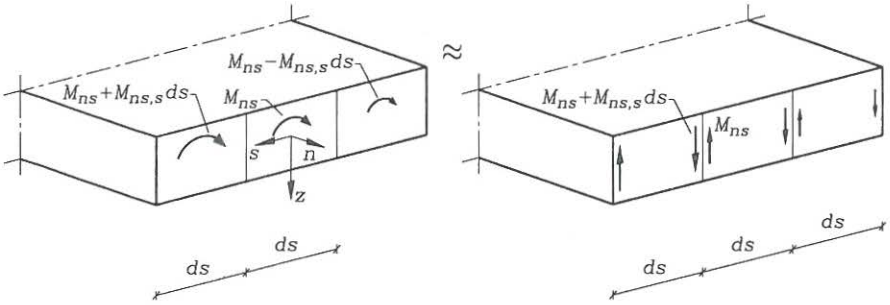

Fig. 6.11: The torsional moment M_{ns} and equivalent forces M_{ns}.

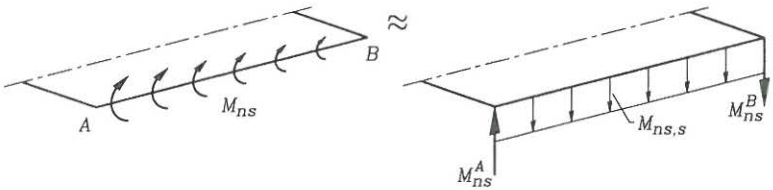

Fig. 6.12: The torsional moment M_{ns}, equivalent shear force $M_{ns,s}$ and concentrated corner shear forces M_{ns}.

Let us look at corner shear forces at a rectangular corner, and just to illustrate the concept let us use a coordinate system which is orientated according to the corner as shown in fig. 6.13. By looking at the orientation of the torsional moments M_{12}, M_{21}, and by using the idea of force equivalents it becomes clear that there must be a corner shear force of

$$\hat{Q} = M_{12} + M_{21} = 2M_{12} \tag{6.82}$$

at rectangular corners. For non-rectangular corners the sum of the force contributions can be calculated by using the two different local coordinate systems at the corner (n^1, s^1) or (n^2, s^2) as shown in fig. 6.14. Because of the difference in orientation of the (x_1, x_2)-coordinate system and the (n^2, s^2)-coordinate system the expression for the corner shear force becomes

$$\begin{aligned} \hat{Q} &= M_{ns}^2 - M_{ns}^1 \\ &= s_\alpha^2 n_\beta^2 M_{\alpha\beta} - s_\alpha^1 n_\beta^1 M_{\alpha\beta} \end{aligned} \tag{6.83}$$

where the superscripts are references to the relevant coordinate axes.

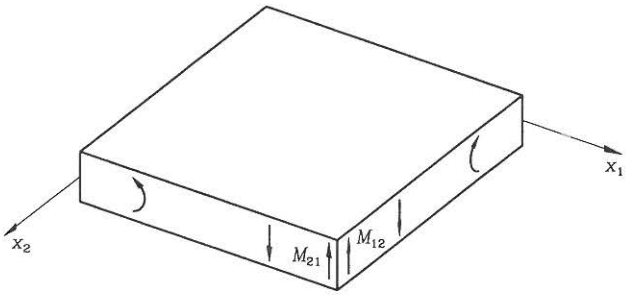

Fig. 6.13: Corner shear forces at rectangular corners.

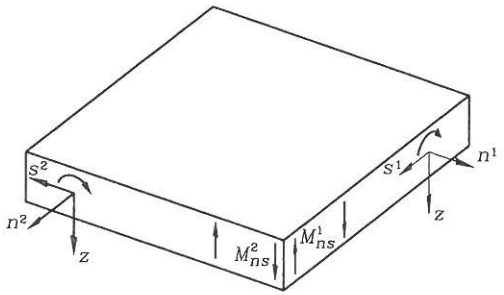

Fig. 6.14: Contributions to the corner shear force.

- **Problem 6.1**

A thin rectangular plate is $a_1 = 1000\,\text{mm}$ by $a_2 = 2000\,\text{mm}$ and has a thickness of $t = 10\,\text{mm}$. The material is steel with an elastic modulus $E = 2.1 \cdot 10^5\,\text{MPa}$ and a Poisson ratio of $\nu = 0.3$. The plate is supported along the boundary and the plate displacements are given by:

$$\begin{aligned} v_1 &= \frac{1}{100} x_1 \\ v_2 &= -\frac{\nu}{100} x_2 \\ w &= \frac{1}{20} a_1 \sin(\frac{\pi x_1}{a_1}) \sin(\frac{\pi x_2}{a_2}) \end{aligned}$$

where the coordinates are in the ranges $x_1 \in [0, a_1]$ and $x_2 \in [0, a_2]$. The plate is assumed to follow the Kirchhoff plate theory and it has a non-uniform distributed load p and no distributed in-plane loads $p_\beta = 0$.

a) Make a sketch of the in-plane displacements v_ν and another sketch of the out-of-plane displacements w.

b) Find the middle surface strain components $\bar{\varepsilon}_{\alpha\beta}$.

c) Find the membrane forces $N_{\alpha\beta}$ and show that they fulfil the equilibrium equations within the plate.

d) Find the membrane boundary forces $\bar{N}_\beta$ and describe the in-plane load situation.

e) Use the displacement equilibrium equations for a Kirchhoff plate to find a mathematical expression for the distributed transverse load $p(x_\nu)$.

f) Find the curvatures $\kappa_{\alpha\beta}$.

g) Find the moments $M_{\alpha\beta}$ and show that they fulfil the static equilibrium equations.

h) Find the boundary moments $\bar{M}_n$ and the equivalent shear force distribution $\bar{Q} + \bar{M}_{s,s}$.

i) Find the corner shear forces $\hat{Q}$.

Chapter 7

Yield Line Analysis of Plates

The elastic analysis of plates using the differential equations or virtual work functionals described in the previous chapter determines the elastic moment distributions and the transverse displacements. However, this gives no indication of the transverse load-carrying capacities. The load at first yielding in a plate is much lower than the experimental load-carrying capacity, due to the plastic capacity of the material. Due to the plastification and the ability of the material to yield, the moments in the plate are redistributed and the plastic zones grow until eventually a plastic flow mechanism is formed, much like in the plastic hinge theory for beams. The plastic flow mechanism is also called a collapse mechanism.

The main idea is to assume that the plastic flow mechanism consists of moving (rotating) rigid parts of the plate, where the parts are connected along yield lines, i.e. plastic hinge lines, as shown in fig. 7.1. Along the yield lines there are mutual rotations between neighbouring rigid parts. We assume that the plastic flow is quasi static, so that we shall be able to use energy considerations and the principle of virtual work. For this type of quasi static plastic flow mechanism we may assume virtual displacements corresponding to a virtual yield line lay-out and calculate the total (plastic) virtual work δW_p, by assuming that the moments have plastified. The (plastic) principle of virtual work $\delta W_p \geq 0$ then gives an upper bound for the load-carrying capacity of the plate. The upper bound can then be minimized by variations in the yield line lay-out.

The yield line theory was developed in 1943 by Johansen [27], [28], and [29]. The theory was mainly developed for reinforced concrete slabs (plates), but since then it has been extended to other materials, such as metals. General theories for perfectly plastic materials were developed independently by Gvozdev about 1936 and Prager about 1951. Modern treatments of the plasticity theories are given by Chen & Han [18], Nielsen [30], Martin [31] and Save & Massonnet [32], see also the work by Prager [33] and by Hodge [34]. Introductory texts in Danish are given by Nielsen & Rathkjen [26] and by Nielsen [24].

The presentation in this chapter will be limited to the yield line theory based on the principle of virtual work and a short introduction to the strip method based on equilibrium solutions as developed in 1956 by Hillerborg, see [35] or [36]. The yield line theory establishes upper bounds for the load-carrying capacity, and the

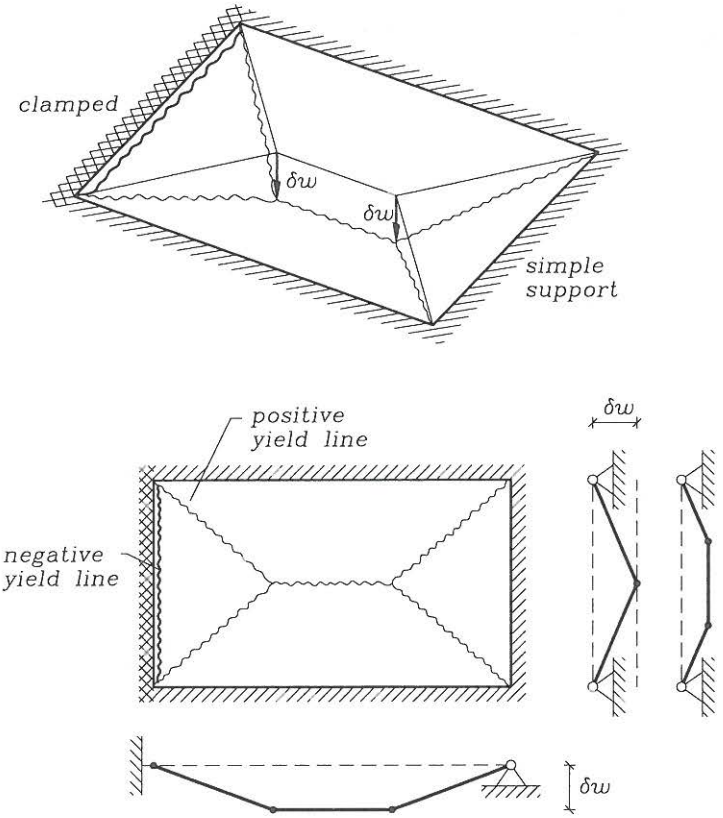

Fig. 7.1: A plastic flow mechanism for a plate.

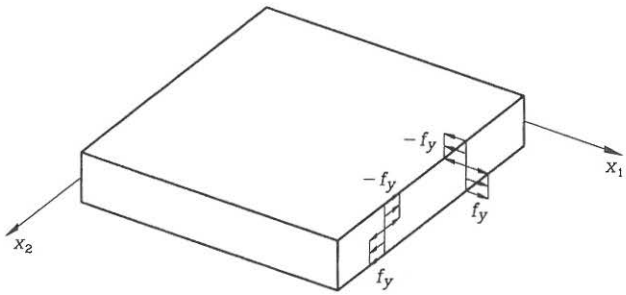

Fig. 7.2: Stress distribution used to define M_p.

strip method establishes lower bounds for the load-carrying capacity through the use of statically admissible moment distributions. Before the yield line method is treated we need to introduce a few basic concepts of perfect plasticity theory for plates.

Yield Criterion and Flow Rule

When a combination of plate moments at some point reaches a certain level it is assumed that the material becomes perfectly plastic and yields at this point. The combination of moments at which the material becomes perfectly plastic is described by a yield criterion. In plasticity theory the yield criterion is described by a yield function $f(M_{\alpha\beta})$. The yield function often includes a referencial plastification moment M_p, *(where p is a reference index, i.e. no summation)* or M_p^+ and M_p^- if the positive and negative plastification moments differ. The plastification moment M_p for an isotropic material can be determined by use of the uniaxial yield stress f_y, *(where y is a reference index)*, corresponding to the stress distributions shown in fig. 7.2 as follows:

For an isotropic plate material with equal compression and tension yield stress the referencial plastification moment is:

$$M_p = \left| \int_t z\sigma_y \, dz \right| = \frac{1}{4} t^2 f_y \tag{7.1}$$

If the yield function is less than zero, $f(M_{\alpha\beta}) < 0$, then the material has not reached the plastification level, and when the function reaches zero $f(M_{\alpha\beta}) = 0$, then the material yields. A perfectly plastic material can never be in a state where the yield function is positive. The yield criterion can be described by a socalled yield surface in moment space, i.e. as a function of the moments $M_{\alpha\beta}$. The yield surface is the surface in moment space at which the yield function is zero:

$$f(M_{\alpha\beta}) = 0 \tag{7.2}$$

For isotropic materials the yield criterion and the yield function can be formulated in principal moments, if the material remains direction independent (during and after yielding). For these materials the principal axes of moments and curvatures are identical. Some classic yield criteria (surfaces) for plates are shown in fig. 7.3. The von Mises and Tresca yield criteria are based on integrated plane stress yield criteria and Johansen's (simple) yield criterion is, to some extent, based on experimental knowledge of reinforced concrete plates. The von Mises yield criterion is formulated so that it preserves the material volume during plastic flow, which is generally the case for metals. Let us summarize.

The constitutive state of the material is described by the yield function

$$f(M_{\alpha\beta}) \begin{cases} < 0 & \textit{linear elastic state} \\ = 0 & \textit{perfecly plastic state} \\ > 0 & \textit{impossible state} \end{cases} \tag{7.3}$$

The yield surface in moment space is given by:

$$f(M_{\alpha\beta}) = 0 \tag{7.4}$$

How do we link the curvature rates and the moments for perfectly plastic plates? Let us use the dissipation assumption originally used by von Mises: *The rate at which plastic energy is dissipated is the maximum possible*, (sometimes referenced as the Hill-Mandel maximum dissipation principle). The rate of energy dissipation $\dot{d}$ per area in a plate is determined by the work of the plastic moments through the curvature rate:

$$\dot{d} = M_{\alpha\beta}\dot{\kappa}_{\alpha\beta} \tag{7.5}$$

According to the von Mises assumption the dissipated energy $\dot{d}$ is the maximum possible, i.e. the material makes the maximum possible resistance. A necessary condition for a maximum is that, the variation of the energy dissipation is zero $\delta\dot{d} = 0$, i.e. the rate of energy dissipation is stationary. Variations with respect to the moments on the yield surface gives:

$$\dot{\kappa}_{\alpha\beta}\,\delta M_{\alpha\beta} = 0 \tag{7.6}$$

For consistence the moments must remain on the yield surface for the used variations. This is expressed mathematically by use of the yield criterion as follows:

$$\frac{\partial f}{\partial M_{\alpha\beta}}\,\delta M_{\alpha\beta} = 0 \tag{7.7}$$

which just states that the value of f remains stationary $\delta f = 0$ (and thus equal to zero) for the variation $\delta M_{\alpha\beta}$. The term $\frac{\partial f}{\partial M_{\alpha\beta}}$ is normal to the yield surface. The (dot) product between this normal and the variation in moments must therefore be zero. Let us examine the two equations. If the two equations (7.6) and (7.7) are fulfilled for any moment variation on the yield surface, then we conclude that the

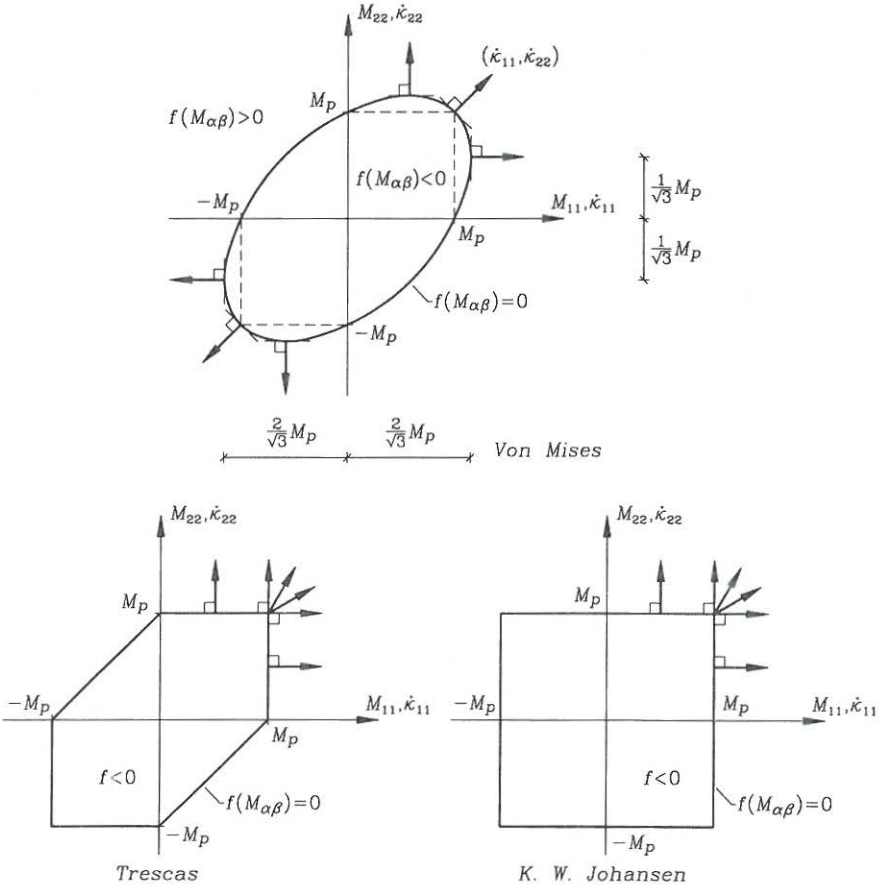

Fig. 7.3: Some plate yield criteria.

coefficients $\dot{\kappa}_{\alpha\beta}$ and $\frac{\partial f}{\partial M_{\alpha\beta}}$ are proportional. Thus the constitutive relation, or let us say the flow rule, takes the form

$$\dot{\kappa}_{\alpha\beta} = \dot{\lambda} \frac{\partial f}{\partial M_{\alpha\beta}} \tag{7.8}$$

In the flow rule $\dot{\lambda}$ is a flow rate proportionality factor. Since plastic flow only occurs on the yield surface we write the flow rule in the following manner:

The associated flow rule for perfectly plastic materials

$$\dot{\kappa}_{\alpha\beta} = \begin{cases} \dot{\lambda} \dfrac{\partial f}{\partial M_{\alpha\beta}} & \text{if} \quad f(M_{\alpha\beta}) = 0 \\ 0 & \text{if} \quad f(M_{\alpha\beta}) < 0 \end{cases} \tag{7.9}$$

This flow rule is an associated flow rule since the plastic flow $\dot{\kappa}_{\alpha\beta}$ is directly associated with the yield surface $f = 0$. The flow rule states that the curvature flow rate is proportional to the normal of the yield surface, so it is also referred to as the normality condition or the normality flow rule. Note that the dissipation assumption of von Mises is not always correct and hence, non-associative flow rules exist. Let us discuss the implication of the von Mises assumption. The stationarity of the energy dissipation $\delta \dot{d} = 0$ is a sufficient condition for a maximum, if the yield surface is convex. To show this let us compare the energy dissipation rate for a neighbouring moment state $M_{\alpha\beta} + \Delta M_{\alpha\beta}$ on the yield surface with the maximum energy dissipation state $M_{\alpha\beta}$ for given curvature rates $\dot{\kappa}_{\alpha\beta}$ as follows:

$$\begin{aligned} (M_{\alpha\beta} + \Delta M_{\alpha\beta})\dot{\kappa}_{\alpha\beta} &< M_{\alpha\beta}\dot{\kappa}_{\alpha\beta} \quad \Downarrow \\ \Delta M_{\alpha\beta}\dot{\kappa}_{\alpha\beta} &< 0 \end{aligned} \tag{7.10}$$

The first inequality is true since $M_{\alpha\beta}\dot{\kappa}_{\alpha\beta}$ is the maximum possible energy dissipation. The curvature rate $\dot{\kappa}_{\alpha\beta}$ at maximum energy dissipation is normal to the yield surface, and the second equation states that the projection of the moments on this normal must be negative, which is the same as stating that the yield surface must be convex, as shown in fig. 7.4. The derivations have been made assuming continuity of the functions. However, the demand for a continuous convex yield surface is often relaxed to allow for linearly varying parts. It is worth noting that for a given set of curvature rates it is possible to find a unique solution for the moments only if the yield surface is convex. However, for both convex yield surfaces and yield surfaces with relaxed convexity the rate of energy dissipation is unique for a given set of curvature rates.

- **Example 7.1** What are the moments for a given set of curvature rates?

  Let us compare the linear elastic constitutive relations for plates and the perfectly plastic constitutive relations, i.e. the flow rule, for a given set of uniaxial curvatures and curvature rates. The curvature state in a yield line corresponds to a localized uniaxial curvature. The material is assumed to obey the von Mises yield criterion

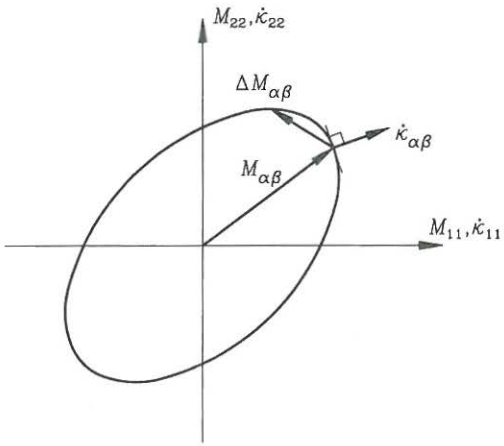

Fig. 7.4: Neighbouring moment state on a convex yield surface.

shown in fig. 7.3. Let us assume the following positive uniaxial curvatures and curvature rates:

$$\begin{pmatrix} \kappa_{11} \\ \kappa_{22} \\ 2\kappa_{12} \end{pmatrix} = \begin{pmatrix} \kappa_{11} \\ 0 \\ 0 \end{pmatrix} \qquad \begin{pmatrix} \dot{\kappa}_{11} \\ \dot{\kappa}_{22} \\ 2\dot{\kappa}_{12} \end{pmatrix} = \begin{pmatrix} \dot{\kappa}_{11} \\ 0 \\ 0 \end{pmatrix}$$

In the elastic case we use the constitutive relations (6.28) or (6.33) and find

$$\begin{pmatrix} M_{11} \\ M_{22} \\ M_{12} \end{pmatrix} = D\kappa_{11} \begin{pmatrix} 1 \\ \nu \\ 0 \end{pmatrix}$$

In the plastic case we use the flow rule (7.9), which states that the curvatures are normal to the von Mises yield surface, shown in fig. 7.3. The curvature state corresponds to the localized curvature in a yield line parallel to the x_2-axis. In the yield line the twist is zero, $\dot{\kappa}_{12} = 0$, and the principal coordinate directions are orientated as the yield line, which means that the torsional moment is zero, $M_{12} = 0$. We thus just find the one point on the von Mises yield surface, which has the normal vector $(\kappa_{11}, \kappa_{22}) = (1, 0)$. This gives us the following moments in the plastic case:

$$\begin{pmatrix} M_{11} \\ M_{22} \\ M_{12} \end{pmatrix} = \frac{2}{\sqrt{3}} M_p \begin{pmatrix} 1 \\ \frac{1}{2} \\ 0 \end{pmatrix} \simeq 1.15 M_p \begin{pmatrix} 1 \\ 0.5 \\ 0 \end{pmatrix}$$

In both the elastic and the plastic case it is seen that a uniaxial curvature κ_{11} or $\dot{\kappa}_{11}$ results in a transverse moment M_{22}. It is also noted that the maximum moment for the perfectly plastic von Mises material is higher than the reference moment M_p. This is due to biaxial state of stress in the plate. If, instead, we had used Tresca's or Johansen's yield surfaces the maximum moment in the yield line would be exactly M_p.

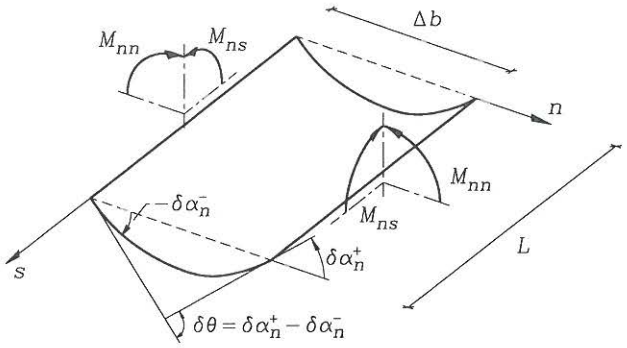

Fig. 7.5: A virtual hinge line of width Δb and curvature $\delta\kappa_{nn}$.

Virtual Work, Hinge Lines and Yield Lines

The yield criterion is assumed to be independent of both axial forces and transverse shear forces. The assumption is also made in the plastic hinge theory for beams. For the assumption to be valid the plate must be thin enough compared to the spans of the plate, i.e. the shear forces must be small enough. The yield criteria can be derived using the kinematic assumptions of the Kirchhoff plate theory and a general plane stress yield criterion. Let us not get into the implications of the assumptions made. The flexural part of the virtual work functional on which the yield line theory is based:

$$\delta W \;=\; \int_A \left(M_{\alpha\beta}\,\delta\kappa_{\alpha\beta} - \lambda p\delta w\right) dA - \int_{\partial A} \left(\bar{M}_\beta \delta\alpha_\beta + \bar{Q}\delta w\right)\, ds \tag{7.11}$$

in which $\delta\alpha_\beta = -\delta w_{,\beta}$ are the virtual middle surface inclinations and $\delta\kappa_{\alpha\beta} = -\delta w_{\alpha\beta}$ are the virtual curvatures, both derivable from the virtual middle surface displacement δw. Furthermore, a load factor λ has been introduced, so that the total transverse load intensity p^t is given by $p^t = \lambda p$. (This λ is not related directly to the flow rate proportionality factor $\dot{\lambda}$ in the previous subsection).

The virtual work in a virtual hinge line is the basis of the derivations of the upper and lower-bound theorems. Let us consider a band with the width Δb, which only has virtual curvature in the normal direction $\delta\kappa_{nn}$ as shown in fig. 7.5. The band is described using a local (n, s)-coordinate system with the n-axis as a normal and the s axis in the direction of the band. At opposite sides of the band the edge moments M_{nn} and M_{ns} are assumed equal. The principle of virtual work $\delta W = 0$ gives us

$$\lim_{\Delta b\to 0}\left(\int_A M_{\alpha\beta}\,\delta\kappa_{\alpha\beta}\,dA - \int_{\partial A}\bar{M}_\beta\delta\alpha_\beta\,ds\right) \;=\; 0 \quad \Downarrow$$

$$\lim_{\Delta b\to 0}\int_A M_{nn}\,\delta\kappa_{nn}\,dA \;=\; \int_L M_{nn}\delta\theta\,ds \tag{7.12}$$

in which the integration index L is the length of the hinge line. The normal moment and the mutual rotations are related to the original coordinate system as follows:

$$M_{nn} = n_\beta n_\alpha M_{\alpha\beta} \tag{7.13}$$

$$\begin{aligned} \delta\theta &= \delta\alpha_n^+ - \delta\alpha_n^- = \Delta(\delta\alpha_n) \\ &= n_\beta(\delta\alpha_\beta^+ - \delta\alpha_\beta^-) = n_\beta\,\Delta(\delta\alpha_\beta) \end{aligned} \tag{7.14}$$

Thus, the internal virtual work in a hinge line δW_{int} is found by integrating the product of the moment M_{nn} and the virtual mutual rotation $\delta\theta$ in the line, i.e.

$$\delta W_{int} = \int_L M_{nn}\delta\theta\, ds \tag{7.15}$$

Using only virtual displacements with hinge lines and rigid plate parts the virtual work functional takes the following form

Virtual work functional (for virtual displacements with hinge lines)

$$\delta W = \sum_{\text{hinge lines}} \int_L M_{nn}\delta\theta\, ds - \lambda \int_A p\delta w\, dA \tag{7.16}$$

If the hinge line is a yield line, then we can find the yield moment in the line $M_{nn} = M_\ell$ by use of the flow rule. In the yield line the curvature state is given by κ_{nn} with $\kappa_{ss} = \kappa_{ns} = 0$. The normal to the yield surface is given by the curvature state and we can find the yield line moment by identifying a point on the yield surface with this normal. For the yield surfaces shown the moment in the yield line is found to be:

The moment M_{nn} in a yield line is

$$M_\ell = \pm\frac{2}{\sqrt{3}} M_p \qquad \textit{von Mises' yield criterion} \tag{7.17}$$

$$M_\ell = \pm M_p \qquad \textit{Tresca's yield criterion} \tag{7.18}$$

$$M_\ell = \begin{cases} M_p^+ \\ -M_p^- \end{cases} \qquad \textit{Johansen's yield criterion} \tag{7.19}$$

where the positive values correspond to yield lines with positive mutual rotation $\delta\theta > 0$ and the negative values to yield lines with negative mutual rotations $\delta\theta < 0$.

Thus, the non-negative plastic virtual work in a yield line is

$$\delta W_{int} = \int_L M_\ell\delta\theta\, ds = LM_\ell\delta\theta \tag{7.20}$$

where a straight yield line has been assumed in the last equality.

In yield lines the moments are given directly by the flow rule, but it must be

emphasized that the hinge line is assumed to be a real yield line. The plastic virtual work functional takes the following form:

Plastic virtual work functional (for virtual displacements with yield lines)

$$\delta W_p = \sum_{\text{yield lines}} \int_L M_\ell \delta\theta \, ds - \lambda_p \int_A p\delta w \, dA \tag{7.21}$$

The virtual work functional δW and the plastic virtual work functional δW_p will be used in the next two sections for evaluation of the upper and lower-bound theorems for plates.

The determination of the internal plastic virtual work may sometimes be simplified as described in the following. For straight yield lines we may define the following components L_β of the yield line length L and likewise the mutual rotation $\delta\theta$ as:

$$\begin{aligned} \delta\theta_\beta &= n_\beta \delta\theta \\ L_\beta &= n_\beta L \end{aligned} \tag{7.22}$$

The length L_2 is the projection of L on the x_1-axis and the length L_1 is the projection on the x_2-axis. (Note that $\delta\theta_\beta = \Delta(\delta\alpha_\beta)$). The introduced components enable us to rewrite the internal virtual work as follows:

$$\begin{aligned} \delta W_{int} &= M_\ell L \delta\theta = M_\ell n_\beta L_\beta \delta\theta = M_\ell L_\beta n_\beta \delta\theta \\ &= M_\ell L_\beta \delta\theta_\beta \end{aligned} \tag{7.23}$$

With this format we can decompose the mutual rotations in convenient coordinate directions and use the projections of the yield line length on these directions. The assumption of straight yield lines is not necessary, but may be easier to understand.

- **Example 7.2** A rectangular plate with opposite edge supports.

  A rectangular plate with simple supports at two opposite sides is loaded by a uniform transverse load $p = 1\text{kN/m}^2$. The plate is isotropic with a referencial plastification moment of $M_p = 8\,\text{kNm/m}$ and follows Tresca's yield criterion. The geometry with $a = 2$ m and the assumed yield line is shown in fig. 7.6. For a Tresca material the moment in the yield line is $M_\ell = M_p$. Assuming that the yield line is the correct one we use the principle of virtual work $\delta W_p = 0$ to find the load-carrying capacity as follows:

$$\begin{aligned} \int_L M_\ell \delta\theta \, ds - \lambda_p \int_A p\delta w \, dA &= 0 \quad \Downarrow \\ M_p 2\frac{\delta w}{a} a - \lambda_p \, p \, 2a^2 \, \frac{\delta w}{2} &= 0 \quad \Downarrow \end{aligned}$$

$$\lambda_p = \frac{2M_p}{pa^2} = \frac{16\,\text{kNm/m}}{1\,\text{kN/m}^2(2\,\text{m})^2} = 4$$

  If this is the correct yield line lay-out at failure, then the total load-carrying capacity for a uniform transverse load is $p^t = 4\,\text{kN/m}^2$.

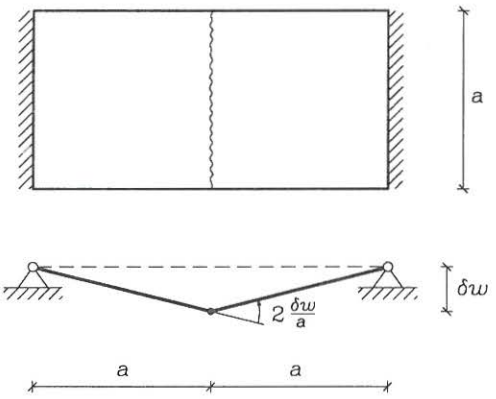

Fig. 7.6: A simple yield line example.

Reinforced Concrete Plates

In reinforced concrete plates with orthogonal reinforcement the amount of reinforcement in the two directions may vary and the yield criterion therefore becomes orthotropic. Let us use a main x_ν-coordinate system with axes along the orthotropic directions, i.e. orientated as the reinforcement. The referencial plastification moments are $M_{p\beta}$, i.e. with M_{p1} corresponding to the plastification moment with reinforcement in the x_1 direction and M_{p2} corresponding to the plastification moment with reinforcement in the x_2 direction. There may also be a difference between positive and negative plastification moments and we thus introduce the sign as an upper index as $M^+_{p\beta}$ for positive and $M^-_{p\beta}$ for negative plastification moments. Johansen's generalized yield surface for reinforced concrete plates is shown in fig. 7.7. The moment M_ℓ in an orthotropic yield line can be found using the definition of the normal moment M_{nn} as follows

$$\begin{aligned} M_\ell &= n_\beta n_\alpha M_{\alpha\beta} \\ &= n_1^2 M_{11} + n_2^2 M_{22} + 2 n_1 n_2 M_{12} \end{aligned} \tag{7.24}$$

For Johansen's generalized yield surface, which has $M_{12} = 0$ in the plastic zone, the moment in positive or negative yield lines is given by:

$$\begin{aligned} M^+_\ell &= n_1^2 M^+_{p1} + n_2^2 M^+_{p2} \\ M^-_\ell &= -(n_1^2 M^-_{p1} + n_2^2 M^-_{p2}) \end{aligned} \tag{7.25}$$

The virtual work in an orthotropic yield line using Johansen's yield surface is then given by:

$$\begin{aligned} \delta W_\ell &= L M_\ell \delta\theta \\ &= \left| L(n_1^2 M_{p1} + n_2^2 M_{p2})\delta\theta \right| \end{aligned} \tag{7.26}$$

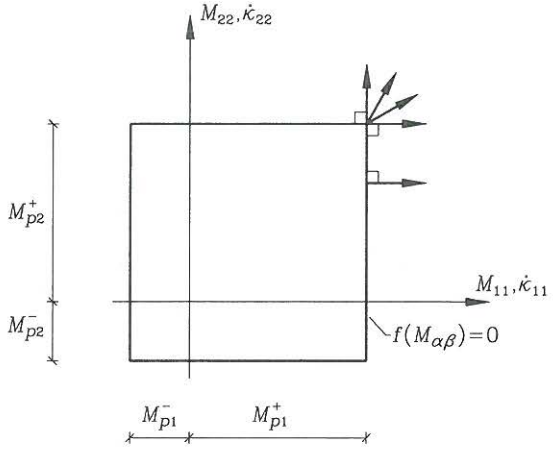

Fig. 7.7: Johansen's generalized yield surface.

This formula becomes easier in practical analysis if we project the length L of the yield line onto the reinforcement axes as L_β, and likewise the mutual rotation $\delta\theta$ as $\delta\theta_\beta$. Using (7.22) the virtual work takes the following form:

$$\delta W_\ell \;=\; |L_1 M_{p1}\delta\theta_1 + L_2 M_{p2}\delta\theta_2\,| \tag{7.27}$$

Note that the definition of $L_\beta = n_\beta L$ implies that L_1 is along the x_2-axis and L_2 is along the x_1-axis. In the isotropic case the formula reduces to $\delta W_\ell = |M_p L_\beta \delta\theta_\beta|$, which has in fact already been shown.

- **Example 7.3** A simple orthotropic skew plate.

  A skew plate with simple supports at two opposite sides is loaded by a uniform transverse load $p = 1\,\mathrm{kN/m^2}$. The plate is orthotropic with referencial plastification moments of $M_{p1} = 8\,\mathrm{kNm/m}$ and $M_{p2} = 0.5M_{p1}$. The plate is a reinforced concrete plate (RFC) and it follows Johansen's yield criterion. The geometry with $a = 2\,\mathrm{m}$ and the assumed yield line is shown in fig. 7.8.

  For the shown yield line the normal vector has the components

$$\begin{aligned} n_1 &= \cos v = \sqrt{2}/2 \\ n_2 &= \sin v = \sqrt{2}/2 \end{aligned}$$

  Since the mutual rotation in the yield line is $\delta\theta = 2\sqrt{2}\,\delta w/a$ the rotation components become

$$\begin{aligned} \delta\theta_1 &= n_1\delta\theta = 2\delta w/a \\ \delta\theta_2 &= n_2\delta\theta = 2\delta w/a \end{aligned}$$

  The lengths of the yield line projections are $L_1 = L_2 = a$.

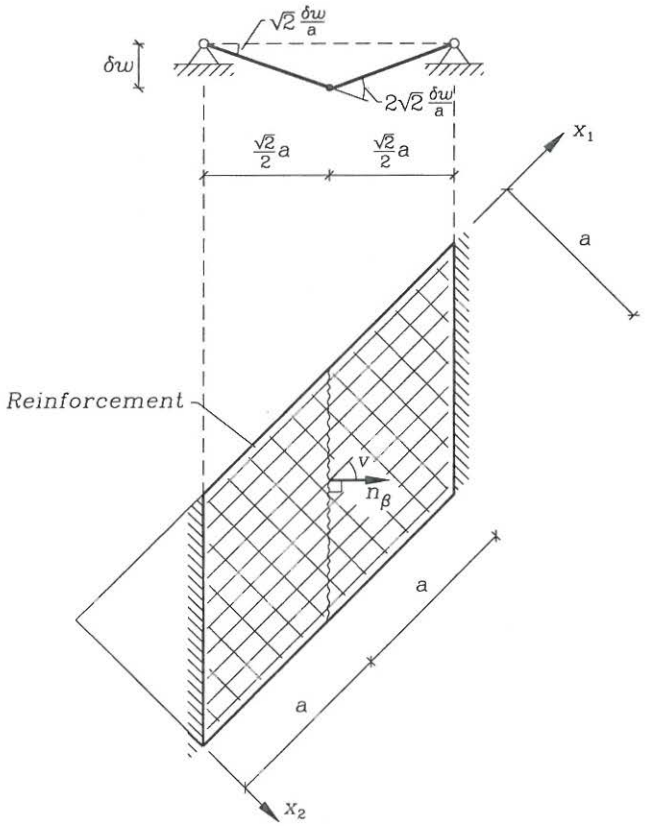

Fig. 7.8: A simple yield line example for an orthotropic RFC-plate.

Assuming that the yield line is the correct one we use the principle of virtual work $\delta W_p = 0$ to find the load-carrying capacity as follows:

$$\begin{aligned} \int_L M_\ell \delta\theta \, ds - \lambda_p \int_A p\delta w \, dA &= 0 \quad \Downarrow \\ aM_{p1} 2\frac{\delta w}{a} + aM_{p2} 2\frac{\delta w}{a} - \lambda_p \, p \, 2a^2 \, \frac{\delta w}{2} &= 0 \quad \Downarrow \\ 3M_{p1}\delta w - \lambda_p \, p \, a^2 \, \delta w &= 0 \quad \Downarrow \end{aligned}$$

$$\lambda_p = 3\frac{M_{p1}}{pa^2} = \frac{24\,\text{kNm/m}}{1\,\text{kN/m}^2(2\,\text{m})^2} = 6$$

If this is the correct yield line lay-out at failure, then the total load-carrying capacity for a uniform transverse load is $p^t = 6\,\text{kN/m}^2$.

7.1 Upper Bounds by the Yield Line Method

In this section the upper-bound theorem will be introduced in much the same way as in the chapter on plastic hinge analysis. The use of the principle of virtual work $\delta W = 0$ to find the load-carrying capacity is based upon the use of the real moment field $M_{\alpha\beta}$. However, through the use of a kinematic approach we may obtain an upper bound on the load-carrying capacity by exchanging the real moments in a virtual hinge line with the plastified moments. By anticipating that the moment in the virtual hinge line is the plastified normal moment M_ℓ we violate the principle of virtual work by increasing the internal virtual work, since $|M_\ell| \geq |M_{nn}|$ and therefore the plastic virtual work is greater than the real virtual work, i.e. $\delta W_p \geq \delta W = 0$. This leads to the upper-bound theorem for plates:

The upper-bound theorem

An upper bound, λ^+, for the plastic load-carrying capacity, λ_p, can be found by introducing kinematicly admissible virtual displacements with virtual yield lines into the virtual work functional and using that this virtual work is greater than or equal to zero, $\delta W_p \geq 0$.

The inequality leads to the following formulation:

$$\delta W_p = \sum_{\text{yield lines}} \int_L M_\ell \delta\theta \, ds - \lambda_p \int_A p \, \delta w \, dA \geq 0 \quad \Downarrow$$

$$\lambda_p \leq \lambda^+ \tag{7.28}$$

where the upper-bound load factor is given by

$$\lambda^+ = \frac{\sum_{\text{yield lines}} \int_L M_\ell \delta\theta \, ds}{\int_L p \, \delta w \, dA} \tag{7.29}$$

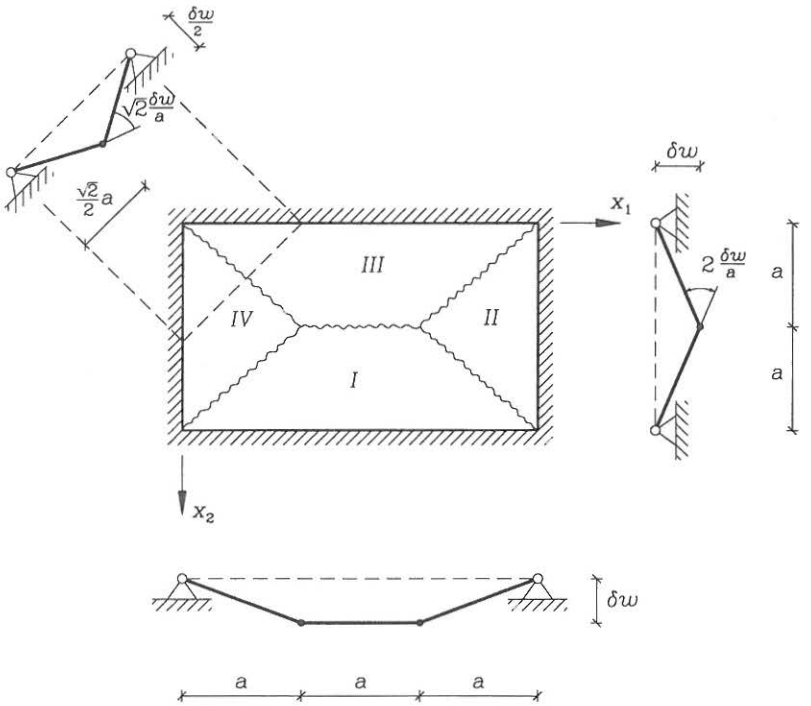

Fig. 7.9: Uniformly loaded rectangular plate.

There are many formulations of the upper-bound theorem. In many texts the equations are derived in an energy rate format, but the present formulation gains through the use of the concept of virtual hinge/yield lines.

Today the best way to validate the upper-bound solutions is through the use of advanced computational techniques which utilize the concepts of modern plasticity theory. However, even with these modern techniques the final flow mechanism may be difficult to obtain, even though the load factor is very close to the found upper-bound load factor. A few analytical examples exist, where both upper and lower-bound results can be found. It is time to illustrate the practical use of the upper-bound theorem.

- **Example 7.4** Uniformly loaded rectangular plate.

  A rectangular plate of isotropic perfectly plastic material is loaded by a uniform transverse load λp, where $p = 1\,\mathrm{kN/m^2}$. The plate geometry with $a = 2\,\mathrm{m}$ and the anticipated virtual yield layout is shown in fig. 7.9. The plastification moment is $M_p = 7\,\mathrm{kNm/m}$ for both positive and negative moments. Let us find the upper-bound load factor λ^+ for the shown virtual yield line lay-out.

  The virtual work of the external load can be found as follows, since the distributed

load is constant:

$$\delta W_{ext} = \lambda^+ \int_A p\delta w \, dA = \lambda^+ p \int_A \delta w \, dA$$

where $\int_A \delta w \, dA$ is the volume of the traverse space. Using this we find:

$$\delta W_{ext} = 2\lambda^+ p(\frac{1}{2}a^2\delta w) + 8\lambda^+ p(\frac{1}{3}\frac{a^2}{2}\delta w) = \frac{7}{3}\lambda^+ pa^2\delta w$$

Alternatively we can calulate the external work as the sum of the work performed by the resultant load on each individual rigid part of the plate. This method is used for more complicated load cases.

The internal work of the yield lines is straightforward for the central yield line, where the mutual rotation is $\delta\theta = 2\delta w/a$, whereas the diagonal yield lines become more difficult. However, by looking at a section through the plate which is perpendicular to the diagonal yield line we see that the mutual rotation becomes $\sqrt{2}\delta w/a$. The internal work becomes:

$$\delta W_{int} = \sum_{\text{yield lines}} M_\ell L\delta\theta = M_\ell a 2\frac{\delta w}{a} + 4M_\ell\sqrt{2}\, a\sqrt{2}\frac{\delta w}{a} = 10M_\ell\delta w$$

The upper-bound theorem results in

$$\lambda^+ = \frac{10M_\ell\delta w}{\frac{7}{3}pa^2\delta w} = \frac{30}{7}\frac{M_\ell}{pa^2}$$

If the material has Johansen's or Tresca's yield criterion then $M_\ell = M_p$ and we find the following upper-bound load factor:

$$\lambda^+ = \frac{30}{7}\frac{M_p}{pa^2} = \frac{15}{2} = 7.5$$

If, however, the material has the von Mises yield criterion then $M_\ell = \frac{2}{\sqrt{3}}M_p$ and we find $\lambda^+ \simeq 1.15 \cdot 7.5 \simeq 8.6$ which is 15% higher.

To find the lowest possible upper-bound load factor different variable yield line layouts must be tried and minimized. However, we are never sure, that we have found the lowest possible upper bound, unless of course we can find a corresponding lower-bound solution. However, the minimum is usually very flat and the upper-bound technique is in fact used in practice without consulting lower-bound techniques.

Practical Solution Technique

The internal work in the virtual yield lines may be calculated in a more practical manner, where the problem of determining the mutual rotation in a yield line is circumvented. Each rigid part of the plate is considered individually and the total virtual work is found by summation over the individual rigid parts. The virtual work of the shear forces is neglected, since they do not contribute to the total virtual work. The virtual work of the yield moments in a rigid part I of the plate, which has a constant inclination, $\delta\alpha_{\beta}^{I}$, can be found. Using that the normal inclination is

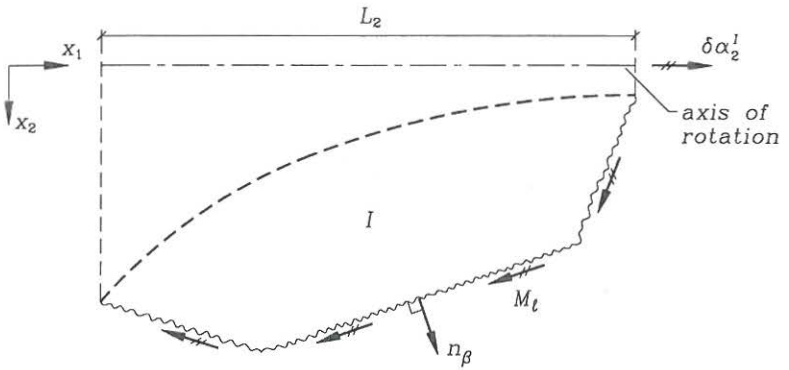

Fig. 7.10: Calculation of internal work for each rigid part.

$\delta\alpha_n^I = n_\beta \delta\alpha_\beta^I$ and that the component lengths L_β are found by the integral of $n_\beta ds$ along the line, i.e. $L_\beta = \int_L n_\beta ds$, it follows that:

$$\begin{aligned} \delta W_{int}^I &= \int_L M_\ell \delta\alpha_n^I \, ds = \int_L M_\ell \delta\alpha_\beta^I \, n_\beta \, ds = M_\ell \delta\alpha_\beta^I \int_L n_\beta \, ds \\ &= M_\ell L_\beta \delta\alpha_\beta^I \end{aligned} \tag{7.30}$$

where the yield moment M_ℓ is assumed to be constant and L_1 is the yield line projection on the x_2-axis and L_2 is the projection on the x_1-axis, (summing up overlapping parts). If the yield moment is piecewise constant, the calculation can be performed piecewise. If the coordinate system is orientated with an axis parallel to the axis of rotation, then the calculation only involves one term. For example if the local x_1-axis is chosen parallel to the axis of rotation for part I, then the internal work becomes $\delta W_{int}^I = M_\ell L_2 \delta\alpha_2^I$, since one inclination vanishes, as shown in fig. 7.10, i.e. $\delta\alpha_1^I = 0$.

- **Example 7.5** Uniformly loaded rectangular plate, revisited.

  Let us try the more practical technique on the previous, fairly simple example, shown in fig. 7.9. The individual rigid parts of the plate rotate about the support lines, which in this rectangular case are parallel to the chosen coordinate system. All the plate rotations in the current yield line lay-out are identical and equal to $\delta w/a$. The projected lengths of the yield lines are $L_2 = 3a$ for parts I and III, and $L_1 = 2a$ for parts II and IV. Thus, the internal virtual work can simply be calculated as:

$$\delta W_{int} = \sum_{\text{parts}} M_\ell L_\beta \delta\alpha_\beta = M_\ell (3a + 2a + 3a + 2a) \frac{\delta w}{a} = 10 M_\ell \delta w$$

  which of course is the same as found previously. The practical technique becomes the easiest method for complicated yield line lay-outs.

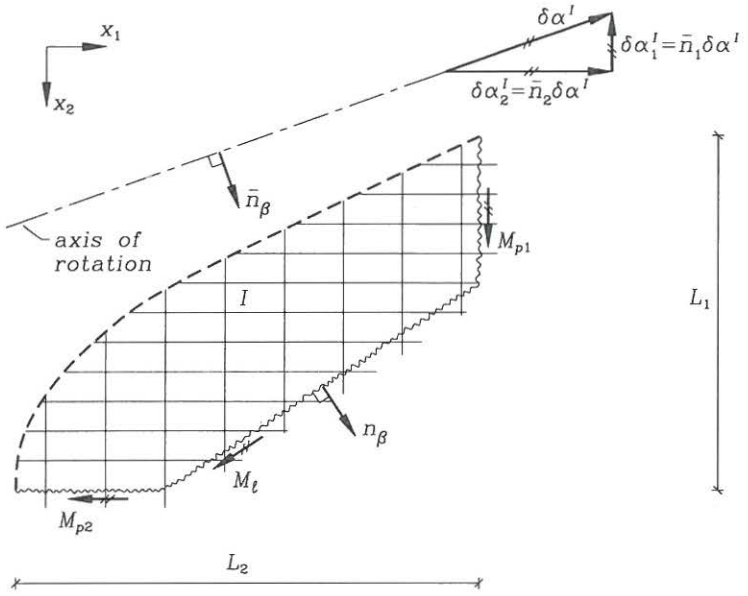

Fig. 7.11: Calculation of internal work in an orthotropic rigid part.

For orthotropic reinforced concrete plates the solution technique is practically the same. The difference lies in the choice of coordinate axes. In the orthotropic case we choose the orthotropic axes as shown in fig. 7.11. The internal work of the moments along the boundary of each rigid part is calculated and the contributions from all parts are summed. The rotation $\delta\theta$ in a yield line between two rigid parts can be split into the inclinations (rotations) of the individual parts $\delta\alpha$ on either side of the yield line by $\delta\theta = \delta\alpha_n^+ - \delta\alpha_n^-$. The internal work in a yield line is thus determined as follows:

$$\begin{aligned}
\delta W_{int}^I &= \int_L M_\ell \delta\alpha_n^I \, ds \\
&= \int_L (n_1^2 M_{p1} + n_2^2 M_{p2}) \delta\alpha_n^I \, ds \\
&= \int_L M_{p1} \, n_1 \delta\alpha_n^I \, n_1 ds + \int_L M_{p2} \, n_2 \delta\alpha_n^I \, n_2 ds \\
&= \int_L M_{p1} \, \delta\alpha_1^I \, dx_1 + \int_L M_{p2} \, \delta\alpha_2^I \, dx_2 \\
&= M_{p1} L_1 \delta\alpha_1^I + M_{p2} L_2 \delta\alpha_2^I
\end{aligned} \tag{7.31}$$

where it is important to note that the coordinate axes and the reinforcement axes must be identical. The inclination $\delta\alpha^I$ of the rigid part considered must be decomposed in inclination components along the reinforcement axes as $\delta\alpha_1^I$ and $\delta\alpha_2^I$.

- **Example 7.6** A simple orthotropic skew plate, revisited.

Let us revisit the orthotropic skew plate of example 7.3 shown in fig. 7.8 and analyse it by considering the individual rigid parts. The inclination angle (rotation) of the rigid part is determined by the rotation about the line support and the central displacement as:

$$\delta\alpha = \frac{\delta w}{\frac{\sqrt{2}}{2}a} = \sqrt{2}\delta w/a$$

The coordinate axes are orientated as the orthotropic reinforcement, and the line of rotation has the normal (in this example $u = v$):

$$\begin{aligned} \bar{n}_1 &= \cos u = \sqrt{2}/2 \\ \bar{n}_2 &= \sin u = \sqrt{2}/2 \end{aligned}$$

The inclination components are thus given by:

$$\begin{aligned} \delta\alpha_1 &= \bar{n}_1\delta\alpha = \delta w/a \\ \delta\alpha_2 &= \bar{n}_2\delta\alpha = \delta w/a \end{aligned}$$

The length of the yield line is $L = \sqrt{2}a$ and the yield line projections on the coordinate axes are also in this example given as:

$$\begin{aligned} L_1 &= n_1 L = a \\ L_2 &= n_2 L = a \end{aligned}$$

The internal work in one rigid part, part I, can then be found using equation (7.31), which gives us:

$$\delta W^I_{int} = M_{p1}a\frac{\delta w}{a} + M_{p2}a\frac{\delta w}{a} = (M_{p1} + M_{p2})\delta w$$

since there are two identical rigid parts and since $M_{p2} = 0.5M_{p1}$ the total internal work becomes:

$$\delta W_{int} = 2(M_{p1} + M_{p2})\delta w = 3M_{p1}\delta w$$

The external work is also in this example found to be:

$$\delta W_{ext} = \lambda_p p a^2 \delta w$$

The upper-bound load factor can thus be found as

$$\lambda^+ = 3\frac{M_{p1}}{pa} = 6$$

which was also found in example 7.3.

- **Example 7.7** Uniformly loaded rectangular plate, revisited once again.

Let the rectangular plate analysed in examples 7.4 and 7.5 be an orthotropic reinforced concrete plate with reinforcement directions parallel to the edges, so that

the reinforcement in the x_1-direction leads to $M_{p1} = \mu M_p$ and in the x_2-direction to $M_{p2} = M_p$.

The internal works by the rigid parts I and II, shown in fig. 7.9, are found using equation (7.31) as follows:

$$\begin{aligned} \delta W_{int}^{I} &= M_{p2} L_2 \delta\alpha_2^I = M_p\, 3a\, \delta w/a = 3M_p\delta w \\ \delta W_{int}^{II} &= M_{p1} L_1 \delta\alpha_1^{II} = \mu M_p\, 2a\, \delta w/a = 2\mu M_p\delta w \end{aligned}$$

The total internal work is then found by summation of the internal work performed by each rigid part as:

$$\delta W_{int} = 2\delta W_{int}^{I} + 2\delta W_{int}^{II} = (6+4\mu)M_p\delta W$$

The external work has been found in example 7.4 as $\delta W_{ext} = \frac{7}{3}\lambda^+ pa^2\delta w$ and the upper-bound load factor thus becomes:

$$\lambda^+ = \frac{3}{7}(6+4\mu)\frac{M_p}{pa^2}$$

By inserting $\mu = 1$ the result is identical to that already found for the isotropic rectangular plate in examples 7.4 and 7.5.

Admissible Yield Line Lay-Outs

The yield line lay-out must be geometricly possible, so that the virtual displacements only involve discontinuities in the plate inclinations $\delta\theta = \Delta(\delta\alpha_s)$ at yield lines and not discontinuities in the virtual displacement, i.e. $\Delta(\delta w) = 0$. If a rigid part of the plate is supported by a column, then the rotation axis of this part must go through the support point. Through geometric analysis it can be shown that the rotation axes and the yield line between two connected plates must intersect. An intersection point at infinity is also acceptable. This leaves us with the following statement:

Geometricly admissible yield line lay-out.

The yield line lay-out is geometricly admissible, if the intersection point of the rotation axes of mutually connected rigid parts is also intesected by their mutual yield line (and its extension).

The rotation axis of parts supported by columns must intersect the support point.

For plates supported along the edges some geometricly admissible yield line lay-outs are shown in fig. 7.12 and fig. 7.13 some admissible lay-outs are shown for a plate supported by two columns and along an edge.

Corner Levers

Plates are more or less geometricly fixed at corners where both edges are supported. Due to this there is a tendency for the yield lines to separate and form socalled

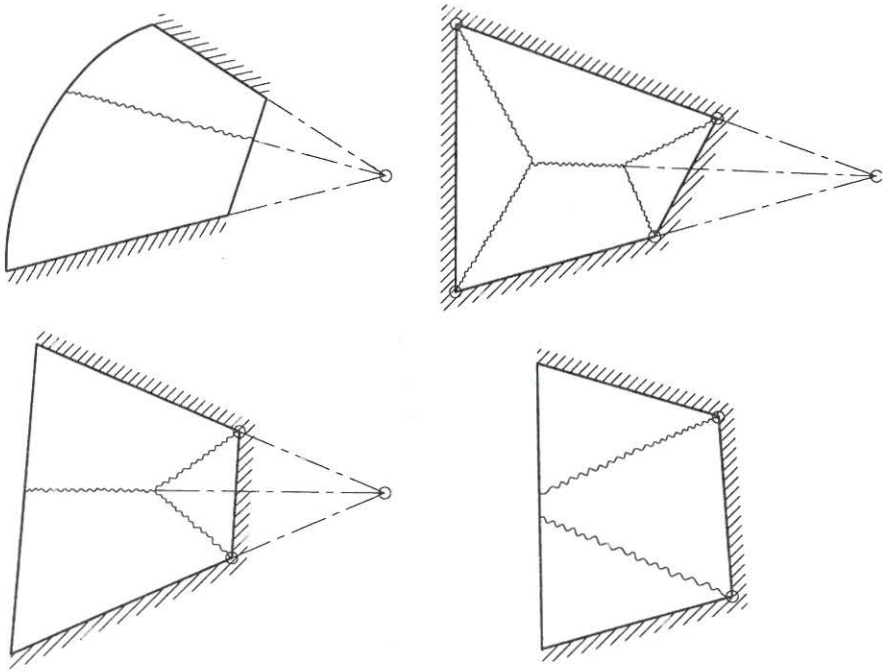

Fig. 7.12: Geometricly admissible yield line lay-outs.

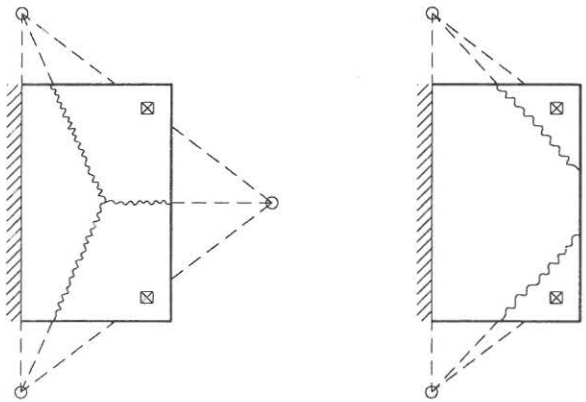

Fig. 7.13: Geometricly admissible yield line lay-out including columns.

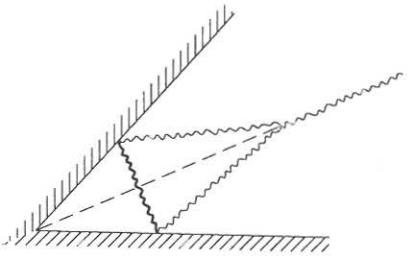

Fig. 7.14: A corner lever.

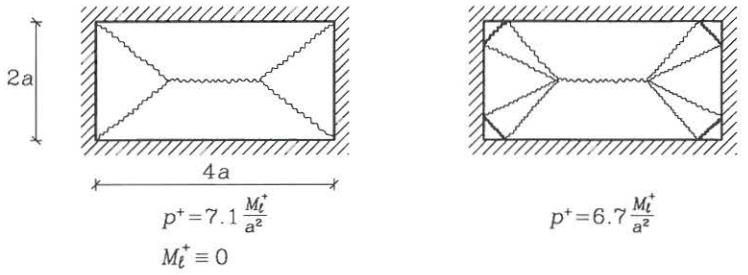

Fig. 7.15: A rectangular plate.

corner levers with a negative yield line, as shown in fig. 7.14. For small corner angles the tendency of the existence of a lever is increased due to firmer fixation at the corner. The corner levers usually give a small correction to the original upper bound, and the best way to find a minimum upper bound is first to find the minimum yield line lay-out and then introduce corner levers. The small influence of corner levers is illustrated in the in fig. 7.15 and 7.16 for uniformly loaded isotropic reinforced concrete plates with $M_\ell^- = 0$.

Concentrated Shear Forces

Since the shear forces have been neglected in the yield criteria we must be sure that the shear forces can be sustained by the plate, especially at the yield lines. There are concentrated shear forces at the corners and we have to be sure that their magnitude is acceptable. At the free edges of a plate where a yield line ends there are also concentrated shear forces. We may estimate these forces by use of the yield line lay-out, which must be close to the lay-out of the real flow mechanism.

Let us use a local coordinate system as shown in fig. 7.17 with the x_1-direction parallel to the yield line and just analyse one part of the plate. The angle between the yield line and the edge of the plate is φ. The moments in the yield line are the principal moments and therefore $M_{22} = M_\ell$ and $M_{12} = 0$. On the edge we assume

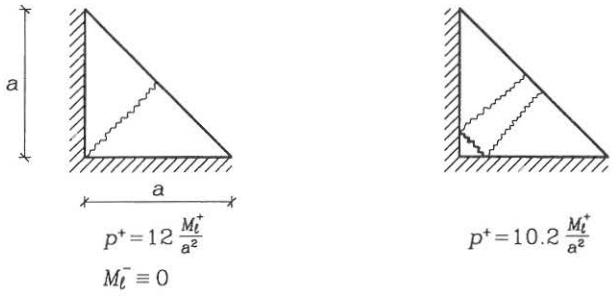

Fig. 7.16: A triangular plate.

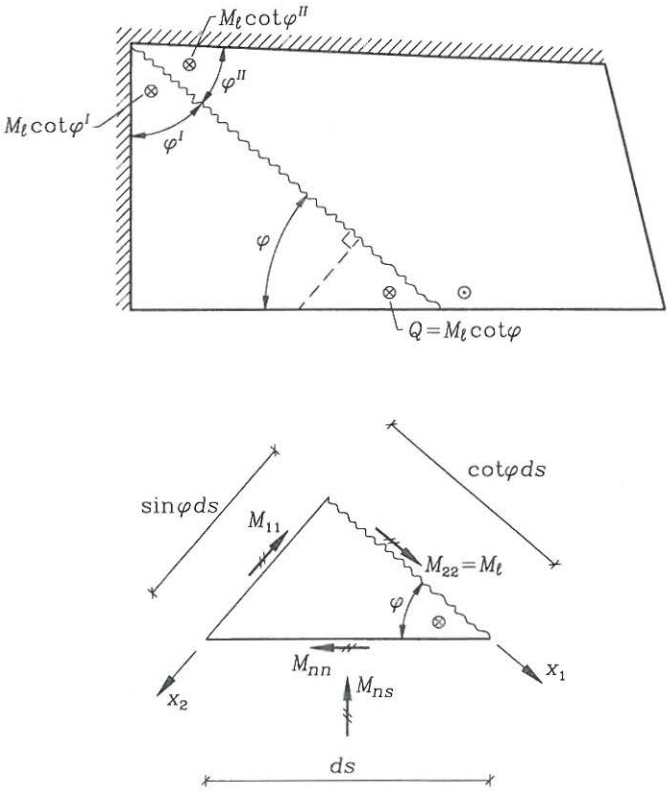

Fig. 7.17: Yield line section at an edge.

that the normal moment M_{nn} is given, for example for a free edge or a simply supported edge $M_{nn} = 0$ and for a fixed edge with a negative yield line $M_{nn} = M_\ell^-$.

We need to find M_{ns} along the edge. To do so we consider moment equilbrium about the x_1-axis as follows:

$$(-M_{ns}\sin\varphi - M_{nn}\cos\varphi)ds + M_\ell \cos\varphi \, ds = 0 \quad \Downarrow$$

$$M_{ns} = (M_\ell - M_{nn})\cot\varphi \tag{7.32}$$

The concentrated shear force is given by equation (6.83), which in the present system with $M_{21} = 0$ takes the form:

$$\begin{aligned} Q &= M_{ns} - M_{21} = M_{ns} \\ &= (M_\ell - M_{nn})\cot\varphi \end{aligned} \tag{7.33}$$

At a free edge with $M_{nn} = 0$ the concentrated internal shear force must be determined at either side of the yield line. On one side of the yield line the edge shear force is

$$Q_{edge} = M_\ell \cot\varphi \tag{7.34}$$

and on the other side of the yield line the edge shear force just changes sign, since $\cot(\pi - \varphi) = -\cot\varphi$. At corners there are two rigid parts of the plate each contributing with one concentrated shear force. There are two angles, φ^I and φ^{II} at such a corner. The corner shear force has to be transferred to the supports. For two simple supports meeting at a corner the concentrated shear force is:

$$Q_{corner} = M_\ell(\cot\varphi^I + \cot\varphi^{II}) \tag{7.35}$$

For corners with two fixed supports (with negative yield lines along the edges) we find:

$$Q_{corner} = (|M_\ell^+| + |M_\ell^-|)(\cot\varphi^I + \cot\varphi^{II}) \tag{7.36}$$

These shear forces are only approximations and they are only realistic if the yield line lay-out corresponds to the real plastic flow mechanism for the plate. For thin plates the concentrated shear forces are transferred over yield lines or to supports over an in-plane distance approximately equal to the thickness of the plate. Note that $\cot\varphi$ changes sign around $\varphi = \pi/2$ so that for angles lower than $\pi/2$ the shear force is positive and directed downwards.

Point Loads

At point loads or at column supports local circular or elliptical flow mechanisms have to be checked. For isotropic plates with point loads the flow mechanism has a negative outer circular yield line and positive internal radial yield lines. For anisotropic plates the outer yield line is elliptical. It is also interesting that the upper bound does not depend on the diameter of the flow mechanism, as we shall see in the following. Let us analyse an isotropic plate with a point load, for example the one shown in fig. 7.18. Let $d\varphi$ be the angle between the radial yield lines. The

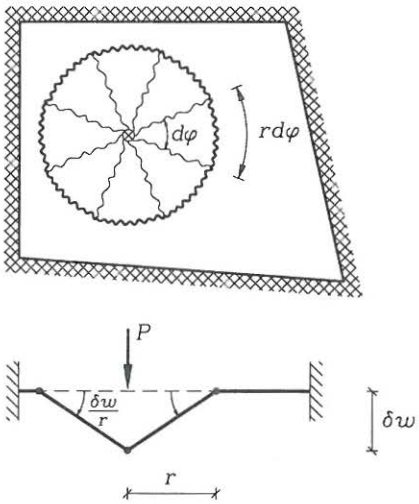

Fig. 7.18: Isotropic plate with a point load.

central displacement is δw and the radius is r. Thus, the external work is

$$\delta W_{ext} = P\delta w \tag{7.37}$$

The internal work can be found by projection on the axis of rotation for the individual rigid parts. The individual part rotates $\delta w/r$ about the negative yield line, which has the length $rd\varphi$. One rigid part thus contributes to the internal work with

$$\delta W^I_{int} = (M^+_\ell + |M^-_\ell|)\frac{\delta w}{r} rd\varphi \tag{7.38}$$

The total internal plastic virtual work becomes:

$$\delta W_{int} = \int_0^{2\pi} (M^+_\ell + |M^-_\ell|)\delta w \, d\varphi = 2\pi(M^+_\ell + |M^-_\ell|)\delta w \tag{7.39}$$

The principle of virtual work, $\delta W = \delta W_{int} - \delta W_{ext} = 0$, then gives:

$$P^+ = 2\pi(M^+_\ell + |M^-_\ell|) \tag{7.40}$$

For plates with equally positive and negative yield moments we thus find that $P^+ = 4\pi M_\ell$. At corners the above principles may be used and the formulas modified adequately.

7.2 Lower-Bound Theorem

A lower bound on the plastic load factor can be found by a static approach. The idea is to use statically admissible moment fields $M_{\alpha\beta}$, which are within the yield

surface and therefore safe, i.e. $f(M_{\alpha\beta}) \leq 0$ and thereby find a lower-bound load factor λ^-. Statically admissible moment fields are moment fields which satisfy the static equilibrium equations:

$$\begin{aligned} M_{\alpha\beta,\alpha\beta} + p &= 0 \quad \Downarrow \\ M_{11,11} + 2M_{12,12} + M_{22,22} + p &= 0 \end{aligned} \tag{7.41}$$

In a virtual hinge line the statically admissible normal moment is given as

$$M_S = M_{nn} = n_\beta n_\alpha M_{\alpha\beta} \tag{7.42}$$

If the moment field is safe the moments in the hinge line are within or on the yield surface $f(M_{\alpha\beta}) \leq 0$ and therefore the normal moments are less than the yield line moments, i.e. $|M_S| \leq |M_\ell|$.

To show the lower-bound theorem for plates let us first use the yield lines of the real flow mechanism to find an exact expression for the plastic load factor λ_p, then let us use a safe statically admissible moment distribution with the real yield line lay-out and show that this gives a lower bound λ^-. Let us begin. The real flow mechanism with $\delta\theta = \dot{\theta}$ and $\delta w = \dot{w}$ is introduced into the principle of virtual work $\delta W = 0$ and it is used that the moments are plastified in the yield lines, i.e. $M_{nn} = M_\ell$. This gives us the real plastic load factor as follows:

$$\delta W = \sum_{\text{hinge lines}} \int_L M_\ell \dot{\theta}\, ds - \lambda \int_A p\dot{w}\, dA = 0 \quad \Downarrow$$

$$\lambda_p = \frac{\sum_{\text{hinge lines}} \int_L M_\ell \dot{\theta}\, ds}{\int_A p\dot{w}\, dA} \tag{7.43}$$

Next let us use a statically admissible moment distribution M_S in equilibrium with the load $\lambda^- p$. The principle of virtual work is exact for a given equilibrium state and we can use any virtual displacement field to find the load factor. This load factor is a lower bound if we make sure that the statically admissible moment field is safe, i.e. $f(M_{\alpha\beta}) \leq 0$ everywhere or equivalently that $|M_S| \leq |M_\ell|$ is satisfied for any hinge line lay-out. Since we can use any virtual hinge line lay-out let us try the yield line lay-out of the real flow mechanism. This gives us:

$$\delta W = \sum_{\text{hinge lines}} \int_L M_S \delta\theta\, ds - \lambda^- \int_A p\delta w\, dA = 0 \quad \Downarrow$$

$$\lambda^- = \frac{\sum_{\text{hinge lines}} \int_L M_S \delta\theta\, ds}{\int_A p\delta w\, dA} = \frac{\sum_{\text{hinge lines}} \int_L M_S \dot{\theta}\, ds}{\int_A p\dot{w}\, dA} \leq \lambda_p \tag{7.44}$$

where the last inequality is obtained using (7.43) and that $M_S\dot{\theta} \leq M_\ell\dot{\theta}$, since the statically admissible moment distribution is safe everywhere.

The lower-bound theorem

If a statically admissible moment field, $M_{\alpha\beta}$, in equilibrium with the factored external loads, $\lambda^- p$, is safe, $f(M_{\alpha\beta}) \leq 0$, then the load factor, λ^-, is a lower bound for the real plastic load factor λ_p, i.e. $\lambda^- \leq \lambda_p$.

The lower-bound theorem is very seldom used in combination with the upper-bound theorem, since it is very difficult to find good lower bound values. The linear-elastic plate theory results in lower-bound solutions if they are scaled to satisfy the yield criterion everywhere in the plate.

The Strip Method

Following Hillerborg [36] statically admissible moment fields may be found by taking the twisting moment as zero, $M_{12} = 0$, and carrying the load in two orthogonal directions through the moments M_{11} and M_{22}. If the twisting moment is zero in the static equilibrium equation (7.41) for transverese loads, we obtain the following equilibrium equation:

$$M_{11,11} + M_{22,22} + p = 0 \tag{7.45}$$

This equation can be split into two by separating the transverse load p into the part ψp carried in the x_1-direction and the part $(1-\psi)p$ carried in the x_2-direction, where the parameter ψ governs the dispersion of the load in the two directions. This leads to the following set of equations:

$$\begin{aligned} M_{11,11} + \psi p &= 0 \\ M_{22,22} + (1-\psi)p &= 0 \end{aligned} \tag{7.46}$$

These equations are equivalent to two beam equilibrium equations. The idea of approximating a plate by orthogonal beams is old, and Hillerborg gives a systematic treatment of the subject with respect to reinforced concrete plates. Hillerborg considers the "beams" as strips of plate in which the load is carried in the strip direction. In reinforced concrete beams the reinforcement can then be chosen for the individual strip. This is the main advantage of the strip method. However, today reinforcement is seldom varied much in the plate, due to prefabrication of reinforcement. Reinforced concrete plates, however, usually have a boundary zone with increased top reinforcement.

A plate is subdivided into different regions in which the dispersion parameter ψ is constant. The dispersion parameter is usually chosen so that the load in a given point is carried/dispersed in the most optimal direction. For a rectangular beam with uniform transverse load two such subdivisions are shown in figs. 7.19 and 7.20. In fig. 7.19 the plate is simply supported at all edges, and the subdivision has been related to the yield line lay-out of a probable plastic flow mechanism and in each subplate the load is carried in one direction only. In fig. 7.20 the rectangular plate has one free edge and three simply suported edges. The subdivision includes an edge strip, which transfers load to the supports.

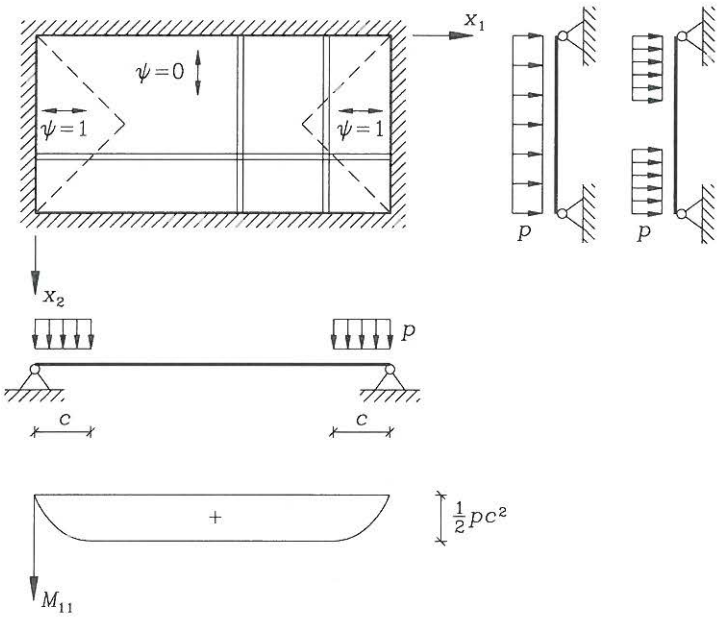

Fig. 7.19: Subdivision of rectangular plate.

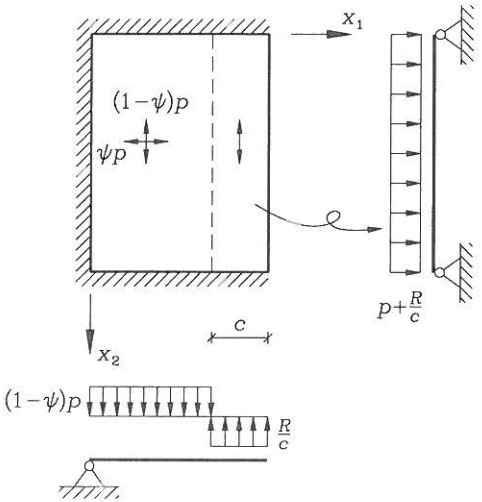

Fig. 7.20: Another subdivision of a rectangular plate.

- **Example 7.8** Lower-bound solution for plate in fig. 7.9.

  The rectangular plate is loaded by a uniform transverse load $p = 1\,\mathrm{kN/m^2}$ and the geometry is shown in fig. 7.9 with $a = 2\,\mathrm{m}$. The referencial plastification moment is $M_p = 7\,\mathrm{kNm/m}$. Let us assume that the load is carried by orthogonal strips in the x_1 and x_2 directions. The strips have pinned ends and the maximum moments in the strips are thus determined by $\frac{1}{8}pL^2$. The optimal choice of the dispersion parameter is thus determined by the square of the span lengths. For a Tresca material the moments in the two transverse directions should be equal and we thus choose the dispersion parameter by equalizing the moments in the two transverse strips as follows:

$$\begin{aligned} \frac{1}{8}\psi p(3a)^2 &= \frac{1}{8}(1-\psi)p(2a)^2 \quad \Downarrow \\ \psi &= \frac{4a^2}{4a^2+9a^2} = \frac{4}{13} \end{aligned}$$

  The maximum moments thus become:

$$M_{11} = M_{22} = \frac{4\cdot 9}{13\cdot 8}pa^2 = \frac{9}{26}pa^2$$

  Let us scale the loads and thereby the maximum moments by a load factor λ^-, so that the central moments are on the yield surface:

$$\begin{aligned} \lambda^- \frac{9}{26}pa^2 &\le M_p \quad \Downarrow \\ \lambda^- &= \frac{26M_p}{9pa^2} \simeq 5.1 \end{aligned}$$

  which should be compared with the upper bound $\lambda^+ = 7.5$ found in the previous example. The lower bound $\lambda^- = 5.1$ is also a lower bound for the von Mises material, since the point $(M_{11}, M_{22}) = (M_p, M_p)$ is on the von Mises yield surface.

Rectangular Plates

A simple statically admissible moment distribution, which satisfies the plate equilibrium equation (7.41) including the torsional term can be found for uniformly loaded rectangular plates as outlined in the the following.

The equilibrium equation only includes second order partial derivatives of the moments M_{11} and M_{22} in the directions x_1 and x_2, respectively. It also includes a mixed second order derivative of the torsional moment M_{12}. The solution could therefore be parabolic in M_{11} and M_{22}, and hyperbolic for the torsional moment M_{12}. Such a moment distribution is given by:

$$\begin{aligned} M_{11} &= a_{10} + a_{11}x_1 + a_{12}x_1^2 \\ M_{22} &= a_{20} + a_{21}x_2 + a_{22}x_2^2 \\ M_{12} &= a_0 + a_1x_1 + a_2x_2 + a_3x_1x_2 \end{aligned} \tag{7.47}$$

where the constants $a_{...}$ depend on the boundary conditions and boundary moments chosen. Inserting the moment field into the equilibrium equation results in:

$$2a_{12} + 2a_{22} + 2a_3 + p = 0 \tag{7.48}$$

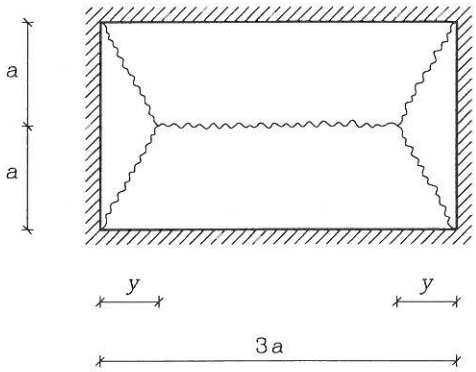

Fig. 7.21: Optimal choice of y for a rectangular plate.

which corresponds to dividing the load between the three moment distributions. By analysis of the moment distribution the boundary terms are found to be constant, as briefly described in the following. The normal moments $\bar{M}_n = M_{nn}$ are constant along the boundary. The torsional moments $\bar{M}_s = M_{ns}$ are transformed into constant shear force contributions $\bar{M}_{s,s} = M_{ns,s}$ along the boundaries and into point shear forces at the corners. The non-torsional shear force is $\bar{Q} = M_{nn,n} + M_{ns,s}$ and the total equivalent shear force is $\bar{Q} + \bar{M}_{s,s} = M_{nn,n} + 2M_{ns,s}$. Since the partial derivative of the torsional moment is in the tangential direction this contribution also becomes constant. The concentrated shear forces at corners are $-2\bar{M}_s = -2M_{ns}$. The solution is treated thoroughly by Nielsen [30] for different boundary conditions.

- **Problem 7.1**

  For the uniformly loaded and simply supported rectangular plate shown in fig. 7.21, find the optimal distance y which minimizes the upper bound for the load-carrying capacity and compare with $y = a$ in the previous example. The geometry is given in the figure. (It may be used that an extremum of a fraction $\frac{g(y)}{h(y)}$ is also an extremum of the fraction of the numerator and denominator derivatives, i.e. $\frac{g'(y)}{h'(y)}$, where the prime corresponds to differentiation with respect to y).

  What is the upper-bound load factor if the material is a Tresca material and if the load is $p = 1\ \mathrm{kN/m^2}$, the distance $a = 2$ m and the plastification moment $M_p = 8\ \mathrm{kNm/m}$.

- **Problem 7.2**

  Analyse the uniformly loaded angle plate with simple supports and two free edges shown in fig. 7.22.

  a) Find the upper-bound load factor for the shown yield line lay-out.

  b) Find the nodal shear forces at the two corners and state the direction of the shear force and the corner reaction.

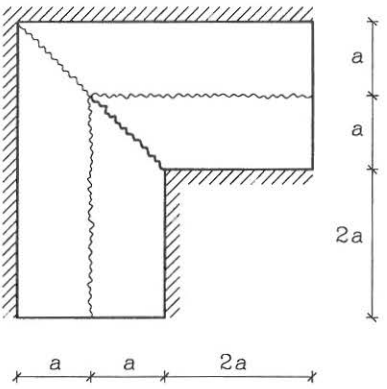

Fig. 7.22: A special geometry including a negative yield line.

- **Problem 7.3**
  Find upper bounds for the uniformly loaded square plate shown in fig. 7.23. The plate has three simply supported edges and one free edge. Try at least two different yield line lay-outs and optimize the best lay-out.

  For the final lay-out, find the concentrated edge shear forces.

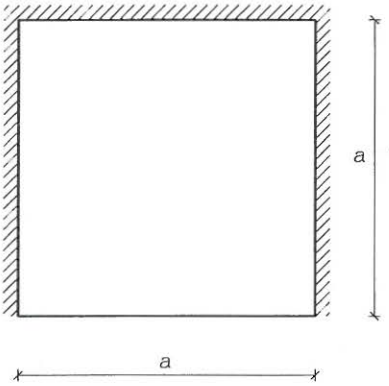

Fig. 7.23: Find the lowest possible upper bound.

Bibliography

[1] Simmonds, J. G., *A Brief on Tensor Analysis*, Springer Verlag, New York, 1982.

[2] Kay, D. C., *Theory and Problems of Tensor Calculus*. Schaum's Outline Series, McGraw-Hill, 1988.

[3] Synge, J. L. and Shield, A., *Tensor Calculus*, University of Toronto Press, Toronto, 1949.

[4] Washizu, K., *Variational Methods in Elasticity and Plasticity*, Second Edition, Pergamon Press, Oxford, 1975.

[5] Krenk, S., *Three-Dimensional Elastic Beam Theory*, draft manuscript, Lecture notes F114 and F115. Department of Structural Engineering, Technical University of Denmark, 2800 Lyngby, Denmark, 1989.

[6] Malvern, L. E., *Introduction to the Mechanics of a Continuous Medium*, Prentice-Hall, Englewood Cliffs, New Jersey, 1969.

[7] Flügge, W., *Tensor Analysis and Continuum Mechanics*, Springer-Verlag, Berlin, 1972.

[8] Love, A. E. H., *A Treatise on the Mathematical Theory of Elasticity*, Fourth Edition, Dover, New York, 1944.

[9] Timoshenko, S. P. and Goodier, J. N., *Theory of Elasticity*, Second Edition, McGraw-Hill, New York, 1951.

[10] Timoshenko, S. P., *History of Strength of Materials*, McGraw-Hill, New York, 1953.

[11] Timoshenko, S. P. and Gere, J. M., *Theory of Elastic Stability*, Second Edition, McGraw-Hill, New York, 1961.

[12] Gere, J. M. and Timoshenko, S. P., *Mechanics of Materials*, Third SI Edition, Chapman and Hall, London, 1991.

[13] Lanczos, C., *The Variational Principles of Mechanics*, Third Edition, University of Toronto Press, Toronto, 1966.

[14] Bažant, Z. P., and Cedolin, L., *Stability of Structures, Elastic, Inelastic, Fracture and Damage Theories*, Oxford University Press, 1991.

[15] Massonnet, C. E. and Save, M. A., *Plastic Analysis and Design*, Blaisdell Publishing Company, New York, 1965.

[16] Neal, B. G., *The Plastic Methods of Structural Analysis*, Third (S.I.) Edition, Chapmann & Hall Ltd., Third (S.I.) Edition, London, 1977.

[17] Neal, B. G. and Symmonds, P. S., The Rapid Calculation of the Plastic Collapse Load for a Framed Structure, *Proc. Inst. Civil Engrs.*, 1, (Part 3), 58, 1952.

[18] Chen, W. F. and Han, D. J., *Plasticity for Structural Engineers*, Springer-Verlag, New York, 1988.

[19] Kirchhoff, G., Über das Gleichgewicht und die Bewegung einer elastichen Scheibe, *Journal für die Reine und Angewandte Mathematik*, **40**, 51-8, 1850.

[20] Reissner, E., The Effect of Transverse Shear Deformation on the Bending of Elastic Plates, *J. Appl. Mech.*, **12**, 69-76, 1945.

[21] Mindlin, R. D., Influence of Rotatory Inertia and Shear in Flexural Motions of Isotropic Elastic Plates, *J. Appl. Mech.*, **18**, 31-8, 1951.

[22] Timoshenko, S, and Woinowsky-Krieger, S., *Theory of Plates and Shells*, 2nd Ed., McGraw-Hill, New York, 1959.

[23] Boresi, A. P., Sidebottom, O. M., Seely, F. B, and Smith, J. O., *Advanced Mechanics of Materials*, Third Edition, Wiley, New York, 1978.

[24] Nielsen, L. O., *Pladers Statik*, 4 udgave, F141, Department of Structural Engineering, Technical University of Denmark, 1994.

[25] Nielsen, M. P. and Rathkjen, A., *Mekanik 5.1, del 1, Skiver og plader*, Den private Ingeniørfond ved Danmarks tekniske Højskole, København, 1981.

[26] Nielsen, M. P. and Rathkjen, A., *Mekanik 5.1, del 2, Skiver og plader*, Den private Ingeniørfond ved Danmarks tekniske Højskole, København, 1981.

[27] Johansen, K. W., *Brudlinieteorier* (Yield line theories), (a doctoral thesis), Gjellerup, Copenhagen, 1943.

[28] Johansen, K. W., *Yield Line Theory*, English translation of *Brudlinieteorier*, Cement and Concrete Association, London, 1962.

[29] Johansen, K. W., *Pladeformler, Formelsamling*, (Slab Formulas), Two Volumes. Polyteknisk Forening, Copenhagen, 1949.

[30] Nielsen, M. P., *Limit Analysis and Concrete Plasticity*, Prentice-Hall, Inc., Englewood Cliffs, New Jersey, 1984.

[31] Martin, J. B., *Plasticity: Fundamentals and General Results*, Cambridge, Mass., MIT Press, 1975.

[32] Save, M. A. and Massonnet, C. E., *Plastic Analysis and Design of Plates, Shells and Disks*, North-Holland Publishing Company, Amsterdam, 1972.

[33] Prager, W., *An Introduction to Plasticity*, Reading, Mass., Addison-Wesley, 1959.

[34] Hodge, P. G., *Plastic Analysis of Structures*, New York, McGraw-Hill 1959.

[35] Hillerborg, A., *Strimlemetoden*, (The Strip Method), Stockholm, Almqvist & Wiksell, 1974.

[36] Hillerborg, A., *Strip Method of Design*, Viewpoint Publications, William Clowes & Sons, London, 1975.

Index